Study of Simple and Complex Structures in Composite Materials

SIMÃO PEDRO BRISSOS SOUSA JESUS GAMITO

(Licenciado em Engenharia Mecânica)

Dissertação para obtenção do grau de Mestre em Engenharia Mecânica, na Área de Especialização de Produção e Manutenção

Orientadores:

Doutor Afonso Manuel da Costa de Sousa Leite

Doutora Maria Amélia Ramos Loja

Júri:

Presidente: Doutor Mário José Gonçalves Cavaco Mendes

Vogais: Doutor Ivo Manuel Ferreira de Bragança

Doutor Afonso Manuel da Costa de Sousa Leite

Dezembro de 2024

Study of Simple and Complex Structures in Composite Materials

SIMÃO PEDRO BRISSOS SOUSA JESUS GAMITO

(Licenciado em Engenharia Mecânica)

Dissertação para obtenção do grau de Mestre em Engenharia Mecânica, na Área de Especialização de Produção e Manutenção

Orientadores:

Doutor Afonso Manuel da Costa de Sousa Leite, ISEL/IPL

Doutora Maria Amélia Ramos Loja, ISEL/IPL

Júri:

Presidente: Doutor Mário José Gonçalves Cavaco Mendes, ISEL/IPL

Vogais: Doutor Ivo Manuel Ferreira de Bragança, ISEL/IPL

Doutor Afonso Manuel da Costa de Sousa Leite, ISEL/IPL

Dezembro de 2024

Acknowledgements

This thesis or the motivation behind it couldn't be made possible without the contrition of numerous individuals, too many to enumerate. Here are some examples of such wonderful people:

To my master thesis advisor, Professor Maria Amélia Ramos Loja, I would like to thank for the wisdom transmitted throughout my academic journey and or the tenacity that has become engraved in my person. To my thesis adviser, Professor Afonso Manuel da Costa de Sousa Leite, thank you for all the motivation and availability in my academic studies, as well as the many inputs and suggestions throughout the experimental and numerical methods. Truly, thank you both.

To my mother and father, for always believing in me, even when I couldn't. To my brother, for being himself, because that is more than enough.

To my girlfriend Ana, for being my better half and my anchor.

To my friends at ISEL, Renato Cabrita, Ricardo Parente, Rui Roque for the encouragement and friendship.

To my friend, José Luz for helping with the experimental procedure.

Statement of integrity

I declare that this dissertation is the result of my personal and independent research. Its content is original, and all sources listed in the bibliographic references were consulted and are duly mentioned in the text. I further declare that all scientific and technical references relevant to the development of the work are duly cited and included in the bibliographic references.

The author

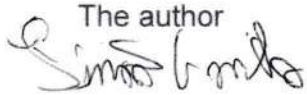

Lisbon, 18/12/2024

Estudo de Estruturas Simples e Complexas em Materiais Compósitos

Resumo

O uso de materiais compósitos tem aumentado exponencialmente nas mais variadas áreas da engenharia, não apenas em relação a materiais à base de fibra, mas também a compósitos de partículas, como os conhecidos Materiais Funcionalmente Graduados (FGM). Este trabalho é especificamente focado em materiais fibrosos que, ao considerar a direção da fibra dentro de cada camada, permite atingir diferentes valores de propriedades mecânicas e, portanto, um uso generalizado. No entanto, devido à natureza heterogênea e ortotrópica desses materiais, a previsão de falha torna-se complexa. O uso combinado de métodos analíticos (frequentemente realizados usando plataformas de computação simbólica) e/ou métodos numéricos permite prever a falha. Apesar de usar uma abordagem de métodos únicos ou combinados, é necessário verificar os resultados obtidos com referências alternativas.

Este estudo teve como objetivo desenvolver e implementar uma abordagem numérico-analítica e experimental para caracterizar o comportamento mecânico de placas compósitas à base de fibra com matriz epóxi. O estudo considerou placas de fibra de carbono/epóxi com diferentes números de camadas e orientações de fibra. Quatro abordagens foram empregadas: a primeira e a segunda abordagens, baseadas no Método de Elementos Finitos (FEM) usando ANSYS Mechanical Parametric Design Language (Mechanical APDL) e ANSYS WORKBENCH, respectivamente; a terceira abordagem envolveu resultados analíticos obtidos através do software de computação simbólica MAPLESOFT; a quarta abordagem baseou-se em ensaios de tração experimentais das placas, utilizando extensómetria para medir as deformações resultantes, assim como um dispositivo de tração bi-axial. Posteriomente, um estudo estático tridimensional de um guiador de triatlo foi calculado usando o software FEM Solidworks Simulation.

Os resultados mostram que, embora alguns métodos numéricos possam prever a falha no contexto de materiais compósitos com alguma precisão, essa previsão está fundamentalmente ligada ao critério de falha adotado na análise.

Palavras-Chave

Materiais fibrosos;
Critérios de falha em materiais compósitos;
”User Programmable Feature” (UPF);

Study of Simple and Complex Structures in Composite Materials

Abstract

The use of composite materials has been increasing exponentially in various engineering fields, not only in fiber-based materials but also in advanced particle composites, such as Functionally Graded Materials (FGM). This work focuses on fiber-based materials, which, by considering the appropriate fiber direction within each layer, can achieve different mechanical properties, leading to widespread use. However, due to the heterogeneous and orthotropic nature of these materials, failure prediction becomes challenging. Combining analytical methods (often using symbolic computing platforms) and/or numerical methods allows for failure prediction. Despite using a single or combined method approach, verifying the results with alternative references is crucial.

This study aimed to develop and implement a numerical-analytical and experimental approach to characterize the mechanical behavior of fiber-based composite plates with an epoxy matrix. The study considered carbon fiber/epoxy plates with varying numbers of layers and fiber orientations. Four approaches were employed: the first and second approaches, based on the Finite Element Method (FEM) using ANSYS Mechanical Parametric Design Language (Mechanical APDL) and ANSYS WORKBENCH, respectively; the third approach involved analytical results obtained through the MAPLESOFT symbolic computing software; the fourth approach relied on experimental tensile tests of the composite plates, using strain gauges to measure resulting strains from a bi-axial tensile device. Additionally, a three-dimensional static study of a triathlon guide was calculated using Solidworks Simulation FEM software.

The results indicate that while some numerical methods can predict failure in composite materials with reasonable accuracy, this prediction is fundamentally linked to the failure criterion used in the analysis.

Keywords

Fiber based materials;
Composite failure criteria;
User Programmable Feature (UPF).

Nomenclature and abbreviations

Roman Alphabet

E	Young's Modulus	[GPa]
P	Load	[N]
A	Transversal Area	[m^2]
$Pult$	Ultimate Load	[N]
X	Ultimate Stress in x direction	[Pa]
Y	Ultimate Stress in y direction	[Pa]
G	Shear Modulus	[Pa]
V_f	Fiber Volume	[m^3]
A_f	Fiber Area	[m^2]
A_m	Matrix Area	[m^2]
V_m	Matrix Volume	[m^3]
L	Initial Length	[m]
W	Initial Thickness	[m]
u	X displacement	[m]
v	Y displacement	[m]
w	Z displacement	[m]
k	Neutral surface curvatures	[m]
Q	Elastic Stiffness Coefficient	[Pa]
$\overline{Q}$	Transformed Reduced Elastic Stiffness Coefficients	[Pa]
t	Plate Thickness	[m]
N	Resultant Force	[N]
M	Resultant Moment	[N·m]
A	Membrane Stiffness Matrix	[Pa·m]
B	Membrane-Bending Stiffness Matrix	[Pa·m]
D	Bending Stiffness y Matrix	[Pa·m]
I_f	Inverse Failure Index	[-]
R	Strength Index	[-]

Roman Alphabet

F_1t	Ultimate Traction Force in direction 1	[N]
F_2t	Ultimate Traction Force in direction 2	[N]
F_3t	Ultimate Traction Force in direction 3	[N]
F_{12}	Ultimate Shear Force in direction 12	[N]
F_{23}	Ultimate Shear Force in direction 23	[N]
F_{13}	Ultimate Shear Force in direction 13	[N]
F_{1c}	Ultimate Compression Force in direction 1	[N]
F_{2c}	Ultimate Compression Force in direction 2	[N]
F_{3c}	Ultimate Compression Force in direction 3	[N]
h	Layer Thickness	[m]
a	Plate Width	[m]
b	Plate Length	[m]
H_f	Fiber Thickness	[m]
H_m	Matrix Thickness	[m]
H_t	Total Thickness	[m]
$\overline{x}$	Average	[-]
s	Standard deviation	[-]

Greek Alphabet

ϵ	Strain	[-]
σ	Stress	[Pa]
ν	Poisson's coefficient	[-]
τ	Shear Stress	[Pa]
γ	Distortion	[-]
ρ	Mass density	[kg/m^3]
δ_l	Length Variation	[m]
δ_W	Thickness Variation	[m]
β	Rotation	[-]
θ	Angle of rotation	[º]

Abbreviations

APDL	*Ansys Parametric Design Language*
ASTM	*American Society for Testing and Materials*
CFaEM	*Carbon Fiber and Epoxy Matrix*
CLT	*Classical Lamination Theory*
FEM	*Finite Element Method*
FGM	*Functionally Graded Materials*
FGaEM	*Fiber Glass and Epoxy Matrix*
UPF	*User Programmable Feature*
MDF	*Medium Density Fiber*

Contents

List of Figures

List of Tables

Chapter 1

Introduction

1.1 Motivation and Goal

The combination of materials with different mechanical properties plays a vital role in various industries such as mechanical, civil and aerospace. So, the demand for new and innovative materials and composite structures is ever-present. Fiber-based composite materials consist of using fibers, which may be or not, from different materials, and embedding them within adhesives elements, also known as matrices. There are several reasons justifying the growing use of these materials, such as the lower density of the materials used, the need for greater strength of the structure, limited fracture/fatigue occurrences or corrosion-resistant properties which will inevitably affect the cost/performance ratio.

In the present industrial sector, there can be found numerous variants and combinations of composite materials. One example is the particular case of fiber-based composite materials in simple manufacturing procedures, such as plates. With this in mind, the goal of the present document is to study the displacement and inverse failure criteria of plates in the numerical/experimental context, in order to applied the results in the context of more complex geometry.

To study the mechanical failure in composite plates, two different material/fiber orientations were considered for three different loading configurations. The numerical model used in Mechanical APDL for both configurations was obtained through the study proposed by [1], although numerical model studied in ANSYS Workbench was created with the same principles found in the present study. Regarding the analytical model, the present work relied on the MAPLESOFT software, to implement the Classical Lamination Theory (CLT), wherein the concepts of plain stress, transformation coordinate system [2] and load-displacement relations [3] are fundamental. Lastly, the experimental results were obtained by performing a tensile test on the two material configurations.

The two material configurations analyzed, considered the use of: Carbon Fiber and Epoxy Matrix (CFaEM), with the stacking sequence of [0/0/0/0], hereafter named E1; and CFaEM with the stacking sequence of [30/90/-30/60], hereafter named E2. The properties of the materials will be obtained via tensile testing and the plates will be studied for three load configurations (NX, NXY and NY) with five test steps each, incrementally increasing the load value, on both numerical and analytical form, with experimental testing being conducted via bi-axial tensile device to be optimized. Finally, a comparative study will be conducted between the different approaches and conclusions will be accordingly presented. The conclusions will then influence the complex geometry study, in the form of a FEM model of a triathlon handlebar.

1.2 Thesis Structure

The present document is divided into eight chapters, including the introduction. The remainder of this document has the following constitution:

- Chapter II refers to the State of the Art, which begins by describing the CLT, as well as the fundamentals associated with the numerical, analytical and experimental model;
- Chapter III details the design, manufacturing, and subsequent use of the experimental device, as well as the specimens for tensile testing;
- Chapter IV details the presentation of the numerical study using Mechanical APDL and ANSYS Workbench, and the analytical model implemented in Maplesoft;
- Chapter V details the design and results of the triathlon FEM model;
- Chapter VI presents the comparison of the results obtained in Chapter III-IV;
- Chapter VII, presents the conclusions drawn from the analysis of the results presented in previous chapters, as well as the possible future developments.

Chapter 2

State of the Art

2.1 Laminated Composite Plates

Although composite plates can be considered simple within regards to the manufacturing and initial application, there are many industrial applications of these structures, mainly due to the combination of mechanical properties involved, resistance to corrosion of the final product, as well as the overall specific strength and specific elasticity [4] (evidenced in figure 2.1.).As such, the applications of composite plates include aircraft structures, automobile panels and sensors [5], with a continued evolution and growth as an industry standard [6].

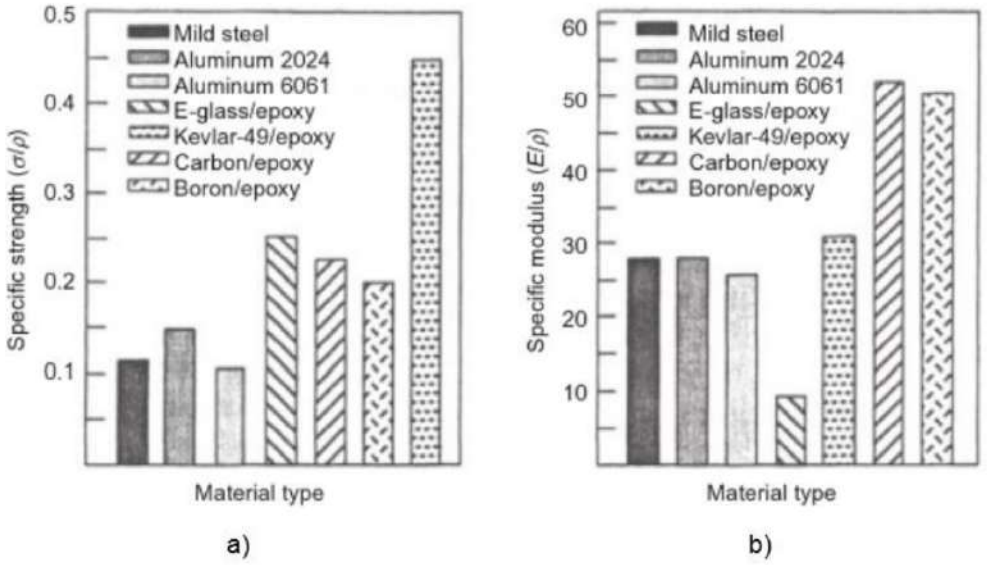

Figure 2.1: Comparison within conventional composite materials of a) Specific strength; b) Specific elasticity [4].

In regard to the materials used in the synthesis of composite plates, these can be divided into two categories: The matrix and the reinforcement, as expanded in figures 2.2 and 2.3.

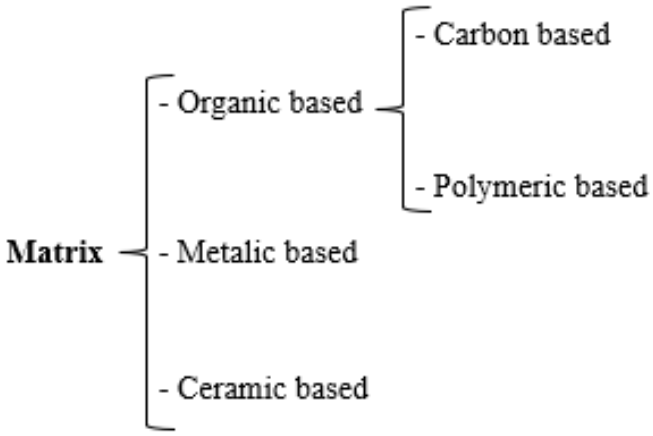

Figure 2.2: Matrix type, based on [7].

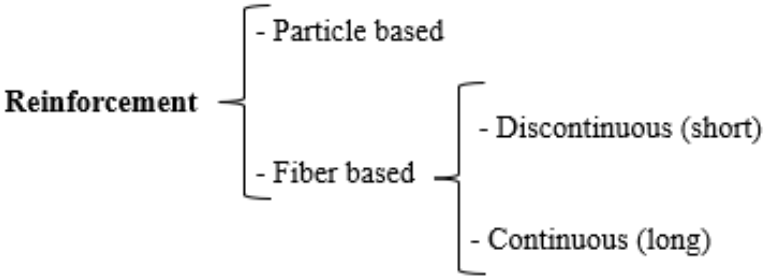

Figure 2.3: Reinforcement type, based on [7].

A laminated composite plate is constituted by stacking layers of long fiber materials, whose orientation regarding the Cartesian coordinate system of the laminated [10] may vary on a layer-by-layer basis (as shown in figure 2.4). Laminated composite plates can be described using the orientation and number of plies in the stacking sequence, following the standard laminated code presented in table 2.1.

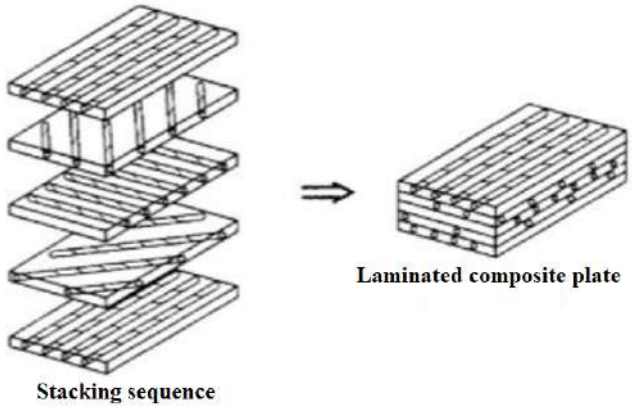

Figure 2.4: Common laminated composite plate formation [10].

Table 2.1: Standard laminated code examples, based on [10],[11].

Laminated types	Example of fiber orientation [°]	Standard laminated code
Quasi-isotropic symmetric	[0/90/+45/-45/-45/-45/+45/90/0]	$[0/90/\pm45]_s$
Crossed symmetric	[0/90/90/0]	$[0/90]_s$
Unidirectional	[0/0/0/0/0/0]	$[0_6]$
Angled symmetric	[+45/-45/-45/+45]	$[\pm45]_s$
Angled anti-symmetric	[+30/-30/+30/-30/+30/-30/+30/-30]	$[\pm30]_4$

2.2 Mechanical Behaviour of Laminated Plates

To better understand the contents of this work, there is a need to explore the mechanical behavior of laminated plates. For this, both the experimental/theoretical and relations must be laid out, at the macroscopic and the microscopic level. Both the experimental and theoretical approaches to the mechanical behavior of laminated need, at the first instance, to be defined at the layer level. As such, the macro and micro mechanic behavior of the different layers can be defined as follows.

2.2.1 Macroscopic mechanics

In regards to the mechanical behaviour at the macroscopic level, the basis for these properties is defined using normalized test patterns. These test patterns are regulated via the American Society for Testing Materials (ASTM), namely the ASTM D 3039/D 3039M [8] and ASTM D 3518/D 3518M [9] standards, which regulates the standard test methods for tensile properties and in-plane response of polymer matrix composite materials.

As such, using the guidelines at ASTM D 3039/D 3039M [8] and performing the necessary tensile testing of unidirectional fiber composites, both in the direction 1 and direction 2, as shown in figure 2.5 and figure 2.6, respectively. With the results of these tests, we can define the relations between both the displacement planar components and the respective traction applied.

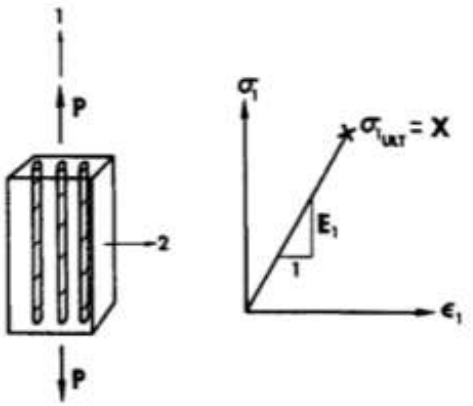

Figure 2.5: Uni-axial load in the direction 1 [10].

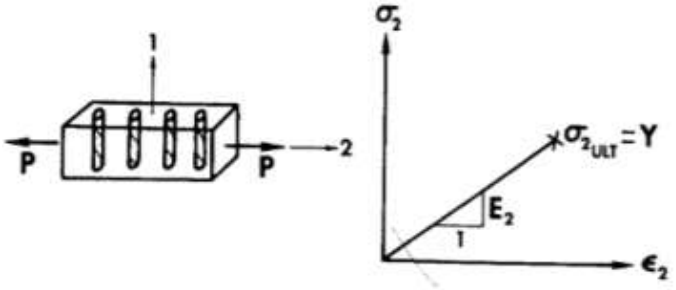

Figure 2.6: Uni-axial load in the direction 2 [10].

In the present analysis, both the deformations ϵ_1 and ϵ_2, for both direction 1 and 2, can be obtained via the relations in equations 2.1 and 2.2. With this, the poisson coefficient υ_{12} can be defined as shown in the equation 2.3.

$$\epsilon_1 = \frac{\sigma_1}{E_1} \tag{2.1}$$

$$\epsilon_2 = -\frac{\upsilon_{12}\sigma_1}{E_1} \tag{2.2}$$

$$\upsilon_{12} = -\frac{\epsilon_2}{\epsilon_1} \tag{2.3}$$

However, given the relation between σ_1 and the transversal area A (equation 2.4) and if the load P is equal to ultimate load P_{ult}, X can be defined as per equation 2.5.

$$\sigma_1 = \frac{P}{A} \tag{2.4}$$

$$X = \frac{P_{ult}}{A} \tag{2.5}$$

Similarly, for the uni-axial load in the direction 2, the deformations ϵ_1 and ϵ_2 are defined via equations 2.6 and 2.7. Both the relations present in equations 2.5 can be applied with σ_2, as shown in equation 2.8, and Y as the ultimate strength in direction 2 (equation 2.9).

$$\epsilon_1 = -\frac{\upsilon_{12}\sigma_2}{E_2} \tag{2.6}$$

$$\epsilon_2 = \frac{\sigma_2}{E_2} \tag{2.7}$$

With both the σ_2, υ_{21} and Y being defined as:

$$\sigma_2 = \frac{P}{A} \tag{2.8}$$

$$Y = \frac{P_{ult}}{A} \tag{2.9}$$

Similarly, using a 45 degree fiber angle specimen in a uni-axial load (figure 2.7), as per the guidelines found in ASTM D 3518/D3039M, the shear modulus can be obtained via the equation found in 2.10.

$$G_{12} = \frac{\tau_{12}}{\gamma_{12}} \tag{2.10}$$

2.2.2 Microscopic mechanics

In regards to the microscopic scale of composite materials, the mechanical aspect seeks to define the relations between the properties of the composite and its components [10]. As such, the Voigt method method for finding the elastic coefficients properties, including the shear modulus method, will be discussed as follows.

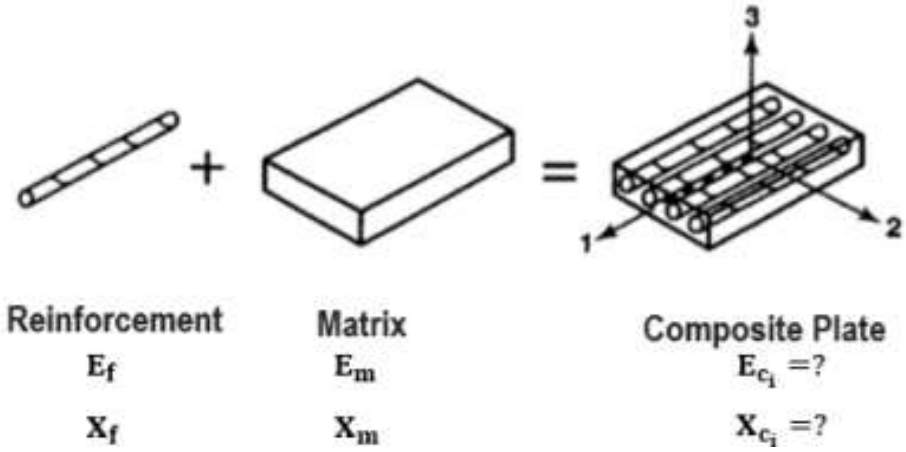

Figure 2.7: Micromechanical key problem [10].

2.2.2.1 Voigt method

The Voigt method refers to the correlations found between the volume of the fiber/matrix and the resultant Young's module of the laminate [12]. As such, the Young modulus E_1 can be obtained through the tensile analysis of a segmented bi-dimensional cell [10]. With this, both the fiber volume fraction V_f and matrix volume fraction V_m can be defined using the equations 2.11 and 2.12, respectively.

$$V_f = \frac{A_f}{A_f + A_m} \tag{2.11}$$

$$V_m = \frac{A_m}{A_f + A_m} \tag{2.12}$$

Thus, under the tensile testing represented in figure 2.8, the cell will deform axially, where this deformation is represented by the index Δl. By assuming that the deformed area is sufficiently further away from the point of the force's application, the extension suffered by the matrix is equal to the fiber [10], thus producing the relation found in equation 2.13.

$$\epsilon_{f1} = \epsilon_{m1} = \epsilon_1 \frac{\Delta l}{L} \tag{2.13}$$

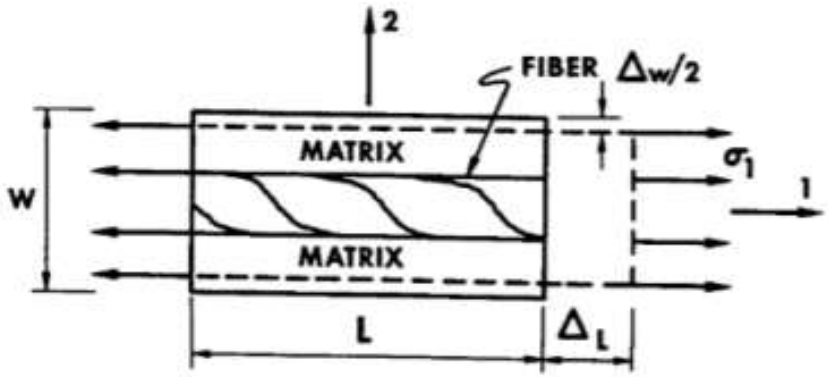

Figure 2.8: Elemental cell under strength test [10].

With the total force applied to the elemental cell being separated between the matrix and fiber components (as evidenced by equation 2.14), as well as the known relations between the stress σ_1, the Young Modulus E_1 and the extension ϵ_1 (shown in equation 2.15), one can separate the stress present in the fibers σ_{f1} and the stress in the matrix σ_{m1} as two different relations, The relations in question can be found in equation 2.16 and equation 2.17 for the stress in the fibers and the stress in the matrix, respectively.

$$\sigma_1(A_f + A_m) = \sigma_{f1f} + \sigma_{m1} \cdot A_m \tag{2.14}$$

$$\sigma_1 = E_1 \cdot \epsilon_1 \tag{2.15}$$

$$\sigma_{f1} = E_f \cdot \epsilon_{f1} \tag{2.16}$$

$$\sigma_{m1} = E_m \cdot \epsilon_{m1} \tag{2.17}$$

By resolving the previous equations in order of E_1, the Rule of Mixtures is obtained:

$$E_1 = E_f \cdot V_f + E_m \cdot V_m \tag{2.18}$$

In regard to the calculation of the Poisson coefficient, both the fiber and matrix longitudinal extensions are considered equal and are directly correlated with the overall longitudinal extension [10]. Both these relations, as well as transversal extension relations, are shown as follows:

$$\Delta W = W_f \cdot \epsilon_{f2} + W_m \cdot \epsilon_{m2} \tag{2.19}$$

In which, similar to equations 2.15 through 2.17, the relations between the fiber extension ϵ_{f2} and the matrix extension ϵ_{m2} can be considered as separate relations [10], as shown in equations 2.20 to 2.22.

$$\epsilon_2 = -\nu_{21} \cdot \epsilon_1 \tag{2.20}$$

$$\epsilon_{f2} = -\nu_f \cdot \epsilon_1 \tag{2.21}$$

$$\epsilon_{m2} = -\nu_m \cdot \epsilon_1 \tag{2.22}$$

Replacing both equations and solving for ν_{12}, the Poisson coefficient is defined as follows:

$$\epsilon_2 = \frac{\Delta W}{w} \tag{2.23}$$

$$\epsilon_2 = V_f \cdot \epsilon_{f2} + V_m \cdot \epsilon_{m2} \tag{2.24}$$

$$\nu_{12} = V_f \cdot \nu_f + (1 - V_f) \cdot \nu_m \tag{2.25}$$

2.2.2.2 Shear Modulus

The value of the shear modulus can be obtained via the shear test in figure 2.9. As with the Voigt and Reuss Method, the shear stress presented by the fibers is equal in value and direction to the shear tension in the matrix [10]. The total deformation cause by shear tension $\triangle$ can be defined via the equation 2.26.

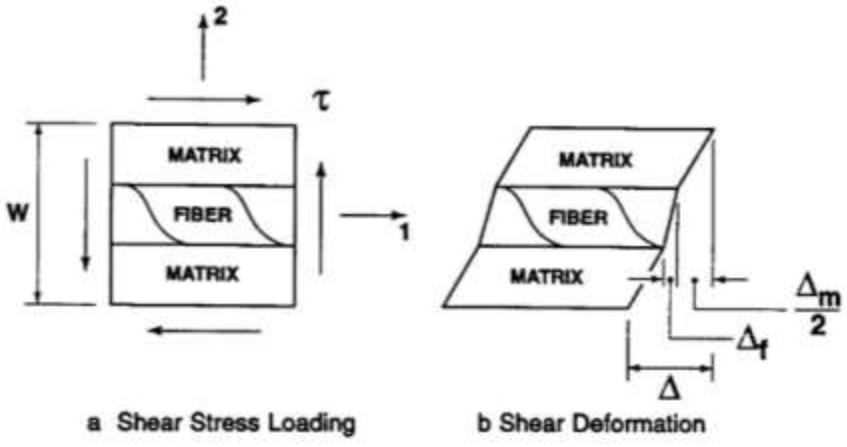

Figure 2.9: Elemental cell under shear tension test [10].

$$\Delta = \gamma \cdot W = \gamma_{f12} \cdot W_f + \gamma_{m12} \cdot W_{m12} \tag{2.26}$$

With the relation of the total deformation caused by the shear tension and the same principal of separation of fiber and matrix properties found previously, the shear deformations are described as follows:

$$\gamma_{12} = \frac{\tau_{12}}{G_{12}} \tag{2.27}$$

Replacing both expressions, the longitudinal shear modulus is defined as:

$$G_{12} = \frac{G_{f12} \cdot G_m}{G_{f12} \cdot V_m + G_m \cdot V_f} \tag{2.28}$$

2.2.3 Classic Lamination Theory

The Classical Lamination Theory is an extension of the Classical Plate Theory, with Kirchhoff's assumptions as a basis [2]. In it, their domain falls in the following assumptions:

- The laminate is an approximately thin rectangular plate, in which the thickness h is much reduced compared to the other plate dimensions;

- The perpendicular sections to the plate plane (such as a (x,y) plane), remain unaltered after the loading has occurred. This implies that the transverse shear strains are null (both in the yxz and yyz directions);

- It is assumed that the thickness h is constant throughout the length of the plate and that the normal sections to the plane of the plate are not extensible;

- The normal stress σ_z is reduced when compared to the other stress components and as such, can be neglected.

Regarding the Kirchhoff's hypothesis, the displacements u, v and w of the laminate in the xy plane and z direction are derived from the transversal deformation of the laminate (figure 2.10). In this case, the B displacement in the x direction of the neutral surface is transcribed into u_0, meaning that the $_0$ index will be used to define the possible points within the neutral surface.

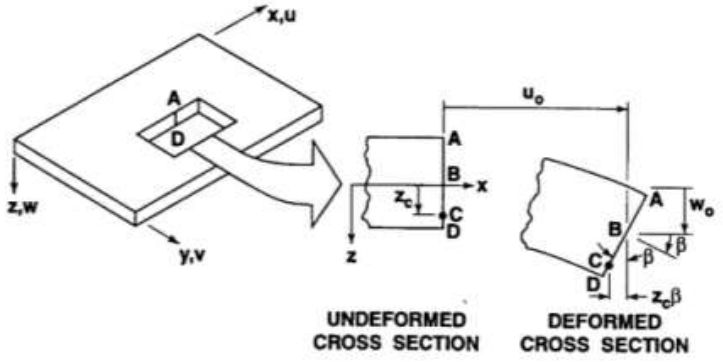

Figure 2.10: Deformation in the xz plane [10].

It's also worth noting that the perpendicular line to the neutral surface ($ABCD$) is unchanged after the plate suffers deformation. With this, the displacement of the C point and the neutral surface rotation of β can be described in equations 2.29 and 2.30, respectively.

$$u_c = u_0 - z_c \cdot \beta \tag{2.29}$$

$$\beta = \frac{dw}{dx} \tag{2.30}$$

Accordingly, any z point on the plate surface has a u and v displacement derived from the rotation β as such:

$$u = u_0 - z \cdot \frac{dw_0}{dx} \tag{2.31}$$

$$v = v_0 - z \cdot \frac{dw_0}{dy} \tag{2.32}$$

As such, through the Kirchhoff's assumptions, the deformations on the laminate are ϵ_x, ϵ_y and $\gamma_x y$ (in which ϵ_z = $\gamma_x z$ = $\gamma_y z$ = 0):

$$\epsilon = \begin{bmatrix} \epsilon_x \\ \epsilon_y \\ \gamma_{xy} \end{bmatrix} = \begin{bmatrix} \frac{du}{x} \\ \frac{dv}{dy} \\ \frac{du}{y} + \frac{dv}{dx} \end{bmatrix} \tag{2.33}$$

Thus, considering the displacement field and the kinematical relations of Elasticity for small deformations, one obtains for the deformations in CLT:

$$\begin{bmatrix} \epsilon_x \\ \epsilon_y \\ \gamma_{xy} \end{bmatrix} = \begin{bmatrix} \epsilon_{x0} \\ \epsilon_{y0} \\ \gamma_{xy0} \end{bmatrix} + z \cdot \begin{bmatrix} \mathrm{k}_x \\ \mathrm{k}_y \\ \mathrm{k}_{xy} \end{bmatrix} \tag{2.34}$$

In which k represents the neutral surface curvatures:

$$k = \begin{bmatrix} k_x \\ k_y \\ k_x y \end{bmatrix} = - \begin{bmatrix} \frac{d^2 w0}{dx^2} \\ \frac{d^2 w0}{dy^2} \\ 2\frac{d^2 w0}{dxdy} \end{bmatrix} \tag{2.35}$$

Given the previous 2 dimension stress status (σ_3=σ_4=σ_5=0), constitutive relations of the laminate can be defined as follows [2]:

$$\begin{bmatrix} \sigma_1 \\ \sigma_2 \\ \tau_{12} \end{bmatrix} = \begin{bmatrix} Q_{11} & Q_{12} & 0 \\ Q_{12} & Q_{22} & 0 \\ 0 & 0 & Q_{66} \end{bmatrix} \cdot \begin{bmatrix} \epsilon_1 \\ \epsilon_2 \\ \gamma_{12} \end{bmatrix} \tag{2.36}$$

In which the reduced elastic stiffness coefficients Q with different indexes are defined as:

$$Q_{11} = \frac{E_1}{1 - \nu_{12} \cdot \nu_{21}} \tag{2.37}$$

$$Q_{12} = \frac{\nu_{12} \cdot E_2}{1 - \nu_{12} \cdot \nu_{21}} = \frac{\nu_{12} \cdot E_1}{1 - \nu_{12} \cdot \nu_{21}} \tag{2.38}$$

$$Q_{22} = \frac{E_2}{1 - \nu_{12} \cdot \nu_{21}} \tag{2.39}$$

$$Q_{66} = G_{12} \tag{2.40}$$

Regarding the transformation of stress status in another cartesian coordinate system, such as the one associated to each fiber direction, the transformation matrix can be applied (equation 2.41) [2].

$$\begin{bmatrix} \sigma_x \\ \sigma_y \\ \sigma_z \\ \sigma_{yz} \\ \sigma_{xz} \\ \sigma_{xy} \end{bmatrix} = \begin{bmatrix} \mathrm{c}^2 & \mathrm{s}^2 & 0 & 0 & 0 & -2\mathrm{cs} \\ \mathrm{s}^2 & \mathrm{c}^2 & 0 & 0 & 0 & 2\mathrm{cs} \\ 0 & 0 & 1 & 0 & 0 & 0 \\ 0 & 0 & 0 & \mathrm{c} & \mathrm{s} & 0 \\ 0 & 0 & 0 & -\mathrm{s} & \mathrm{c} & 0 \\ \mathrm{cs} & -\mathrm{cs} & 0 & 0 & 0 & \mathrm{c}^2 - s^2 \end{bmatrix} = \begin{bmatrix} \sigma_1 \\ \sigma_2 \\ \sigma_3 \\ \sigma_4 \\ \sigma_5 \\ \sigma_6 \end{bmatrix} \tag{2.41}$$

With the coefficients c, s and $2cs$ being derived from the trignometry of the angle of rotation θ:

$$c = cos(\theta) \tag{2.42}$$

$$s = sin(\theta) \tag{2.43}$$

$$2cs = sin(2\theta) \tag{2.44}$$

After the application of the transformation matrix, the constitutive relations of the laminate present themselves as follows:

$$\begin{bmatrix} \sigma_{xx} \\ \sigma_{yy} \\ \sigma_{xy} \end{bmatrix} = \begin{bmatrix} \overline{Q_{11}} & \overline{Q_{12}} & \overline{Q_{16}} \\ \overline{Q_{12}} & \overline{Q_{22}} & \overline{Q_{26}} \\ \overline{Q_{16}} & \overline{Q_{26}} & \overline{Q_{66}} \end{bmatrix} \cdot \begin{bmatrix} \epsilon_{xx} \\ \epsilon_{yy} \\ \gamma_{xy} \end{bmatrix} \tag{2.45}$$

with the transformed reduced elastic stiffness coefficients $\overline{Q}$ with different indexes given as:

$$\overline{Q_{11}} = Q_{11} \cdot cos(\theta)^4 + 2 \cdot (Q_{12} + 2 \cdot Q_{66}) \cdot sin(\theta)^2 \cdot cos(\theta)^2 + Q_{22} \cdot sin(\theta)^4 \tag{2.46}$$

$$\overline{Q_{12}} = (Q_{11} + Q_{22} - 4 \cdot Q_{66}) \cdot sin(\theta)^2 \cdot cos(\theta)^2 + Q_{12} \cdot (sin(\theta)^4 + cos(\theta)^4) \tag{2.47}$$

$$\overline{Q_{22}} = Q_{11} \cdot sin(\theta)^4 + 2 \cdot (Q_{12} + 2 \cdot Q_{66}) \cdot sin(\theta)^2 \cdot cos(\theta)^2 + Q_{22} \cdot cos(\theta)^4 \tag{2.48}$$

$$\overline{Q_{16}} = (Q_{11} - Q_{12} - 2 \cdot Q_{66}) \cdot sin(\theta) \cdot cos(\theta)^3 + (Q_{12} - Q_{22} + 2 \cdot Q_{66}) \cdot sin(\theta)^3 \cdot cos(\theta) \tag{2.49}$$

$$\overline{Q_{26}} = (Q_{11} - Q_{12} - 2 \cdot Q_{66}) \cdot sin(\theta)^3 \cdot cos(\theta) + (Q_{12} - Q_{22} + 2 \cdot Q_{66}) \cdot sin(\theta) \cdot cos(\theta)^3 \tag{2.50}$$

$$\overline{Q_{66}} = (Q_{11} + Q_{22} - 2 \cdot Q_{12} - 2 \cdot Q_{66}) \cdot sin(\theta)^2 \cdot cos(\theta)^2 + Q_{66} \cdot (sin(\theta)^4 \cdot cos(\theta)^4) \tag{2.51}$$

2.2.4 In-plane force and moment resultants

Assuming the disposition of in-plane forces and moment as per figure 2.11, the in-plane force and moment resultants associated to the stress state of the laminate, is obtained by integrating the stresses σ_x, σ_y and σ_{xy} through the laminate thickness t.

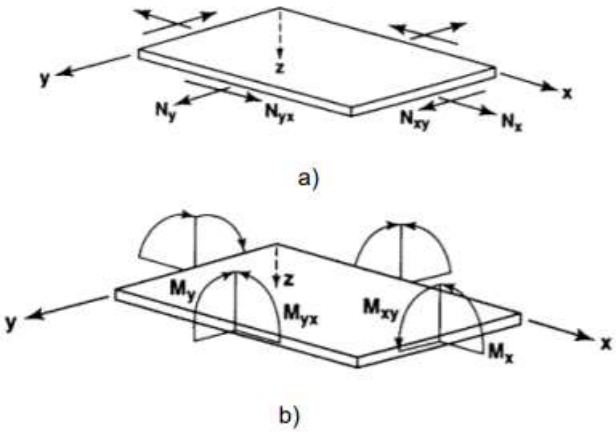

Figure 2.11: In-plate force (a) and moment (b) [10].

$$\begin{bmatrix} N_x \\ N_y \\ N_{xy} \end{bmatrix} = \int_{-t/2}^{t/2} \begin{bmatrix} \sigma_x \\ \sigma_y \\ \sigma_{xy} \end{bmatrix} dz = \sum_{k=1}^{n} \int_{z_x}^{z_{x+1}} \begin{bmatrix} \sigma_x \\ \sigma_y \\ \sigma_{xy} \end{bmatrix} dz \tag{2.52}$$

$$\begin{bmatrix} M_x \\ M_y \\ M_{xy} \end{bmatrix} = \int_{-t/2}^{t/2} \begin{bmatrix} \sigma_x \\ \sigma_y \\ \sigma_{xy} \end{bmatrix} \cdot z dz = \sum_{k=1}^{n} \int_{z_x}^{z_{x+1}} \begin{bmatrix} \sigma_x \\ \sigma_y \\ \sigma_{xy} \end{bmatrix} \cdot z dz \tag{2.53}$$

As such, the in-plane force and moment resultants (per unit of length) are calculated layer by layer z_k (shown in figure 2.12).

Thus, replacing the previous equation with equation 2.34, the fundamental equation of CLT are as follows:

$$\begin{bmatrix} N_x \\ N_y \\ N_{xy} \end{bmatrix} = \sum_{k=1}^{n} \int_{z_x}^{z_{x+1}} \begin{bmatrix} \sigma_x \\ \sigma_y \\ \sigma_{xy} \end{bmatrix} dz = \sum_{k=1}^{n} \int_{z_x}^{z_{x+1}} \begin{bmatrix} \overline{Q_{11}} & \overline{Q_{12}} & \overline{Q_{16}} \\ \overline{Q_{12}} & \overline{Q_{22}} & \overline{Q_{26}} \\ \overline{Q_{16}} & \overline{Q_{26}} & \overline{Q_{66}} \end{bmatrix}^k \cdot \begin{bmatrix} zk_x \\ zk_y \\ \gamma_{xy} \end{bmatrix} dz \tag{2.54}$$

and for the moment:

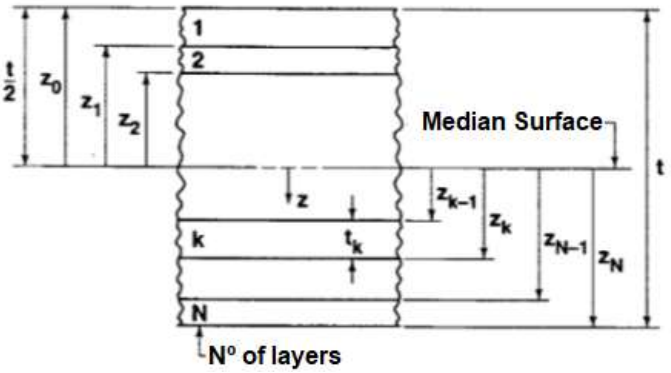

Figure 2.12: Geometry of N layer laminate [10].

$$\begin{bmatrix} M_x \\ M_y \\ M_{xy} \end{bmatrix} = \sum_{k=1}^{n} \int_{z_x}^{z_{x+1}} \begin{bmatrix} \sigma_x \\ \sigma_y \\ \sigma_{xy} \end{bmatrix} \cdot z \, dz = \sum_{k=1}^{n} \int_{z_x}^{z_{x+1}} \begin{bmatrix} \overline{Q_{11}} & \overline{Q_{12}} & \overline{Q_{16}} \\ \overline{Q_{12}} & \overline{Q_{22}} & \overline{Q_{26}} \\ \overline{Q_{16}} & \overline{Q_{26}} & \overline{Q_{66}} \end{bmatrix}^{k} \cdot \begin{bmatrix} zk_x \\ zk_y \\ \gamma_{xy} \end{bmatrix} \cdot z \, dz \tag{2.55}$$

The matrices A_{ij}, B_{ij} and D_{ij} (responsible for the membrane stiffness, membrane-bending and bending stiffness respectively) are defined via the equation 2.56, equation 2.57 and equation 2.58, respectively.

$$A_{ij} = \sum_{k=1}^{n} \overline{Q_{ij}}^{k} \cdot (z_k - z_{k-1}) \tag{2.56}$$

$$B_{ij} = \frac{1}{2} \cdot \sum_{k=1}^{n} \overline{Q_{ij}}^{k} \cdot (z_k^2 - z_{k-1}^2) \tag{2.57}$$

$$D_{ij} = \frac{1}{3} \cdot \sum_{k=1}^{n} \overline{Q_{ij}}^{k} \cdot (z_k^3 - z_{k-1}^3) \tag{2.58}$$

As such, by replacing the former relations we get the CLT equations that can be found in equations 2.59 and 2.60.

$$\begin{bmatrix} N_x \\ N_y \\ N_{xy} \end{bmatrix} = \begin{bmatrix} A_{11} & A_{12} & A_{16} \\ A_{12} & A_{22} & A_{26} \\ A_{16} & A_{26} & A_{66} \end{bmatrix} \cdot \begin{bmatrix} \epsilon_x \\ \epsilon_y \\ \gamma_{xy} \end{bmatrix} + \begin{bmatrix} B_{11} & B_{12} & B_{16} \\ B_{12} & B_{22} & B_{26} \\ B_{16} & B_{26} & B_{66} \end{bmatrix} \cdot \begin{bmatrix} k_x \\ k_y \\ k_{xy} \end{bmatrix} \tag{2.59}$$

$$\begin{bmatrix} M_x \\ M_y \\ M_{xy} \end{bmatrix} = \begin{bmatrix} B_{11} & B_{12} & B_{16} \\ B_{12} & B_{22} & B_{26} \\ B_{16} & B_{26} & B_{66} \end{bmatrix} \cdot \begin{bmatrix} \epsilon_x \\ \epsilon_y \\ \gamma_{xy} \end{bmatrix} + \begin{bmatrix} D_{11} & D_{12} & D_{16} \\ D_{12} & D_{22} & D_{26} \\ D_{16} & D_{26} & D_{66} \end{bmatrix} \cdot \begin{bmatrix} k_x \\ k_y \\ k_{xy} \end{bmatrix} \tag{2.60}$$

2.3 Failure Criteria

Failure criteria allow for the characterization of stress, present when the failure occurs. In this case, though the relation between the stress provided by the loading σ_L and the rupture strength σ_R, the failure index is defined [12]. In this case, if $I_f \geq 1$ then failure will always occur.

$$I_f = \frac{\sigma_L}{\sigma_R} \tag{2.61}$$

2.3.1 Maximum Stress Criteria

The Maximum Stress Criteria refers to the non-interactive (there is no interaction between the stress components) failure criteria based on the maximum stress applied [12]. In it, the failure occurs when one of the stress components is equal to the rupture stress of the subject [17]:

$$I_f = max \left\{ \begin{array}{llllll} \frac{\sigma_1}{F_{1t}} & if & \sigma_1 > 0 & or & -\frac{\sigma_1}{F_{1c}} & if \quad \sigma_1 < 0 \\ \frac{\sigma_2}{F_{2t}} & if & \sigma_2 > 0 & or & -\frac{\sigma_2}{F_{2c}} & if \quad \sigma_2 < 0 \\ \frac{\sigma_3}{F_{3t}} & if & \sigma_3 > 0 & or & -\frac{\sigma_3}{F_{3c}} & if \quad \sigma_3 < 0 \\ |\frac{\sigma_{12}}{F_{12}}| & & & & & \\ |\frac{\sigma_{23}}{F_{23}}| & & & & & \\ |\frac{\sigma_{13}}{F_{13}}| & & & & & \end{array} \right\} \tag{2.62}$$

2.3.2 Tsai-Hill Criteria

The Tsai-Hill failure criteria is a quadratic and interactive criterion, based on the tension that identifies failure [17]:

$$\begin{aligned} I_f = (G_2 + G_3) \cdot \sigma_1^2 + (G_1 + G_3) \cdot \sigma_2^2 + (G_1 + G_2) \cdot \sigma_3^2 \\ -2G_3\sigma_1\sigma_2 - 2G_2\sigma_1\sigma_3 - 2G_1\sigma_2\sigma_3 + 2G_4\tau_{23}^2 + 2G_5\tau_{13}^2 + 2G_6\tau_{12}^2 \end{aligned} \tag{2.63}$$

In which the coefficients $G1$, $G2$ and $G6$ can be defined as:

$$G_1 = \frac{1}{2}\left(\frac{2}{F_{2T}^2} - \frac{1}{F_{1T}^2}\right) \tag{2.64}$$

$$G_2 = \frac{1}{2}\left(\frac{1}{F_{1T}^2}\right) = G_3 \tag{2.65}$$

$$G_6 = \frac{1}{2}\left(\frac{1}{F6^2}\right) \tag{2.66}$$

2.3.3 Tsai-Wu Criteria

The Tsai-Wu Criteria is defined as follows, with c_{12}, c_{23} and c_{13} as the coupling Tsai-Wu coefficients, being -1 [17].

$$I_f = \left[-\frac{B}{2A} + \sqrt{(\frac{B}{2A})^2} + \frac{1}{A} \right]^{-1} \tag{2.67}$$

In which A and B are defined as:

$$A = \frac{\sigma_1^2}{F_{1t} \cdot F_{1c}} + \frac{(\sigma_2)^2}{F_{2t} \cdot F_{2c}} + \frac{(\sigma_3)^2}{F_{3t} \cdot F_{3c}} + \frac{(\sigma_{12})^2}{F_{12}^2} + \frac{(\sigma_{23})^2}{F_{23}^2} + \frac{(\sigma_{13})^2}{F_{12}^2}$$
$$+c_{12} \cdot \frac{(\sigma_1 \sigma_2)}{\sqrt{(F_{1t} \cdot F_{1c} \cdot F_{2t} \cdot F_{2c})}} + c_{23} \cdot \frac{(\sigma_2 \sigma_3)}{\sqrt{(F_{2t} \cdot F_{2c} \cdot F_{3t} \cdot F_{3c})}} + c_{13} \cdot \frac{(\sigma_1 \sigma_3)}{\sqrt{(F_{1t} \cdot F_{1c} \cdot F_{3t} \cdot F_{3c})}} \tag{2.68}$$

$$B = (F_{1_t}^{-1} - F_{1_c}^{-1}) \cdot \sigma_1 + (F_{2_t}^{-1} - F_{2_c}^{-1}) \cdot \sigma_2 + (F_{3_t}^{-1} - F_{3_c}^{-1}) \cdot \sigma_3 \tag{2.69}$$

2.3.4 Hashin-Rotem Criteria

The Hashin-Rotem criterion is partially interactive and is focused on compromising the fiber and matrix rupture points, being divided into those two failure modes [12]. In terms of the failure of the fiber, it can be defined as:

$$-F_{1c} < \sigma_1 < F_{1t} \tag{2.70}$$

The failure criteria of the matrix, which is assumed to be parallel to the fibers, can be defined as:

$$\left(\frac{\sigma_2}{F_2}\right)^2 + \left(\frac{\sigma_6}{F_6}\right)^2 = 1 \tag{2.71}$$

In which F_1 and F_2 can be defined as follows:

$$\left\{ \begin{array}{llll} F_1 = F_{1t} & if & \sigma_1 > 0 \\ F_1 = F_{1c} & if & \sigma_1 < 0 \\ F_2 = F_{2t} & if & \sigma_2 > 0 \\ F_2 = F_{2c} & if & \sigma_2 < 0 \end{array} \right\} \tag{2.72}$$

However, the criteria only allow for the prediction of failure in their respective fields (i.e. only in the matrix and in the fiber), neglecting the possibility of the matrix-fiber interface failure mode [18]. As such, the Hashin 2D criteria is established as:

- Fiber fracture in traction ($\sigma_1 \geq 0$) :

$$\left(\frac{\sigma_1}{F_{1t}}\right)^2 + \left(\frac{\sigma_6}{F_{6t}}\right)^2 = 1 \tag{2.73}$$

- Fiber fracture in compression ($\sigma_1 < 0$):

$$|\sigma_1| = F_{1c} \tag{2.74}$$

- Matrix fracture in traction ($\sigma_2 \geq 0$) :

$$\left(\frac{\sigma_2}{F_{2t}}\right)^2 + \left(\frac{\sigma_6}{F_{6t}}\right)^2 = 1 \tag{2.75}$$

- Matrix fracture in compression ($\sigma_2 < 0$):

$$\left(\frac{\sigma_2}{2F_4}\right)^2 + \left[\left(\frac{F_{2c}}{2F_4}\right)^2 - 1\right] \cdot \frac{\sigma_2}{F_{2c}} + \left(\frac{\sigma_6}{F_6}\right)^2 = 1 \tag{2.76}$$

2.4 Bi-axial tensile testing device

Given the nature of the testing device, there needs to be a concern in regards to the boundary conditions and freedom degrees permitted [13]. As such, there is a need to cut the specimens to be tested (as per figure 2.13), in order to analyze the strain in the different directions [13]. The placement of the strain gauges must also be in the middle of the crucible, in order to more accurately measure the strain in each direction [13].

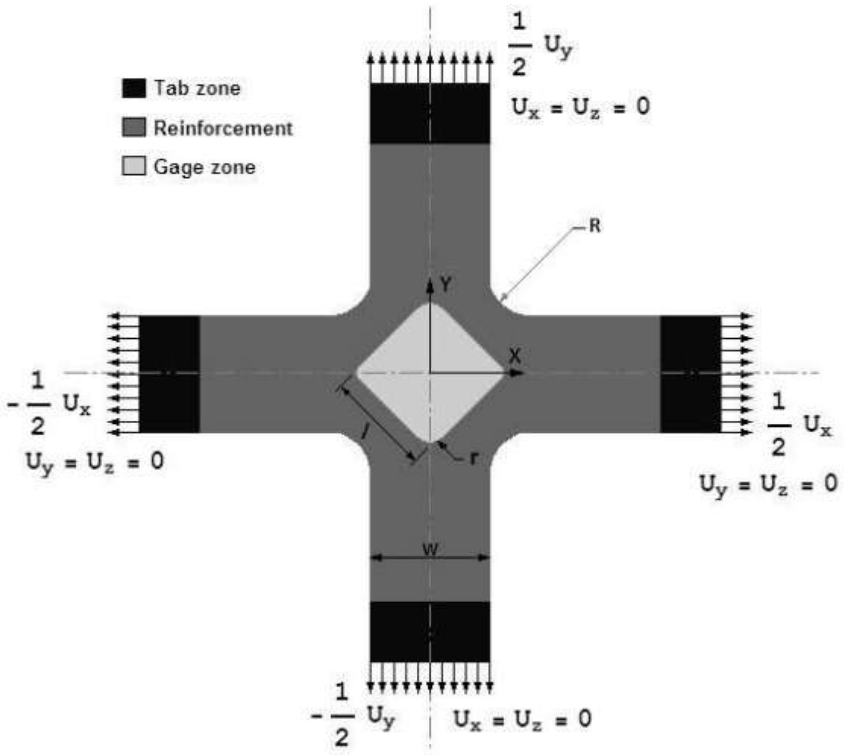

Figure 2.13: Crucible like specimen [13].

However, the clamping sub-assemblies are required to minimize the appearance of improper reactions [15] to be installed on rails [10]. With this, the design of the clamping subassembly should resemble the one found in figure 2.14. In the present thesis, however, the specimens are to be pulled via cables and pulleys with calibrated weights.

Figure 2.14: Clamping assembly example [15].

There is also a need to validate and improve the parameters obtained [14]. Such optimization process can be achieved utilized the example given in figure 2.15, with a numerical study running in parallel with the experimentation process.

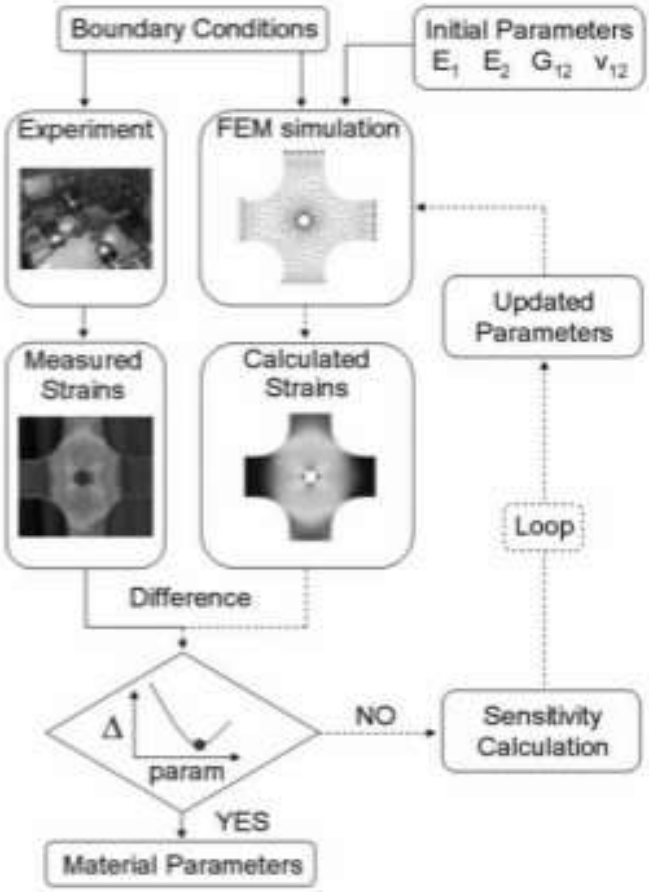

Figure 2.15: Optimization example [14].

Chapter 3

Experimental program

The present chapter has the purpose of exposing the procedures considered to perform the different studies. Beginning with the properties of the selected fiber and matrix, as well as the specimen manufacturing and the proof of concept of the bi-axial tensile device.

3.1 Specimen manufacturing

The mechanical properties of the material used to fabricate the two different case studies (E1 and E2), with different compositions and load configurations, were obtained via tensile testing [8], [9]. As such, the specimens for the tensile testing were manufactured using the wet-hand layup technique (figure 3.1), followed by a vacuum cure for 4 hours (figure 3.2). This process entails the fiber impregnation manually, using peel-ply, absorbent sponge sheets and plastic film in that order. Due to the nature of this process, the probability of premature curing of the matrix is high, making it a hasty but delicate procedure.

Figure 3.1: Wet hand layup process.

Figure 3.2: Vacuum bag curing process.

The 90 and 45 degree specimens were made under the same vacuum seal, whereas the 0 degree specimen was made a standalone one, as shown in figure 3.3.The same specimens were cut in accordance with [8] and [9], with the measurements shown in table 3.1. However, due to miscalculation in the cutting procedure, two of the specimens were not in the specifications. As such, only three specimens were considered for each stacking sequence.

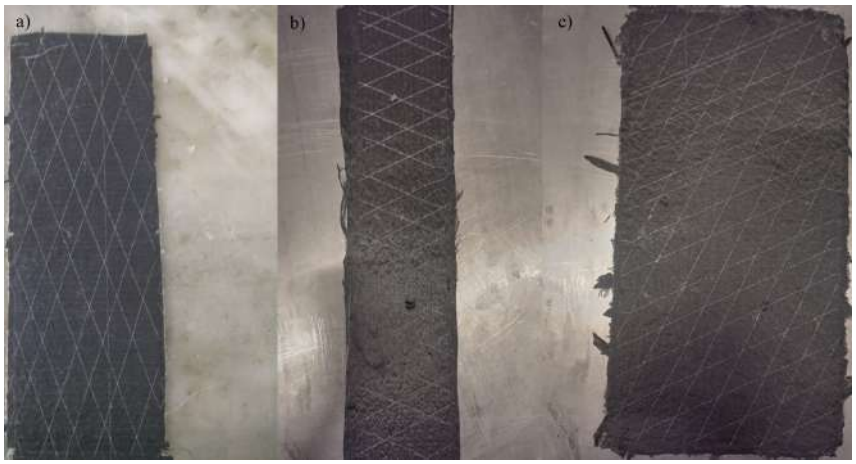

Figure 3.3: Specimens for tensile testing [8], [9]: a) 0 degree; b) 90 degree ; c) 45 degree.

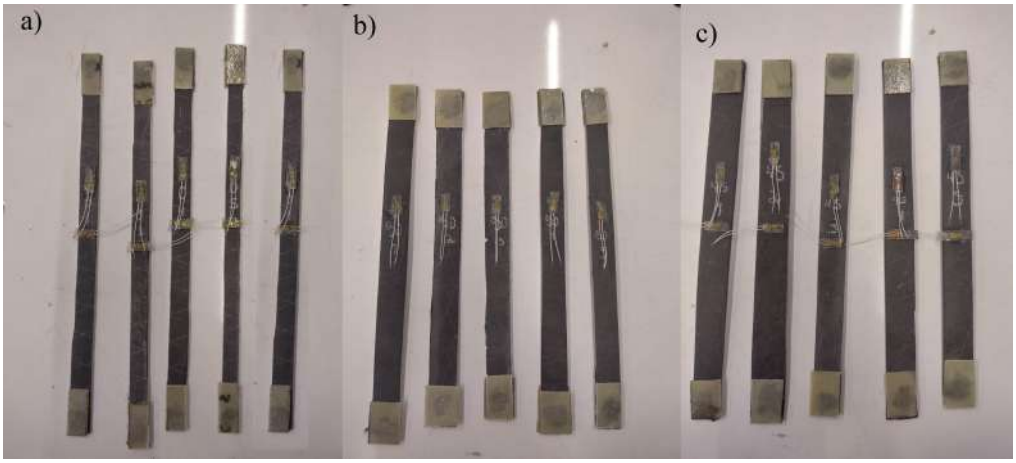

Figure 3.4: Specimens for tensile testing with strain gauges: a) 0 degree; b) 90 degree; c) 45 degree.

Table 3.1: Dimensions of specimens.

Type of Specimens	Specimen Nº	Nº of layers	Thickness [mm]	Height [mm]	Width [mm]
90 degree specimens- Transversal direction	1	4	1,20	312,00	14,80
	2	4	1,10	315,00	15,20
	3	4	1,30	313,00	14,40
0 degree specimens- Longitudinal direction	4	4	1,10	311,00	25,20
	5	4	1,20	315,00	24,60
	6	4	1,40	314,00	24,70
±45 degree specimens	7	4	1,20	314,00	25,80
	8	4	1,10	315,00	24,40
	9	4	1,10	314,00	25,20

3.2 Instrumentation and data acquisition

The specimens were wired with the 1-CLY41-6/120ZE strain gauges and CA80 glue (figure 3.4). After this, the strain gauges where soldered to wire and connected to the amplifier/wheatstone bridge [25] interface as per the figures 3.5, 3.6 and 3.7.

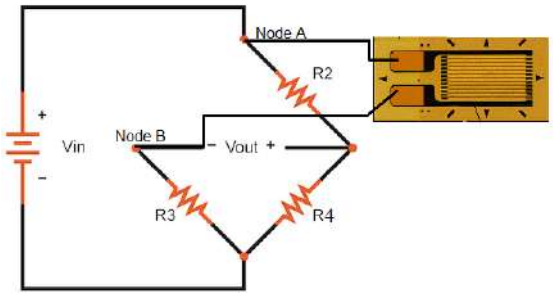

Figure 3.5: Wheatstone bridge diagram, adapted from [25].

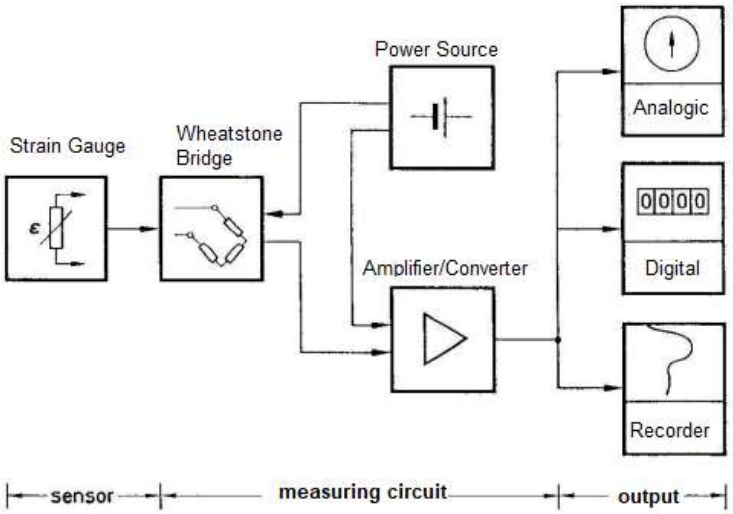

Figure 3.6: Data gathering circuit, adapted from [26].

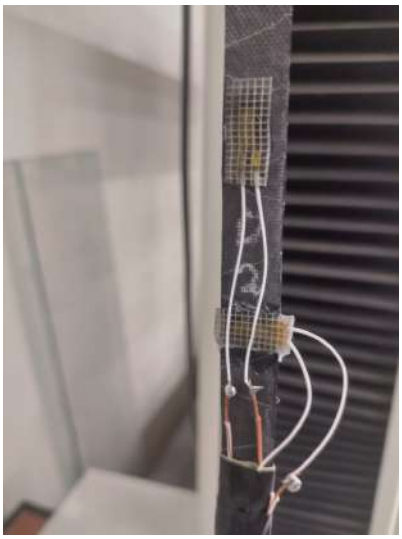

Figure 3.7: Specimen with strain gauge wired.

In the present case, the measuring circuit is composed by the ”Spider 8” interface (figure 3.8) and it’s subsequent data output is acquired via the ”Catman Easy” (figure 3.9). All the technical data of the instrumentation process can be found in Annex B.

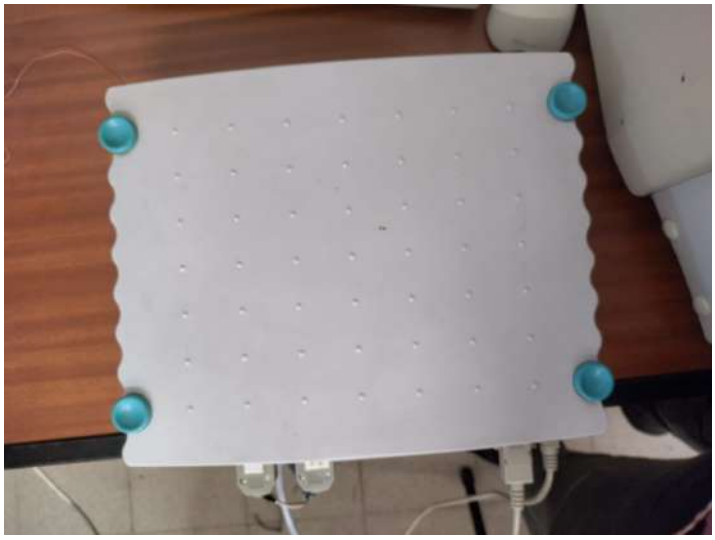

Figure 3.8: Spider 8 interface utilized.

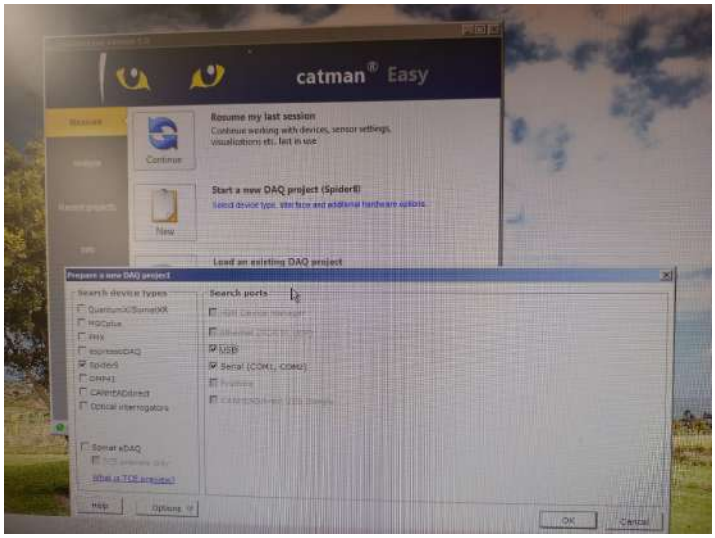

Figure 3.9: Data output acquisition software utilized.

3.3 Repeatability of results

As with every experimental procedure, errors will arise, whether it be random or systematic. The random error has is related with the accuracy of the device and/or conditions of testing and can only be mitigated. In regards to the systematic error, it has its roots on human intervention and can be related to the reading phase or the calibration of the equipment. As such, the average $\bar{x}$ and standard deviation s must be calculated to evaluate the accuracy of the results.

$$\bar{x} = \frac{\sum_i x_i}{n} \tag{3.1}$$

$$s = \sqrt{\frac{\sum_i (x_i - \bar{x})^2}{n-1}} \tag{3.2}$$

3.4 Tensile test of 90 degree specimens

With the specimens ready for testing, they were put in the tensile machine (figure 3.10), the data acquisition was setup and the test steps were defined [24].

Figure 3.10: Tensile testing setup used.

The 90 degree specimens were subjected to five test steps, from 0 to 500 N producing the material strains and machine displacement shown in table 3.2 to 3.4.

Table 3.2: Results in 90 degree for specimen 1.

Transversal Young's Modulus (E2)- specimen 1			**Section Area [m^2]= 3,91E-05**
F [N]	**Material Strain [10^-3]**	**Machine Displacement [mm]**	**Stress [MPa]**
0	0,00	0,00	0,00
100	0,50	0,17	2,56
200	1,00	0,34	5,12
300	1,50	0,50	7,68
400	1,99	0,67	10,24
500	2,49	0,85	12,80

Table 3.3: Results in 0 degree for specimen 2.

Transversal Young's Modulus (E2)- specimen 2			Section Area [m^2]= 4,03E-05
F [N]	**Material Strain [10^-3]**	**Machine Displacement [mm]**	**Stress [MPa]**
0	0,00	0,00	0,00
100	0,63	0,17	2,48
200	1,16	0,33	4,96
300	1,70	0,50	7,44
400	2,19	0,66	9,92
500	2,75	0,87	12,40

Table 3.4: Results in 0 degree for specimen 3.

Transversal Young's Modulus (E2)- specimen 3			Section Area [m^2]=3,99E-05
F [N]	**Strain [10^-3]**	**Machine Displacement [mm]**	**Stress [MPa]**
0	0,00	0	0,00
100	0,15	0,09	2,51
200	0,32	0,18	5,01
300	0,30	0,27	7,52
400	0,70	0,36	10,03
500	0,88	0,47	12,53

With this, a linear regression between the material strain and stress results can be applied, resulting in a value of the slope Transversal Young's Modulus [21]. These results are shown in figure 3.11 to 3.13.

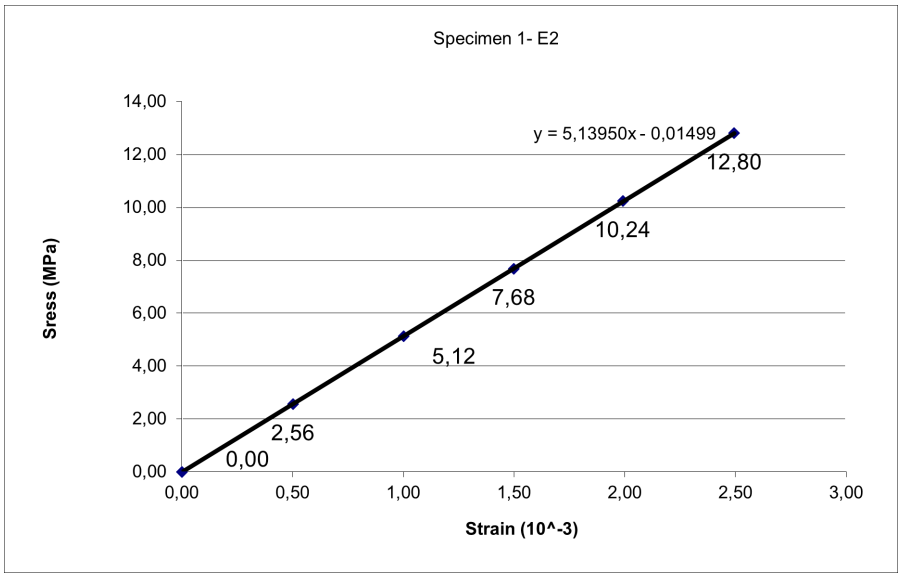

Figure 3.11: Transversal Young's Modulus- specimen 1.

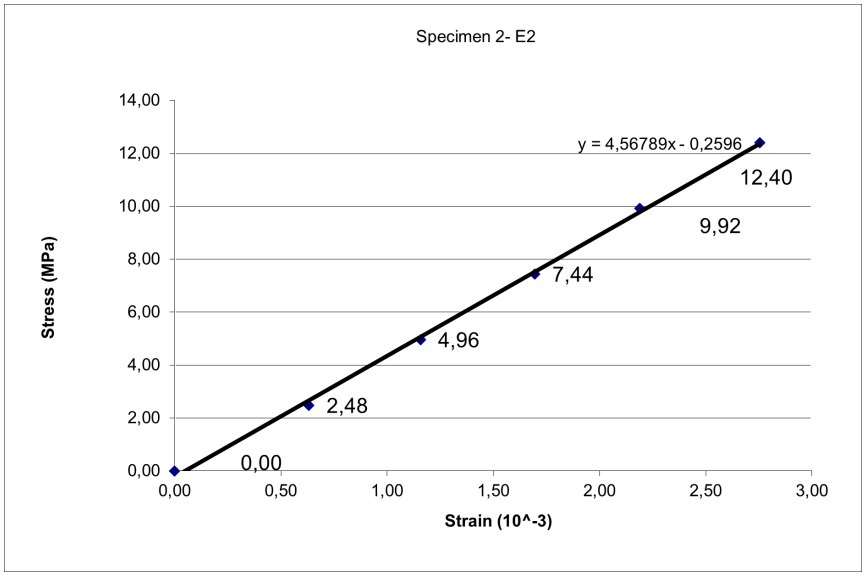

Figure 3.12: Transversal Young's Modulus- specimen 2.

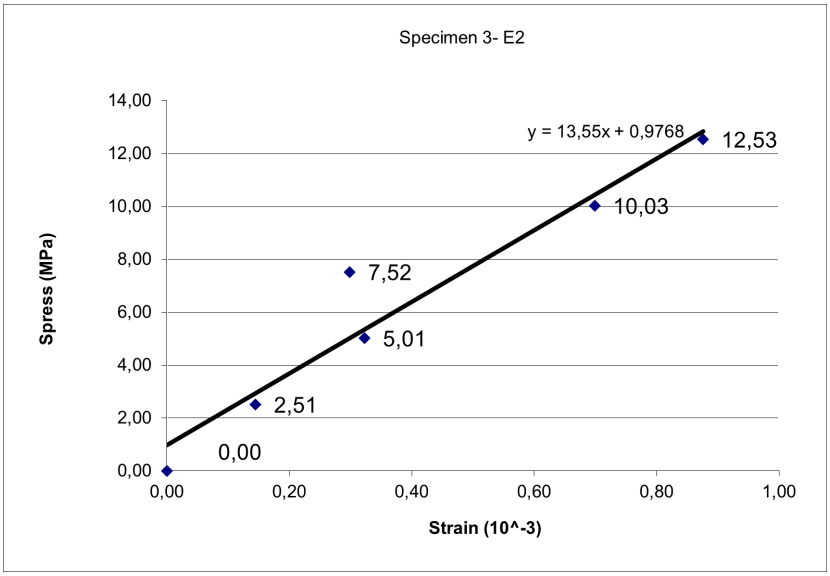

Figure 3.13: Transversal Young's Modulus- specimen 3.

3.5 Tensile test of 0 degree specimens

Similarly, the 0 degree specimens were subjected to ten test steps, from to 1000 N, this time producing the longitudinal and transversal material strain (e1 and e2, in the context of the testing) shown in table 3.5 to 3.8.

Table 3.5: Results in 0 degree for specimen 4.

Longitudinal Young's Modulus (E1) and ν- specimen 4				**Section Area [m^2]= 2,38E-05**
F [N]	**e1 [10^-3]**	**e2 [10^-3]**	**Machine Displacement [mm]**	**Stress [MPa]**
0	0,00	0,00	0,00	0,00
100	0,08	-0,04	0,06	4,21
200	0,16	-0,08	0,12	8,42
300	0,23	-0,12	0,17	12,63
400	0,30	-0,16	0,22	16,84
500	0,37	-0,20	0,27	21,04
600	0,43	-0,24	0,32	25,25
700	0,49	-0,28	0,37	29,46
800	0,55	-0,34	0,47	33,67
900	0,59	-0,40	0,58	37,88
1000	0,65	-0,45	0,68	42,09

Table 3.6: Results in 0 degree for specimen 5.

Longitudinal Young's Modulus (E1) and ν - specimen 5				**Section Area [m^2]= 1,91E-05**
F[N]	**e1 [10^-3]**	**e2 [10^-3]**	**Machine Displacement [mm]**	**Stress [MPa]**
0	0,00	0,00	0,00	0,00
100	0,05	-0,03	0,07	5,25
200	0,08	-0,05	0,13	10,50
300	0,11	-0,07	0,18	15,75
400	0,14	-0,10	0,22	21,00
500	0,18	-0,12	0,27	26,25
600	0,22	-0,15	0,31	31,50
700	0,26	-0,17	0,35	36,75
800	0,30	-0,19	0,39	41,99
900	0,35	-0,21	0,44	47,24
1000	0,41	-0,23	0,50	52,49

Table 3.7: Results in 0 degree for specimen 6.

Longitudinal Young's Modulus (E1) and ν- specimen 6				Section Area [m^2]= 2,21E-05
F [N]	**e1 [10^-3]**	**e2 [10^-3]**	**Machine Displacement [mm]**	**Stress [MPa]**
0	0,00	0,00	0,00	0,00
100	0,06	-0,03	0,08	4,53
200	0,10	-0,07	0,13	9,06
300	0,14	-0,10	0,18	13,59
400	0,18	-0,13	0,22	18,12
500	0,22	-0,16	0,27	22,64
600	0,26	-0,19	0,30	27,17
700	0,30	-0,22	0,34	31,70
800	0,34	-0,25	0,38	36,23
900	0,38	-0,28	0,42	40,76
1000	0,41	-0,31	0,45	45,29

Similarly, the Longitudinal Young's Modulus and ν can be calculated via a linear regression of the longitudinal material strain /stress and transversal material strain/longitudinal material strain for 0 degree specimens, respectively. These results can be found in figure 3.14 to 3.19.

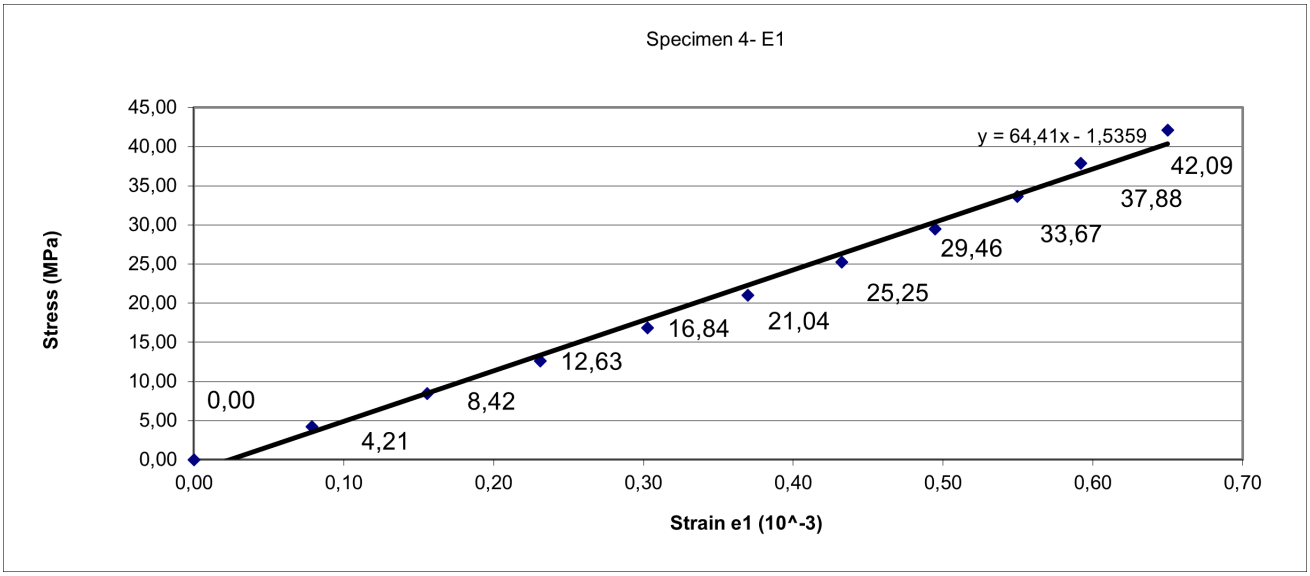

Figure 3.14: Longitudinal Young's Module- specimen 4.

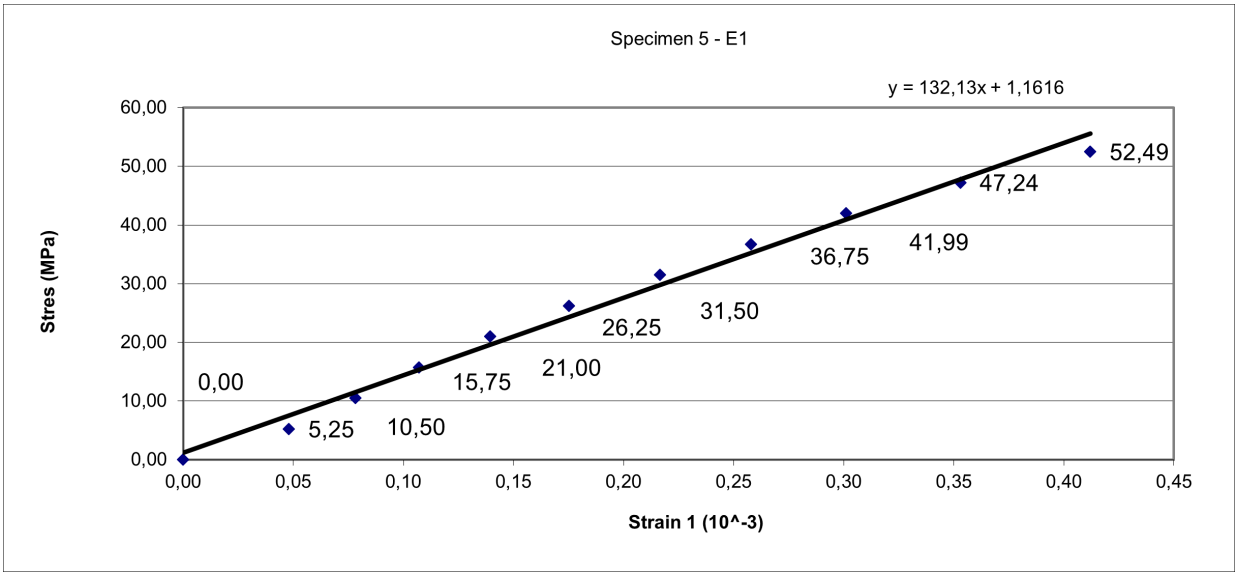

Figure 3.15: Longitudinal Young's Module- specimen 5.

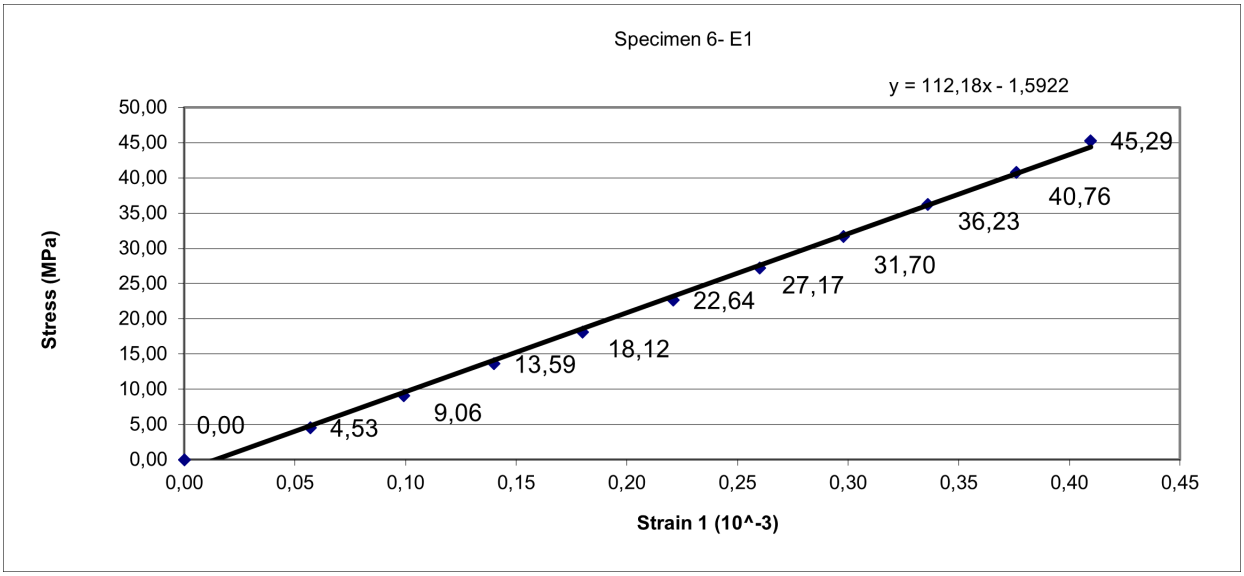

Figure 3.16: Longitudinal Young's Module- specimen 6.

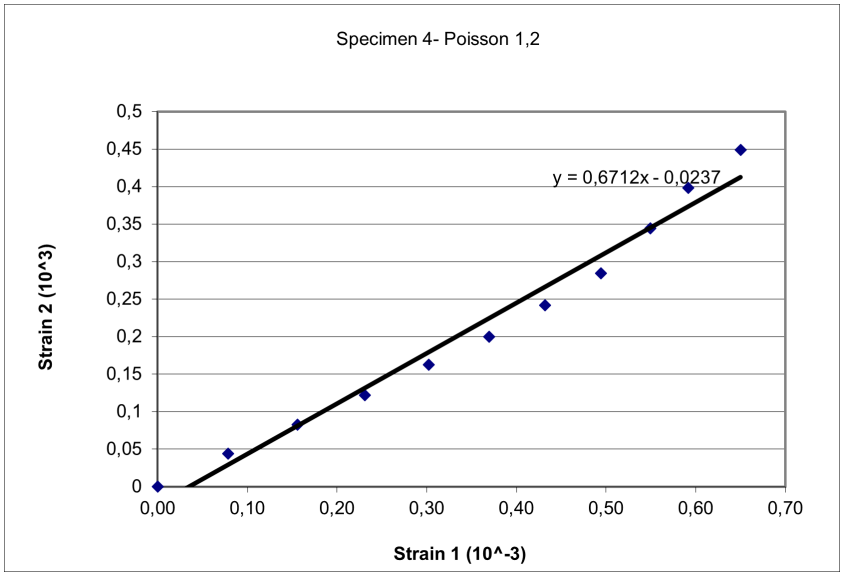

Figure 3.17: Poisson - specimen 4.

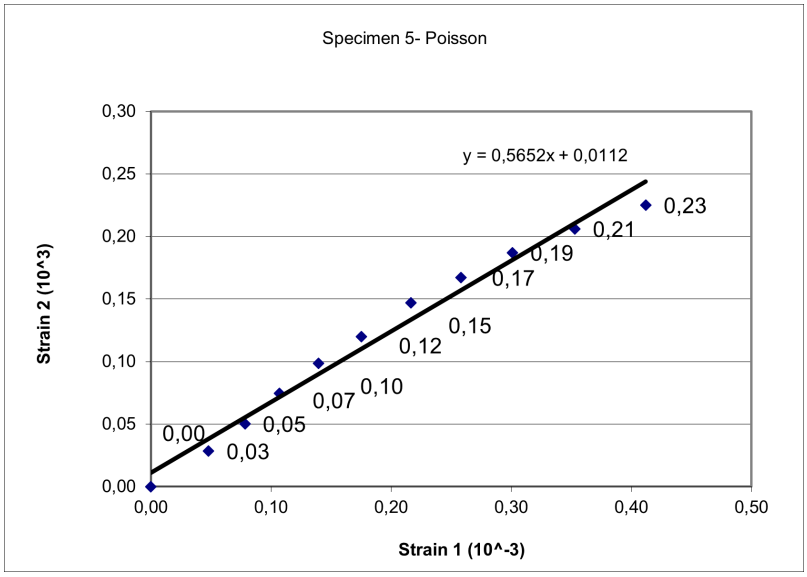

Figure 3.18: Poisson - specimen 5.

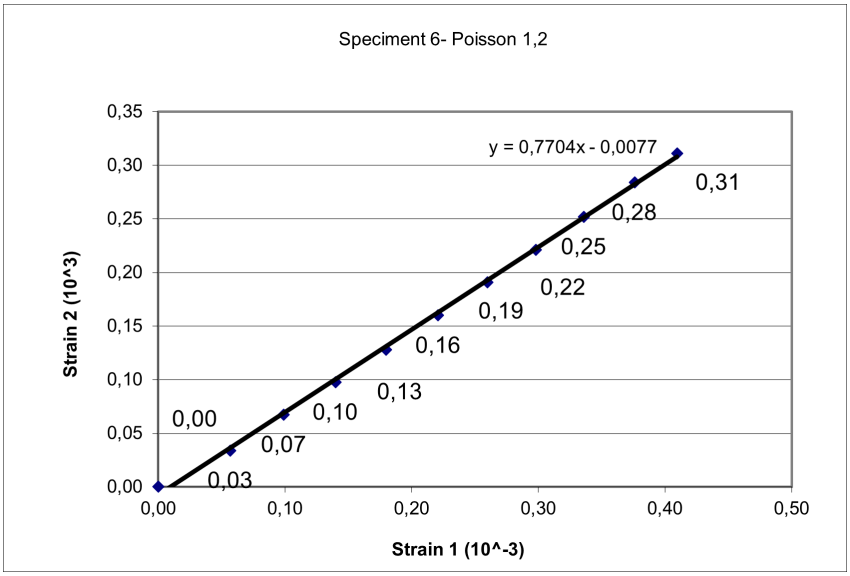

Figure 3.19: Poisson - specimen 6.

3.6 Tensile test of 45º/-45 degree specimens

Finally, the 45º/-45º specimens were subjected to the same test steps of 0º specimens, producing the longitudinal and transversal material strain shown in table 3.8 to 3.10.

Table 3.8: Results in 45 degree for specimen 7.

G12- specimen 7				Section Area [m^2]= 7,78E-05	
F [N]	**e1 [10^-3]**	**e2 [10^-3]**	**Machine Displacement [mm]**	**Shear Stress [MPa]**	**Shear Strain**
0	0,00	0,00	0	0,00	0,00
100	0,15	-0,04	0,07	0,64	0,19
200	0,29	-0,09	0,14	1,29	0,38
300	0,44	-0,15	0,22	1,93	0,59
400	0,58	-0,21	0,28	2,57	0,79
500	0,73	-0,27	0,36	3,22	1,00
600	0,87	-0,34	0,43	3,86	1,21
700	1,02	-0,41	0,51	4,50	1,43
800	1,18	-0,48	0,60	5,14	1,66

Lastly, the G12 can be calculated via e1 and e2, resulting in the calculation of shear strain. After this, a linear regression of the shear strain and shear stress for 45º/-45º specimens can be made, resulting in the value of G12. These results can be found in figure 3.20 to 3.22.

Table 3.9: Results in 45 degree for specimen 8.

G12- specimen 8				Section Area [m^2]= 8,15E-05	
F [N]	**e1 [10^-3]**	**e2 [10^-3]**	**Machine Displacement [mm]**	**Shear Stress [MPa]**	**Shear Strain**
0	0,00	0,00	0,00	0,00	0,00
100	0,13	-0,09	0,07	0,61	0,19
200	0,26	-0,17	0,13	1,23	0,38
300	0,37	-0,25	0,19	1,84	0,59
400	0,49	-0,34	0,26	2,45	0,79
500	0,59	-0,41	0,31	3,07	1,00
600	0,71	-0,50	0,38	3,68	1,21
700	0,82	-0,58	0,45	4,29	1,43
800	0,92	-0,65	-0,53	4,91	1,66

Table 3.10: Results in 45 degree for specimen 9.

G12- specimen 9				Section Area [m^2]= 8,26E-05	
F [N]	**e1 [10^-3]**	**e2 [10^-3]**	**Machine Displacement [mm]**	**Shear Stress [MPa]**	**Shear Strain**
0	0,00	0,00	0,00	0,00	0,00
100	0,05	-0,01	0,08	0,61	0,19
200	0,14	-0,04	0,15	1,21	0,38
300	0,24	-0,08	0,21	1,82	0,59
400	0,34	-0,13	0,27	2,42	0,79
500	0,45	-0,17	0,32	3,03	1,00
600	0,56	-0,22	0,38	3,63	1,21
700	0,69	-0,27	0,44	4,24	1,43
800	0,82	-0,33	0,49	4,84	1,66

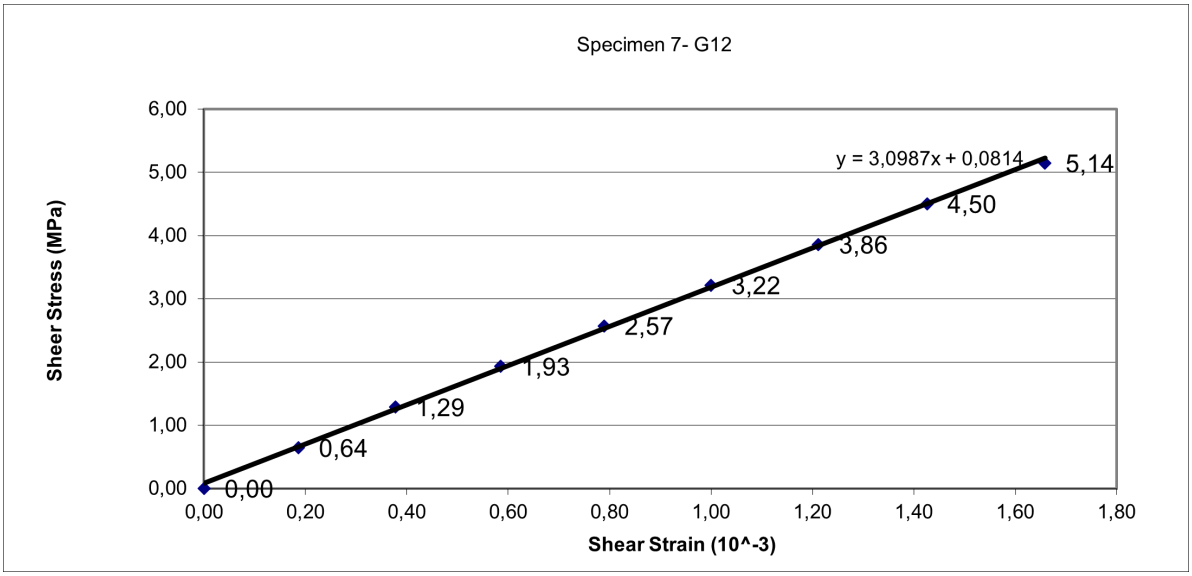

Figure 3.20: G12- specimen 7.

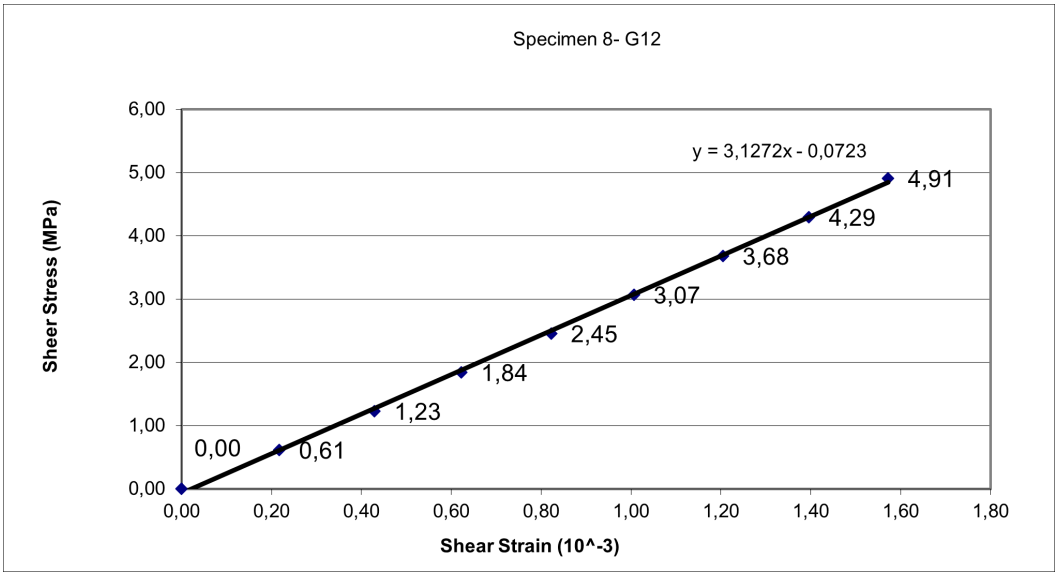

Figure 3.21: G12- specimen 8.

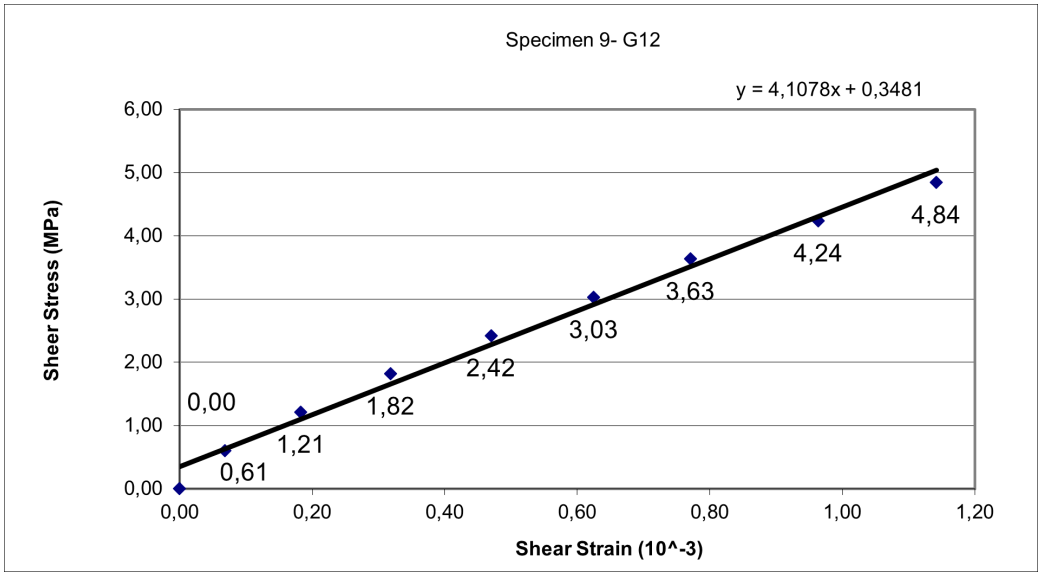

Figure 3.22: G12- specimen 9.

3.7 Mechanical Properties

Table 3.11: Mean and standard deviation of mechanical properties.

Nº	Young Modulus E1 [GPa]	Median	Std Dev	Young Modulus E2 [GPa]	Median	Std Dev	G12 [GPa]	Median	Std Dev	Poisson [N/A]	Median	Std Dev
1	64,41	112,18	25,66	5,14	5,14	3,86	3,09	3,13	0,44	0,67	0,67	0,07
2	132,13			4,57			3,13			0,56		
3	112,18			13,55			4,11			0,77		

With this, the mechanical properties can be summarized in the table 3.11, with their respective mean and standard deviation. The standard deviation for $E2$ can be derived from the specimen nº 3, due to smaller width of the specimen, resulting in the strain gauge to be applied on the side of the specimen. There is also a indentation present in the specimen used to calculate $E1$ that could have affected this result. However, the high poisson values could be attributed to the straightness of the specimens studied. The same happens in $G12$ values. As such, the mechanical and geometrical properties can be resumed in table 3.12 and 3.13.

Table 3.12: Mechanical properties and strengths.

Properties	Unit	Designation	Case E1 and E2
E1	GPa	Longitudinal Young's Module	112,18
E2 = E3	GPa	Transversal Young's Module	5,14
G12 = G13	GPa	Shear Module	3,13
ν_{12}	N/A	Poisson's coefficient	0,67
ν_{21}	N/A	Poisson's coefficient	0,03
ρ	kg/m^3	Density	1500
F1T	MPa	Longitudinal tensile rupture strength	1950 [21]
F2T = F3T	MPa	Transversal tensile rupture strength	48 [21]
F1C	MPa	Longitudinal compressive rupture strength	1480 [21]
F2C=F3C	MPa	Transversal compressive rupture strength	200 [21]
F4 = F5	MPa	Shear rupture strength	1000 [21]
F6	MPa	Shear rupture strength	79 [21]

Table 3.13: Geometrical properties [19].

Parameters	Unit	Description	Case E1	Case E2
N	N/A	Nº of layers	4	4
h	mm	Layer thickness	0,125	0,125
Stacking sequence	N/A		[0/0/0/0]	[30/90/-30/60]
z	N/A	Neutral plane	0	0
a	mm	Width	150	50
b	mm	Length	150	50

3.8 Testing device

Given the fact that a bi-axial tensile device was not available in the ISEL facilities, and such a device was considered necessary it was designed and built using a Medium Density Fiber (MDF) board, as well as the use of Bosch profile beams [23], ball-bearing linear guides and clamping jaws. The initial design of the bi-axial tensile device was partially based on [22], without using the crucible plate design. However, the first design presented problems in regards to the clamping jaw configurations. In it, the clamping jaws were found to be much too heavy for the Bosch profile beams, which would inevitably hinder the clamping of the plates to be tested. As such, the present design serves as a proof of concept. The 3D model design was achieved via the software Solidworks, as well as the technical drawing found in Appendix D.

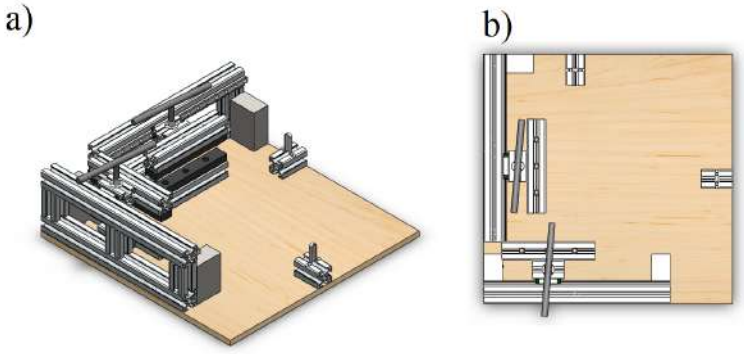

Figure 3.23: 3D model of the testing device: a) isometric view; b) Top view.

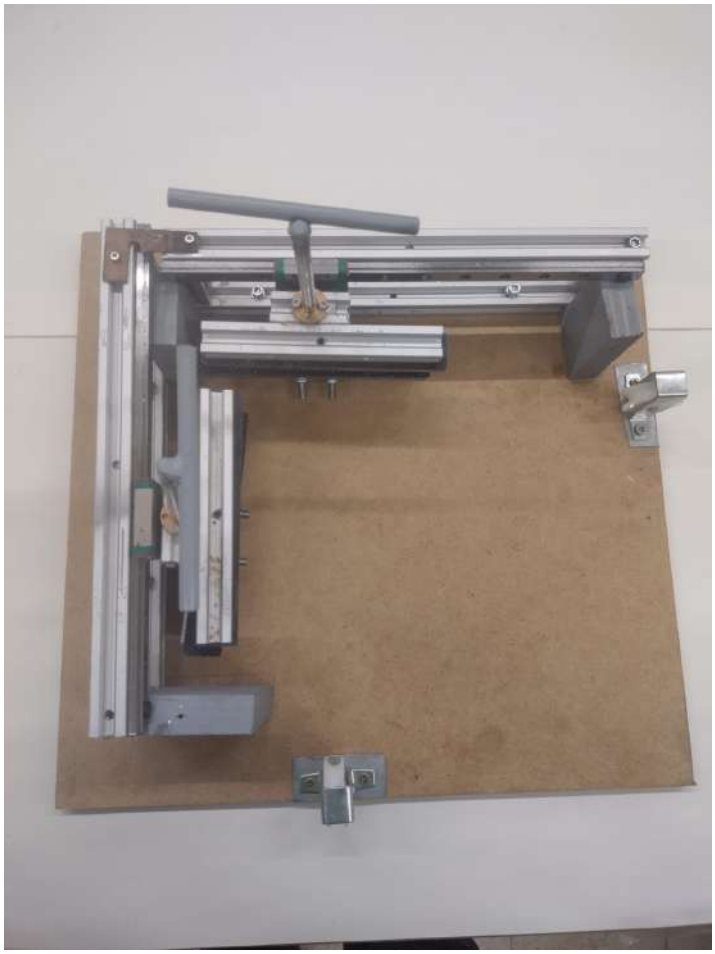

Figure 3.24: First iteration of clamping jaw.

However, due the weight of the clamping jaws, the plate could not be properly clamped. With this, the design was updated, with a new set of clamping jaws, as shown in figure 4.3. In it, the testing procedure is defined as such:

- The composite plate is clamped in the left and bottom clamp jaws (figure 3.22);

- In the Nx test, the composite plate is connected via a string to a steel weight, passing in the right pulley;

- For the Ny test, the connection to the composite plate is achieved via a string to a steel weight, passing on the top pulley;

- For the Nxy test, both the right and top pulley are connected via string to two steel weights.

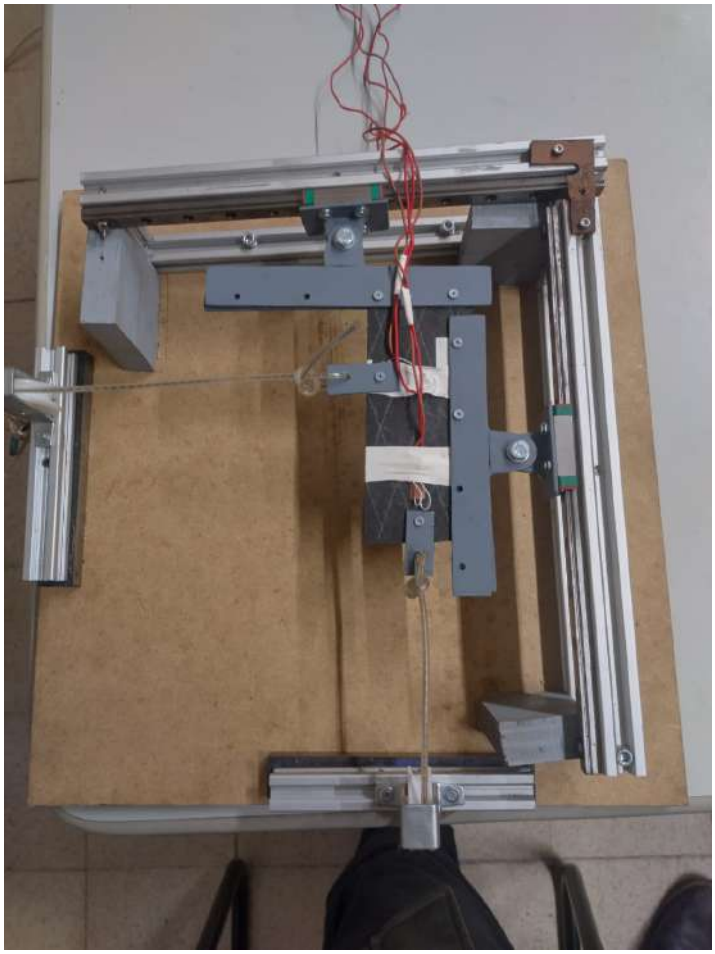

Figure 3.25: Clamping jaw configuration.

3.9 Plate Design

The present study is based on a composite plate with a force applied in the same direction as the boundary. Each composite plate is composed of a layer of unidirectional fibers with the thickness Hf, epoxy resin Hm and the total plate thickness Ht. The figures 3.23 and 3.24 show the down-up stacking sequence of both the E1 and E2 case studies. To ensure repeatability of results, each case study test step will have a total of three tested samples, making the total number of samples equal to fifteen.

Table 3.14: Plate's geometrical characteristics.

Case study	Hf [mm]	Hm [mm]	Ht [mm]	Nº of samples
E1	0,25	0,25	1	3
E2	0,25	0,25	1	3

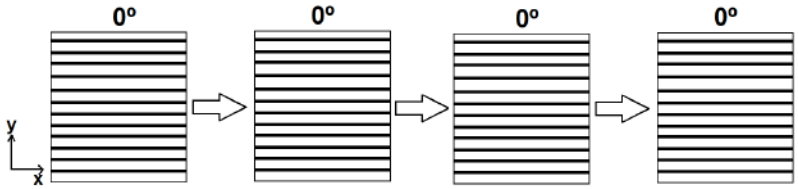

Figure 3.26: Stacking Sequence of E1 case study.

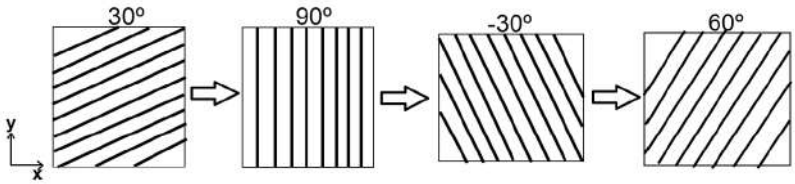

Figure 3.27: Stacking Sequence of E2 case study.

The fibers and adhesives used were 24 K carbon fiber for both E1 and E2 case studies, as well as Sicomin epoxy resin SR 1500 (and SD 2505 hardener). The technical data-sheets these materials can be found in Annex A. In regards to the instrumentation process, it was adapted a similar layout for the strain gauges.

Chapter 4

Numerical and analytical plate study

4.1 Numerical Method

4.1.1 Mechanical APDL

The present section aims to explain the implementation of the elements that contribute to the Mechanical APDL analysis of the two different cases. However, before the implementation of those parameters, there is a need to define the Tsai-Wu and Hashin failure criteria in the context of the APDL simulation. As such, the implementation of the Tsai-Wu and Hashin failure criteria follows the UPF method and is presented as follows.

4.1.1.1 User Programmable Feature Implementation

Because of the exemption of the Tsai-Wu and Hashin failure criteria in the default APDL module, the necessity for user-based modification of the software arises and as such, different UPF routines must be created [20]. With this, the code for both failure criteria is developed [20] using the Fortran programming language. For this, both the ”Intel oneAPI 64 for visual studio” and the ”Intel oneAPI IA32” compilers have to be installed.

```
c  input arguments:
c     variable (typ,siz,intent)    description
c     elem     (int,sc,in)       - element number
c     elim     (dp,ar(9),in)     - failure strains at the current temperature
c                                  (see FC command input with Lab1 = EPEL)
c     slim     (dp,ar(12),in)    - failure stresses and coupling coefficients
c                                  at the current temperature
c                                  (see FC command input with Lab1 = S)
c                                 xten = 1
c                                 xcmp = 2
c                                 xy = 7
c                                 xycp = 10
c     eps      (dp,ar(6),in)     - vector of strains
c     sig      (dp,ar(6),in)     - vector of stresses
c     tem      (dp,sc,in)        - temperature at this point in the model
c     matlay   (int,sc,in)       - material number
c     iott     (int,sc,in)       - unit number for writing
c
c  output arguments:
c     variable (typ,siz,intent)    description
c     nfcOut   (int,sc, out)     - number of user fc computed
c     fc       (dp,ar(9),out)    - user failure criterion
c
#include "impcom.inc"
c
      external vmax, vzero
      integer  elem,matlay,iott, nfcOut, iloc
      double precision
     x       eps(6),sig(6), fc(9),tem,elim(9),slim(12), vmax,vect(9)
      double precision fi
      double precision tmp(2), tmp1, tmp2, tmpa, tmpb
c
c
c  - nfcOut must be set to 1 or greater if the user subroutine is to be used
c   (see example below)
      nfcOut = 4
c
c
```

Figure 4.1: Input arguments for UPF [20].

By implementing the code into the APDL system, an executable of the program will be created for each UPF. Meaning that in total, three different executable applications were created (one for Tsai-Wu, one for Hashin and the default APDL), since the UPF's can be executed in parallel with each other or the default APDL module [20].

```
c Hashin example - output is inverse of strength ratio
c  by sheldon
c Meant to be an example of implementing user-defined failure criteria
c "Fiber" direction assumed to be "x"
c "Matrix" value of "y" used
c  fi = failure index
c
      call vzero (fc(1), 9)
c     usr1 = fiber tension or compression
      if (sig(1) .ge. 0.0d0) then
        call vzero (tmp(1), 2)
        tmp1 = (sig(4)**2.0d0 + sig(6)**2.0d0)/(slim(7)**2.0d0)
c       take sqrt
        tmp(1) = sqrt(tmp1 + (sig(1)/slim(1))**2.0d0)
        tmp(2) = sig(1)/slim(1)
        fc(2) = vmax (tmp(1), 2, iloc)
      else
        fc(2) = abs(sig(1)/slim(2))
      endif
c     usr2 = matrix
      tmp2 = sig(2) + sig(3)
      if (tmp2 .gt. 0.0d0) then
        tmp1 = ((sig(2) + sig(3))**2.0d0) / slim(3)**2.0d0
        tmp1 = tmp1 + ((sig(5)**2.0d0) - sig(2)*sig(3))/(slim(8)**2.0d0)
        fi = tmp1 + (sig(4)**2.0d0 + sig(6)**2.0d0)/(slim(7)**2.0d0)
        fc(3) = sqrt(fi)
      else if (tmp2 .lt. 0.0d0) then
        tmp1 = (slim(4)/(2.0d0*slim(8)))**2.0d0 - 1.0d0
        tmpb = tmp1*(tmp2)/slim(4)
        tmp1 = (tmp2**2.0d0)/(4.0d0*(slim(8)**2.0d0))
        tmp1 = tmp1 + ((sig(5)**2.0d0) - sig(2)*sig(3))/(slim(8)**2.0d0)
        tmpa = tmp1 + (sig(4)**2.0d0 + sig(6)**2.0d0)/(slim(7)**2.0d0)
        tmp1 = sqrt((tmpb/(2.0d0*tmpa))**2.0d0 + 1.0d0/tmpa)
        fc(3) = 1.0d0/(tmp1 - tmpb/(2.0d0*tmpa))
      else
        fc(3) = 0.0d0
      endif
c     usr3 = delamination
c       tmp1 = (sig(4)**2.0d0 + sig(6)**2.0d0)/(slim(7)**2.0d0)
c       fi = tmp1 + (sig(3)/slim(3))**2.0d0
c     largest
      call vzero (tmp(1), 2)
      tmp(1) = fc(2)
      tmp(2) = fc(3)
      fc(1) = vmax (tmp(1), 2, iloc)
      fc(4) = iloc*(-1.0d0)
ccccccccccccccccccccccccccccccccccccccccccccccccccccccccccccccccccccccccc
c
c
      return
      end
```

```
c Tsai-Wu example
c  by sheldon
c Meant to serve as simple example for study
c Compare with results of existing model in ANSYS for verification
c
c     usr1 = strength index
c     usr2 = inverse of strength ratio
c
c     A
      twa = -(sig(1)**2.0d0)/(slim(1)*slim(2))
      twa = twa - (sig(2)**2.0d0)/(slim(3)*slim(4))
      twa = twa - (sig(3)**2.0d0)/(slim(5)*slim(6))
      twa = twa + (sig(4)**2.0d0)/(slim(7)**2.0d0)
      twa = twa + (sig(5)**2.0d0)/(slim(8)**2.0d0)
      twa = twa + (sig(6)**2.0d0)/(slim(9)**2.0d0)
      tmp = slim(10)*sig(1)*sig(2)/sqrt(slim(1)*slim(2)*slim(3)*slim(4))
      twa = twa + tmp
      tmp = slim(11)*sig(3)*sig(2)/sqrt(slim(5)*slim(6)*slim(3)*slim(4))
      twa = twa + tmp
      tmp = slim(12)*sig(1)*sig(3)/sqrt(slim(1)*slim(2)*slim(5)*slim(6))
      twa = twa + tmp
c     B
      twb = sig(1)*(1.0d0/slim(1) + 1.0d0/slim(2))
      twb = twb + sig(2)*(1.0d0/slim(3) + 1.0d0/slim(4))
      twb = twb + sig(3)*(1.0d0/slim(5) + 1.0d0/slim(6))
c     TSI
      fc(1) = twa + twb
c     TSR
      tmp = sqrt((twb/(2.0d0*twa))**2.0d0 + 1.0d0/twa)
      fc(2) = 1.0d0/(tmp - twb/(2.0d0*twa))
ccccccccccccccccccccccccccccccccccccccccccccccccccccccccccccccccccccccccc
c
c
      return
      end
```

Figure 4.2: UPF code for Hashin and Tsai-Wu criteria [20].

4.1.1.2 Mechanical APDL code

Regarding the mesh configurations used, the complexity of the plates only require a 15x15 element mesh.

Regarding the boundary conditions used for the different studies, they are defined as follows:

Table 4.1: Boundary Conditions Implemented [1].

Type	Boundary Condition	APDL Code
NX	X displacement in line 4	DL,4,UX,0
NX	Z displacement in line 4	DL,4,UZ,0
NX	Z displacement in line 2	DL,2,UZ,0
NXY	Y displacement in line 1	DL,1,UY,0
NXY	Z displacement in line 1	DL,1,UZ,0
NXY	X displacement in line 4	DL,4,UX,0
NXY	Z displacement in line 4	DL,4,UZ,0
NXY	Z displacement in line 2	DL,2,UZ,0
NXY	Z displacement in line 3	DL,3,UZ,0
NY	Y displacement in line 1	DL,1,UY,0
NY	Z displacement in line 1	DL,1,UZ,0
NY	Z displacement in line 3	DL,3,UZ,0

Concerning the loads applied, as previously mentioned, both the application, magnitude and direction are presented in figure 4.3 and table 4.2.

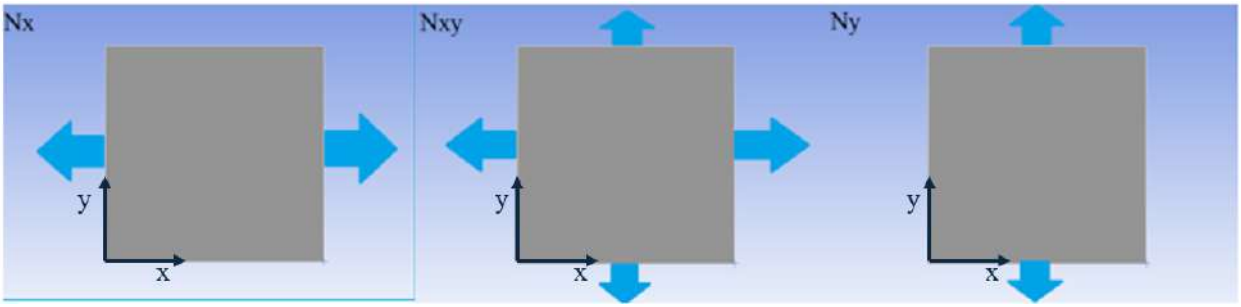

Figure 4.3: Application and direction of the loads applied.

Table 4.2: Loading values.

Parameters	Unit	Description	Case E1	Case E2
Nx	N/mm	Loading values on the ”x” coordinate	150 to 200 by 10	50 to 100 by 10
Nxy	N/mm	Loading values on the ”x” and ”y” coordinates	150 to 200 by 10	50 to 100 by 10
Ny	N/mm	Loading values on the ”y” coordinate	150-200 by 10	50 to 100 by 10

The implementation of the failure criteria used in each case study is feasible due to the ”PLESOL” command (giving the nodal value). As mentioned previously, the results calculated in this step are the total deformation, as well as the Failure Index of the Maximum Stress, Tsai-Wu, Hashin and Tsai-Hill failure criteria.

The APDL codes adapted from [1] (for both the Hashin and Tsai-Wu UPF, as well as the Max Stress and Tsai-Hill pre-implemented) can be found in their totality in Appendix A of the present document.

4.1.2 Workbench

Similarly to the APDL application, the Workbench numerical study starts with the definition of the properties of the materials. Following this, both the geometry and mesh are defined using the Pre-ACP module.

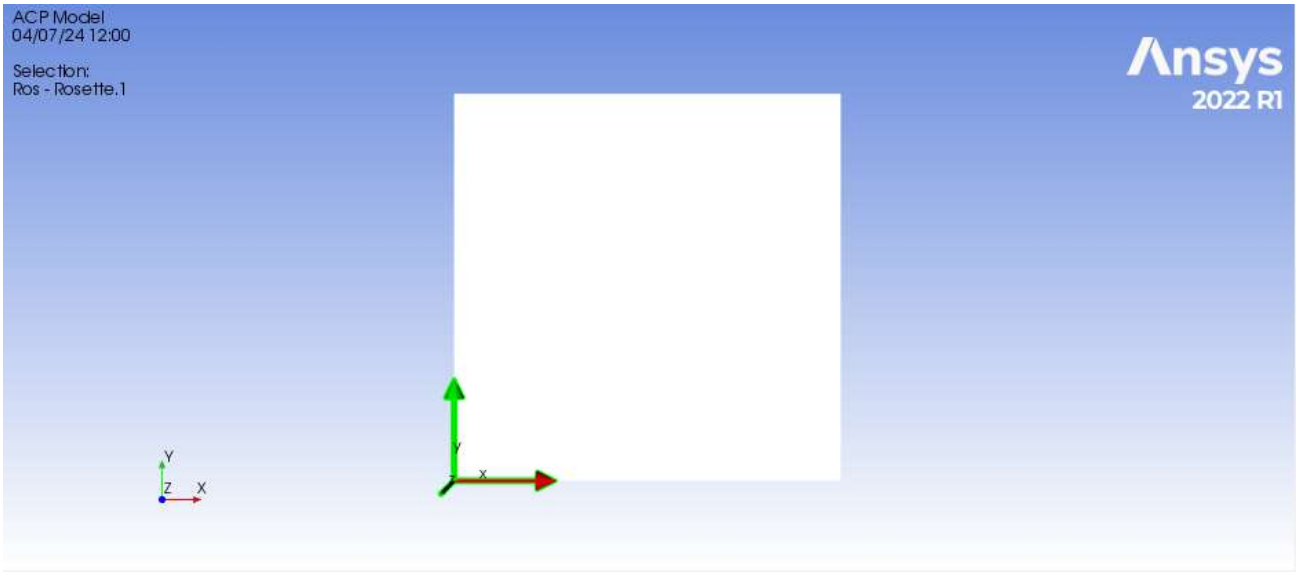

Figure 4.4: Coordinate system used for the study.

Utilizing the stacking sequence used in the E1 and E2 cases, as well as the type of fiber integration (unidirectional, in both the case studies), the basis for the study is established. With this, the structure for both the studies are presented in figure 4.5:

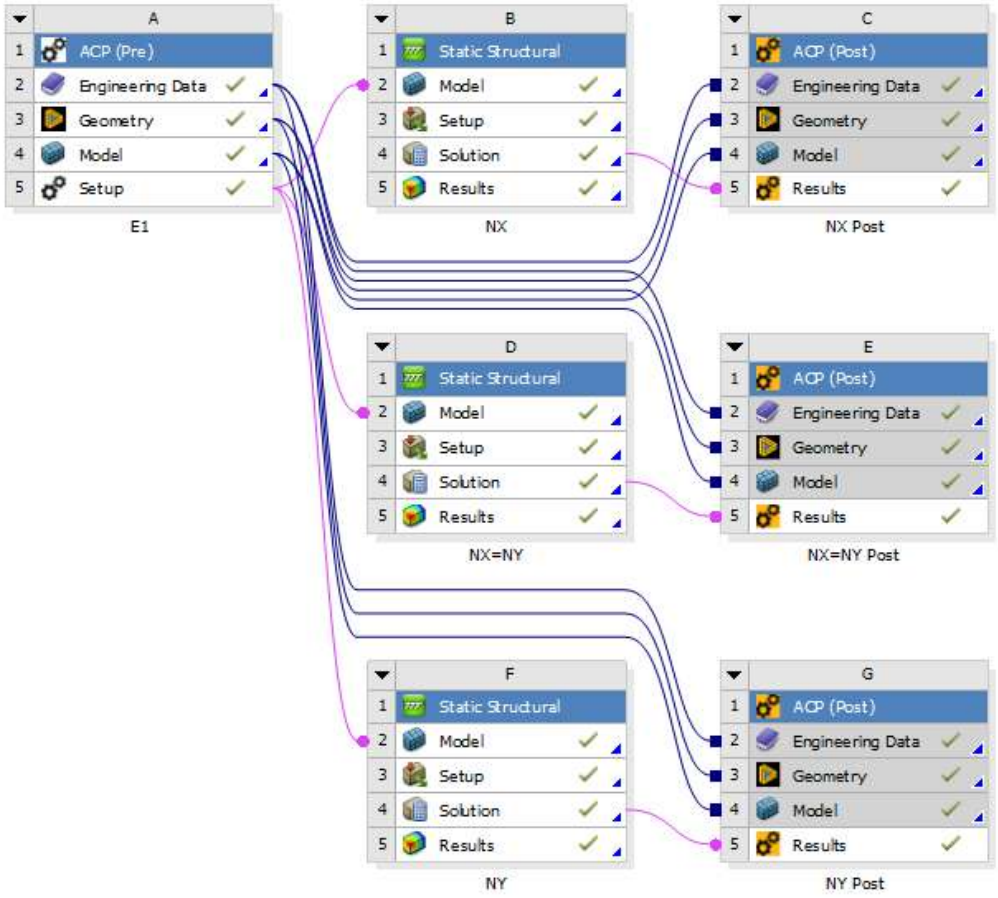

Figure 4.5: Study structure. Example: E1 case study.

In this structure, the setup given by the Pre-ACP module is fed into each Static Structural study. After importing the model characteristics, the next step is the definition of boundary conditions and load applications.

Given that the present study requires different incremental loads in each case, the step loads were configured as shown in figure 4.6:

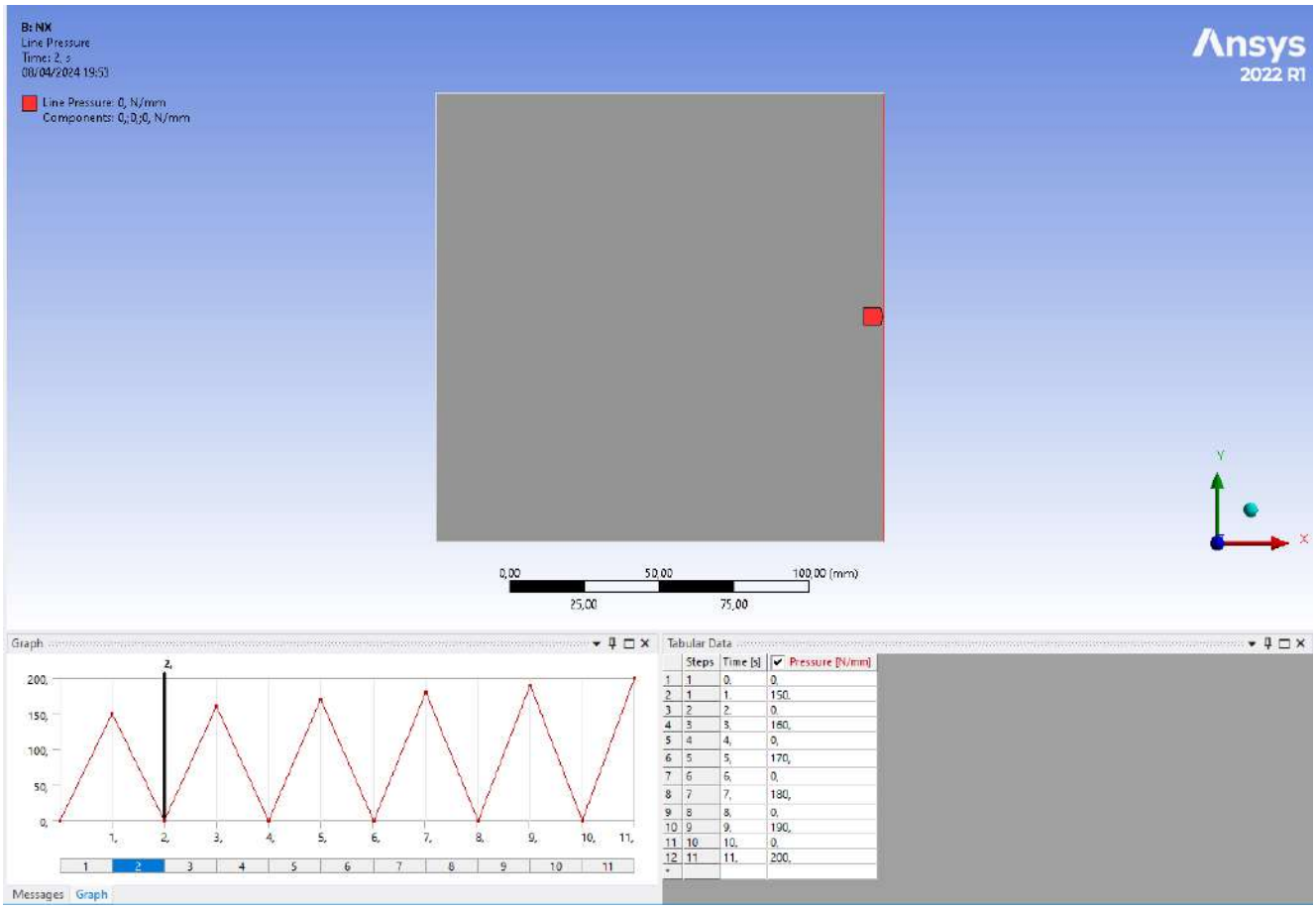

Figure 4.6: Line pressure application. Example: E1 case study, NX load.

Both the boundary conditions of E1 and E2 cases are the same and are represented by figures found in Appendix B. Given this, the boundary conditions implemented in table 4.3.

Table 4.3: Boundary Conditions Implemented. Example: E1 case study.

Type	Boundary Condition	Figure
NX	Left Rotation	Figure B.1-A
NX	Left Displacement	Figure B.1-B
NX	Right Rotation	Figure B.1-C
NX	Right Displacement	Figure B.1-D
NXY	Left Rotation	Figure B.2-A
NXY	Left Displacement	Figure B.2-B
NXY	Bottom Rotation	Figure B.2-C
NXY	Bottom Displacement	Figure B.2-D
NXY	Right Rotation	Figure B.2-E
NXY	Right Displacement	Figure B.2-F
NXY	Top Rotation	Figure B.2-G
NXY	Top Displacement	Figure B.2-H
NY	Bottom Rotation	Figure B.3-A
NY	Bottom Displacement	Figure B.3-B
NY	Top Rotation	Figure B.3-C
NY	Top Displacement	Figure B.3-D

4.2 Analytical Method

The analytical method implemented is based on the CLTP and the failure criteria previously exposed. As such, the procedure for the MAPLE implementation is as follows:

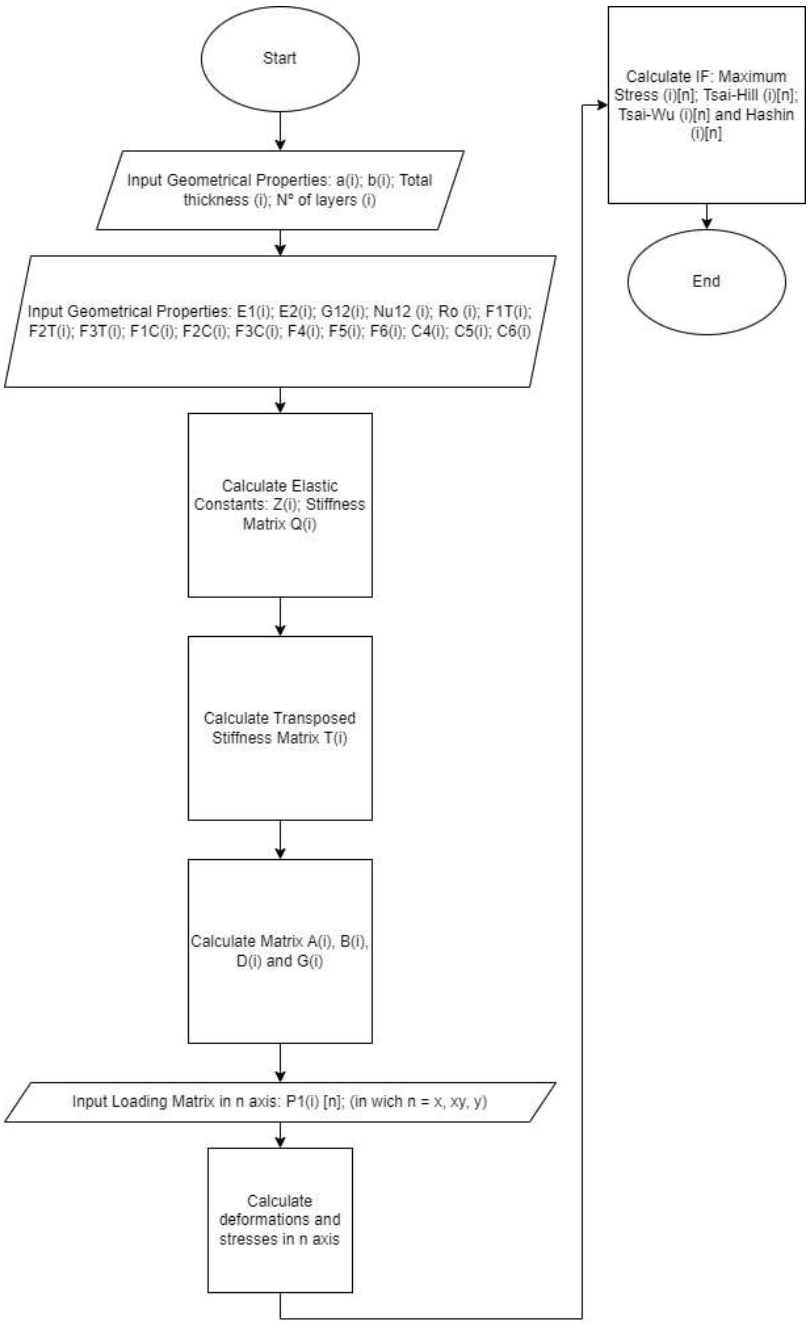

Figure 4.7: Analytical Calculation Flowchart in a Symbolic Computation Platform.

As such, the laminate stiffness matrices (A, B and D) calculated for the case study E1 are as follows:

$$A = \begin{bmatrix} 114.48 & 3.51 & 0 \\ 3.51 & 5.26 & 0 \\ 0 & 0 & 3.13 \end{bmatrix} MPa \tag{4.1}$$

$$B = \begin{bmatrix} 0 & 0 & 0 \\ 0 & 0 & 0 \\ 0 & 0 & 0 \end{bmatrix} MPa \tag{4.2}$$

$$D = \begin{bmatrix} 9.54 & 0.29 & 0 \\ 0.29 & 0.44 & 0 \\ 0 & 0 & 0.26 \end{bmatrix} Pa \tag{4.3}$$

Similarly, the laminate stiffness matrices for E2 are:

$$A = \begin{bmatrix} 14.29 & 7.15 & 4.65 \\ 13.97 & 27.95 & 1.26 \\ 1.26 & 4.65 & 8.41 \end{bmatrix} MPa \tag{4.4}$$

$$B = \begin{bmatrix} -4440.90 & 173.80 & -2348.8 \\ 118.60 & 2386.50 & 870.60 \\ -3196.20 & 1718.00 & 538.10 \end{bmatrix} Pa \tag{4.5}$$

$$D = \begin{bmatrix} 3.163 & 1.69 & 1.67 \\ 1.97 & 3.73 & 1.53 \\ 1.53 & 1.67 & 1.72 \end{bmatrix} Pa \tag{4.6}$$

The full exported MAPLE code can be found in Appendix C.

Chapter 5

Triathlon Handlebar

5.1 Design, Setup and Mesh

In the present chapter, the design in Solidworks Computer Assisted Drawing of the handlebar is shown. Given the design provided by [28] as a basis, the handlebar was designed more rudimentary aerodynamically speaking, but was also optimized in terms of strength of the materials previously studied. As such, the handlebar is given design can be found on figure 5.1, as well as the stacking sequence in figure 5.2 and fiber orientation for both the left and right handle (figure 5.3 and figure 5.4, respectively).

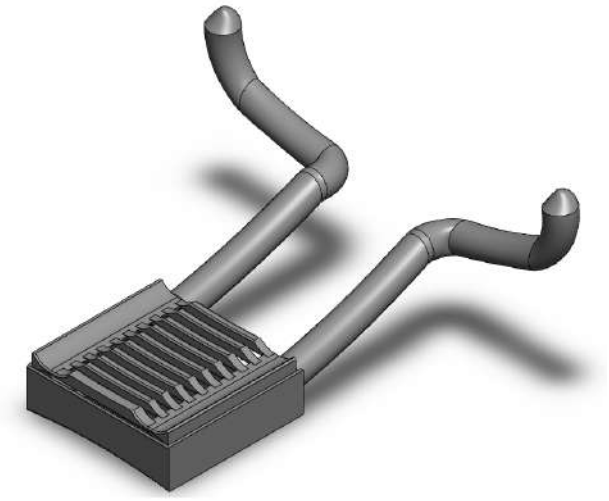

Figure 5.1: Triathlon Handlebar Design.

Ply	Thickness	Angle	Material
1	1	90	CARBON FIBER+EPOX
2	1	45	CARBON FIBER+EPOX
3	1	-45	CARBON FIBER+EPOX
4	1	90	CARBON FIBER+EPOX

Figure 5.2: Stacking Sequence adopted [28].

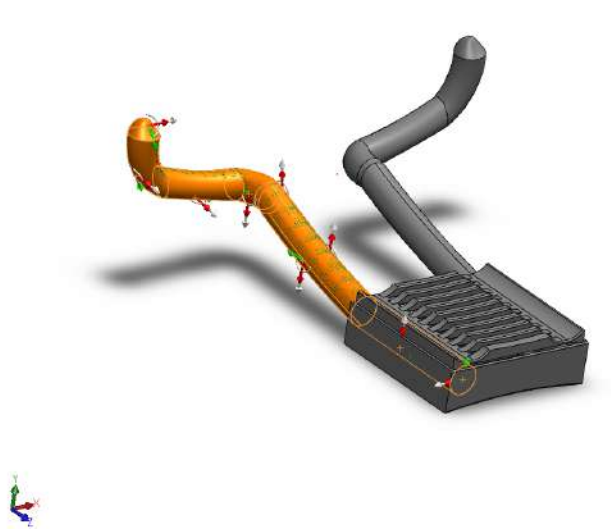

Figure 5.3: Left handle fiber orientation [28].

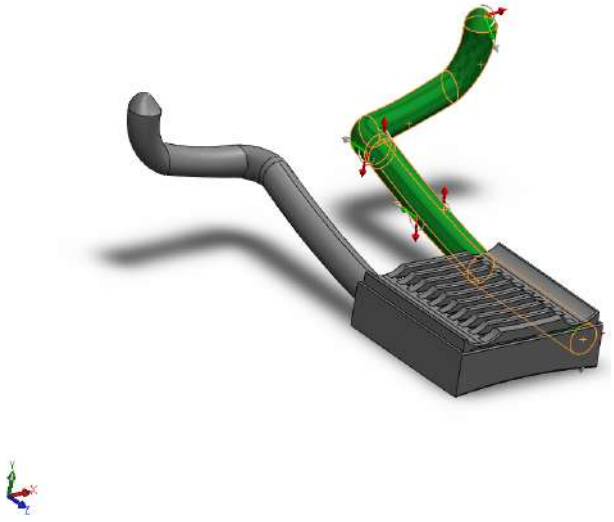

Figure 5.4: Right handlebar fiber orientation [28].

In regards to the load value and position/orientation, there is defined a value of 392N, as it represents to half of the body weight of a 80 kilogram athlete, in both the left and right arm of the handlebar [28]. The fixtures utilized represent the restriction in movement and rotation of the handlebar, as it is sited in the steering wheel [28]. The mesh utilized was a standard mixed mesh with an element size of 32mm and tolerance of 1.63 mm, as per [28]. The load configurations, fixtures and mesh can be found in figures 5.5, 5.6 and 5.7, respectively.

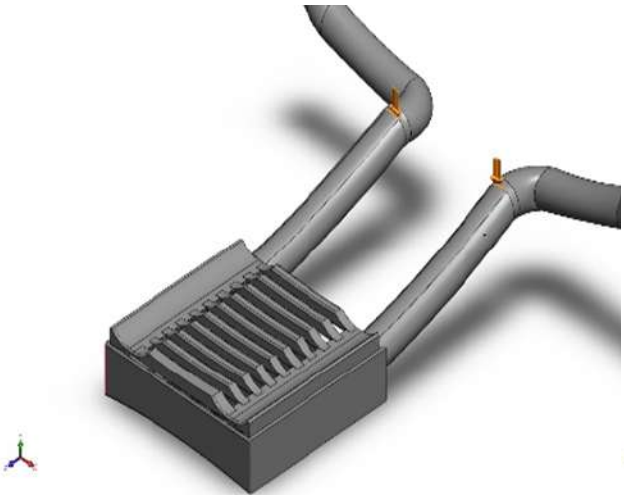

Figure 5.5: Load configuration utilized [28].

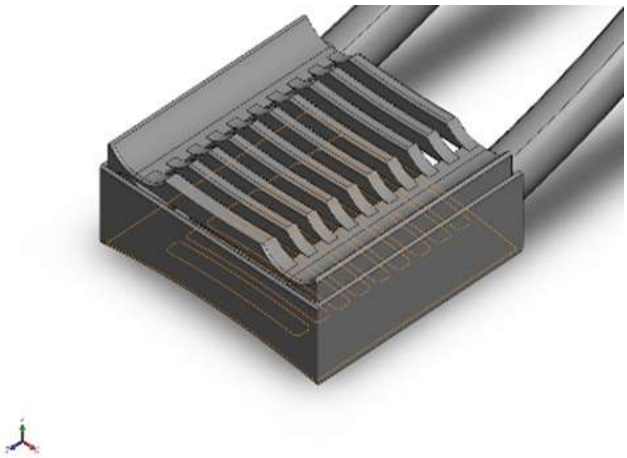

Figure 5.6: Fixture configuration [28].

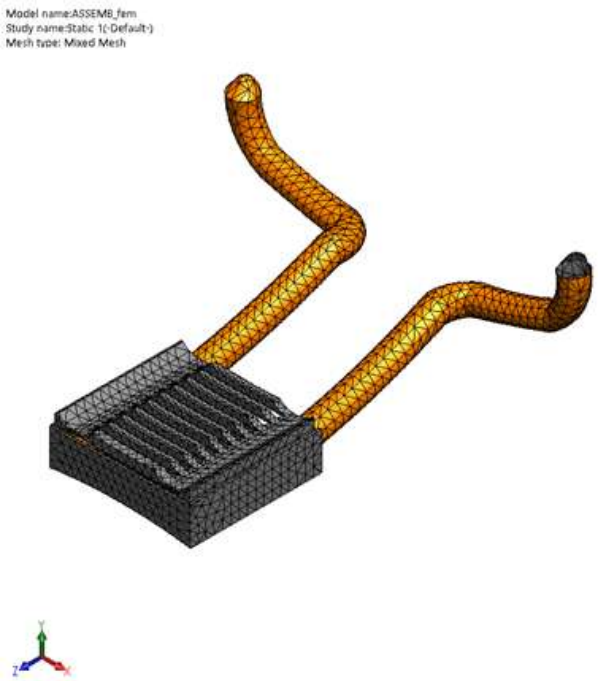

Figure 5.7: Mesh utilized [28].

5.2 Results

Using the previously exposed setup, the strain, displacement, and Sx stress found in figure 5.8 to figure 5.11, as well as the IF. The failure criteria utilized for the present study is the Tsai-Hill failure criteria.

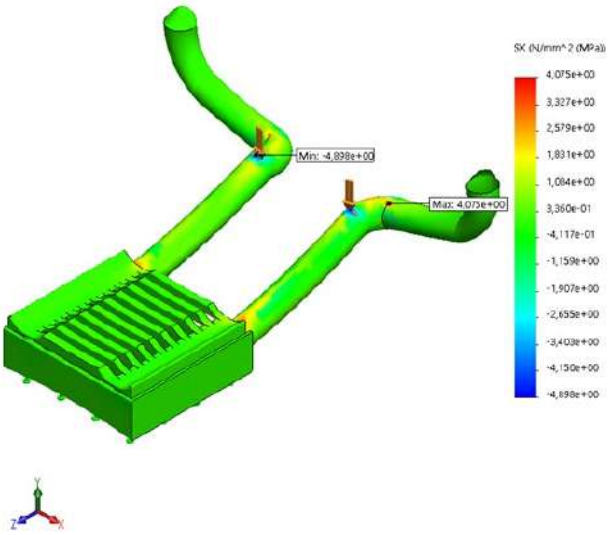

Figure 5.8: Sx results.

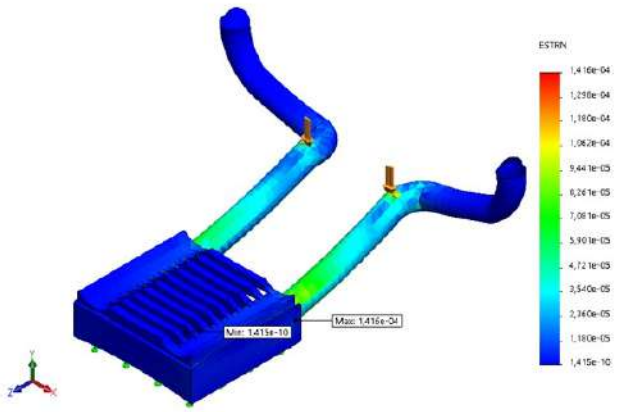

Figure 5.9: Strain results.

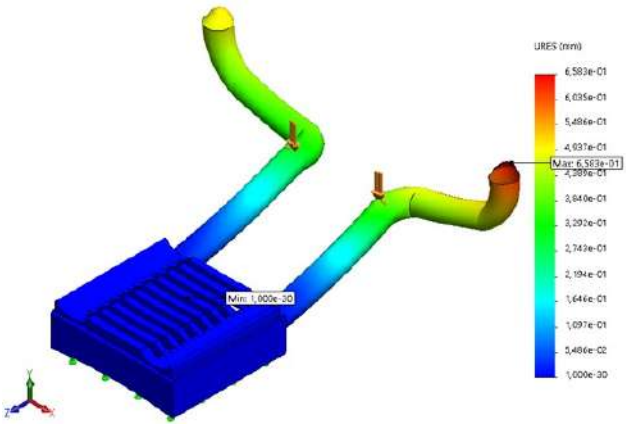

Figure 5.10: Displacement results.

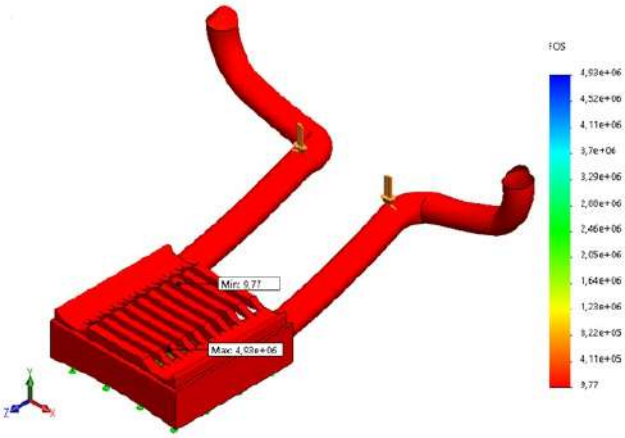

Figure 5.11: Factor of safety results.

The results show that, although the handlebar is within the failure limits of Tsai-Hill IF, the same would benefit from mass and ergonomic improvements.

Chapter 6

Plate Results and Analysis

6.1 Results for E1 Case Study

In this section, the results for the E1 case study are presented for the different load configurations, throughout the different methods adopted. As such, both the Maplesoft, Mechanical APDL and Workbench results for the E1 case study are given by table 6.1. Regarding the Failure Index, there is a clear relation between the load configuration and the methods used to calculate the results. For instance, in the NX load configuration, the value of Failure Index achieves it's maximum value in the Workbench method, regardless of the failure criterion adopted. However, the NX loading configuration in both the MAPLESOFT, Mechanical APDL and Workbench procedures do not reach the rupture point on all the failure criteria studied.This is to be expected, given that the fiber orientation is collinear with the loading direction. Leading to the conclusion that the Workbench method is conservative in regards to IF values far from the rupture point in the E1 case study.

Table 6.1: E1 Study Case Results.

E1 Case Study [APDL]															
	NX					NX=NY					NY				
P[N/mm]	Tsai-Wu	Tsai-Hill	Max Stress	Hashin	Maximum Displacement [mm]	Tsai-Wu	Tsai-Hill	Max Stress	Hashin	Maximum Displacement [mm]	Tsai-Wu	Tsai-Hill	Max Stress	Hashin	Maximum Displacement [mm]
150,00	0,08	0,08	0,08	0,07	0,24	3,07	4,57	3,13	4,57	4,24	3,13	4,72	3,13	4,72	4,38
160,00	0,08	0,08	0,08	0,08	0,26	3,28	5,03	3,33	5,03	4,53	3,33	5,20	3,33	5,20	4,67
170,00	0,09	0,09	0,09	0,09	0,27	3,48	5,51	3,54	5,51	4,81	3,54	5,70	3,54	5,70	4,96
180,00	0,09	0,09	0,09	0,09	0,29	3,69	6,01	3,75	6,01	5,09	3,75	6,23	3,75	6,23	5,26
190,00	0,10	0,10	0,10	0,10	0,30	3,89	6,53	3,96	6,53	5,38	3,96	6,77	3,96	6,77	5,55
200,00	0,10	0,10	0,10	0,10	0,32	4,09	7,07	4,17	7,07	5,66	4,17	7,33	4,17	7,33	5,84
E1 Case Study [Workbench]															
	NX					NX=NY					NY				
P[N/mm]	Tsai-Wu	Tsai-Hill	Max Stress	Hashin	Maximum Displacement [mm]	Tsai-Wu	Tsai-Hill	Max Stress	Hashin	Maximum Displacement [mm]	Tsai-Wu	Tsai-Hill	Max Stress	Hashin	Maximum Displacement [mm]
150,00	0,13	0,15	0,11	0,11	0,21	3,07	3,13	3,13	3,13	4,24	3,60	3,60	3,59	3,60	4,37
160,00	0,14	0,16	0,12	0,12	0,23	3,28	3,33	3,33	3,33	4,53	3,84	3,84	3,84	3,84	4,67
170,00	0,14	0,17	0,12	0,12	0,24	3,48	3,54	3,54	3,54	4,81	4,08	4,08	4,08	4,08	4,96
180,00	0,15	0,18	0,13	0,13	0,26	3,69	3,75	3,75	3,75	5,09	4,32	4,32	4,32	4,32	5,24
190,00	0,16	0,19	0,14	0,14	0,27	3,89	3,96	3,96	3,96	5,38	4,56	4,56	4,56	4,56	5,55
200,00	0,17	0,19	0,15	0,15	0,29	4,09	4,17	4,17	4,17	5,66	4,79	4,79	4,79	4,80	5,83
E1 Case Study [MAPLESOFT]															
	NX					NX=NY					NY				
P[N/mm]	Tsai-Wu	Tsai-Hill	Max Stress	Hashin	Maximum Displacement [mm]	Tsai-Wu	Tsai-Hill	Max Stress	Hashin	Maximum Displacement [mm]	Tsai-Wu	Tsai-Hill	Max Stress	Hashin	Maximum Displacement [mm]
150,00	0,06	0,06	0,06	0,08	0,24	4,87	6,96	5,28	6,96	4,19	4,87	6,96	5,28	6,96	4,33
160,00	0,06	0,06	0,06	0,08	0,25	5,03	7,19	5,36	7,19	4,47	5,03	7,19	5,36	7,19	4,62
170,00	0,06	0,06	0,06	0,08	0,27	5,16	7,63	5,44	7,41	4,75	5,19	7,41	5,44	7,41	4,90
180,00	0,07	0,06	0,06	0,08	0,29	5,33	7,84	5,52	7,63	5,03	5,34	7,63	5,52	7,63	5,19
190,00	0,07	0,06	0,06	0,08	0,30	5,48	7,84	5,59	7,84	5,31	5,48	7,84	5,59	7,84	5,48
200,00	0,07	0,07	0,06	0,09	0,32	5,62	8,04	5,67	8,04	5,59	5,63	8,04	5,67	8,04	5,77

However, it is also noticeable that both the NXY and NY loading configurations yield a similar result in the magnitude of the Inverse Failure criterion studied, with the analytical method outputting the highest values. From these results, one can also conclude that, although the maximum displacement values are similar within each load configuration, the Tsai-Hill and Hashin Failure Index (figure 6.3 and figure 6.4, respectively) are conservative when in the presence of a possible rupture point for stacking sequences similar to the one found in E1 Case Study.

In regards to the deviation of these results (figures 6.1 to 6.5), as shown previously,the Mechanical APDL approach offers the most precision based results, followed by the analytical model and finally the Workbench approach. Note that the deviation in maximum displacement results are much smaller when compared to those found in the IF (figure 6.5). Given the fact that the displacement is the first variable calculated in the FEA study, the propagation of deviation is inevitable and will affect the final calculated variable (as shown in figure 6.5).

In summary, the results shown suggest the application of the Tsai-Hill or Hashin-Rottem Failure Criterion, utilizing the Mechanical APDL approach, for stacking sequences similar to E1 Case Study.

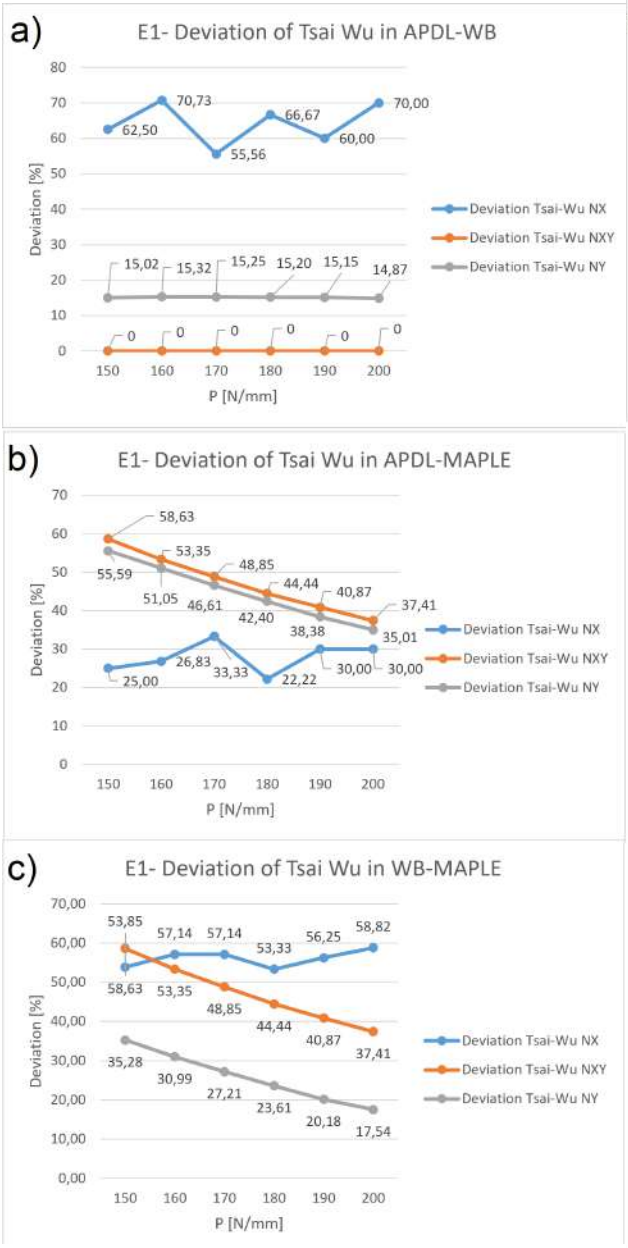

Figure 6.1: Deviation in Tsai Wu IF on E1 case Study in: a) APDL- Workbench; b) APDL-MAPLESOFT; c) Workbench-MAPLESOFT.

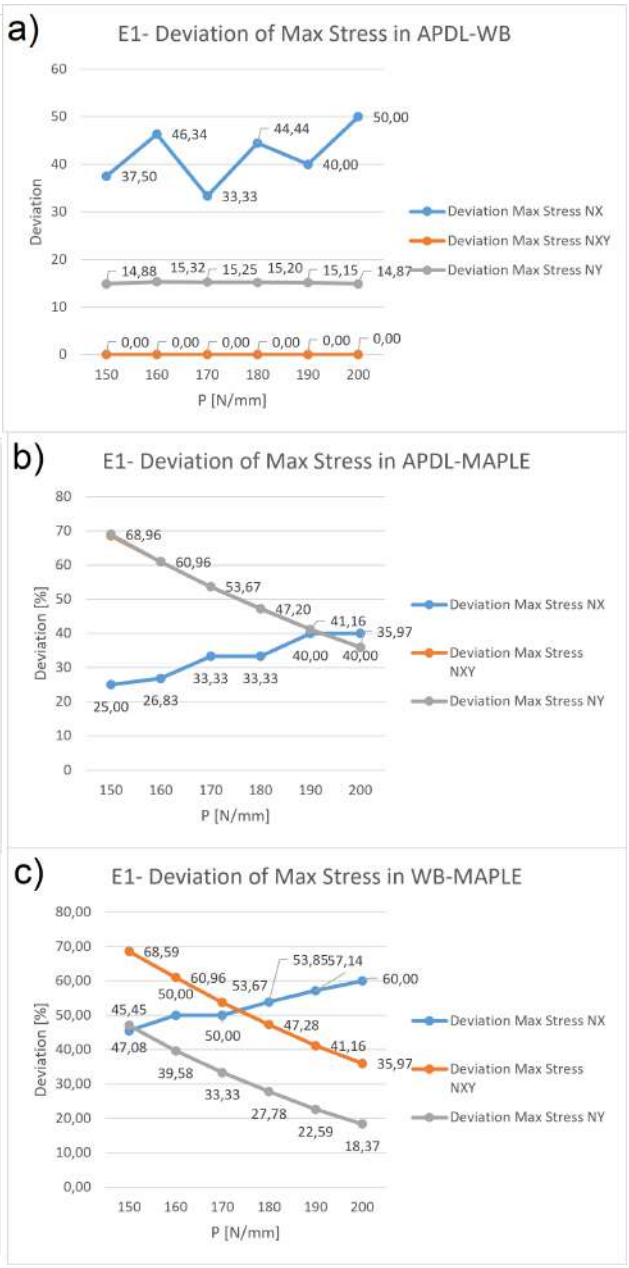

Figure 6.2: Deviation in Maximum Stress IF on E1 case Study in: a) APDL- Workbench; b) APDL-MAPLESOFT; c) Workbench-MAPLESOFT.

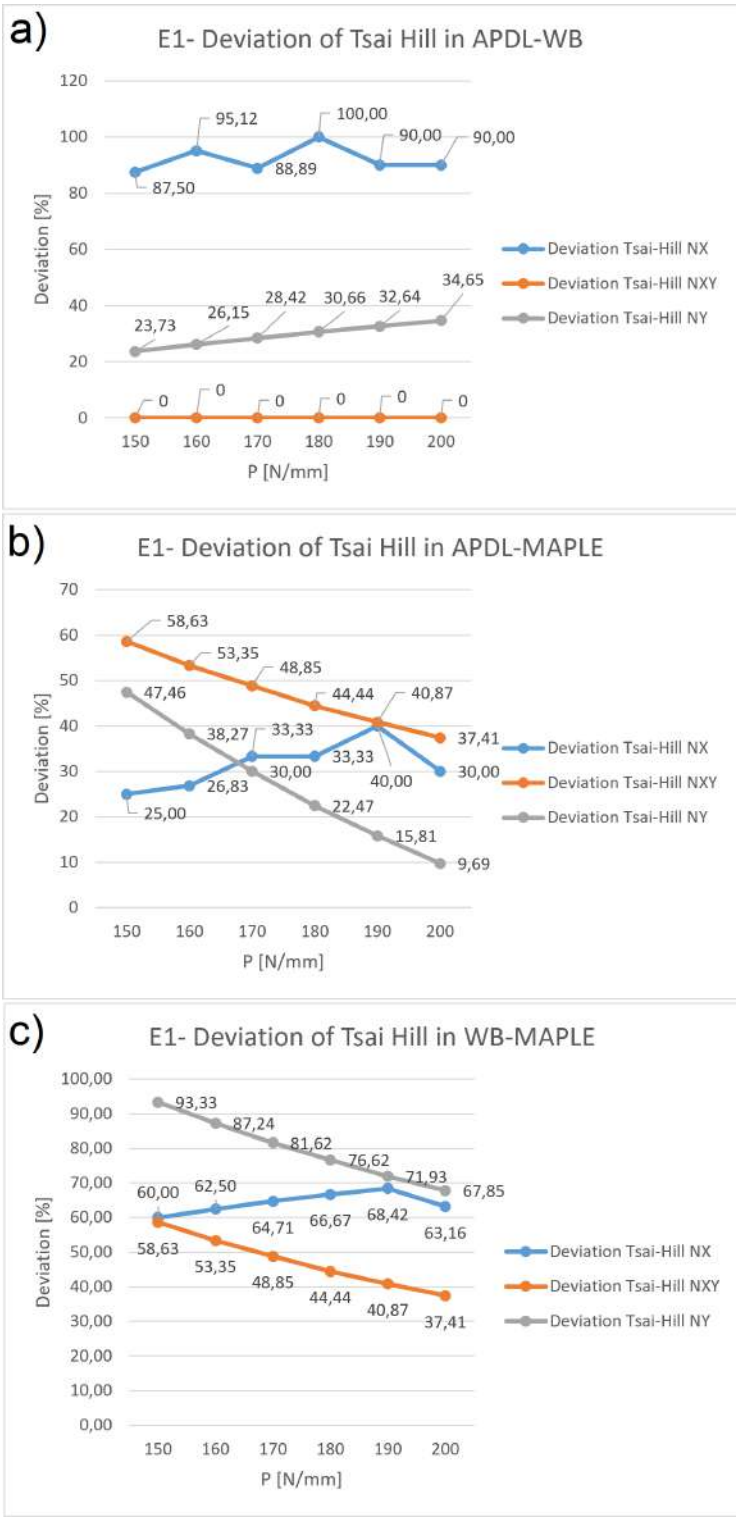

Figure 6.3: Deviation in Tsai-Hill IF on E1 case Study in: a) APDL- Workbench; b) APDL-MAPLESOFT; c) Workbench-MAPLESOFT.

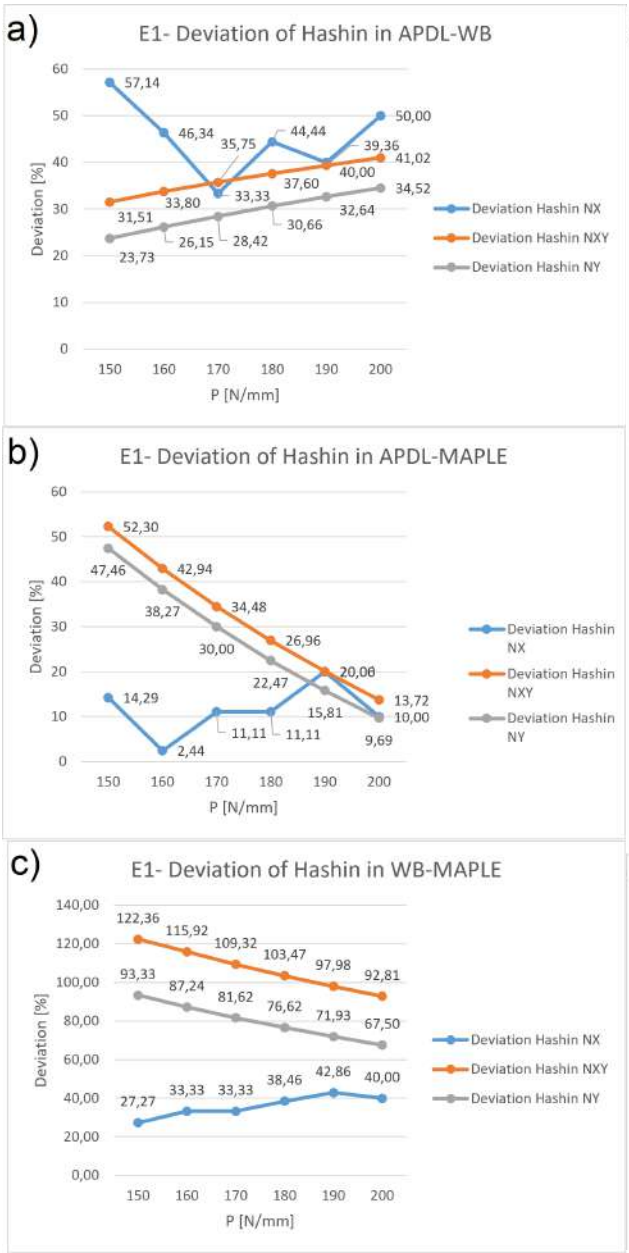

Figure 6.4: Deviation in Hashin IF on E1 case Study in: a) APDL- Workbench; b) APDL-MAPLESOFT; c) Workbench-MAPLESOFT.

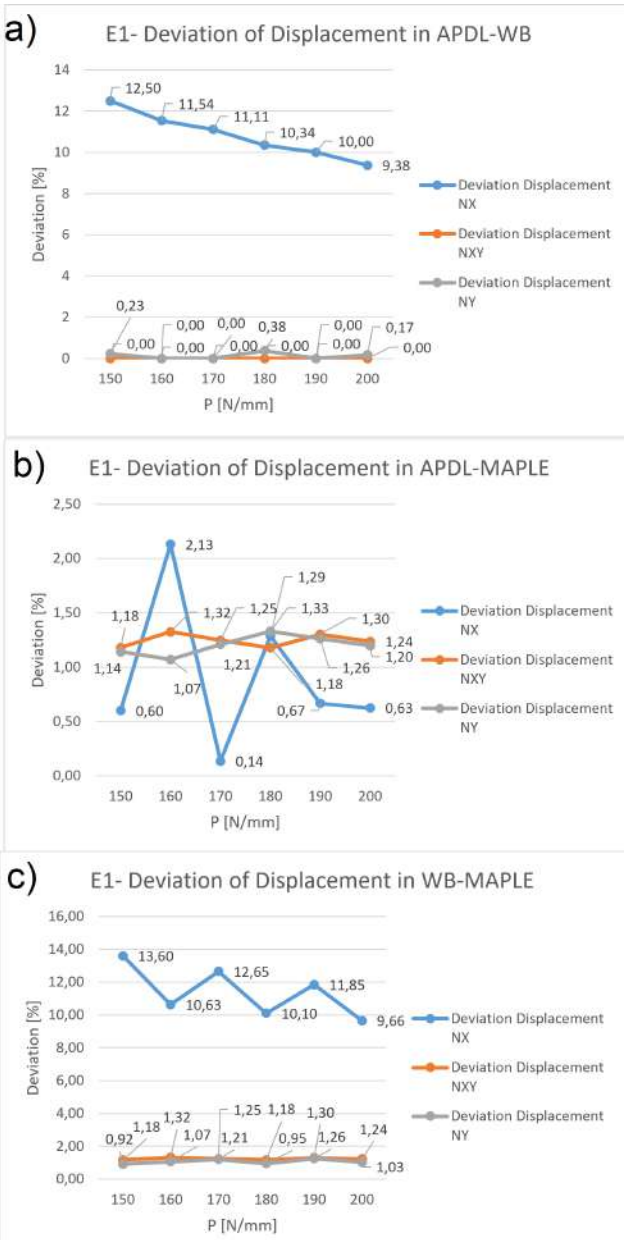

Figure 6.5: Deviation in Displacement on E1 case Study in: a) APDL- Workbench; b) APDL-MAPLESOFT; c) Workbench-MAPLESOFT.

6.2 Results for E2 Case Study

Given the results for the E1 Case Study, with special remarks to the deviation of the IF's in Workbench method and the values in which failure occurs, one would expect the same trend to continue in the more complex E2 Case Study.

Table 6.2: E2 Study Case Results.

E2 Case Study [APDL]															
	NX					NXY					NY				
P[N/mm]	Tsai-Wu	Tsai-Hill	Max Stress	Hashin	Maximum Displacement [mm]	Tsai-Wu	Tsai-Hill	Max Stress	Hashin	Maximum Displacement [mm]	Tsai-Wu	Tsai-Hill	Max Stress	Hashin	Maximum Displacement [mm]
50,00	0,26	0,26	0,20	0,26	1,42	0,33	0,39	0,39	0,39	0,29	0,56	0,56	0,51	0,56	17,76
60,00	0,31	0,31	0,24	0,31	1,70	0,39	0,47	0,47	0,47	0,34	0,68	0,68	0,61	0,68	21,32
70,00	0,36	0,36	0,28	0,36	1,99	0,46	0,55	0,55	0,55	0,40	0,79	0,79	0,72	0,79	24,87
80,00	0,42	0,42	0,32	0,42	2,27	0,52	0,63	0,63	0,63	0,46	0,90	0,90	0,82	0,90	28,42
90,00	0,47	0,47	0,36	0,47	2,56	0,59	0,70	0,70	0,70	0,51	1,02	1,02	0,92	1,02	31,98
100,00	0,52	0,52	0,40	0,52	2,84	0,66	0,78	0,78	0,78	0,57	1,13	1,18	1,02	1,18	35,53
E2 Case Study [Workbench]															
	NX					NX=NY					NY				
P[N/mm]	Tsai-Wu	Tsai-Hill	Max Stress	Hashin	Maximum Displacement [mm]	Tsai-Wu	Tsai-Hill	Max Stress	Hashin	Maximum Displacement [mm]	Tsai-Wu	Tsai-Hill	Max Stress	Hashin	Maximum Displacement [mm]
50,00	0,47	0,52	0,52	0,52	0,55	0,27	0,35	0,33	0,33	0,18	0,30	0,31	0,31	0,31	18,41
60,00	0,57	0,62	0,62	0,62	0,66	0,33	0,41	0,39	0,39	0,21	0,36	0,37	0,37	0,37	21,80
70,00	0,66	0,73	0,73	0,73	0,77	0,38	0,48	0,46	0,46	0,25	0,42	0,43	0,43	0,43	24,37
80,00	0,75	0,83	0,83	0,83	0,88	0,43	0,55	0,53	0,53	0,28	0,49	0,49	0,49	0,49	28,88
90,00	0,85	0,93	0,94	0,94	0,99	0,49	0,62	0,59	0,60	0,32	0,55	0,55	0,55	0,55	31,92
100,00	0,94	1,04	1,04	1,04	1,09	0,54	0,69	0,66	0,66	0,36	0,61	0,62	0,62	0,62	35,87
E2 Case Study [MAPLE]															
	NX					NX=NY					NY				
P[N/mm]	Tsai-Wu	Tsai-Hill	Max Stress	Hashin	Maximum Displacement [mm]	Tsai-Wu	Tsai-Hill	Max Stress	Hashin	Maximum Displacement [mm]	Tsai-Wu	Tsai-Hill	Max Stress	Hashin	Maximum Displacement [mm]
50,00	0,26	0,20	0,22	0,22	0,93	0,29	0,30	0,30	0,36	0,31	0,63	0,56	0,38	0,56	16,01
60,00	0,27	0,22	0,23	0,23	1,11	0,30	0,33	0,32	0,37	0,37	0,66	0,62	0,39	0,62	19,30
70,00	0,28	0,24	0,24	0,24	1,30	0,31	0,36	0,33	0,39	0,43	0,68	0,67	0,41	0,62	22,53
80,00	0,29	0,25	0,25	0,25	1,49	0,32	0,38	0,34	0,40	0,44	0,70	0,71	0,42	0,67	25,75
90,00	0,30	0,27	0,26	0,26	1,67	0,33	0,40	0,35	0,41	0,49	0,73	0,76	0,43	0,71	28,97
100,00	0,31	0,28	0,26	0,26	1,86	0,34	0,40	0,36	0,42	0,55	0,75	0,80	0,44	0,79	32,19

However, due to the nature of the stacking sequence, the IF's calculated are lower in magnitude (with only achieving maximum value of 1.04 in the NY loading, as shown in table 6.2. The rupture is present, however, in almost every IF calculated (NXY load configuration not achieving IF$>$1) and it's value is more prevalent in the NY loading configuration. These values of IF can be explain due to the layer of 90º in the stacking sequence, being directly co linear to the loading configuration in question.

In the present case study, the highest values of IF for NX load configuration were achieved utilizing the Workbench method, while the NXY and NY load configuration result values were achieved in Mechanical APDL.

As shown previously, the values obtained via the Mechanical APDL are overall higher when in the presence of a possible rupture point for all the failure criterion. Leading to the conclusion that the this stacking sequence is more likely to enter the rupture point, but also that the method of calculation that is more optimized to calculate failure in E1 Case Study has applicability in a more complex stacking sequence.

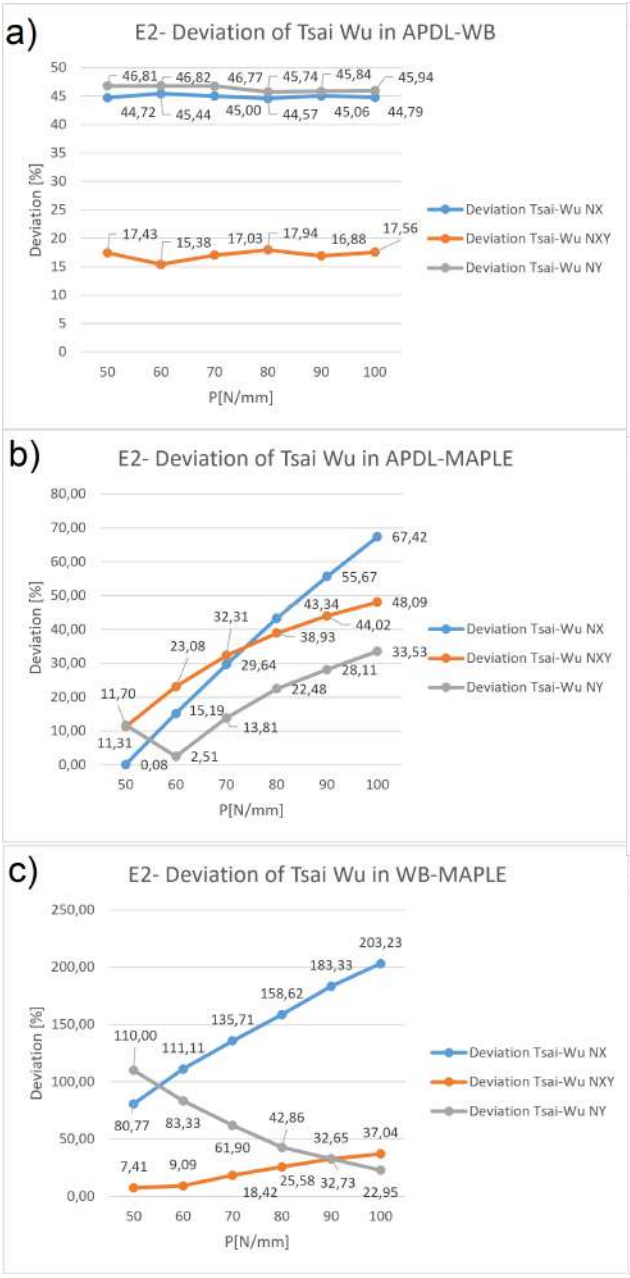

Figure 6.6: Deviation in Tsai Wu IF on E2 case Study in: a) APDL- Workbench; b) APDL-MAPLESOFT; c) Workbench-MAPLESOFT.

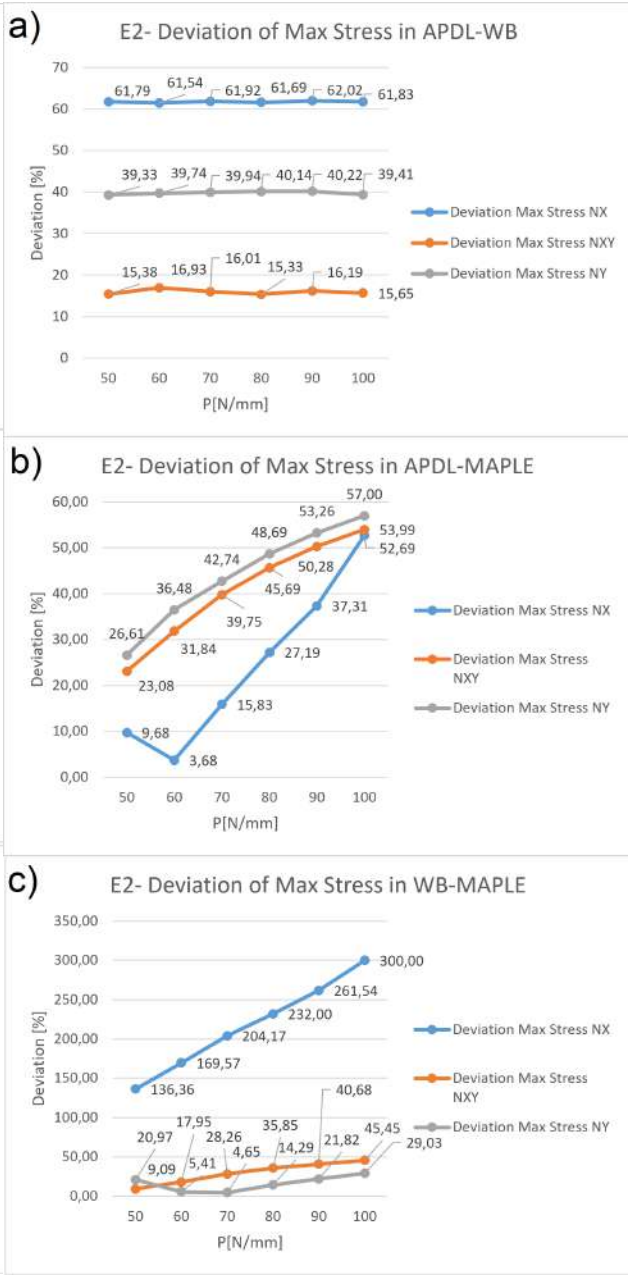

Figure 6.7: Deviation in Maximum Stress IF on E2 case Study in: a) APDL- Workbench; b) APDL-MAPLESOFT; c) Workbench-MAPLESOFT.

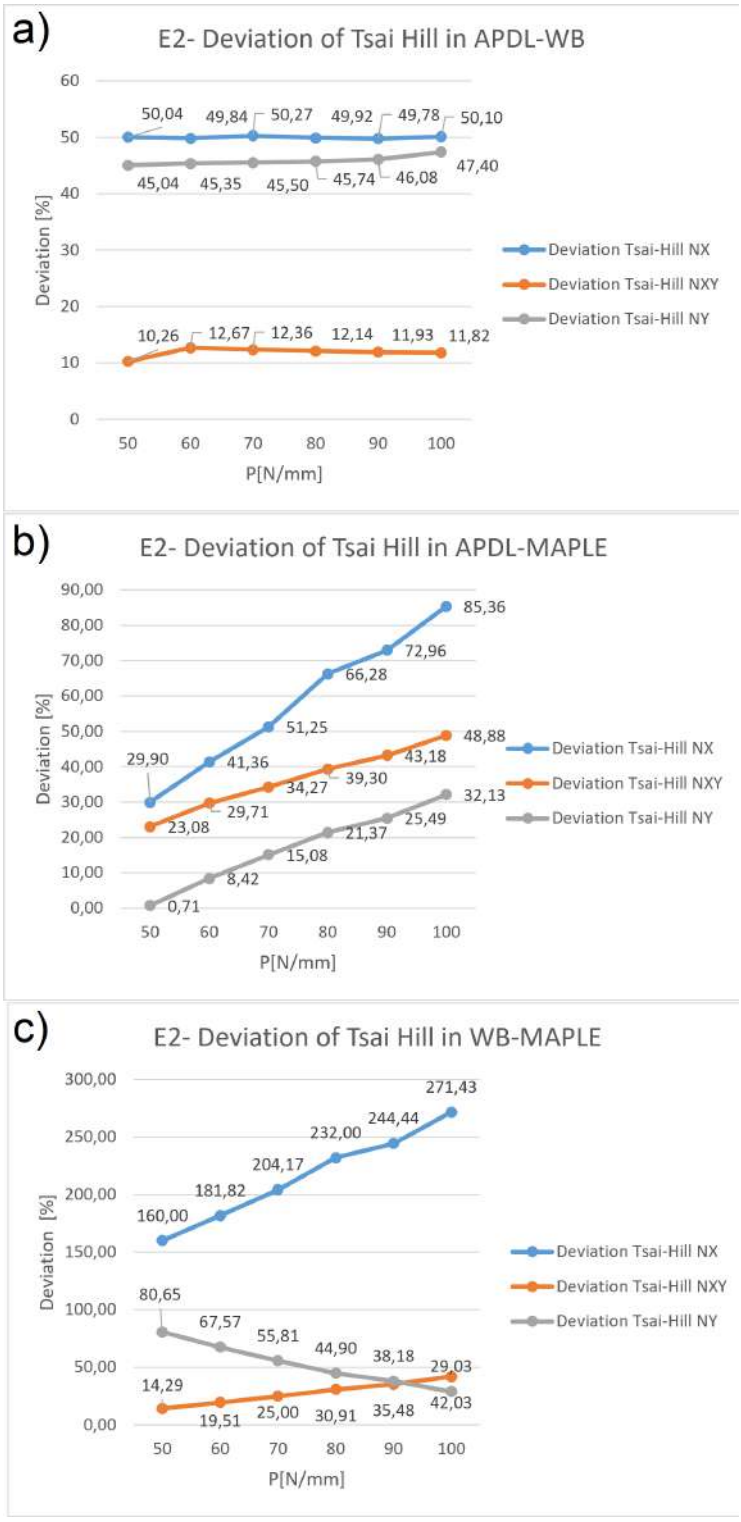

Figure 6.8: Deviation in Tsai-Hill IF on E2 case Study in: a) APDL- Workbench; b) APDL-MAPLESOFT; c) Workbench-MAPLESOFT.

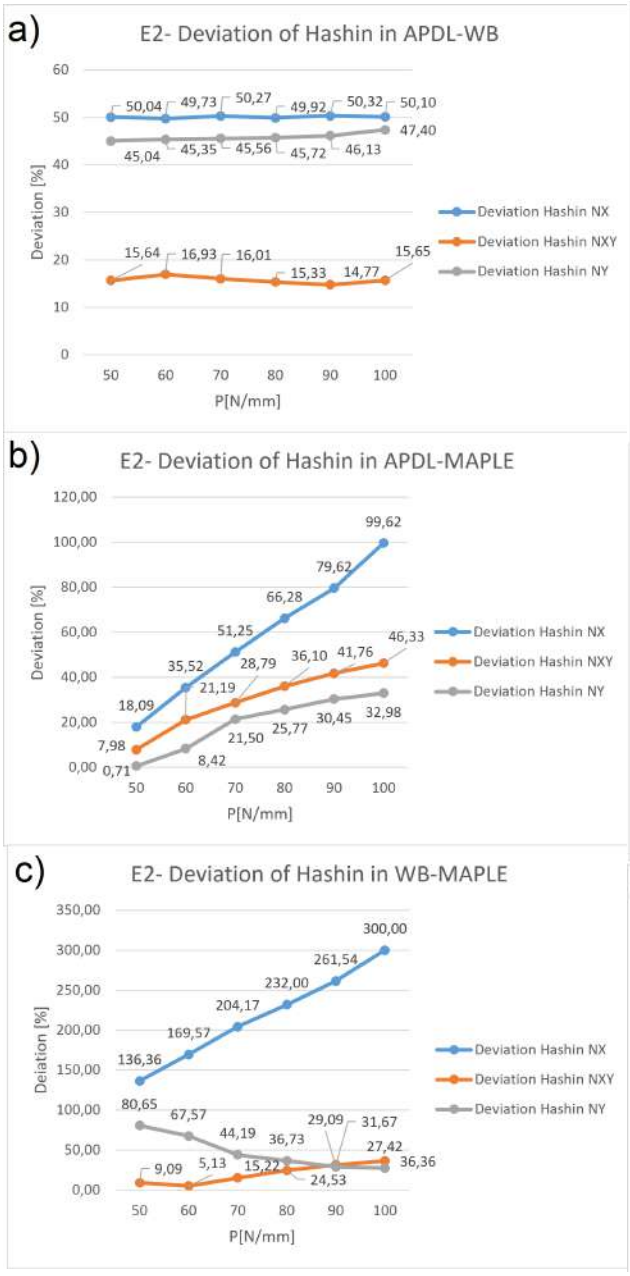

Figure 6.9: Deviation in Hashin IF on E2 case Study in: a) APDL- Workbench; b) APDL-MAPLESOFT; c) Workbench-MAPLESOFT.

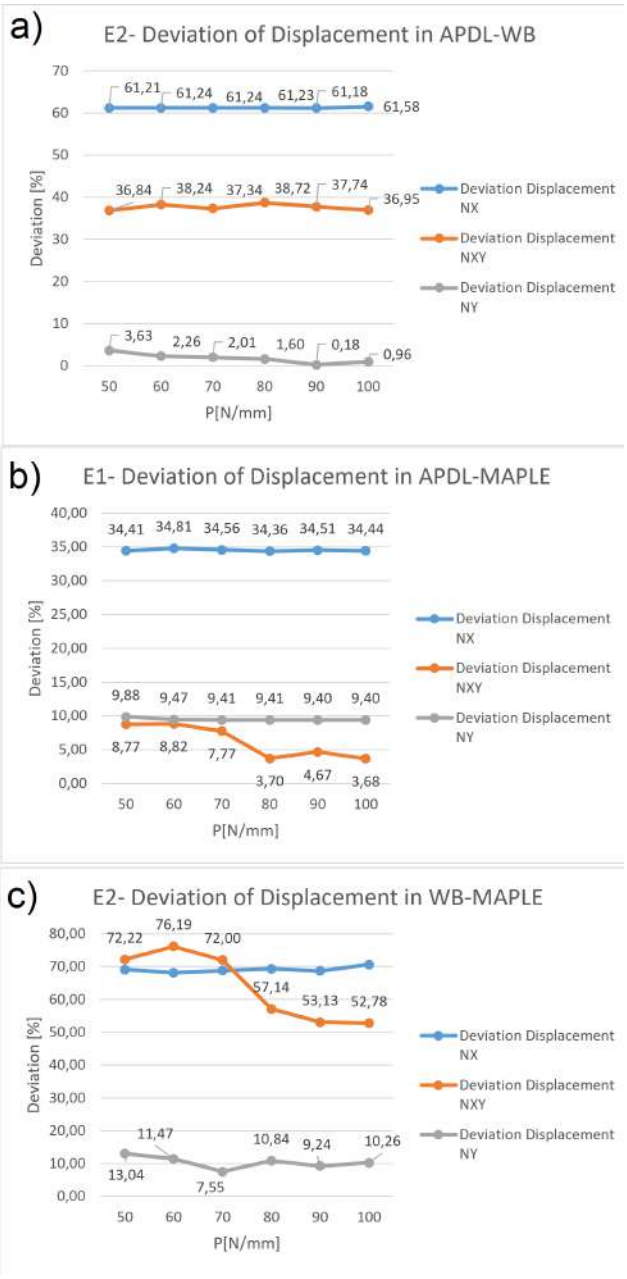

Figure 6.10: Deviation in Displacement on E2 case Study in: a) APDL- Workbench; b) APDL-MAPLESOFT; c) Workbench-MAPLESOFT.

Moreover, when analyzing the maximum displacement, the values reached have an overall order of magnitude completely different to the E1 Case Study. This will not only contribute to the over all higher volume of IF$>$1 present in the E2 Case Study at hand, but also the deviation of the same results (figure 6.6 to 6.10).The results with the most severe deviation are found not only on E2 (the subject with the most complex stacking sequence) as well as on the subjects that reached failure. Due to the sudden reduction of stiffness, when in the presence of crush/cracking, it introduces numerical instability to the model [27].

In summary, the results shown suggest the application of the Tsai-Hill or Hashin-Rottem Failure Criterion, much like the E1 Case Study. Utilizing the Mechanical APDL is also applicable for stacking sequences similar to E2 Case Study.

Chapter 7

Conclusions and Future works

7.1 Conclusions

Both the study of laminated plates and the triathlon handlebar study present a good comparison term between simple and complex geometry in the simulation setting.

In regards to the experimental mechanical properties of the specimens, both the E1 case study ([0/0/0/0])and E2 case study ([30/90/-30/60]) results were within the industry standard. However, the ν results were lower in value to the industry standard. This can be attributed to the possible presence of air bubbles that were trapped within the matrix in the manufacturing process.

In regards to the experimental phase, the same could not be achieved given the fact that both the E2 plates did not cure during the vacuum seal, as well as the bi-axial tensile device not properly clamping the test subjects. The E2 plates were made utilizing an older resin and curing agent that could have affected the result, as well as the instability of the vacuum seal in the curing phase.

Regarding the bi-axial tensile device, the clamping jaws did not fully cover the clamping area (only securing the very edge of the specimen).

In regards to the numerical/analytical studies, there is a clear indication of the degree and nature of the Hashin-Rottem and Tsai-Hill failure criterion in regards to the loads applied. When in the presence of relatively low loads (and therefore lower IF values), the Hashin-Rottem and Tsai-Hill IF show an overall decrease in value when compared to other failure criterion. However, when closer to the rupture point, both the criterion present a higher value of IF then the Maximum Stress and Tsai-Wu failure criterion. This results are applied on simpler stacking sequences (like the one found in E1 Case Study), as well as more complex stacking sequences (e.g. E2 Case Study).

There is also a clear relation between the methods utilized. Both analytical and Mechanical APDL method produced results very similar to the expected. However, the results produced via the Workbench method are easily spotted as outliers. There is a clear propagation of error in regards to the Workbench method, most likely stemming from the displacement calculation. The deviation is more prominent in NX loading configurations, in both case studies. The same conclusions can be drawn for the maximum displacement study.

In regards to the complex geometry study (triathlon handlebar), the design utilized did not interfered with the IF calculated.

7.2 Future Work

In regards to future work, the following developments are recommended:

- Improve the design of the bi-axial tensile testing device;
- Manufacture and test E1 and E2 case study plates;
- Optimize the triathlon handlebar design for mass, ergonomics and aerodynamics;
- Manufacture and test the triathlon handlebar model in a experimental setting;
- Study the effect of Puck and LARC03 Failure Criteria for both study cases;
- Study the effects of compression loads for both study cases.

References

[1] S.N. Mula, A.M.S. Leite and M.A.R. Loja. Analytical and numerial study of failure in composite plates. *Technopress*, Volume 4, Number 1: 23–41, 2022.

[2] J.N. Reddy. Mechanics of Laminated Composite Plates: Theory and Analysis. *CRC Press*. Second Edition. 112–156, 2004.

[3] I.M. Daniel and O. Ishai. Engineering Mechanics of Composite Materials. *Oxford University Press*. Second Edition. 63-90. 2006.

[4] G.H. Staab. Laminar Composites. *Butterworth-Heinemann*. Second Edition. 1999.

[5] M.E. Moreno, V. Tita, and F.D. Marques. Influence of boundary conditions on the determination of effective material properties for active fiber composites. *Proceedings... Pan-American Congress of Applied Mechanics*. Foz do Iguaçu, Brazil. 2010.

[6] M.F. Ashby. Materials Selection in Mechanical Design. *Butterworth-Heinemann*. Second Edition. 3-4. 2005.

[7] D.B. Miracle and S.L. Donaldson. ASM Handbook- Composites. *ASM International*. Second Edition. Vol. 21. 2001.

[8] ASTM D 3039/D 3039M. Standard Test Method for Tensile Properties of Polymer Matrix Composite Materials.

[9] ASTM D 3518/D 3518M. Standard Test Method for In-Plane Shear Response of Polymer Matrix Composite Materials by Tensile Test of a ±45º Laminate.

[10] R.M. Jones. Mechanics of Composite Materials. *Taylor and Francis*, Second Edition. 1999.

[11] P.K. Mallick. Fiber-Reinforced Composites: Material, Manufacturing and Design. *CRC Press*. Thrid Edition, 2007.

[12] M.F.S.F. Moura, A.B. Morais and A.G. Magalhães. Materiais Compósitos - Materiais, fabrico e comportamento mecânico. *Publindústria*, 200.

[13] D.A.A. Escárpita, D. Cárdenas, H. Elizalde, R. Ramirez and O. Probst. Biaxial Tensile Strength Characterization of Textile Composite Materials. Composites And Their Properties, 6, 2012.

[14] D.V. Hemelrijck, A. Makris, C. Ramault, E. Lamkanfi, W.V. Paepegem and D. Lecompte. Biaxial testing of fiber reinforced composite laminates. Materials: Design and Applications, 3, 2008.

[15] A.B. Pereira, F.A.O. Fernandes, A.B. de Morais and J. Maio. Biaxial Testile Machine: Development and Evaluation. MPDI, 2020.

[16] J.B.M. Sousa and A.R. da Silva. Analytical and numerical analysis of multilayered beams with interlayer slip. *Engineering Structures*, 32: 1671–1680, 2010.

[17] E.J. Barbero. Finite Element Analysis of Composite Materials. *Taylor and Francis Group*, Second Edition, 2014.

[18] F. París. A Study of Failure Criteria of Fibrous Composite Materials. NASA/CR-2001-210661. George Washington University, 2001

[19] P.D. Soden, M.J. Hinton and A.S. Kaddour. Lamina properties, lay-up configurations and loading conditions for a range of fiber-reinfornced composite laminates. Composites Science and Technology, 48, 1998.

[20] S. Imaoka. User-Defined Failure Criteria. ANSYS Release. 12.0.1, 2009.

[21] S. Yang, H. Gao, Q.Wu, S. Yuan, Z. Ye and Y. Zhao. Comprehensive mechanical properties and damage mechanisms of a new type multiphase fibers braided/phenolic resin composites. Journal of Alloys and Compounds. 7, 2024.

[22] M. Schemmann, J. Lang, A. Helfrich, T. Seelig, and T. Böhlke. Cruciform Specimen Design for Biaxial Tensile Testing of SMC.Discontinuous Fiber Composites, 2, 2018.

[23] D. Wyciągnięcie. Design of Bosch 30X30. GrabCad.com, 2015.

[24] M.T. Rafat, T.Z. Shuchi, F.R. Evan and M.A.Rahman. Mechanical and absorption properties of carbon-basalt and glass fiber reinforced composites: A comprehensive study with implications for advanced manufacturing technologyResults in Materials, 8, 2024.

[25] T. R. Kuphaldt. Chapter 8- DC Measuring circuits. Lessons in Electric Circuits, Vol.1-DC, 2000.

[26] H.H.F. Martins, M.B.F. Filho. Utilização de extensômetros para aquisição de forças no protótipo. Laboratório de Projeto de Engenharia, Universidade de São Paulo, 2019.

[27] ANSYS INC. ANSYS Mechanical APDL Performance Guide, 2013.

[28] M. Morais. Extensão de Aerodinâmica de Triatlo. Unidade Curricular de Projeto Mecânico, Área Departamental de Engenharia Mecânica Instituto Superior de Engenharia de Lisboa, 2021.

Annex A- Fiber and matrices technical data

UNIDIRECTIONAL CARBON FABRIC

24K and 300 gsm (width: 63 cm)

DESCRIPTION

300 gsm UNIDIRECTIONAL 24K CARBON FABRIC suitable for production of composite parts and tools with epoxy, vinyl ester and urethane-acrylic (Crestapol) resins. Ideal for specific reinforcements in certain directions of the composite part or tool.

Supplied covered with a protective and sealing plastic film. Additionally, the fabric yarns are held together thanks to the application of a thin thermoplastic thread on one side of the fabric. This thread is compatible with all thermosetting resins. Roll width: 63 cm.

CHARACTERISTICS

Test Report Nº	12458026-11
Item	SIGRATEX C U300-0/SO
Fiber type	SIGRAFIL C T24-4.8/240-E100
Carbon thread type	24K y 1600 tex
Areal Weight	303 +/-5%
Width	600 +/- 2%
Crimp	Scrimp on one side

TYPE OF SUPPLY

- 300 gsm Unidirectional 24K Carbon fabric x 1 linear m (0.63 m^2), supplied rolled in a cardboard box
- 300 gsm Unidirectional 24K Carbon fabric x 5 linear m (3.15 m^2), supplied rolled in a cardboard box
- 300 gsm Unidirectional 24K Carbon fabric x 25 linear m (15.75 m), supplied rolled in a cardboard box

*This technical data sheet has been created based on our latest knowledge and according to the best information and knowledge currently available. As we are unable to check if our products are used as recommended, we cannot guarantee the results. In spite of this, we will be glad to give an advice.

RESINAS CASTRO S.L.
Pol. Ind. A Granxa, 3ª Paralela
C/Cíes 190, 36400 O Porriño – ESPAÑA

Tlf.: +34 986 342 955 Fax: +34 986 342 520
E-mail: shop@castrocomposites.com
Web: www.castrocomposites.com

SR 1500
Système époxyde de stratification

Fort pouvoir mouillant et débullant.
Excellente adhésion sur tout type de renforts (verre, aramide, carbone, polyester...)
Réactivité modulable par le choix du durcisseur.
Durcisseurs miscibles en toutes proportions.
Systèmes utilisables après 7 à 14 jours à 20-25°C pour les durcisseurs **SD 2507**, **SD 2505** et **SD 2503**.
Post cuisson à 40 °C minimum, pour une tenue en température supérieure à 60 °C.
Développé pour: construction navale, aéronautique, prototypes automobiles, outillage.

Utilisations spécifiques :

SR 1500 / SD 2507, SD 2806 :
Stratifiés de faible épaisseur, durcissement à basse température (10 – 15°C).
Réparations et collages rapides, retouches, mastics...

SR 1500 / SD 2505, SD 2503:
Systèmes standards de stratification: pièces toutes dimensions, moules, joint-congés...

SR 1500 / SD 7561
Pièces de grandes dimensions ou de forte épaisseur de stratifié, injection, coulée
Long temps de travail du stratifié
Température de post-cuisson : 55 °C minimum

Autres formulations à base de résine SR 1500 :

SR 1500 i : Résine ignifugée M1
SR 1500 / SD 597.20: Coulée de gros volume et mousses syntactiques
SR 1500 JV : Contient un contrôleur de dosage. Résine jaune translucide devenant violette au contact du durcisseur. Dosages avec les durcisseurs standard inchangés.

Polymérisation :

Les durcisseurs **SD 2507**, **SD 2806** et **SD 2505** ont été développés pour offrir d'excellentes propriétés mécaniques à température ambiante

Sicomin, 31 avenue de la Lardière, 13220 Châteauneuf les Martigues, France
T: +33 (0)4 42 42 30 20 / F: +33 (0)4 42 81 29 29 / E: info@sicomin.com / www.sicomin.com

	SR 1500 / SD 2507 **SR 1500 / SD 2806** **SR 1500 / SD 2505**	**SR 1500 / SD 2503**	**SR 1500 / SD 7561**
Attendre à 20°C avant cuisson	2 à 4 heures	12 heures	24 heures
Cycle de cuisson minimum	2 à 7 jours à 20-25 °C	14 jours à 20-25 °C	12 heures à 60 °C
Cycle de cuisson préconisé	2 à 7 jours à 20 °C Ou 12 heures à 40 °C Ou 6 heures à 60 °C	14 jours à 20 °C Ou 24 heures à 40 °C Ou 8 heures à 60 °C	6 h à 40 °C + 12 heures à 60 °C

Résine époxy SR 1500

		SR 1500
Aspect		Liquide
Couleur		Claire
Viscosité (mPa.s)	15 °C	5 300 ± 1 000
Rhéomètre	20 °C	2 300 ± 500
CP 50 mm	25 °C	1 250 ± 250
gradient de	30 °C	750 ± 150
cisaillement 10 s^{-1}	40 °C	300 ± 60
Densité : Picnomètre NF EN ISO 2811-1	20 °C	1.13 ± 0.01
Stabilité au stockage:		24 mois, ne critallise pas

Durcisseurs SD xxxx

		SD 2507	**SD 2806**	**SD 2505**	**SD 2503**	**SD 7561**
Aspect / couleur:		Liquide jaune	Liquide jaune	Liquide jaune	Liquide jaune	Liquide transparent
Réactivité		Rapide	Réactivités intermédiaires			Ultra lent
Viscosité (mPa.s)						
Rhéomètre	20 °C	1 600 ± 300	300 ± 60	350 ± 70	210 ± 40	60 ± 15
CP 50 mm	25 °C	1 000 ± 200	200 ± 40	230 ± 40	150 ± 30	45 ± 10
gradient de cisaillement 10 s^{-1}	30 °C	600 ± 100	140 ± 30	150 ± 30	100 ± 20	35 ± 5
Densité Picnomètre NF EN ISO 2811-1	20 °C	1.09 ± 0.01	1.07 ± 0.01	1.00 ± 0.01	1.00 ± 0.01	0.96 ± 0.01

Mélanges SR 1500 / SD xxxx

		SR 1500 / SD 2507	SR 1500 / SD 2806	SR 1500 / SD 2505	SR 1500 / SD 2503	SR 1500 / SD 7561
Dosage en poids		**100 / 33 g**	**100 / 33 g**	**100 / 33 g**	**100 / 33 g**	**100 / 33 g**
Dosage volumique		**100 / 35 ml**	**100 / 35 ml**	**100 / 37 ml**	**100 / 37 ml**	**100 / 39 ml**
Viscosité (mPa.s)						
Rhéomètre	20 °C	2 200 ± 400	1 000 ± 200	800 ± 150	750 ± 150	650 ± 120
PP 50 mm	25 °C	1 500 ± 300	800 ± 150	650 ± 120	600 ± 120	450 ± 100
gradient de cisaillement 10 s^{-1}	30 °C	800 ± 150	550 ± 100	500 ± 100	400 ± 80	350 ± 70

Réactivité en masse sur 500 g de mélange

	SR 1500 / SD 2507	SR 1500 / SD 2806	SR 1500 / SD 2505	SR 1500 / SD 2503	SR 1500 / SD 7561
Température d'exothermie (°C) sur 500 g mélange:					
30°C	> 215 °C	> 215 °C	> 215 °C	> 215 °C	190 °C
25°C	> 215 °C	> 215 °C	> 215 °C	> 215 °C	117 °C
20°C	> 215 °C	> 215 °C	> 215 °C	> 215 °C	26 °C
Temps pour atteindre l'exothermie sur 500 g de mélange:					
30°C	11'	13'	15'	27'	2h 33'
25°C	10'	17'	20'	42'	4h 30'
20°C	13'	22'	30'	57'	8h
Temps pour atteindre 50°C sur 500 g de mélange:					
30°C	4'	9'	10'	18'	1h 50'
25°C	5'	12'	14'	33'	4h
20°C	11'	18'	25'	45'	-

Exotherme sur 500 g à 20 °C

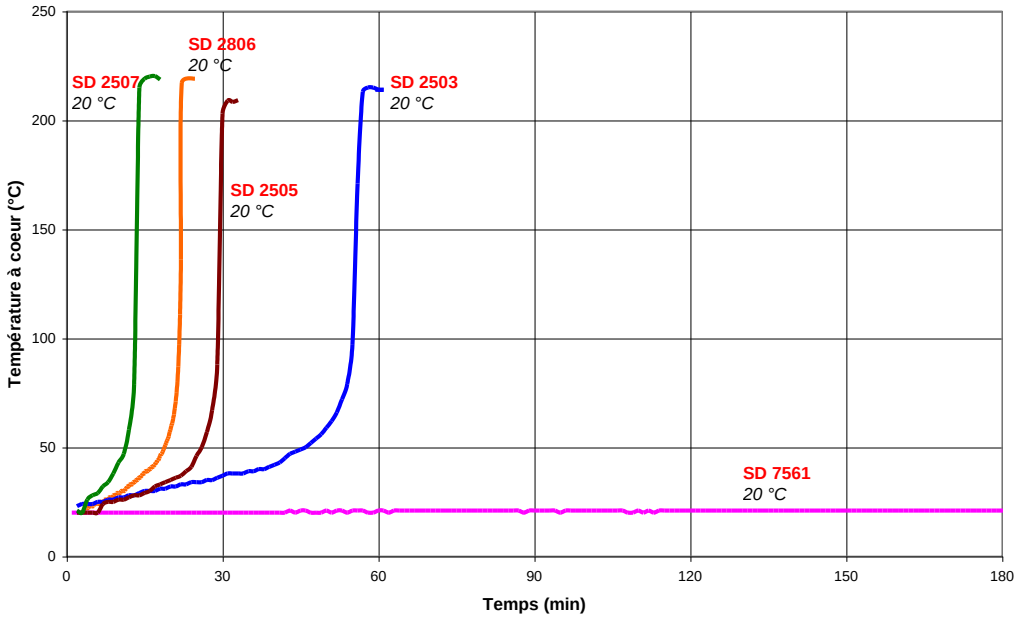

Réactivité - Suivi de viscosité sur film de 1 mm d'épaisseur

- **à 20 °C**

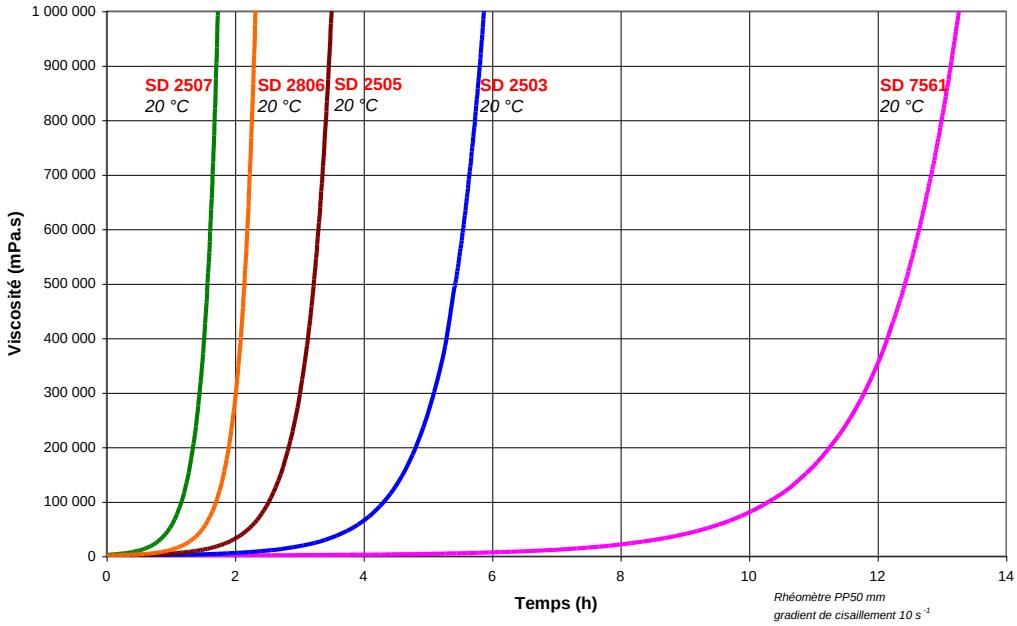

- **à 30 °C**

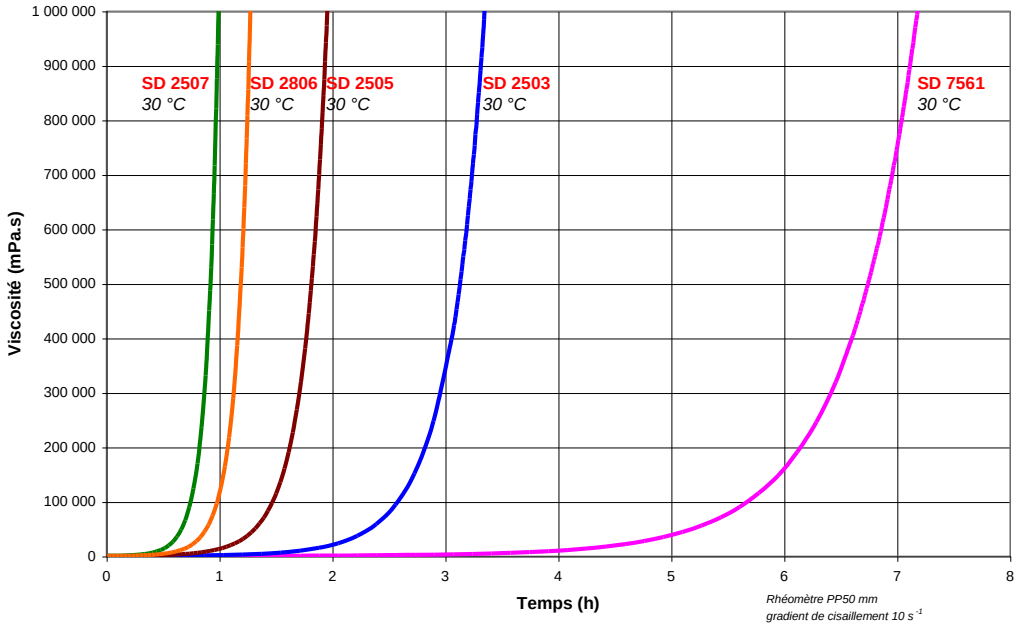

Propriétés mécaniques sur résine pure :

		SR 1500 / SD 2507			SR 1500 / SD 2806		
Cycles de polymérisation		14 jours 23 °C	24 h 23°C + 24h 40°C	24 h 23°C + 8h 60 °C	14 jours 23 °C	24 h 23°C + 24h 40°C	24 h 23°C + 16h 60 °C
Traction							
Module	N/mm^2	3300	3200	3140	3490	3340	3250
Résistance maximum	N/mm^2	80	80	80	68	79	81
Résistance à la rupture	N/mm^2	74	72	74	68	66	70
Allongement à l'effort maximum	%	3.7	3.9	4.3	2.3	3.7	4.0
Allongement à la rupture	%	4.5	4.7	5.6	2.3	6.0	7.0
Flexion							
Module	N/mm^2	3450	3400	3300	3580	3480	3420
Résistance maximum	N/mm^2	123	121	123	111	117	118
Allongement à l'effort maximum	%	4.8	5.0	5.4	3.9	9.5	5.0
Allongement à la rupture	%	7.8	8.1	8.4	4.7	4.6	8.8
Choc Charpy							
Résilience	kJ/m^2	19	27	24	13	8	8
Transition vitreuse							
Tg1	°C	55	69	73	54	65	62
Tg1 max.	°C			75			72

Essais réalisés sur des éprouvettes de résine pure coulée, sans dégazage préalable, entre des plaques en acier.
Mesures effectuées suivant les normes :

Traction :	NF T51-034
Flexion :	NF T51-001
Compression:	NF T 51-101
Choc Charpy:	NF T51-501
Transition vitreuse:	ISO 11357-2 : 1999 -5°C/180°C sous azote Tg1 ou Onset : 1er point à 20 °C/mn Tg1 maximum ou Onset : deuxième passage

Sicomin, 31 avenue de la Lardière, 13220 Châteauneuf les Martigues, France
T: +33 (0)4 42 42 30 20 / F: +33 (0)4 42 81 29 29 / E: info@sicomin.com / www.sicomin.com

Propriétés mécaniques sur résine pure :

		SR 1500 / SD 2505			SR 1500 / SD 2503		SR 1500 / SD 7561		
Cycles de polymérisation		14 jours 23 °C	24 h 23°C + 24h 40°C	24 h 23°C + 8h 60 °C	14 jours 23 °C	24 h 23°C + 8h 60 °C	14 jours 23 °C	24 h 23°C + 24h 40°C	24 h 23°C + 16h 60 °C
Traction									
Module	N/mm^2	3100	2900	2900	3350	2860	3000	3000	2900
Résistance maximum	N/mm^2	77	74	74	77	71	48	67	68
Résistance à la rupture	N/mm^2	71	68	68	72	65	48	67	67
Allongement à l'effort maximum	%	3.6	4.4	4.7	3.6	4.7	1.9	2.7	3.8
Allongement à la rupture	%	4.5	6.0	7.4	5.4	8.0	1.9	2.8	4.2
Flexion									
Module	N/mm^2	3200	3100	3100	3300	2760	3250	3100	3100
Résistance maximum	N/mm^2	115	115	117	125	123	77	112	122
Allongement à l'effort maximum	%	4.8	5.4	5.6	4.6	6.4	2.3	3.7	5.3
Allongement à la rupture	%	7.7	8	7.9	7.2	7.5	2.6	3.8	6.9
Choc Charpy									
Résilience	kJ/m^2	25	30	26	12	30	28	15	24
Transition vitreuse									
Tg1	°C	56	68	72	55	70	55	69	89
Tg1 max.	°C			76		76			92

Essais réalisés sur des éprouvettes de résine pure coulée, sans dégazage préalable, entre des plaques en acier.
Mesures effectuées suivant les normes :

Traction :	NF T51-034
Flexion :	NF T51-001
Compression:	NF T 51-101
Choc Charpy:	NF T51-501
Transition vitreuse:	ISO 11357-2 : 1999 -5°C/180°C sous azote Tg1 ou Onset : 1er point à 20 °C/mn Tg1 maximum ou Onset : deuxième passage

Sicomin, 31 avenue de la Lardière, 13220 Châteauneuf les Martigues, France
T: +33 (0)4 42 42 30 20 / F: +33 (0)4 42 81 29 29 / E: info@sicomin.com / www.sicomin.com

Propriétés mécaniques des stratifiés à base de résine SR 1500 :

Echantillonnage		
Matrice		**SR 1500 / SD 7561**
Renfort		3300
Nombre de couches		15
Mise en œuvre		Presse
Taux massique de renfort (Mf)		76.5
Post-cuisson		16 h 60 °C
Flexion		
Module	N/mm^2	24 600
Résistance maximum	N/mm^2	625
Allongement. à l'effort maximum	%	2.93
Délaminage en flexion		
Contrainte de cisaillement	N/mm^2	55
Choc Charpy		
Résilience	kJ/m^2	211
Absorption d'eau	%poids	0.11
Transition vitreuse		
Tg 1	°C	81
Tg 1 max.	°C	88

Essais réalisés selon les normes:

Flexion :	NF T 57-105
Délaminage en flexion:	NF T 57-104
Choc Charpy:	NF T 57-108
Reprise en eau:	Interne. Polymérisation selon cycle, usinage, pesée, séjour dans eau distillée à 70 °C / 48 heures séchage 24 h à 40°C, pesée, tests mécaniques sur 10 éprouvettes
Transition vitreuse:	ISO 11357-2 : 1999 -5°C/180°C sous azote Tg1 ou Onset : 1er point à 20 °C/mn Tg1 maximum ou Onset : deuxième passage
Renfort 3300:	Sergé 2/2 Verre E, grammage 300 g/m^2

Sicomin, 31 avenue de la Lardière, 13220 Châteauneuf les Martigues, France
T: +33 (0)4 42 42 30 20 / F: +33 (0)4 42 81 29 29 / E: info@sicomin.com / www.sicomin.com

Les informations que nous donnons par écrit ou verbalement dans le cadre de notre assistance technique et de nos essais n'engagent pas notre responsabilité. Nous conseillons aux utilisateurs des systèmes époxydes SICOMIN, de vérifier par des essais pratiques si nos produits conviennent aux procédés et applications envisagés. L'utilisation, la mise en oeuvre et la transformation des produits fournis échappent à notre contrôle et relèvent exclusivement de votre responsabilité.
Si notre responsabilité devait néanmoins se trouver engagée, elle se limiterait , pour tous les dommages, à la valeur de la marchandise fournie par nous et mise en oeuvre par vos soins. Nous garantissons la qualité irréprochable de nos produits dans le cadre de nos conditions générales de ventes et de livraison.

Sicomin, 31 avenue de la Lardière, 13220 Châteauneuf les Martigues, France
T: +33 (0)4 42 42 30 20 / F: +33 (0)4 42 81 29 29 / E: info@sicomin.com / www.sicomin.com

an HBK company

Dehnungsmessstreifen
Strain gages
Jauges d'extensométrie

Bestellnummer Order No. No. de référence	**1-CLY41-6/120ZE**
Typ Type Type	6/120ZE LY41
Widerstand Resistance Résistance	120 Ω ±0.35 %
Stückzahl Number of pieces Quantité	10
k-Faktor Gauge factor Facteur k	2.11 ±1.0 %
Temperaturkoeffizient des k-Faktors Temperature coefficient of gauge factor Coefficient de température du facteur k	93 ±10 [10^{-6} / K]
Querempfindlichkeit Transverse sensitivity Sensibilité transverse	0.1 %
Folienlos Foil lot Lot de la feuille	A436/10
Herstellungslos Production batch Lot de fabrication	812115233

Daten / Data / Données

Temperaturkompensation: Ferritischer Stahl mit
Temperature compensation: Ferritic steel with
Compensation de température: Acier avec

$\alpha = 10.8\ [10^{-6}\ /\ K]$

RoHS

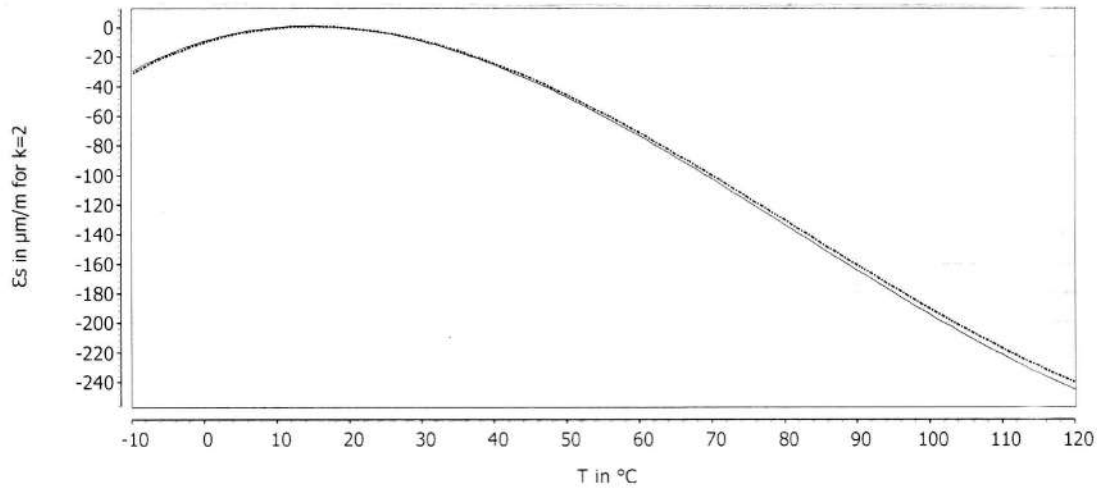

$$\varepsilon_S(T) = -9.22 + 1.48 * \mathbf{T} - 5.63E\text{-}02 * \mathbf{T}^2 + 2.30E\text{-}04 * \mathbf{T}^3$$

Kombinierte Standardunsicherheit zu $\varepsilon_S(T)$
Combined standard uncertainty for $\varepsilon_S(T)$
Incertitude standard combinée pour $\varepsilon_S(T)$

$u_c = \pm 0.30 * \Delta T$

Einfluss Drähte / Kabel
Influence wires / cables
Influence des fils / câbles

$\varepsilon_w = 0.0501 * \Delta T$

Referenztemperatur
Reference temperature
Température de référence

$T_{ref} = 20°C$

Zur leichteren Lesbarkeit sind die Einheiten entfallen. Dehnung in µm/m und Temperatur in °C
For easier readability, the units have been omitted. Elongation in µm/m and temperature in °C
Pour faciliter la lecture, les unités ont été supprimées. Allongement en µm/m et température en °C

$$\Delta T = T - T_{ref}$$

Temperaturgang der Dehnungsmessstreifen bei Applikationen auf Werkstoffen mit dem oben angegebenen Wärmeausdehnungskoeffizienten α.

— **Kennlinie 1:** DMS ohne Anschlussbändchen
Kennlinie 2: DMS mit Anschlussbändchen der Länge 50 mm

The **temperature response** of strain gauges for applications on materials with the coefficient of thermal expansion α specified above.

— **Curve 1:** Strain gauge without leads
Curve 2: Strain gauge with leads of length 50 mm

Réponse en température des jauges de contrainte pour les applications sur des matériaux ayant le coefficient de dilatation thermique α indiqué ci-dessus.

— **Courbe 1:** Jauge d'extensométrie sans fils
Courbe 2: Jauge de contrainte avec des fils de longueur 50 mm

Alle technischen Daten nach VDI/VDE 2635.
All specifications in accordance with VDI/VDE 2635.
Toutes les caractéristiques techniques selon la norme VDI/VDE 2635.

Kopfdaten / Header / Titre

A point (".") is used as decimal separator in data; the separator needs to be configured accordingly for import into Excel.

Rev. 02.2019 HBM Messfolien Folie

Overview of measuring ranges

Type	Unit	SR55 (CF 4,8 kHz)	SR30 (CF 600Hz)	SR01 (DC)
SG/inductive	mV/V	±3; ±12, ±125; ±500		—
Voltage	V	±10		±0,1; ±1; ±10
Current	mA	—		±20; ±200
Resistance	Ω	—		400; 4000
Frequency	kHz	0,1; 1;10; 100; 1000	—	—
Period length	s	0,01; 0,1; 1; 10; 100	—	—
Counter	d	25.000; 2.500.000	—	—

Appendix A- APDL study

In this appendix, both the APDL code for the E1 and E2 cases are shown, for the NX load configurations.

```
    !.....................................................................!
    ! E1NX !
    !.....................................................................!
FINISH
/CLEAR
/filename, E1NX   ! Nome do ficheiro
/PREP7
!/TITLE, Estudo de uma placa em composito Carbono/Epoxi
/UNITS,MPA              ! Unidades: [mm ; MPa ; Newtons]
!.....................................................................................
! DefiniÃ§Ã£o do tipo de elemento
ET,1,SHELL281           ! Tipo de elemento
kEYOPT,1,8,1            ! Mostra a sequÃªncia das lÃ¢minas

! "For cycle" PressÃ£o a aplicar [N/mm]
*DO, P, 150, 200, 10 !For P=150 to 200 [N/mm]
!.....................................................................................
!DefiniÃ§Ã£o das dimenÃ§Ãµes da placa
!Comprimento
C=150           ! [mm]

!Largura
L=150            ! [mm]

!Espessura
h=0.25            ! [mm]

!.....................................................................................
!Definição das placas e das orientações das fibras
!Orientações: [0/90/45/-45]s=[0/90/45/-45/-45/45/90/0]

SECTYPE,1,SHELL
SECDATA,h,1,0      ! 1ª Camada: Espessura 0.25 mm: mat. #1: Theta 0 deg
SECDATA,h,1,0      ! 2ª Camada: Espessura 0.25 mm: mat. #1: Theta 0 deg
SECDATA,h,1,0     ! 3ª Camada: Espessura 0.25 mm: mat. #1: Theta 0 deg
SECDATA,h,1,0     ! 4ª Camada: Espessura 0.25 mm: mat. #1: Theta 0 deg

SECOFFSET,MID      ! Nós na na espessura do laminado do meio
!.....................................................................................
!Propriadades do material AS4/3501-6 (Graphite/Epoxy)
E1=126E+03         ! [MPa]
E2=11E+03          ! [MPa]
E3=11E+03          ! [MPa]

v12=0.28
v13=0.28
v23=0.52

G12=6.6E+03         ! [MPa]
G13=6.6E+03         ! [MPa]
G23=3.618E+03       ! [MPa]

Rho=1.550E-06
!DefiniÃ§Ã£o das propriadades do material
MPTEMP,,,,,,,,          ! Material Ortotropico - Carbono/EpÃ³xi
MPTEMP,1,0
MPDATA,EX,1,,E1
MPDATA,EY,1,,E2
MPDATA,EZ,1,,E3
MPDATA,PRXY,1,,v12
MPDATA,PRXZ,1,,v13
MPDATA,PRYZ,1,,v23
MPDATA,GXY,1,,G12
MPDATA,GXZ,1,,G13
```

```
MPDATA,GYZ,1,,G23

!.....................................................................
!DefiniÃ§Ã£o da geometria e da malha da placa
RECTNG,0,C,0,L           ! Placa retangular cxl [1000x1000]
ESIZE,,15                ! NÃºmero de divisÃµes por cada linha= 15
AMESH,ALL                ! MESH da Ã¡rea (geraÃ§Ã£o da malha)
FINISH                   ! Fim do mÃ³dulo PrÃ©-processamento

/SOLU                    ! MÃ³dulo da soluÃ§Ã£o
ANTYPE,STATIC            ! AnÃ¡lise estÃ¡tica
!.....................................................................
! DefiniÃ§Ã£o das CondiÃ§Ãµes de fronteira
DL,4,1,UX,0   ! Constrangimento de modo a evitar movimento na linha 4
DL,4,1,UZ,0
DK,1,UY,0     ! Constrangimento de modo a evitar movimento no ponto 1
DL,2,1,UZ,0   ! Constrangimento de modo a evitar movimento na linha 2


SFL,2,PRES,-P        ! AplicaÃ§Ã£o da pressÃ£o uniforme aplicada na linha 3 da
placa
/PSF,PRES,NORM,2,1,1 ! Apresenta a pressÃ£o distribuÃda uniformemente na linha 3


SOLVE             ! Resolve o estado da carga em estudo
FINISH            ! Fim do mÃ³dulo de soluÃ§Ã£o
/POST1            ! MÃ³dulo PÃ³s processamento
SET,LAST          ! Apresenta a deformada da placa
RSYS,LSYS         ! Sistema de coordenadas da lÃ¢mina

!.....................................................................
! Fatores de falha da placa
!Propriadades dos fatores de falha AS4/3501-6 (Graphite/Epoxy)
F1t=1950         ! [MPa]
F2t=48           ! [MPa]
F3t=48           ! [MPa]

F1c=1480         ! [MPa]
F2c=200          ! [MPa]
F3c=200          ! [MPa]

F4=1E+04         ! [MPa]
F5=1E+04         ! [MPa]
F6=79            ! [MPa]

!Coeficientes de Tsai-Wu [-1 (predefinido)]
C4=-1
C5=-1
C6=-1
!DefiniÃ§Ã£o do criterio de falha
FC,1,S,XTEN,F1t           ! TensÃ£o de Rotura Longitudinal Ã  TraÃ§Ã£o F1t
FC,1,S,XCMP,-F1c          ! TensÃ£o de Rotura Longitudinal Ã  CompressÃ£o F1c
FC,1,S,YTEN,F2t           ! TensÃ£o de Rotura Transversal Ã  TraÃ§Ã£o F2t
FC,1,S,YCMP,-F2c          ! TensÃ£o de Rotura Transversal Ã  CompressÃ£o F2c
FC,1,S,ZTEN,F3t           ! TensÃ£o de Rotura Transversal Ã  TraÃ§Ã£o F3t
FC,1,S,ZCMP,-F3c          ! TensÃ£o de Rotura Transversal Ã  CompressÃ£o F3c
FC,1,S,XY,F6              ! TensÃ£o de Rotura no plano de Corte F6
FC,1,S,YZ,F4              ! TensÃ£o de Rotura no plano de Corte F4
FC,1,S,XZ,F5              ! TensÃ£o de Rotura no plano de Corte F5
FC,1,S,YZCP,C4            ! Coeficiente de Tsai-Wu C4: Predefinido para -1
FC,1,S,XZCP,C5            ! Coeficiente de Tsai-Wu C5: Predefinido para -1
FC,1,S,XYCPCP,C6          ! Coeficiente de Tsai-Wu C6: Predefinido para -1

!.....................................................................
```

```
!*
RSYS,SOLU
AVPRIN,0
SHELL,MID
AVRES,2,
/EFACET,1

LAYER,3

FORCE,TOTAL
/PLOPTS, DATE, 0
JPEG, COLOR, 0
PLNSOL, FAIL, MAX, 2,1.0
/IMAGE, SAVE,strcat(chrval(P),'TH'), png
PLNSOL, FAIL,TWSR, 2,1.0
/IMAGE, SAVE,strcat(chrval(P),'TWSR'), png
PLNSOL, FAIL, SMAX
/IMAGE, SAVE, strcat(chrval(P),'SMAX'), png
PLNSOL, U, SUM
/IMAGE, SAVE, strcat(chrval(P),'USUM'), png

*ENDDO
```

```
    !.....................................................................!
    ! E2NX !
    !.....................................................................!

FINISH
/CLEAR
/filename, E2NX    ! Nome do ficheiro
/PREP7
!/TITLE, Estudo de uma placa em composito Carbono/Epoxi
/UNITS,MPA              ! Unidades: [mm ; MPa ; Newtons]

!.....................................................................................
! Definição do tipo de elemento
ET,1,SHELL281           ! Tipo de elemento
kEYOPT,1,8,1            ! Mostra a sequência das lâminas

! "For cycle" PressÃ£o a aplicar [N/mm]
*DO, P, 50, 100, 10 !For P=50 to 100 [N/mm]
!.....................................................................................
!Definição das dimenções da placa
!Comprimento
C=150            ! [mm]

!Largura
L=150            ! [mm]

!Espessura
h=0.25            ! [mm]

!.....................................................................................
!Definição das placas e das orientações das fibras
!Orientações: [30/90/-30/30]

SECTYPE,1,SHELL
SECDATA,h,1,30      ! 1ª Camada: Espessura 0.25 mm: mat. #1: Theta 30 deg
SECDATA,h,1,90      ! 2ª Camada: Espessura 0.25 mm: mat. #1: Theta 90 deg
SECDATA,h,1,-30     ! 3ª Camada: Espessura 0.25 mm: mat. #1: Theta -30 deg
SECDATA,h,1,30      ! 4ª Camada: Espessura 0.25 mm: mat. #1: Theta 30 deg

SECOFFSET,MID       ! Nós na na espessura do laminado do meio

!.....................................................................................
!Propriadades do material
E1=45.6E+03         ! [MPa]
E2=16.2E+03         ! [MPa]
E3=16.2E+03         ! [MPa]

v12=0.278
v13=0.278
v23=0.40

G12=5.83E+03        ! [MPa]
G13=5.83E+03        ! [MPa]
G23=5.7E+03         ! [MPa]

Rho=1.550E-06

!Definição das propriadades do material
MPTEMP,,,,,,,,          ! Material Ortotropico - Carbono/Epóxi
MPTEMP,1,0
MPDATA,EX,1,,E1
MPDATA,EY,1,,E2
MPDATA,EZ,1,,E3
MPDATA,PRXY,1,,v12
```

```
MPDATA,PRXZ,1,,v13
MPDATA,PRYZ,1,,v23
MPDATA,GXY,1,,G12
MPDATA,GXZ,1,,G13
MPDATA,GYZ,1,,G23

!.....................................................................
!Definição da geometria e da malha da placa
RECTNG,0,C,0,L           ! Placa retangular cxl [1000x1000]
ESIZE,,15                ! Número de divisões por cada linha= 15
AMESH,ALL                ! MESH da área (geração da malha)
FINISH                   ! Fim do módulo Pré-processamento

/SOLU                    ! Módulo da solução
ANTYPE,STATIC            ! Análise estática
!.....................................................................
! Definição das Condições de fronteira

DL,4,1,UX,0   ! Constrangimento de modo a evitar movimento na linha 4
DL,4,1,UZ,0
DK,1,UY,0     ! Constrangimento de modo a evitar movimento no ponto 1
DL,2,1,UZ,0   ! Constrangimento de modo a evitar movimento na linha 2


SFL,2,PRES,-P        ! Aplicação da pressão uniforme aplicada na linha 3 da
placa
/PSF,PRES,NORM,2,1,1 ! Apresenta a pressão distribuída uniformemente na linha 3

SOLVE             ! Resolve o estado da carga em estudo
FINISH            ! Fim do módulo de solução
/POST1            ! Módulo Pós processamento
SET,LAST          ! Apresenta a deformada da placa
RSYS,LSYS         ! Sistema de coordenadas da lâmina

!.....................................................................
! Fatores de falha da placa
!Propriadades dos fatores de falha
F1t=1280         ! [MPa]
F2t=40           ! [MPa]
F3t=40           ! [MPa]

F1c=800          ! [MPa]
F2c=145          ! [MPa]
F3c=145          ! [MPa]

F4=1E+04         ! [MPa]
F5=1E+04         ! [MPa]
F6=73            ! [MPa]

!Coeficientes de Tsai-Wu [-1 (predefinido)]
C4=-1
C5=-1
C6=-1

!Definição do criterio de falha
FC,1,S,XTEN,F1t           ! Tensão de Rotura Longitudinal à Tração F1t
FC,1,S,XCMP,-F1c          ! Tensão de Rotura Longitudinal à Compressão F1c
FC,1,S,YTEN,F2t           ! Tensão de Rotura Transversal à Tração F2t
FC,1,S,YCMP,-F2c          ! Tensão de Rotura Transversal à Compressão F2c
FC,1,S,ZTEN,F3t           ! Tensão de Rotura Transversal à Tração F3t
FC,1,S,ZCMP,-F3c          ! Tensão de Rotura Transversal à Compressão F3c
FC,1,S,XY,F6              ! Tensão de Rotura no plano de Corte F6
FC,1,S,YZ,F4              ! Tensão de Rotura no plano de Corte F4
FC,1,S,XZ,F5              ! Tensão de Rotura no plano de Corte F5
```

```
FC,1,S,YZCP,C4           ! Coeficiente de Tsai-Wu C4: Predefinido para -1
FC,1,S,XZCP,C5           ! Coeficiente de Tsai-Wu C5: Predefinido para -1
FC,1,S,XYCPCP,C6         ! Coeficiente de Tsai-Wu C6: Predefinido para -1

!.....................................................................
!Resultados para primeira lâmina:
!LAYER,2                  ! Tabela com os resultados da primeira lâmina
!PRNSOL,S,FAIL            ! Apresenta uma tabela com os índices de falha
!PLNSOL,S,TWSR            ! Apresenta o IF para o critério de TSAI-WU
!PLNSOL,S,MAXF            ! Apresenta o IF para o critério da Tensão Máxima

!*
RSYS,SOLU
AVPRIN,0
SHELL,MID
AVRES,2,
/EFACET,1

LAYER,2

FORCE,TOTAL

/DSCALE,ALL,1.0
/EFACET,1
/PLOPTS, DATE, 0
JPEG, COLOR, 0
PLNSOL, FAIL, MAX, 2,1.0
/IMAGE, SAVE,strcat(chrval(P),'TH'), png
PLNSOL, FAIL,TWSR, 2,1.0
/IMAGE, SAVE,strcat(chrval(P),'TWSR'), png
PLNSOL, FAIL, SMAX
/IMAGE, SAVE, strcat(chrval(P),'SMAX'), png
PLNSOL, U, SUM
/IMAGE, SAVE, strcat(chrval(P),'USUM'), png

*ENDDO
```

```
    !.....................................................................!
    ! E1NX !
    !.....................................................................!
FINISH
/CLEAR
/filename, E1NX   ! Nome do ficheiro
/PREP7
!/TITLE, Estudo de uma placa em composito Carbono/Epoxi
/UNITS,MPA              ! Unidades: [mm ; MPa ; Newtons]
!.....................................................................................
! DefiniÃ§Ã£o do tipo de elemento
ET,1,SHELL281           ! Tipo de elemento
kEYOPT,1,8,1            ! Mostra a sequÃªncia das lÃ¢minas

! "For cycle" PressÃ£o a aplicar [N/mm]
*DO, P, 150, 200, 10 !For P=150 to 200 [N/mm]
!.....................................................................................
!DefiniÃ§Ã£o das dimenÃ§Ãµes da placa
!Comprimento
C=150           ! [mm]

!Largura
L=150            ! [mm]

!Espessura
h=0.25            ! [mm]

!.....................................................................................
!Definição das placas e das orientações das fibras
!Orientações: [0/90/45/-45]s=[0/90/45/-45/-45/45/90/0]

SECTYPE,1,SHELL
SECDATA,h,1,0      ! 1ª Camada: Espessura 0.25 mm: mat. #1: Theta 0 deg
SECDATA,h,1,0      ! 2ª Camada: Espessura 0.25 mm: mat. #1: Theta 0 deg
SECDATA,h,1,0     ! 3ª Camada: Espessura 0.25 mm: mat. #1: Theta 0 deg
SECDATA,h,1,0     ! 4ª Camada: Espessura 0.25 mm: mat. #1: Theta 0 deg

SECOFFSET,MID      ! Nós na na espessura do laminado do meio
!.....................................................................................
!Propriadades do material AS4/3501-6 (Graphite/Epoxy)
E1=126E+03         ! [MPa]
E2=11E+03          ! [MPa]
E3=11E+03          ! [MPa]

v12=0.28
v13=0.28
v23=0.52

G12=6.6E+03         ! [MPa]
G13=6.6E+03         ! [MPa]
G23=3.618E+03       ! [MPa]

Rho=1.550E-06
!DefiniÃ§Ã£o das propriadades do material
MPTEMP,,,,,,,,          ! Material Ortotropico - Carbono/EpÃ³xi
MPTEMP,1,0
MPDATA,EX,1,,E1
MPDATA,EY,1,,E2
MPDATA,EZ,1,,E3
MPDATA,PRXY,1,,v12
MPDATA,PRXZ,1,,v13
MPDATA,PRYZ,1,,v23
MPDATA,GXY,1,,G12
MPDATA,GXZ,1,,G13
```

```
MPDATA,GYZ,1,,G23

!.....................................................................
!DefiniÃ§Ã£o da geometria e da malha da placa
RECTNG,0,C,0,L           ! Placa retangular cxl [1000x1000]
ESIZE,,15                ! NÃºmero de divisÃµes por cada linha= 15
AMESH,ALL                ! MESH da Ã¡rea (geraÃ§Ã£o da malha)
FINISH                   ! Fim do mÃ³dulo PrÃ©-processamento

/SOLU                    ! MÃ³dulo da soluÃ§Ã£o
ANTYPE,STATIC            ! AnÃ¡lise estÃ¡tica
!.....................................................................
! DefiniÃ§Ã£o das CondiÃ§Ãµes de fronteira
DL,4,1,UX,0   ! Constrangimento de modo a evitar movimento na linha 4
DL,4,1,UZ,0
DK,1,UY,0     ! Constrangimento de modo a evitar movimento no ponto 1
DL,2,1,UZ,0   ! Constrangimento de modo a evitar movimento na linha 2


SFL,2,PRES,-P        ! AplicaÃ§Ã£o da pressÃ£o uniforme aplicada na linha 3 da
placa
/PSF,PRES,NORM,2,1,1 ! Apresenta a pressÃ£o distribuÃda uniformemente na linha 3


SOLVE             ! Resolve o estado da carga em estudo
FINISH            ! Fim do mÃ³dulo de soluÃ§Ã£o
/POST1            ! MÃ³dulo PÃ³s processamento
SET,LAST          ! Apresenta a deformada da placa
RSYS,LSYS         ! Sistema de coordenadas da lÃ¢mina

!.....................................................................
! Fatores de falha da placa
!Propriadades dos fatores de falha AS4/3501-6 (Graphite/Epoxy)
F1t=1950         ! [MPa]
F2t=48           ! [MPa]
F3t=48           ! [MPa]

F1c=1480         ! [MPa]
F2c=200          ! [MPa]
F3c=200          ! [MPa]

F4=1E+04         ! [MPa]
F5=1E+04         ! [MPa]
F6=79            ! [MPa]

!Coeficientes de Tsai-Wu [-1 (predefinido)]
C4=-1
C5=-1
C6=-1
!DefiniÃ§Ã£o do criterio de falha
FC,1,S,XTEN,F1t           ! TensÃ£o de Rotura Longitudinal Ã  TraÃ§Ã£o F1t
FC,1,S,XCMP,-F1c          ! TensÃ£o de Rotura Longitudinal Ã  CompressÃ£o F1c
FC,1,S,YTEN,F2t           ! TensÃ£o de Rotura Transversal Ã  TraÃ§Ã£o F2t
FC,1,S,YCMP,-F2c          ! TensÃ£o de Rotura Transversal Ã  CompressÃ£o F2c
FC,1,S,ZTEN,F3t           ! TensÃ£o de Rotura Transversal Ã  TraÃ§Ã£o F3t
FC,1,S,ZCMP,-F3c          ! TensÃ£o de Rotura Transversal Ã  CompressÃ£o F3c
FC,1,S,XY,F6              ! TensÃ£o de Rotura no plano de Corte F6
FC,1,S,YZ,F4              ! TensÃ£o de Rotura no plano de Corte F4
FC,1,S,XZ,F5              ! TensÃ£o de Rotura no plano de Corte F5
FC,1,S,YZCP,C4            ! Coeficiente de Tsai-Wu C4: Predefinido para -1
FC,1,S,XZCP,C5            ! Coeficiente de Tsai-Wu C5: Predefinido para -1
FC,1,S,XYCPCP,C6          ! Coeficiente de Tsai-Wu C6: Predefinido para -1

!.....................................................................
```

```
!*
RSYS,SOLU
AVPRIN,0
SHELL,MID
AVRES,2,
/EFACET,1

LAYER,3

FORCE,TOTAL

JPEG, COLOR, 0
/PLOPTS, DATE, 0
PLNSOL, FAIL, MAX, 2,1.0
/IMAGE, SAVE,strcat(chrval(P),'Hashin'), png


*ENDDO
```

```
    !.....................................................................!
    ! E2NX !
    !.....................................................................!

FINISH
/CLEAR
/filename, E2NX    ! Nome do ficheiro
/PREP7
!/TITLE, Estudo de uma placa em composito Carbono/Epoxi
/UNITS,MPA              ! Unidades: [mm ; MPa ; Newtons]

!.....................................................................
! Definição do tipo de elemento
ET,1,SHELL281           ! Tipo de elemento
kEYOPT,1,8,1            ! Mostra a sequência das lâminas

! "For cycle" PressÃ£o a aplicar [N/mm]
*DO, P, 50, 100, 10 !For P=50 to 100 [N/mm]
!.....................................................................
!Definição das dimenções da placa
!Comprimento
C=150            ! [mm]

!Largura
L=150            ! [mm]

!Espessura
h=0.25            ! [mm]

!.....................................................................
!Definição das placas e das orientações das fibras
!Orientações: [30/90/-30/30]

SECTYPE,1,SHELL
SECDATA,h,1,30      ! 1ª Camada: Espessura 0.25 mm: mat. #1: Theta 30 deg
SECDATA,h,1,90      ! 2ª Camada: Espessura 0.25 mm: mat. #1: Theta 90 deg
SECDATA,h,1,-30     ! 3ª Camada: Espessura 0.25 mm: mat. #1: Theta -30 deg
SECDATA,h,1,30      ! 4ª Camada: Espessura 0.25 mm: mat. #1: Theta 30 deg

SECOFFSET,MID       ! Nós na na espessura do laminado do meio

!.....................................................................
!Propriadades do material
E1=45.6E+03         ! [MPa]
E2=16.2E+03         ! [MPa]
E3=16.2E+03         ! [MPa]

v12=0.278
v13=0.278
v23=0.40

G12=5.83E+03        ! [MPa]
G13=5.83E+03        ! [MPa]
G23=5.7E+03         ! [MPa]

Rho=1.550E-06

!Definição das propriadades do material
MPTEMP,,,,,,,,          ! Material Ortotropico - Carbono/Epóxi
MPTEMP,1,0
MPDATA,EX,1,,E1
MPDATA,EY,1,,E2
MPDATA,EZ,1,,E3
MPDATA,PRXY,1,,v12
```

```
MPDATA,PRXZ,1,,v13
MPDATA,PRYZ,1,,v23
MPDATA,GXY,1,,G12
MPDATA,GXZ,1,,G13
MPDATA,GYZ,1,,G23

!.....................................................................
!Definição da geometria e da malha da placa
RECTNG,0,C,0,L           ! Placa retangular cxl [1000x1000]
ESIZE,,15                ! Número de divisões por cada linha= 15
AMESH,ALL                ! MESH da área (geração da malha)
FINISH                   ! Fim do módulo Pré-processamento

/SOLU                    ! Módulo da solução
ANTYPE,STATIC            ! Análise estática
!.....................................................................
! Definição das Condições de fronteira

DL,4,1,UX,0   ! Constrangimento de modo a evitar movimento na linha 4
DL,4,1,UZ,0
DK,1,UY,0     ! Constrangimento de modo a evitar movimento no ponto 1
DL,2,1,UZ,0   ! Constrangimento de modo a evitar movimento na linha 2


SFL,2,PRES,-P        ! Aplicação da pressão uniforme aplicada na linha 3 da
placa
/PSF,PRES,NORM,2,1,1 ! Apresenta a pressão distribuída uniformemente na linha 3

SOLVE             ! Resolve o estado da carga em estudo
FINISH            ! Fim do módulo de solução
/POST1            ! Módulo Pós processamento
SET,LAST          ! Apresenta a deformada da placa
RSYS,LSYS         ! Sistema de coordenadas da lâmina

!.....................................................................
! Fatores de falha da placa
!Propriadades dos fatores de falha
F1t=1280         ! [MPa]
F2t=40           ! [MPa]
F3t=40           ! [MPa]

F1c=800          ! [MPa]
F2c=145          ! [MPa]
F3c=145          ! [MPa]

F4=1E+04         ! [MPa]
F5=1E+04         ! [MPa]
F6=73            ! [MPa]

!Coeficientes de Tsai-Wu [-1 (predefinido)]
C4=-1
C5=-1
C6=-1

!Definição do criterio de falha
FC,1,S,XTEN,F1t           ! Tensão de Rotura Longitudinal à Tração F1t
FC,1,S,XCMP,-F1c          ! Tensão de Rotura Longitudinal à Compressão F1c
FC,1,S,YTEN,F2t           ! Tensão de Rotura Transversal à Tração F2t
FC,1,S,YCMP,-F2c          ! Tensão de Rotura Transversal à Compressão F2c
FC,1,S,ZTEN,F3t           ! Tensão de Rotura Transversal à Tração F3t
FC,1,S,ZCMP,-F3c          ! Tensão de Rotura Transversal à Compressão F3c
FC,1,S,XY,F6              ! Tensão de Rotura no plano de Corte F6
FC,1,S,YZ,F4              ! Tensão de Rotura no plano de Corte F4
FC,1,S,XZ,F5              ! Tensão de Rotura no plano de Corte F5
```

```
FC,1,S,YZCP,C4           ! Coeficiente de Tsai-Wu C4: Predefinido para -1
FC,1,S,XZCP,C5           ! Coeficiente de Tsai-Wu C5: Predefinido para -1
FC,1,S,XYCPCP,C6         ! Coeficiente de Tsai-Wu C6: Predefinido para -1

!.....................................................................
!Resultados para primeira lâmina:
!LAYER,2                  ! Tabela com os resultados da primeira lâmina
!PRNSOL,S,FAIL            ! Apresenta uma tabela com os índices de falha
!PLNSOL,S,TWSR            ! Apresenta o IF para o critério de TSAI-WU
!PLNSOL,S,MAXF            ! Apresenta o IF para o critério da Tensão Máxima

!*
RSYS,SOLU
AVPRIN,0
SHELL,MID
AVRES,2,
/EFACET,1

LAYER,2

FORCE,TOTAL

/DSCALE,ALL,1.0
/EFACET,1
/PLOPTS, DATE, 0
JPEG, COLOR, 0
PLNSOL, FAIL, MAX, 2,1.0
/IMAGE, SAVE,strcat(chrval(P),'Hashin'), png

*ENDDO
```

Appendix B- Workbench study

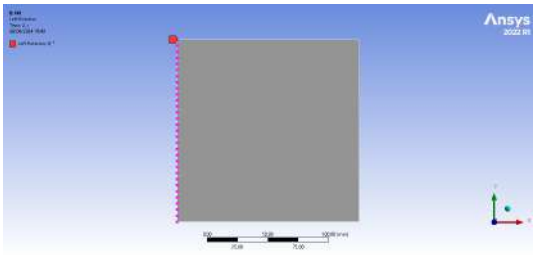

(a) Left Rotation

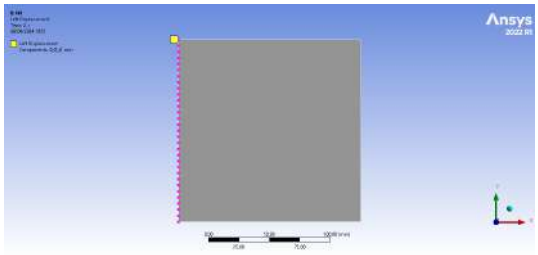

(b) Left Displacement

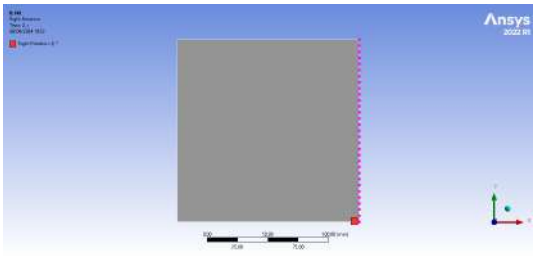

(c) Right Rotation

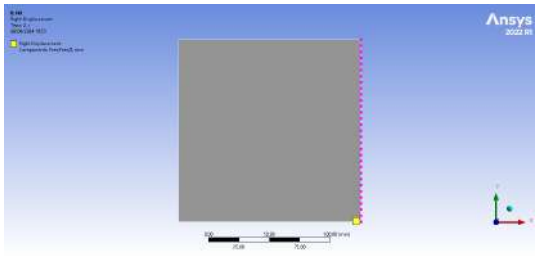

(d) Right Displacement

Figure B.1: Boundary Conditions for NX

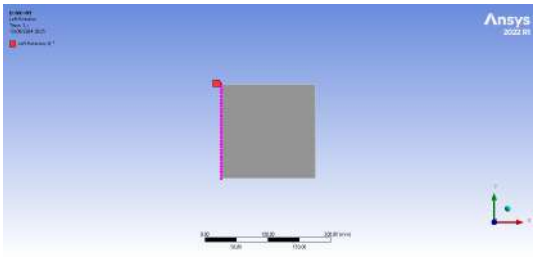

(a) Left Rotation

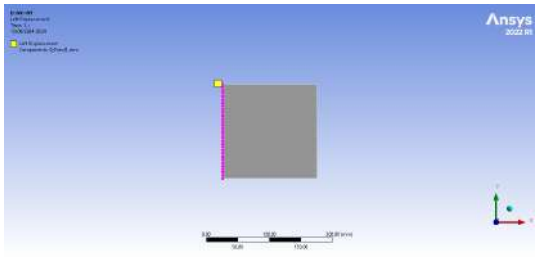

(b) Left Displacement

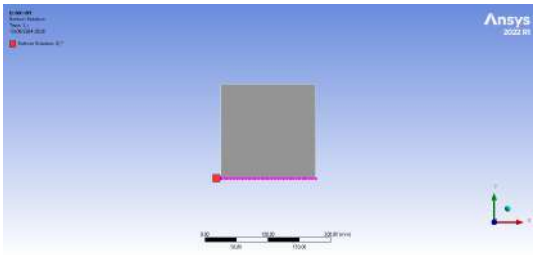

(c) Bottom Rotation

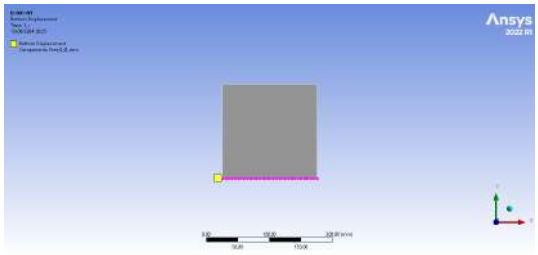

(d) Bottom Displacement

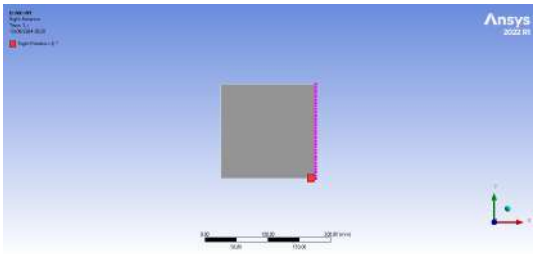

(e) Right Rotation

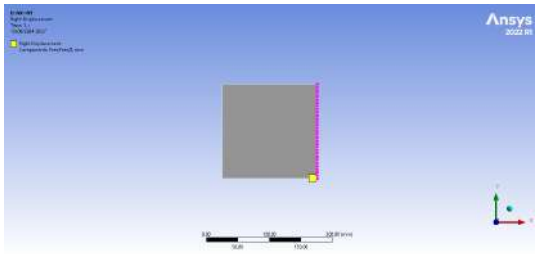

(f) Right Displacement

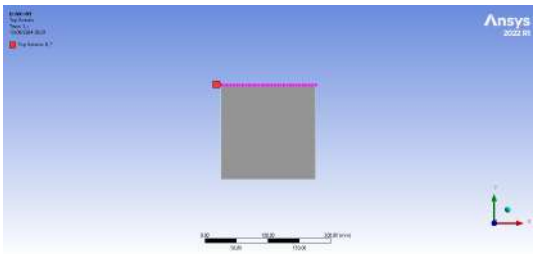

(g) Top Rotation

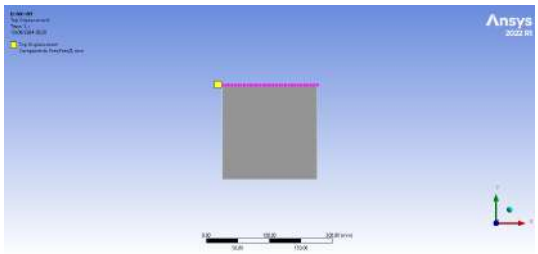

(h) Top Displacement

Figure B.2: Boundary Conditions for NXY

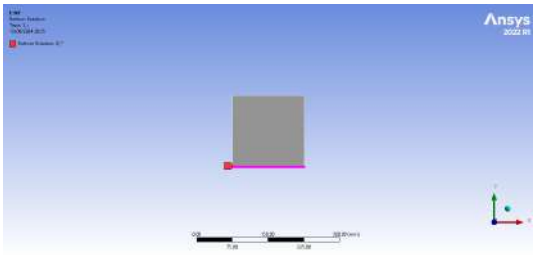

(a) Bottom Rotation

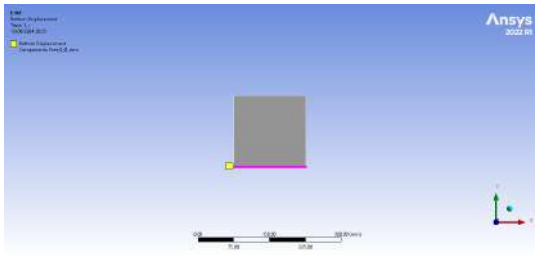

(b) Bottom Displacement

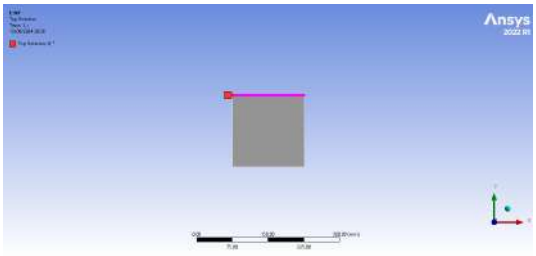

(c) Top Rotation

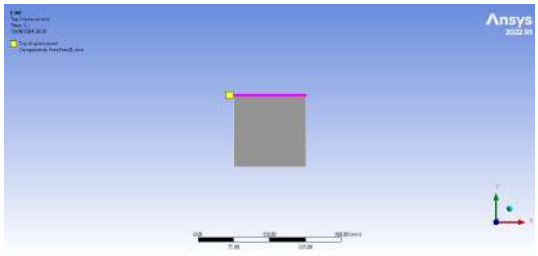

(d) Top Displacement

Figure B.3: Boundary Conditions for NY

Appendix C- Analytical study

1.Initialization

```
> restart:
> with(linalg):
  with(ArrayTools):
  with(LinearAlgebra):
  with(plots):
  Digits:=5:
```

2. Constants

Geometrical Properties

```
> a:=150*10^(-3):
  b:=150*10^(-3):
  ht:=1*10^(-3):#Espessura total do laminado
  Ncamadas_1:=4:#N° Camadas do 1° Caso
  Ncamadas_2:=4:#N° Camadas do 2° Caso
  h1:=ht/Ncamadas_1;#Espessura de cada lâmina do 1° Caso
  h2:=ht/Ncamadas_2;#Espessura de cada lâmina do 2° Caso
```

Material Properties

```
> E1[1]:=112.18*10^9:
  E2[1]:=5.14*10^9:
  G12[1]:=3.13*10^9:
  nu12[1]:=0.67:
  nu21[1]:=0.03:
  ro[1]:=1500:
  F1T[1]:=1950*10^6:
  F2T[1]:=48*10^6:
  F3T[1]:=F2T[1]:
  F1C[1]:=1480*10^6:
  F2C[1]:= 200*10^6:
  F3C[1]:=F2C[1]:
  F4[1]:=1000*10^6:
  F5[1]:=F4[1]:
  F6[1]:=79*10^6:
  C4[1]:=-1:
  C5[1]:=-1:
  C6[1]:=-1:


  E1[2]:=112.18*10^9:
  E2[2]:=5.14*10^9:
  G12[2]:=3.13*10^9:
```

```
nu12[2]:=0.67:
nu21[2]:=0.03:
ro[2]:=1500:
F1T[2]:=1950*10^6:
F2T[2]:=48*10^6:
F3T[2]:=F2T[1]:
F1C[2]:=1480*10^6:
F2C[2]:= 200*10^6:
F3C[2]:=F2C[1]:
F4[2]:=1000*10^6:
F5[2]:=F4[1]:
F6[2]:=79*10^6:
C4[2]:=-1:
C5[2]:=-1:
C6[2]:=-1:
```

3. Elastic constants in the global coordenate system (X,Y)

```
> #1st Case
  #Stacking Sequence [0/ 0 / 0 / 0]


  Z1[0]:=-h1*2;
  Z1[1]:=-h1*1;
  Z1[2]:=-h1*0;# Superfície média
  Z1[3]:=h1*1;
  Z1[4]:=h1*2;
```

```
> #2nd Case
  #Stacking Sequence [30/ 90 / -30 / 60]
  Z2[0] := -h2*2;
  Z2[1] := -h2*1;
  Z2[2] := -h2*0;# Superfície média
  Z2[3] := h2*1;
  Z2[4] := h2*2;
```

Rigidity Matrices Q1[rig] and Q2[rig]

Q1 [rig]

```
Q1[11]:=E1[1]/(1-nu12[1]*nu21[1]):
Q1[22]:=E2[1]/(1-nu12[1]*nu21[1]):
Q1[12]:=nu12[1]*E2[1]/(1-nu12[1]*nu21[1]):
Q1[33]:=G12[1]:
Q1[rig]:=evalm(matrix(3,3,[Q1[11],Q1[12],0,Q1[12],Q1[22],0,0,0,Q1
[33]]));
```

Q2 [rig]

```
Q2[11]:=E1[2]/(1-nu12[2]*nu21[2]):
Q2[22]:=E2[2]/(1-nu12[2]*nu21[2]):
Q2[12]:=nu12[2]*E2[2]/(1-nu12[2]*nu21[2]):
Q2[33]:=G12[2]:
Q2[rig]:=evalm(matrix(3,3,[Q2[11],Q2[12],0,Q2[12],Q2[22],0,0,0,Q2
[33]]));
```

Transposing of coordenates

T sigma- Transposing matrix for tensions

```
> c:=cos(theta):
  s:=sin(theta):
  T[sigma]:=matrix(3,3,[c^2,s^2,2*s*c,s^2,c^2,-2*s*c,-c*s,c*s,c^2
  -s^2]);
  Tinv[sigma]:=simplify(inverse(T[sigma]));
```

T epsilon - Transposing matrix for deformations

```
> T[epsilon]:=matrix(3,3,[c^2,s^2,c*s,s^2,c^2,-c*s,-2*c*s,2*c*s,
  c^2-s^2]);
```

Matrix Q1 barra

```
> Q1[barra]:=Tinv[sigma]*Q1[rig]*T[epsilon];
```

Matrix Q2 barra

```
> Q2[barra]:=Tinv[sigma]*Q2[rig]*T[epsilon];
```

Transposing of the rigidity matrices in each stacking Qbarra, to the coordenate system of the laminate (XY)

1st Case: Stacking Squence [0 / 0 / 0 / 0]

For the 4 layers at 0º, material 1:

```
Q_1[0]:=multiply(simplify(subs(theta=0,evalm
(Tinv[sigma]))),Q1[rig],simplify(subs(theta=0,evalm(T[epsilon]))));
```

2nd Case: Stacking Squence [30/90/-30/60]

For the 2 layers a +30º, material 2:

```
Q_2[+30]:=evalf(multiply(simplify(subs
(theta=Pi/6,evalm(Tinv[sigma]))),Q2[rig],simplify(subs(theta=Pi/6,
evalm(T[epsilon])))));
```

For the layer at -30º, material 2:

```
Q_2[-30]:=evalf(multiply(simplify(subs(theta=
-Pi/3,evalm(Tinv[sigma]))),Q2[rig],simplify(subs(theta=-Pi/6,evalm
(T[epsilon])))));
```

For the layer at +90º, material 2:

```
Q_2[+90]:=evalf(multiply(simplify(subs(theta=
Pi/2,evalm(Tinv[sigma]))),Q2[rig],simplify(subs(theta=Pi/2,evalm(T
[epsilon])))));
```

For the layer at +60º, material 2:

```
Q_2[+60]:=evalf(multiply(simplify(subs(theta=
Pi/3,evalm(Tinv[sigma]))),Q2[rig],simplify(subs(theta=Pi/3,evalm(T
[epsilon])))))
```

```
>
```

Matrix A+B+D=G

1st Case: Stacking Squence [0 / 0 / 0 / 0]

Matrix A

```
A1_1:=evalm(Q_1[0]*(Z1[1]-Z1[0])):
A2_1:=evalm(Q_1[0]*(Z1[2]-Z1[1])):
A3_1:=evalm(Q_1[0]*(Z1[3]-Z1[2])):
A4_1:=evalm(Q_1[0]*(Z1[4]-Z1[3])):
A1:=evalm((A1_1+A2_1+A3_1+A4_1));
```

Inverse of matrix A

```
a_1:=inverse(A1);
```

Elasticity constants of the laminate

```
E1[x]:=1/(Ncamadas_1*h1*a_1[1,1]);
E1[y]:=1/(Ncamadas_1*h1*a_1[1,1]);
G1[xy]:=1/(Ncamadas_1*h1*a_1[3,3]);
nu1[xy]:=-a_1[1,2]/a_1[1,1];
```

Matrix B

```
B1_1:=evalm(Q_1[0]*(Z1[1]^2-Z1[0]^2)):
B2_1:=evalm(Q_1[0]*(Z1[2]^2-Z1[1]^2)):
B3_1:=evalm(Q_1[0]*(Z1[3]^2-Z1[2]^2)):
B4_1:=evalm(Q_1[0]*(Z1[4]^2-Z1[3]^2)):


B1:=evalm((B1_1+B2_1+B3_1+B4_1));
```

Matrix D

```
D1:=evalm((1/3)*(Q_1[0]*(Z1[1]^3-Z1[0]^3)+Q_1[0]*(Z1[2]^3-Z1[1]^3)+
Q_1[0]*(Z1[3]^3-Z1[2]^3)+Q_1[0]*(Z1[4]^3-Z1[3]^3)));
```

General matrix G

```
> G[1]:=blockmatrix(2,2,[A1,B1,B1,D1]);
```

2nd Case: Stacking Squence [30/90/-30/60]

Matrix A

```
A1_2:=evalm(Q_2[+30]*(Z2[1]-Z2[0])):
A2_2:=evalm(Q_2[+90]*(Z2[2]-Z2[1])):
A3_2:=evalm(Q_2[-30]*(Z2[3]-Z2[2])):
A4_2:=evalm(Q_2[+60]*(Z2[4]-Z2[3])):
A2:=evalm((1/2)*(A1_2+A2_2+A3_2+A4_2));
```

Inverse of matrix A

```
a_2:=inverse(A2);
```

Elasticity constants of the laminate

```
E2[x]:=1/(Ncamadas_2*h2*a_2[1,1]);
E2[y]:=1/(Ncamadas_2*h2*a_2[1,1]);
G2[xy]:=1/(Ncamadas_2*h2*a_2[3,3]);
nu2[xy]:=-a_2[1,2]/a_2[1,1];
```

Matrix B

```
B1_2:=evalm(Q_2[+30]*(Z2[1]^2-Z2[0]^2)):
B2_2:=evalm(Q_2[+90]*(Z2[2]^2-Z2[1]^2)):
B3_2:=evalm(Q_2[-30]*(Z2[3]^2-Z2[2]^2)):
B4_2:=evalm(Q_2[+60]*(Z2[4]^2-Z2[3]^2)):
B2:=evalm((1/2)*(B1_2+B2_2+B3_2+B4_2));
```

Matrix D

```
D2:=evalm((1/3)*(Q_2[+30]*(Z2[1]^3-Z2[0]^3)+Q_2[+90]*(Z2[2]^3-Z2[1]
^3)+Q_2[-30]*(Z2[3]^3-Z2[2]^3)+Q_2[+60]*(Z2[4]^3-Z2[3]^3)));
```

General matrix G

```
> G[2]:=blockmatrix(2,2,[A2,B2,B2,D2]);
```

4. Deformations, Tensions and Failures

1st Case

NX

```
> A1_M := convert(A1, Matrix) : B1_M := convert(B1, Matrix) :
    D1_M := convert(D1, Matrix) :
  for i from 150 to 200 by 10 do:
  P1_x[i] := (i);
  N1_x[i] := Matrix(3, 1, [P1_x[i], 0, 0]) / (a);
  d1_x[i] := LinearSolve(A1_M, N1_x[i]) / a;
  D1_x[i] := evalf((sqrt((d1_x[i](1, 1))^2 + (d1_x[i](2, 1))^2)) / (a
     + b)) * 10^3 :
  Sigma1_x_x[i] := E1[x] / (1 - nu12[1]·nu21[1]) ·(d1_x[i](1) + nu21[1]
     ·d1_x[i](2)) :
  Sigma1_x_y[i] := E1[y] / (1 - nu12[1]·nu21[1]) ·(d1_x[i](2) + nu12[1]
     ·d1_x[i](1)) :
  Sigma1_x_xy[i] := G1[xy]·d1_x[i](3) :

  od:
  print(D1_x) :
  print(Sigma1_x_x);
  print(Sigma1_x_y);
  print(Sigma1_x_xy);
```

Max Stress

```
> for i from 150 to 200 by 10 do:
  if Sigma1_x_x[i] ≥ 0 then:
  MSX_1_1[i] := (Sigma1_x_x[i] / F1T[1]) :

  elif Sigma1_x_x[i] < 0 then:
  MSX_1_2[i] := -(Sigma1_x_x[i] / F1C[1]) :

  end if:
  if Sigma1_x_y[i] ≥ 0 then:
  MSX_1_3[i] := Sigma1_x_y[i] / F2T[1] :

  elif Sigma1_x_y[i] < 0 then:
  MSX_1_4[i] := -Sigma1_x_y[i] / F2C[1] :

  end if:
  if Sigma1_x_xy[i] ≥ 0 then:
  MSX_1_5[i] := Sigma1_x_xy[i] / F3T[1] :

  elif Sigma1_x_xy[i] < 0 then:
  MSX_1_6[i] := -Sigma1_x_xy[i] / F3C[1] :

  end if:

  MS1x[i] := max( MSX_1_1[i]^(1/Ncamadas_1) / Ncamadas_1, MSX_1_2[i]^(1/Ncamadas_1) / Ncamadas_1,
    MSX_1_3[i]^(1/Ncamadas_1) / Ncamadas_1, MSX_1_4[i]^(1/Ncamadas_1) / Ncamadas_1,
    MSX_1_5[i]^(1/Ncamadas_1) / Ncamadas_1, MSX_1_6[i]^(1/Ncamadas_1) / Ncamadas_1 ) :
  od:
  print(MS1x) :
```

Tsai-Hill

```
> G1[1] := 1/2 · ( 2/F2T[1]^2 - 1/F1T[1]^2 ) :
  G2[1] := 1/2 · ( 1/(F1T[1])^2 ) :
  G3[1] := 1/2 · ( 1/(F1T[1])^2 ) :
  G6[1] := 1/2 · ( 1/(F6[1])^2 ) :

  for i from 150 to 200 by 10 do:
  TH_x_1[i] := ((G2[1] + G3[1]) · Sigma1_x_x[i]^2 + (G1[1] + G3[1])
```

```
      ·Sigma1_x_y[i]^2 − 2 G3[1]·Sigma1_x_x[i]·Sigma1_x_y[i] + 2
      ·G6[1]·Sigma1_x_xy[i]^2)^(1/Ncamadas_1) :
    od:

    print(TH_x_1) :
```

Tsai-Wu

```
> for i from 150 to 200 by 10 do:
  A[i] := (Sigma1_x_x[i])^2/(F1T[1]·F1C[1]) + (Sigma1_x_y[i])^2/(F2T[1]·F2C[1])
      + (Sigma1_x_xy[i])^2/F4[1]^2
      + C4[1]·(Sigma1_x_x[i]·Sigma1_x_y[i])/sqrt(F1T[1]·F1C[1]·F2T[1]·F2C[1]) :
  B[i] := evalf((F1T[1]^-1 − F1C[1]^-1)·Sigma1_x_x[i] + (F2T[1]^-1
      − F2C[1]^-1)·Sigma1_x_y[i]);

  TW_x_1[i] :=
      evalf(((-B[i]/(2·A[i]) + sqrt((B[i]/(2·A[i]))^2) + 1/A[i])^-1)^(1/Ncamadas_1)) :
  od:
  print(TW_x_1) :
```

Hashin

```
> for i from 150 to 200 by 10 do:

  #Different components
  if Sigma1_x_x[i] ≥ 0 then:
  H1X_1_1[i] := (Sigma1_x_x[i]/F1T[1])^2 + (Sigma1_x_xy[i]/F6[1])^2 :

  H1X_1_2[i] := 0 :
  H1X_1_3[i] := 0 :
  H1X_1_4[i] := 0 :

   elif Sigma1_x_x[i] < 0 then:
   H1X_1_2[i] := abs(Sigma1_x_x[i])/F1C[1] :
   H1X_1_1[i] := 0 :
   H1X_1_3[i] := 0 :
   H1X_1_4[i] := 0 :

   end if:

   if Sigma1_x_y[i] ≥ 0 then:
  H1X_1_3[i] := (Sigma1_x_y[i]/F2T[1])^2 + (Sigma1_x_xy[i]/F6[1])^2 :
```

```
H1X_1_1[i] := 0 :
H1X_1_2[i] := 0 :
H1X_1_4[i] := 0 :

elif Sigma1_x_y[i] < 0 then:

H1X_1_4[i] := ( ( Sigma1_x_y[i] / (2·F4[1]) )^2 + ( ( F2C[1] / (2·F4[1]) )^2 - 1 )
  · Sigma1_x_y[i] / F2C[1] + ( Sigma1_x_xy[i] / F6[1] )^2 ) :
H1X_1_1[i] := 0 :
H1X_1_2[i] := 0 :
H1X_1_3[i] := 0 :
end if:
Hashin1x[i] := max( 10· Ncamadas_1·H1X_1_1[i]^(1/Ncamadas_1), 10
  · Ncamadas_1·H1X_1_2[i]^(1/Ncamadas_1), 10· Ncamadas_1
  ·H1X_1_3[i]^(1/Ncamadas_1), 10· Ncamadas_1·H1 X_1_4[i]^(1/Ncamadas_1) )
  :
od:
print(Hashin1x) :
```

NXY

```
> for i from 150 to 200 by 10 do:
P1_xy[i]:=(i);
N1_xy[i]:=Matrix(3,1,[P1_xy[i],P1_xy[i],P1_xy[i]])/(a);
d1_xy[i]:=LinearSolve(A1_M,N1_xy[i])/(a);
D1_xy[i]:=evalf((sqrt((d1_xy[i](1,1))^2+(d1_xy[i](2,1))^2))/
(a+b))*10^3:
Sigma1_xy_x[i]:=(E1[x])/(1-nu12[1]*nu21[1])*(d1_xy[i](1)+nu21
[1]*d1_xy[i](2)):
Sigma1_xy_y[i]:=(E1[y])/(1-nu12[1]*nu21[1])*(d1_xy[i](2)+nu12
[1]*d1_xy[i](1)):
Sigma1_xy_xy[i]:=G1[xy]*d1_xy[i](3):
od:
print(D1_xy):
print(Sigma1_xy_x);
print(Sigma1_xy_y);
print(Sigma1_xy_xy);
```

Max Stress

```
> for i from 150 to 200 by 10 do:
  if Sigma1_xy_x[i] ≥ 0 then:
  MSXY_1_1[i] := (Sigma1_xy_x[i] / F1T[1]) :

  elif Sigma1_xy_x[i] < 0 then:
  MSXY_1_2[i] := -( Sigma1_xy_x[i] / F1C[1] ) :

  end if:
```

```
if Sigma1_xy_y[i] ≥ 0 then:
MSXY_1_3[i] := Sigma1_xy_y[i] / F2T[1] :

elif Sigma1_xy_y[i] < 0 then:
MSXY_1_4[i] := -Sigma1_xy_y[i] / F2C[1] :


end if:
if Sigma1_xy_xy[i] ≥ 0 then:
MSXY_1_5[i] := Sigma1_xy_xy[i] / F3T[1] :

elif Sigma1_xy_xy[i] < 0 then:
MSXY_1_6[i] := -Sigma1_xy_xy[i] / F3C[1] :

end if:

MS1xy[i] := max( Ncamadas_1·MSXY_1_1[i]^(1/Ncamadas_1), Ncamadas_1
  ·MSXY_1_2[i]^(1/Ncamadas_1), Ncamadas_1·MSXY_1_3[i]^(1/Ncamadas_1),
  Ncamadas_1·MSXY_1_4[i]^(1/Ncamadas_1), Ncamadas_1
  ·MSXY_1_5[i]^(1/Ncamadas_1), Ncamadas_1·MSXY_1_6[i]^(1/Ncamadas_1) ) :
od:
print(MS1xy) :
```

$$\text{table}\left(\left[150 = \max\left(5.27720067101707, 4\,MSXY\_1\_2_{150}^{1/4}, 4\,MSXY\_1\_4_{150}^{1/4}, 4\,MSXY\_1\_6_{150}^{1/4}\right), 180 = \max\left(5.52330365991007, 4\,MSXY\_1\_2_{180}^{1/4}, 4\,MSXY\_1\_4_{180}^{1/4}, 4\,MSXY\_1\_6_{180}^{1/4}\right), 190 = \max\left(5.59846792617014, 4\,MSXY\_1\_2_{190}^{1/4}, 4\,MSXY\_1\_4_{190}^{1/4}, 4\,MSXY\_1\_6_{190}^{1/4}\right), 160 = \max\left(5.36303695905456, 4\,MSXY\_1\_2_{160}^{1/4}, 4\,MSXY\_1\_4_{160}^{1/4}, 4\,MSXY\_1\_6_{160}^{1/4}\right), 170 = \max\left(5.44493907370422, 4\,MSXY\_1\_2_{170}^{1/4}, 4\,MSXY\_1\_4_{170}^{1/4}, 4\,MSXY\_1\_6_{170}^{1/4}\right), 200 = \max\left(5.67072116527397, 4\,MSXY\_1\_2_{200}^{1/4}, 4\,MSXY\_1\_4_{200}^{1/4}, 4\,MSXY\_1\_6_{200}^{1/4}\right)\right]\right) \quad \textbf{(4.1.5.1)}$$

Tsai-Hill

```
> for i from 150 to 200 by 10 do:
TH_xy_1[i] := Ncamadas_1·((G2[1]+G3[1])·Sigma1_xy_x[i]^2
  +(G1[1]+G3[1])·Sigma1_xy_y[i]^2-2 G3[1]·Sigma1_xy_x[i]
  ·Sigma1_xy_y[i]+2·G6[1]·Sigma1_xy_xy[i]^2)^(1/Ncamadas_1)
```

```
od:

print(TH_xy_1) :
```

table([150 = 6.96358647960518, 180 = 7.62809756762986, 190 = 7.83735998785176, 160 = 7.19179263891429, 170 = 7.41328113048253, 200 = 8.04071478035687]) **(4.1.6.1)**

Tsai-Wu

```
> for i from 150 to 200 by 10 do:
```

$$A[i] := \frac{(Sigma1\_xy\_x[i])^2}{F1T[1]\cdot F1C[1]} + \frac{(Sigma1\_xy\_y[i])^2}{F2T[1]\cdot F2C[1]} + \frac{(Sigma1\_xy\_xy[i])^2}{F4[1]^2} + \frac{C4[1]\cdot(Sigma1\_xy\_x[i]\cdot Sigma1\_xy\_y[i])}{sqrt(F1T[1]\cdot F1C[1]\cdot F2T[1]\cdot F2C[1])} :$$

$$B[i] := (F1T[1]^{-1} - F1C[1]^{-1})\cdot Sigma1\_xy\_x[i] + (F2T[1]^{-1} - F2C[1]^{-1})\cdot Sigma1\_xy\_y[i] :$$

$$TW\_xy\_1[i] := Ncamadas\_1 \cdot evalf\left(\left(-\frac{B[i]}{2\cdot A[i]} + sqrt\left(\left(\frac{B[i]}{2\cdot A[i]}\right)^2\right) + \frac{1}{A[i]}\right)^{-1}\right)^{\frac{1}{Ncamadas\_1}} :$$

```
od:
print(TW_xy_1) :
```

table([150 = 4.8700, 180 = 5.3348, 190 = 5.4808, 160 = 5.0296, 170 = 5.1844, 200 = 5.6232]) **(4.1.7.1)**

Hashin

```
> for i from 150 to 200 by 10 do:

#Different components
 if Sigma1_xy_x[i] ≥ 0 then:
```

$$H1XY\_1\_1[i] := \left(\frac{Sigma1\_xy\_x[i]}{F1T[1]}\right)^2 + \left(\frac{Sigma1\_xy\_xy[i]}{F6[1]}\right)^2 :$$

```
 H1XY_1_2[i] := 0 :
 H1XY_1_3[i] := 0 :
 H1XY_1_4[i] := 0 :

 elif Sigma1_xy_x[i] < 0 then:
```

$$H1XY\_1\_2[i] := \frac{abs(Sigma1\_xy\_x[i])}{F1C[1]} :$$

```
 H1XY_1_1[i] := 0 :
 H1XY_1_3[i] := 0 :
 H1XY_1_4[i] := 0 :
end if:
  if Sigma1_xy_y[i] ≥ 0 then:
```

$$H1XY\_1\_3[i] := \left(\frac{Sigma1\_xy\_y[i]}{F2T[1]}\right)^2 + \left(\frac{Sigma1\_xy\_xy[i]}{F6[1]}\right)^2 :$$

```
H1XY_1_1[i] := 0 :
H1XY_1_2[i] := 0 :
H1XY_1_4[i] := 0 :

elif Sigma1_xy_y[i] < 0 then:

H1XY_1_4[i] := ( Sigma1_xy_y[i] / (2·F4[1]) )^2 + ( ( F2C[1] / (2·F4[1]) )^2 - 1 )
  · Sigma1_xy_y[i] / F2C[1] + ( Sigma1_xy_xy[i] / F6[1] )^2 : H1XY_1_1[i] := 0 :

H1XY_1_2[i] := 0 :
H1XY_1_3[i] := 0 :
end if:
Hashin1xy[i] := Ncamadas_1·max(H1XY_1_1[i], H1XY_1_2[i],
   H1XY_1_3[i], H1XY_1_4[i])^(1/Ncamadas_1) :
od: print(Hashin1xy) :
```

table([150 = 6.9636, 180 = 7.6280, 190 = 7.8372, 160 = 7.1920, 170 = 7.4132, 200 = 8.0408]) **(4.1.8.1)**

NY

```
> for i from 150 to 200 by 10 do:
  P1_y[i]:=(i);
  N1_y[i]:=Matrix(3,1,[0,P1_y[i],0])/(b);
  d1_y[i]:=LinearSolve(A1_M,N1_y[i])/b;
  D1_y[i]:=evalf((sqrt((d1_y[i](1,1))^2+(d1_y[i](2,1))^2))/((a+
  b)))*10^3:
  Sigma1_y_x[i] := E1[x]*(d1_y[i](1) + nu21[1]*d1_y[i](2))/(-
  nu12[1]*nu21[1] + 1);
  Sigma1_y_y[i] := E1[y]*(d1_y[i](2) + nu12[1]*d1_y[i](1))/(-
  nu12[1]*nu21[1] + 1);
  Sigma1_y_xy[i] := G1[xy]*d1_y[i](3);
  od:
  print(D1_y):
  print(Sigma1_y_x);
  print(Sigma1_y_y);
  print(Sigma1_y_xy);
```

table([150 = 4.3273, 180 = 5.1930, 190 = 5.4813, 160 = 4.6157, 170 = 4.9043, 200 = 5.7697])

table([150 = −103753.002792733, 180 = −124503.603351279, 190 = −131420.470204129, 160 = −110669.869645582, 170 = −117586.736498430, 200 = −138337.337056978])

table([150 = 1.45416774489902 10^8, 180 = 1.74500129387882 10^8, 190 = 1.84194581020542 10^8, 160 = 1.55111226122562 10^8, 170 = 1.64805677755222 10^8, 200 = 1.93889032653203 10^8])

table([150 = 0., 180 = 0., 190 = 0., 160 = 0., 170 = 0., 200 = 0.]) **(4.1.1)**

Max Stress

```
> for i from 150 to 200 by 10 do:
  if Sigma1_y_x[i] ≥ 0 then:
  MSY_1_1[i] := (Sigma1_y_x[i] / F1T[1]) :
 elif Sigma1_x_x[i] < 0 then:
  MSY_1_2[i] := -(Sigma1_y_x[i] / F1C[1]) :

  end if:
  if Sigma1_y_y[i] ≥ 0 then:
  MSY_1_3[i] := Sigma1_y_y[i] / F2T[1] :
  elif Sigma1_y_y[i] < 0 then:
  MSY_1_4[i] := -Sigma1_y_y[i] / F2C[1] :
  end if:
  if Sigma1_y_xy[i] ≥ 0 then:
  MSY_1_5[i] := Sigma1_y_xy[i] / F3T[1] :
  elif Sigma1_y_xy[i] < 0 then:
  MSY_1_6[i] := -Sigma1_y_xy[i] / F3C[1] :

  end if:

  MS1y[i] := max(Ncamadas_1 · MSY_1_1[i]^(1/Ncamadas_1), Ncamadas_1
    · MSY_1_2[i]^(1/Ncamadas_1), Ncamadas_1 · MSY_1_3[i]^(1/Ncamadas_1),
     Ncamadas_1 · MSY_1_4[i]^(1/Ncamadas_1), Ncamadas_1
    · MSY_1_5[i]^(1/Ncamadas_1), Ncamadas_1 · MSY_1_6[i]^(1/Ncamadas_1)) :
  od:
  print(MS1y) :
```

$$\begin{aligned}&\mathrm{table}\Big(\Big[150 = \max\Big(5.27719702338011,\ 4\,MSY\_1\_1_{150}^{1\,|\,4},\ 4\,MSY\_1\_2_{150}^{1\,|\,4},\ 4\\ &MSY\_1\_4_{150}^{1\,|\,4},\ 4\,MSY\_1\_6_{150}^{1\,|\,4}\Big),\ 180 = \max\Big(5.52329984216505,\ 4\,MSY\_1\_1_{180}^{1\,|\,4},\\ &4\,MSY\_1\_2_{180}^{1\,|\,4},\ 4\,MSY\_1\_4_{180}^{1\,|\,4},\ 4\,MSY\_1\_6_{180}^{1\,|\,4}\Big),\ 190\\ &= \max\Big(5.59846405647107,\ 4\,MSY\_1\_1_{190}^{1\,|\,4},\ 4\,MSY\_1\_2_{190}^{1\,|\,4},\ 4\,MSY\_1\_4_{190}^{1\,|\,4},\ 4\\ &MSY\_1\_6_{190}^{1\,|\,4}\Big),\ 160 = \max\Big(5.36303325208698,\ 4\,MSY\_1\_1_{160}^{1\,|\,4},\ 4\,MSY\_1\_2_{160}^{1\,|\,4},\\ &4\,MSY\_1\_4_{160}^{1\,|\,4},\ 4\,MSY\_1\_6_{160}^{1\,|\,4}\Big),\ 170 = \max\Big(5.44493531012534,\ 4\\ &MSY\_1\_1_{170}^{1\,|\,4},\ 4\,MSY\_1\_2_{170}^{1\,|\,4},\ 4\,MSY\_1\_4_{170}^{1\,|\,4},\ 4\,MSY\_1\_6_{170}^{1\,|\,4}\Big),\ 200\\ &= \max\Big(5.67071724563297,\ 4\,MSY\_1\_1_{200}^{1\,|\,4},\ 4\,MSY\_1\_2_{200}^{1\,|\,4},\ 4\,MSY\_1\_4_{200}^{1\,|\,4},\ 4\\ &MSY\_1\_6_{200}^{1\,|\,4}\Big)\Big]\Big)\end{aligned} \qquad \textbf{(4.1.9.1)}$$

Tsai-Hill

```
> for i from 150 to 200 by 10 do:
  TH_y_1[i] := Ncamadas_1·((G2[1]+G3[1])·Sigma1_y_x[i]^2+(G1[1]
    +G3[1])·Sigma1_y_y[i]^2-2 G3[1]·Sigma1_y_x[i]
    ·Sigma1_xy_y[i]+2·G6[1]·Sigma1_y_xy[i]^2)^(1/Ncamadas_1) :
  od:

  print(TH_y_1) :
```

table([150 = 6.96228478072591, 180 = 7.62667159007897, 190 = 7.83562898597497, 160 = 7.19044817542409, 170 = 7.41189537368262, 200 = 8.03921164730172]) **(4.1.10.1)**

Tsai-Wu

```
> for i from 150 to 200 by 10 do:
  A[i] := (Sigma1_y_x[i])^2/(F1T[1]·F1C[1]) + (Sigma1_y_y[i])^2/(F2T[1]·F2C[1])
    + (Sigma1_y_xy[i])^2/F4[1]^2
    + C4[1]·(Sigma1_y_x[i]·Sigma1_y_y[i])/sqrt(F1T[1]·F1C[1]·F2T[1]·F2C[1]) :
  B[i] := (F1T[1]^-1-F1C[1]^-1)·Sigma1_y_x[i]+(F2T[1]^-1-F2C[1]^-1)
    ·Sigma1_y_y[i]:

  TW_y_1[i] := Ncamadas_1
    ·evalf((-B[i]/(2·A[i])+sqrt((B[i]/(2·A[i]))^2)+1/A[i])^-1)^(1/Ncamadas_1)
  od:
  print(TW_y_1) :
```

table([150 = 4.8732, 180 = 5.3380, 190 = 5.4844, 160 = 5.0328, 170 = 5.1880, 200 = 5.6268]) **(4.1.11.1)**

Hashin

```
> for i from 150 to 200 by 10 do:

  #Different components
   if Sigma1_y_x[i] ≥ 0 then:
  H1Y_1_1[i] := (Sigma1_y_x[i]/F1T[1])^2+(Sigma1_y_xy[i]/F6[1])^2 :

   H1Y_1_2[i] := 0 :
   H1Y_1_3[i] := 0 :
   H1Y_1_4[i] := 0 :

   elif Sigma1_y_x[i] < 0 then:
   H1Y_1_2[i] := abs(Sigma1_y_x[i])/F1C[1] :
   H1Y_1_1[i] := 0 :
   H1Y_1_3[i] := 0 :
   H1Y_1_4[i] := 0 :
```

```
end if:
if Sigma1_y_y[i] ≥ 0 then:
H1Y_1_3[i] := ( Sigma1_y_y[i] / F2T[1] )^2 + ( Sigma1_y_xy[i] / F6[1] )^2 :
H1Y_1_1[i] := 0 :
H1Y_1_2[i] := 0 :
H1Y_1_4[i] := 0 :

elif Sigma1_y_y[i] < 0 then:

H1Y_1_4[i] := ( Sigma1_y_y[i] / (2·F4[1]) )^2 + ( ( F2C[1] / (2·F4[1]) )^2 - 1 )
  · Sigma1_y_y[i] / F2C[1] + ( Sigma1_y_xy[i] / F6[1] )^2 : H1Y_1_1[i] := 0 :
H1Y_1_2[i] := 0 :
H1Y_1_4[i] := 0 :
end if:
Hashin1y[i] := Ncamadas_1·max(H1Y_1_1[i], H1Y_1_2[i],
   H1Y_1_3[i], H1Y_1_4[i])^(1/Ncamadas_1) :

od:
print(Hashin1y) :
```

```
table([150 = 6.96218920748028, 180 = 7.62667076578038, 190
    = 7.83576116842657, 160 = 7.19061954413440, 170 = 7.41189457264173,
    200 = 8.03933395544778])
```

(4.1.12.1)

2nd Case

> NX:

```
> A2_M := convert(A2, Matrix):
  B2_M := convert(B2, Matrix):
  D2_M := convert(D2, Matrix):


  for i from 50 by 10 to 100 do:
  P2_x[i] := i:
  N2_x[i] := Matrix(3, 1, [P2_x[i], 0, 0])/(a+b):
  M2_x[i]:= Matrix(3, 1, [0, 0, 0])/(a+b):
  d2_x_1[i]:=LinearSolve(A2_M,N2_x[i])/(a+b):
  d2_x_2[i]:=LinearSolve(B2_M,N2_x[i])/(a+b):
  D2_x_1[i] := evalf(sqrt(d2_x_1[i](1, 1)^2 + d2_x_1[i](2, 1)^2
  + d2_x_1[i](3, 1)^2)/(a))*10^3:
  D2_x_2[i] := evalf(sqrt(d2_x_2[i](1, 1)^2 + d2_x_2[i](2, 1)
  ^2+d2_x_1[i](3,1)^2)/(a)):
  D2_x[i] := evalf(D2_x_1[i]+D2_x_2[i]);
```

```
Sigma2_x_x[i] := evalf(E2[x]*(d2_x_1[i](1) + nu21[2]*d2_x_1
[i](2))/(-nu12[2]*nu21[2] + 1));
Sigma2_x_y[i] := evalf(E2[y]*(d2_x_1[i](2) + nu12[2]*d2_x_1
[i](2))/(-nu12[2]*nu21[2] + 1));
Sigma2_x_xy[i] := evalf(G2[xy]*d2_x_1[i](3));


od:
print(D2_x_1);
print(D2_x_2);
print(D2_x);
print(Sigma2_x_x);
print(Sigma2_x_y);
print(Sigma2_x_xy);
```

table([50 = 0.37019, 60 = 0.44423, 70 = 0.51827, 90 = 0.66635, 80 = 0.59231, 100 = 0.74040])

table([50 = 0.55801, 60 = 0.66960, 70 = 0.78120, 90 = 1.0044, 80 = 0.89287, 100 = 1.1160])

table([50 = 0.92820, 60 = 1.1138, 70 = 1.2995, 90 = 1.6708, 80 = 1.4852, 100 = 1.8564])

table([50 = 558330., 60 = 670000., 70 = 781660., 90 = $1.0050\ 10^{6}$, 80 = 893330., 100 = $1.1167\ 10^{6}$])

table([50 = −478860., 60 = −574630., 70 = −670400., 90 = −861950., 80 = −766180., 100 = −957720.])

table([50 = 55063., 60 = 66076., 70 = 77088., 90 = 99113., 80 = 88101., 100 = 110130.]) **(4.2.1)**

Max Stress

```
> for i from 50 to 100 by 10 do:
  if Sigma2_x_x[i] ≥ 0 then:

  MSX_2_1[i] := (Sigma2_x_x[i] / F1T[2]) :

  elif Sigma2_x_x[i] < 0 then:
  MSX_2_2[i] := -(Sigma2_x_x[i] / F1C[2]) :

  end if:
  if Sigma2_x_y[i] ≥ 0 then:
  MSX_2_3[i] := Sigma2_x_y[i] / F2T[2] :

  elif Sigma2_x_y[i] < 0 then:
  MSX_2_4[i] := -Sigma2_x_y[i] / F2C[2] :

  end if:
  if Sigma2_x_xy[i] ≥ 0 then:
  MSX_2_5[i] := Sigma2_x_xy[i] / F3T[2] :

  elif Sigma2_x_xy[i] < 0 then:
```

```
    MSX_2_6[i] := -Sigma2_x_xy[i] / F3C[2] :

    end if:

    MS2x[i] := evalf(max(MSX_2_1[i]^(1/Ncamadas_2),
       MSX_2_2[i]^(1/Ncamadas_2), MSX_2_3[i]^(1/Ncamadas_2),
       MSX_2_4[i]^(1/Ncamadas_2), MSX_2_5[i]^(1/Ncamadas_2),
     MSX_2_6[i]^(1/Ncamadas_2))) :
    od:
    print(MS2x) :
```

$$\text{table}\left(\left[50 = \max\left(0.22120, MSX\_2\_2_{50}^{1/4}, MSX\_2\_3_{50}^{1/4}, MSX\_2\_6_{50}^{1/4}\right), 60\right.\right. \qquad \textbf{(4.2.1.1)}$$

$$= \max\left(0.23152, MSX\_2\_2_{60}^{1/4}, MSX\_2\_3_{60}^{1/4}, MSX\_2\_6_{60}^{1/4}\right), 70$$

$$= \max\left(0.24062, MSX\_2\_2_{70}^{1/4}, MSX\_2\_3_{70}^{1/4}, MSX\_2\_6_{70}^{1/4}\right), 90$$

$$= \max\left(0.25622, MSX\_2\_2_{90}^{1/4}, MSX\_2\_3_{90}^{1/4}, MSX\_2\_6_{90}^{1/4}\right), 80$$

$$= \max\left(0.24879, MSX\_2\_2_{80}^{1/4}, MSX\_2\_3_{80}^{1/4}, MSX\_2\_6_{80}^{1/4}\right), 100$$

$$\left.\left. = \max\left(0.26306, MSX\_2\_2_{100}^{1/4}, MSX\_2\_3_{100}^{1/4}, MSX\_2\_6_{100}^{1/4}\right)\right]\right)$$

Tsai-Hill

```
> G1[2] := 1/2 · (2/F2T[2]^2 - 1/F1T[2]^2) :
    G2[2] := 1/2 · (1/(F1T[2])^2) :
    G3[2] := 1/2 · (1/(F1T[2])^2) :
   G6[2] := 1/2 · (1/(F6[2])^2) :

    for i from 50 to 100 by 10 do:
    TH_x_2[i] := 2·((G2[2]+G3[2])·Sigma2_x_x[i]^2 + (G1[2]+G3[2])
      ·Sigma2_x_y[i]^2 - 2 G3[2]·Sigma2_x_x[i]·Sigma2_x_y[i] + 2
      ·G6[2]·Sigma2_x_xy[i]^2)^(1/Ncamadas_2) :

    od:

    print(TH_x_2) :
```

$$\text{table}\left(\left[50 = 0.20008, 60 = 0.21918, 70 = 0.23674, 90 = 0.26844, 80 = 0.25308, 100\right.\right. \qquad \textbf{(4.2.2.1)}$$

$$\left.\left. = 0.28296\right]\right)$$

Tsai-Wu

```
> for i from 50 to 100 by 10 do:
```

$$A[i] := \frac{(\text{Sigma2\_x\_x}[i])^2}{\text{F1T}[2]\cdot\text{F1C}[2]} + \frac{(\text{Sigma2\_x\_y}[i])^2}{\text{F2T}[2]\cdot\text{F2C}[2]} + \frac{(\text{Sigma2\_x\_xy}[i])^2}{\text{F4}[2]^2} + \frac{(\text{Sigma2\_x\_xy}[i])^2}{\text{F5}[2]^2} + \frac{\text{C4}[2]\cdot(\text{Sigma2\_x\_x}[i]\cdot\text{Sigma2\_x\_y}[i])}{\text{sqrt}(\text{F1T}[2]\cdot\text{F1C}[2]\cdot\text{F2T}[2]\cdot\text{F2C}[2])} + \frac{\text{C5}[2]\cdot(\text{Sigma2\_x\_x}[i])}{\text{sqrt}(\text{F1T}[2]\cdot\text{F1C}[2])} + \frac{\text{C6}[2]\cdot(\text{Sigma2\_x\_y}[i])}{\text{sqrt}(\text{F2T}[2]\cdot\text{F2C}[2])};$$

$$B[i] := evalf\left(\left(\text{F1T}[2]^{-1} - \text{F1C}[2]^{-1}\right)\cdot\text{Sigma2\_x\_x}[i] + \left(\text{F2T}[2]^{-1} - \text{F2C}[2]^{-1}\right)\cdot\text{Sigma2\_x\_y}[i]\right);$$

$$\text{TW\_x\_2}[i] := evalf\left(\left(-\frac{B[i]}{2\cdot A[i]} + \text{sqrt}\left(\left(\frac{\text{B}[i]}{2\cdot\text{A}[i]}\right)^2\right) + \frac{1}{A[i]}\right)^{-1}\right)^{\frac{1}{Ncamadas\_2}}:$$

od:

$print(TW\_x\_2):$

table([50 = 0.25972, 60 = 0.27179, 70 = 0.28244, 90 = 0.30070, 80 = 0.29201, 100 = 0.30869]) **(4.2.3.1)**

Hashin

```
> for i from 50 to 100 by 10 do:

  #Different components
   if Sigma2_x_x[i] ≥ 0 then:
  H2X_1_1[i] := ( Sigma2_x_x[i] / F1T[2] )^2 :
  H2X_1_2[i] := 0 :
  H2X_1_3[i] := 0 :
  H2X_1_4[i] := 0 :

   elif Sigma2_x_x[i] < 0 then:
   H2X_1_2[i] := abs(Sigma2_x_x[i]) / F1C[2] :
   H2X_1_1[i] := 0 :
  H2X_1_3[i] := 0 :
  H2X_1_4[i] := 0 :
   end if:

  if Sigma2_x_y[i] ≥ 0 then:
   H2X_1_3[i] := ( Sigma2_x_y[i] / F2T[2] )^2 :
   H2X_1_1[i] := 0 :
  H2X_1_2[i] := 0 :
  H2X_1_4[i] := 0 :
   elif Sigma2_x_y[i] < 0 then:
```

$$H2X\_1\_4[i] := \left(\frac{Sigma2\_x\_y[i]}{2 \cdot F4[2]}\right)^2 + \left(\left(\frac{F2C[2]}{2 \cdot F4[2]}\right)^2 - 1\right) \cdot \frac{Sigma2\_x\_y[i]}{F2C[2]} :$$

```
H2X_1_1[i] := 0 :
H2X_1_2[i] := 0 :
H2X_1_3[i] := 0 :
end if:
Hashin2x[i] := max(H2X_1_1[i], H2X_1_2[i], H2X_1_3[i],
    H2X_1_4[i])^(1/Ncamadas_2) :

od: print(Hashin2x) :
```

table([50 = 0.22065, 60 = 0.23094, 70 = 0.24002, 90 = 0.25558, 80 = 0.24816, 100 = 0.26240]) **(4.2.4.1)**

NXY

```
> for i from 50 to 100 by 10 do:
  P2_xy[i]:=i;
  N2_xy[i]:=Matrix(3,1,[P2_xy[i],P2_xy[i],0])/((a+b));
  d2_xy_1[i]:=LinearSolve(A2_M,N2_xy[i])/((b));
  d2_xy_2[i]:=LinearSolve(B2_M,N2_xy[i])/((b));
  D2_xy_1[i]:=evalf((sqrt((d2_xy_1[i](1,1))^2+(d2_xy_1[i](2,1))
  ^2+(d2_xy_1[i](3,1))^2))/((a+b)))*10^3:
  D2_xy_2[i]:=evalf((sqrt((d2_xy_2[i](1,1))^2+(d2_xy_2[i](2,1))
  ^2+(d2_xy_2[i](3,1))^2))/((a+b)))*10^(-2):
  D2_xy[i]:=evalf(D2_xy_1[i]+D2_xy_2[i]):
  Sigma2_xy_x[i] :=(E2[x])/(1-nu12[2]*nu21[2])*(d2_xy_1[i](1)+
  nu21[2]*d2_xy_1[i](2)):
  Sigma2_xy_y[i] :=(E2[y])/(1-nu12[2]*nu21[2])*(d2_xy_1[i](2)+
  nu12[2]*d2_xy_1[i](2)):
  Sigma2_xy_xy[i] := G2[xy]*d2_xy_1[i](3);
  od:
  print(D2_xy_1):
  print(D2_xy_2):
  print(D2_xy):
  print(Sigma2_xy_x);
  print(Sigma2_xy_y);
  print(Sigma2_xy_xy);
```

table([50 = 0.27594, 60 = 0.33112, 70 = 0.38633, 90 = 0.49670, 80 = 0.44150, 100 = 0.55187])

table([50 = 0.033733, 60 = 0.040480, 70 = 0.047230, 90 = 0.060720, 80 = 0.053973, 100 = 0.067470])

table([50 = 0.30967, 60 = 0.37160, 70 = 0.43356, 90 = 0.55742, 80 = 0.49547, 100 = 0.61934])

table([50 = 943274.182053340, 60 = $1.13192901846401\ 10^6$, 70 = $1.32058385487468\ 10^6$, 90 = $1.69789352769601\ 10^6$, 80

$= 1.50923869128534\ 10^{6}, 100 = 1.88654836410668\ 10^{6}])$

table([50 = −12811.4819308017, 60 = −15373.7783169621, 70
$= -17936.0747031224, 90 = -23060.6674754431, 80 = -20498.3710892828, 100$
$= -25622.9638616035])$

table([50 = −102896.130884227, 60 = −123475.357061072, 70 **(4.2.2)**
$= -144054.583237917, 90 = -185213.035591608, 80 = -164633.809414763, 100$
$= -205792.261768453])$

Max Stress

```
> for i from 50 to 100 by 10 do:
  if Sigma2_xy_x[i] ≥ 0 then:
  MSXY_2_1[i] := (Sigma2_xy_x[i] / F1T[2]) :

  elif Sigma2_xy_x[i] < 0 then:
  MSXY_2_2[i] := -(Sigma2_xy_x[i] / F1C[2]) :

  end if:
  if Sigma2_xy_y[i] ≥ 0 then:
  MSXY_2_3[i] := Sigma2_xy_y[i] / F2T[2] :
  elif Sigma2_xy_y[i] < 0 then:
  MSXY_2_4[i] := -Sigma2_xy_y[i] / F2C[2] :
  end if:
  if Sigma2_xy_xy[i] ≥ 0 then:
  MSXY_2_5[i] := Sigma2_xy_xy[i] / F3T[2] :
  elif Sigma2_xy_xy[i] < 0 then:
  MSXY_2_6[i] := -Sigma2_xy_xy[i] / F3C[2] :
  end if:

  MS2xy[i] := max(2· MSXY_2_1[i]^(1/Ncamadas_2), 2
    · MSXY_2_2[i]^(1/Ncamadas_2), 2· MSXY_2_3[i]^(1/Ncamadas_2), 2
    · MSXY_2_4[i]^(1/Ncamadas_2), 2· MSXY_2_5[i]^(1/Ncamadas_2), 2
    · MSXY_2_6[i]^(1/Ncamadas_2)) :
  od:
  print(MS2xy) :
```

table([50 = max(0.301211991788703, 2 $MSXY\_2\_2_{50}^{1/4}$, 2 $MSXY\_2\_3_{50}^{1/4}$, 2 **(4.2.5.1)**
$MSXY\_2\_5_{50}^{1/4}$), 60 = max(0.315259055012343, 2 $MSXY\_2\_2_{60}^{1/4}$, 2
$MSXY\_2\_3_{60}^{1/4}$, 2 $MSXY\_2\_5_{60}^{1/4}$), 70 = max(0.327645544704080, 2
$MSXY\_2\_2_{70}^{1/4}$, 2 $MSXY\_2\_3_{70}^{1/4}$, 2 $MSXY\_2\_5_{70}^{1/4}$), 90

$= \max\left(0.348891496203969, 2\,MSXY\_2\_2_{90}^{1/4}, 2\,MSXY\_2\_3_{90}^{1/4}, 2\,MSXY\_2\_5_{90}^{1/4}\right), 80 = \max\left(0.338767901251367, 2\,MSXY\_2\_2_{80}^{1/4}, 2\,MSXY\_2\_3_{80}^{1/4}, 2\,MSXY\_2\_5_{80}^{1/4}\right), 100 = \max\left(0.358203443759266, 2\,MSXY\_2\_2_{100}^{1/4}, 2\,MSXY\_2\_3_{100}^{1/4}, 2\,MSXY\_2\_5_{100}^{1/4}\right)\right])$

Tsai-Hill

```
> for i from 50 to 100 by 10 do:
TH_xy_2[i] := Ncamadas_2·2·((G2[2]+G3[2])·Sigma2_xy_x[i]^2
  +(G1[2]+G3[2])·Sigma2_xy_y[i]^2-2 G3[2]·Sigma2_xy_x[i]
  ·Sigma2_xy_y[i]+2·G6[2]·Sigma2_xy_xy[i]^2)^(1/Ncamadas_2) :
od:

print(TH_xy_2) :
```

table([50 = 0.301033027508156, 60 = 0.329765856185961, 70 = 0.356179594421356, 90 = 0.403874183723867, 80 = 0.380774732221325, 100 = 0.425721539651804]) **(4.2.6.1)**

Tsai-Wu

```
> for i from 50 to 100 by 10 do:
A[i] := (Sigma2_xy_x[i])^2/(F1T[2]·F1C[2]) + (Sigma2_xy_y[i])^2/(F2T[2]·F2C[2])
  + (Sigma2_xy_xy[i])^2/F4[2]^2 + (Sigma2_xy_xy[i])^2/F5[2]^2
  + C4[2]·(Sigma2_xy_x[i]·Sigma2_xy_y[i])/sqrt(F1T[2]·F1C[2]·F2T[2]·F2C[2])
  + C5[2]·(Sigma2_xy_x[i])/sqrt(F1T[2]·F1C[2]) + C6[2]·(Sigma2_xy_y[i])/sqrt(F2T[2]·F2C[2]) :
B[i] := evalf((F1T[2]^(-1)-F1C[2]^(-1))·Sigma2_xy_x[i]+(F2T[2]^(-1)
  -F2C[2]^(-1))·Sigma2_xy_y[i]);

TW_xy_2[i] := 2·evalf(-(-B[i]/(2·A[i])+sqrt((B[i]/(2·A[i]))^2)+1/A[i])^(-1))^(1/Ncamadas_2) :
od:
print(TW_xy_2) :
```

table([50 = 0.28700, 60 = 0.30038, 70 = 0.31216, 90 = 0.33236, 80 = 0.32274, 100 = 0.34120]) **(4.2.7.1)**

Hashin

```
> for i from 50 to 100 by 10 do:
```

```
#Different components
 if Sigma2_xy_x[i] ≥ 0 then:
H2XY_1_1[i] := ( Sigma2_xy_x[i] / F1T[2] )^2 :
H2XY_1_2[i] := 0 :
H2XY_1_3[i] := 0 :
H2XY_1_4[i] := 0 :

 elif Sigma2_xy_x[i] < 0 then:
 H2XY_1_2[i] := abs(Sigma2_xy_x[i]) / F1C[2] :
H2XY_1_1[i] := 0 :
H2XY_1_3[i] := 0 :
H2XY_1_4[i] := 0 :

end if:
 if Sigma2_xy_y[i] ≥ 0 then:
 H2XY_1_3[i] := ( Sigma2_xy_y[i] / F2T[2] )^2 :
 H2XY_1_1[i] := 0 :
H2XY_1_2[i] := 0 :
H2XY_1_4[i] := 0 :
 elif Sigma2_xy_y[i] < 0 then:

 H2XY_1_4[i] := ( Sigma2_xy_y[i] / (2·F4[2]) )^2 + ( ( F2C[2] / (2·F4[2]) )^2 - 1 )
    · Sigma2_xy_y[i] / F2C[2] :
H2XY_1_1[i] := 0 :
H2XY_1_2[i] := 0 :
H2XY_1_3[i] := 0 :

 end if:

Hashin2xy[i] := Ncamadas_2· max(H2XY_1_1[i], H2XY_1_2[i],
    H2XY_1_3[i], H2XY_1_4[i])^(1/Ncamadas_2) :


 od:
print(Hashin2xy) :
```

table([50 = 0.356953137332019, 60 = 0.373599708735158, 70 = 0.388278408133491, 90 = 0.413456082983716, 80 = 0.401459039515605, 100 = 0.424491279292993]) **(4.2.8.1)**

NY

```
> for i from 50 to 100 by 10 do:
  P2_y[i]:=(i);
```

```
N2_y[i]:=Matrix(3,1,[0,P2_y[i],0])/(a+b);
d2_y_1[i]:=LinearSolve(A2_M,N2_y[i])/(b);
d2_y_2[i]:=LinearSolve(B2_M,N2_y[i])/(b);
D2_y_1[i]:=evalf((sqrt((d2_y_1[i](1,1))^2+(d2_y_1[i](2,1))^2+
d2_x_1[i](3,1)^2))/(a))*10^3;
D2_y_2[i]:=evalf((sqrt((d2_y_2[i](1,1))^2+(d2_y_2[i](2,1))^2+
d2_x_1[i](3,1)^2))/((a+b)))*10:
D2_y[i]:=evalf(D2_y_1[i]+D2_y_2[i]):
Sigma2_y_x[i] :=(E2[x])/(1-nu12[2]*nu21[2])*(d2_y_1[i](1)+
nu21[2]*d2_y_1[i](2));
Sigma2_y_y[i] := (E2[y])/(1-nu12[2]*nu21[2])*(d2_y_1[i](2)+
nu12[2]*d2_y_1[i](2)):
Sigma2_y_xy[i] := G2[xy]*d2_y_1[i](3);
od:
print(D2_y_1):
print(D2_y_2):
print(D2_y):
print(Sigma2_y_x);
print(Sigma2_y_y);
print(Sigma2_y_xy);
```

table([50 = 0.34817, 60 = 0.41779, 70 = 0.48743, 90 = 0.62669, 80 = 0.55707, 100 = 0.69633])

table([50 = 15.745, 60 = 18.894, 70 = 22.043, 90 = 28.341, 80 = 25.192, 100 = 31.490])

table([50 = 16.093, 60 = 19.312, 70 = 22.530, 90 = 28.968, 80 = 25.749, 100 = 32.186])

table([50 = −173436.341665129, 60 = −208123.609998155, 70 = −242810.878331181, 90 = −312185.414997233, 80 = −277498.146664207, 100 = −346872.683330259])

table([50 = 944949.771842544, 60 = $1.13393972621105\ 10^6$, 70 = $1.32292968057956\ 10^6$, 90 = $1.70090958931658\ 10^6$, 80 = $1.51191963494807\ 10^6$, 100 = $1.88989954368509\ 10^6$])

table([50 = −213022.071925485, 60 = −255626.486310582, 70 = −298230.900695679, 90 = −383439.729465873, 80 = −340835.315080776, 100 = −426044.143850970]) **(4.2.3)**

Max Stress

```
> for i from 50 to 100 by 10 do:
  if Sigma2_y_x[i] ≥ 0 then:
  MSY_2_1[i] := (Sigma2_y_x[i] / F1T[2]) :
  elif Sigma2_y_x[i] < 0 then:
  MSY_2_2[i] := -(Sigma2_y_x[i] / F1C[2]) :
  end if:
  if Sigma2_y_y[i] ≥ 0 then:
  MSY_2_3[i] := Sigma2_y_y[i] / F2T[2] :
  elif Sigma2_y_y[i] < 0 then:
  MSY_2_4[i] := -Sigma2_y_y[i] / F2C[2] :
  end if:
```

```
MS2y[i] := max(MSY_2_1[i]^(1/Ncamadas_2), MSY_2_2[i]^(1/Ncamadas_2),
    MSY_2_3[i]^(1/Ncamadas_2), MSY_2_4[i]^(1/Ncamadas_2)) :
od:
print(MS2y) :
```

$$\text{table}\left(\left[50 = \max\left(0.374577659577483, MSY\_2\_I_{50}^{1/4}, MSY\_2\_4_{50}^{1/4}\right), 60\right. \qquad \textbf{(4.2.9.1)}$$
$$= \max\left(0.392046140945047, MSY\_2\_I_{60}^{1/4}, MSY\_2\_4_{60}^{1/4}\right), 70$$
$$= \max\left(0.407449585846293, MSY\_2\_I_{70}^{1/4}, MSY\_2\_4_{70}^{1/4}\right), 90$$
$$= \max\left(0.433870375872168, MSY\_2\_I_{90}^{1/4}, MSY\_2\_4_{90}^{1/4}\right), 80$$
$$= \max\left(0.421280994947002, MSY\_2\_I_{80}^{1/4}, MSY\_2\_4_{80}^{1/4}\right), 100$$
$$\left. = \max\left(0.445450417890609, MSY\_2\_I_{100}^{1/4}, MSY\_2\_4_{100}^{1/4}\right)\right]\right)$$

Tsai-Hill

```
> for i from 50 to 100 by 10 do:
TH_y_2[i] := Ncamadas_2·(((G2[2]+G3[2])·Sigma2_y_x[i]^2
  +(G1[2]+G3[2])·Sigma2_y_y[i]^2-2 G3[2]·Sigma2_y_x[i]
  ·Sigma2_y_y[i]+2·G6[2]·Sigma2_y_xy[i]^2))^(1/Ncamadas_2) :
od:

print(TH_y_2) :
```

$$\text{table}([50 = 0.563867940927013, 60 = 0.617669967277239, 70 \qquad \textbf{(4.2.10.1)}$$
$$= 0.667171648858564, 90 = 0.756504260174304, 80 = 0.713232397117334,$$
$$100 = 0.797419592245259])$$

Tsai-Wu

```
> for i from 50 to 100 by 10 do:
A[i] := (Sigma2_y_x[i])^2/(F1T[2]·F1C[2]) + (Sigma2_y_y[i])^2/(F2T[2]·F2C[2])
  + (Sigma2_y_xy[i])^2/F4[2]^2 + (Sigma2_y_xy[i])^2/F5[2]^2
  + C4[2]·(Sigma2_y_x[i]·Sigma2_y_y[i])/sqrt(F1T[2]·F1C[2]·F2T[2]·F2C[2])
  + C5[2]·(Sigma2_y_x[i])/sqrt(F1T[2]·F1C[2]) + C6[2]·(Sigma2_y_y[i])/sqrt(F2T[2]·F2C[2]) :
B[i] := evalf((F1T[2]^(-1)-F1C[2]^(-1))·Sigma2_y_x[i]+(F2T[2]^(-1)
  -F2C[2]^(-1))·Sigma2_y_y[i]);

TW_y_2[i] := 2·(-evalf(-B[i]/(2·A[i])+sqrt((B[i]/(2·A[i]))^2)+1/A[i]))^(-1)^(1/Ncamadas_2) :
```

```
od:
print(TW_y_2):
```

table([50 = 0.62590, 60 = 0.65526, 70 = 0.68118, 90 = 0.72574, 80 = 0.70450, 100 = 0.74532]) **(4.2.11.1)**

Hashin

```
> for i from 50 to 100 by 10 do:

#Different components
 if Sigma2_y_x[i] ≥ 0 then:
H2Y_1_1[i] := (Sigma2_y_x[i]/F1T[2])^2 + (Sigma2_y_xy[i]/F6[2])^2 :

H2Y_1_2[i] := 0 :
H2Y_1_3[i] := 0 :
H2Y_1_4[i] := 0 :

 elif Sigma2_y_x[i] < 0 then:
 H2Y_1_2[i] := abs(Sigma2_y_x[i])/F1C[2] :
H2Y_1_1[i] := 0 :
H2Y_1_2[i] := 0 :
H2Y_1_3[i] := 0 :

 end if:
if Sigma2_y_y[i] ≥ 0 then:
 H2Y_1_3[i] := (Sigma2_y_y[i]/F2T[2])^2 + (Sigma2_y_xy[i]/F6[2])^2 :

H2Y_1_1[i] := 0 :
H2Y_1_2[i] := 0 :
H2Y_1_4[i] := 0 :

 elif Sigma2_y_y[i] < 0 then:
 H2Y_1_4[i] := (Sigma2_y_y[i]/(2·F4[2]))^2 + ((F2C[2]/(2·F4[2]))^2 - 1)
   ·Sigma2_y_y[i]/F2C[2] + (Sigma2_y_xy[i]/F6[2])^2 :

H2Y_1_1[i] := 0 :
H2Y_1_2[i] := 0 :
H2Y_1_3[i] := 0 :

 end if:

Hashin2y[i] := max(Ncamadas_2·H2Y_1_1[i]^(1/Ncamadas_2), Ncamadas_2
  ·H2Y_1_2[i]^(1/Ncamadas_2), Ncamadas_2·H2Y_1_3[i]^(1/Ncamadas_2),
   Ncamadas_2·H12Y_1_4[i]^(1/Ncamadas_2)) :
```

```
od:
print(Hashin2y):
```

$$\text{table}\left(\left[50 = \max\left(0.56384, 4\,H12Y\_1\_4_{50}^{1/4}\right), 60 = \max\left(0.61768, 4\,H12Y\_1\_4_{60}^{1/4}\right), 70 = \max\left(0.66716, 4\,H12Y\_1\_4_{70}^{1/4}\right), 90 = \max\left(0.75648, 4\,H12Y\_1\_4_{90}^{1/4}\right), 80 = \max\left(0.71320, 4\,H12Y\_1\_4_{80}^{1/4}\right), 100 = \max\left(0.79740, 4\,H12Y\_1\_4_{100}^{1/4}\right)\right]\right) \quad \textbf{(4.2.12.1)}$$

Appendix D- Technical Drawings

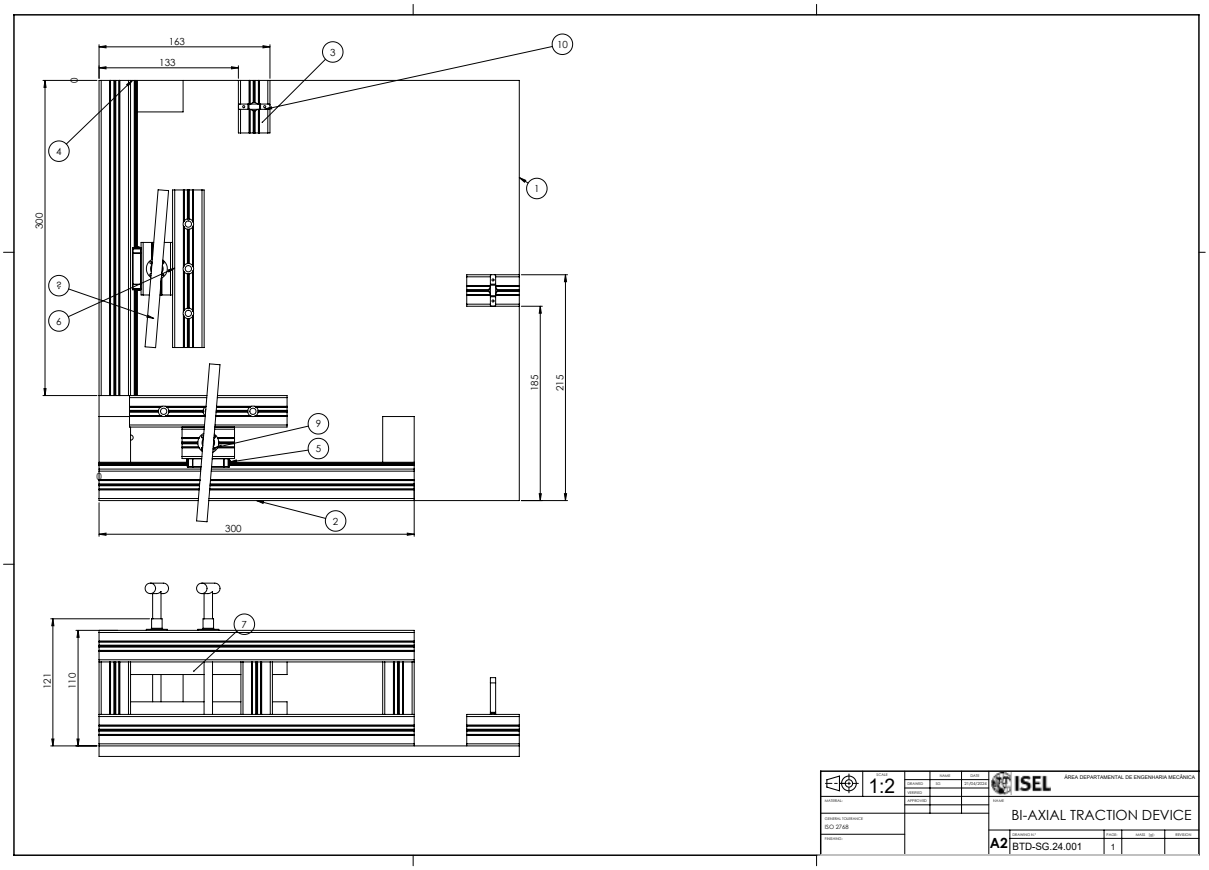
163
133
300
185
215
300
121
110
1
2
3
4
5
6
7
8
9
10
1:2
ISEL
ÁREA DEPARTAMENTAL DE ENGENHARIA MECÂNICA
BI-AXIAL TRACTION DEVICE
ISO 2768
A2
BTD-SG.24.001

Nº	DRAWING Nº	NAME	QUANTITY	MATERIAL	OBS
1	BTD-001	MDF BOARD	1	MDF	
2	BTD-002	BOSCH 30X30X300	4	ALUMINIUM	300 mm V-SLOT BEAM
3	BTD-003	BOSCH 30X30X50	12	ALUMINIUM	50 mm V-SLOT BEAM
4	BTD-004	LINEAR GUIDE SUBASSEMBLY	1	-	
5	BTD-005	M3X6	20	SS304	
6	BTD-006	BOSCH 30X30X150	4	ALUMINIUM	150 mm V-SLOT BEAM
7	BTD-007	CLAMPING JAW	4	CAST IRON	
8	BTD-008	M7 X 30 PIN	2	ANSI STEEL	
9	BTD-009	SUPPORT	2	NICKEL	
10	BTD-010	EYELET	2	ANSI STEEL	

SCALE 1:1

	NAME	DATE
DRAWN	SG	22/04/2024
VERIFIED		
APPROVED		

MATERIAL:

GENERAL TOLERANCE ISO 2768

FINISHING:

ISEL ÁREA DdepartamENTAL DE ENGENHARIA MECÂNICA

NAME

BILL OF MATERIALS

A3	DRAWING Nº	PAGE:	MASS: kg	REVISION:
	BTD-BOM-24	1		

NOTE: THE THICKNESS IS EQUAL TO 10mm

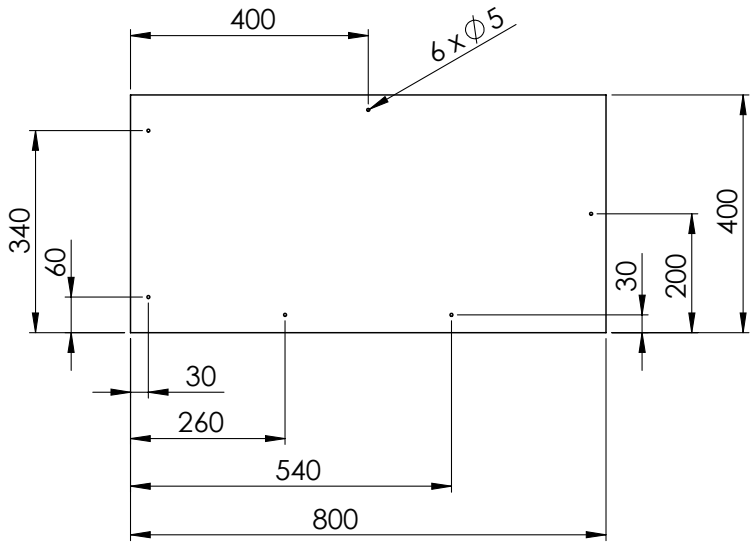

SCALE 1:10		NAME	DATE	ISEL	ÁREA DEPARTAMENTAL DE ENGENHARIA MECÂNICA
	DRAWN	SG	22/04/2024		
	VERIFIED				
MATERIAL: MDF	APPROVED			NAME: MDF BOARD	
GENERAL TOLERANCE ISO 2768					
FINISHING					

A4	DRAWING N.°	PAGE	MASS [g]:	REVISION
	BTD001	1	724.41	

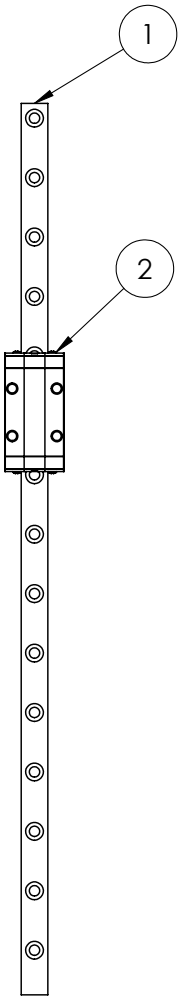

Nº	DRAWING Nº	NAME	QUANTITY	MATERIAL	OBS
1	BTD-004-A	GUIDE BEAM	1	ALUMINIUM	
2	BTD-004-B	CART	2	ALUMINIUM	

SCALE 1:2		NAME	DATE
	DRAWN	SG	22/04/2024
	VERIFIED		
MATERIAL:	APPROVED		
GENERAL TOLERANCE ISO 2768			
FINISHING			

ISEL ÁREA DdepartamENTAL DE ENGENHARIA MECÂNICA

NAME

LINEAR GUIDE SUBASSEMBLY

A4	DRAWING Nº	PAGE	MASS [g]:	REVISION
	BTD-004	1		

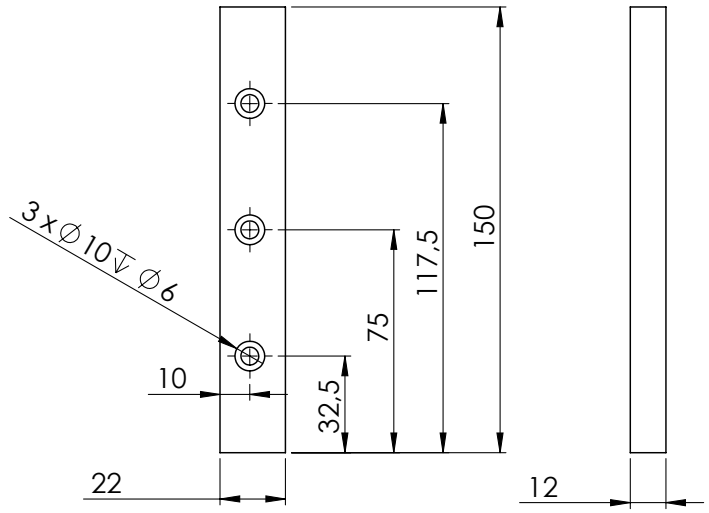

SCALE 1:2		NAME	DATE	ISEL	ÁREA DEPARTAMENTAL DE ENGENHARIA MECÂNICA
	DRAWN	SG	22/04/2024		
	VERIFIED				
MATERIAL: Gray Cast Iron	APPROVED			NAME	CLAMPING JAW
GENERAL TOLERANCE ISO 2768					
FINISHING				A4	DRAWING Nº: BTD-007 / PAGE: 1 / MASS [g]: 269.11 / REVISION:

Appendix E- Mechanical APDL Results

E1 Case Study

NX Load Configuration

- **Hashin-Rottem IF- 150N/mm to 200N/mm**

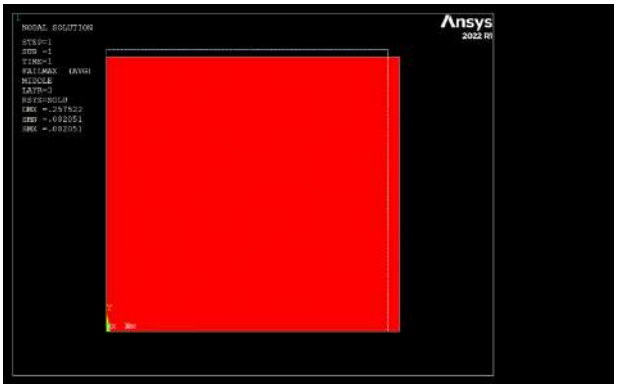

150N/mm

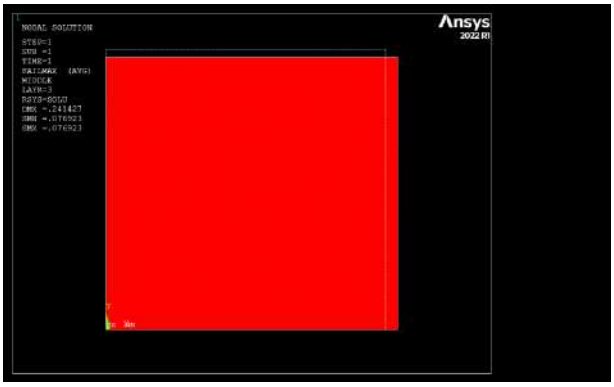

160N/mm

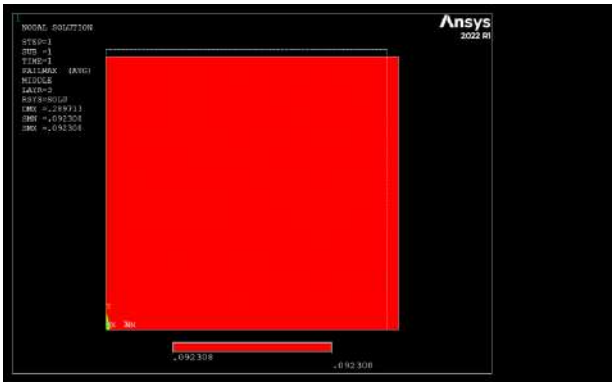

170N/mm

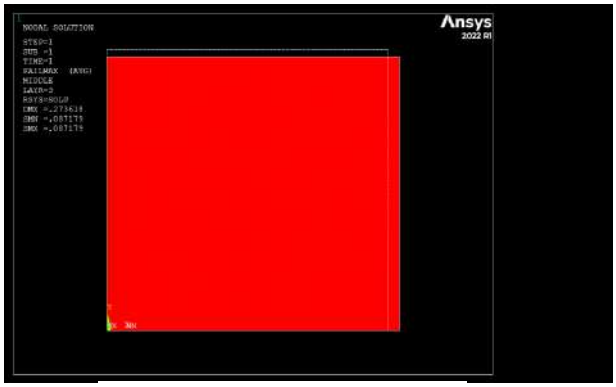

180N/mm

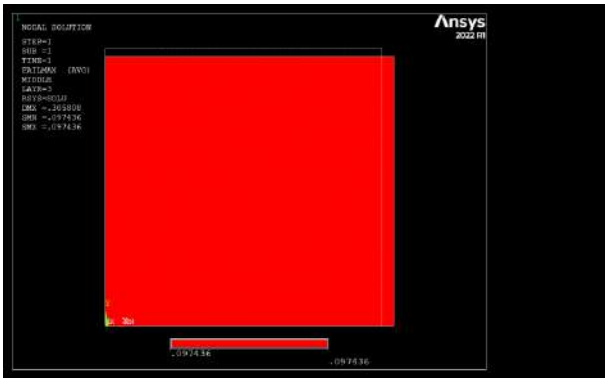

190N/mm

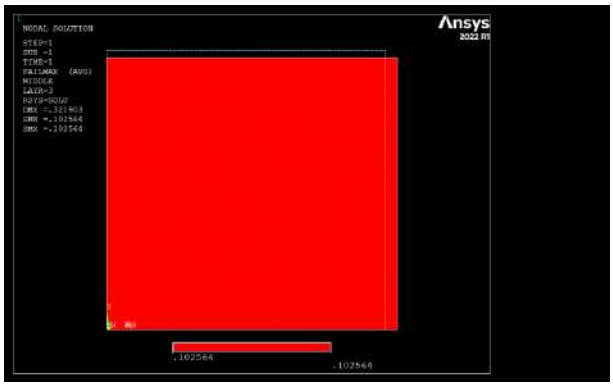

200N/mm

- **Max Stress IF- 150N/mm to 200N/mm**

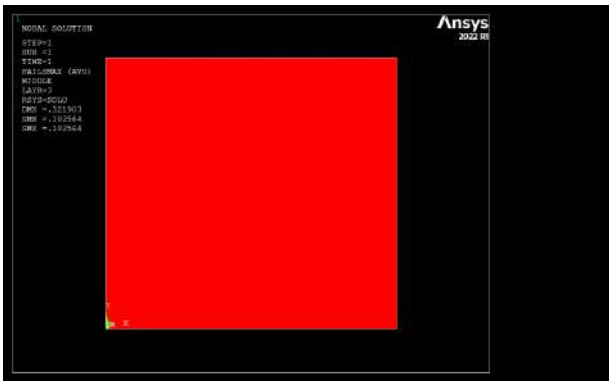

150N/mm

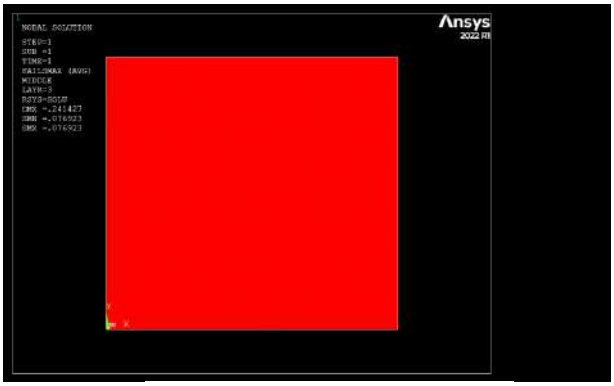

160N/mm

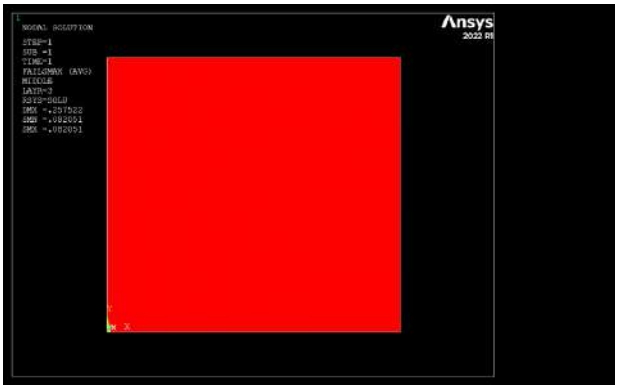

170N/mm

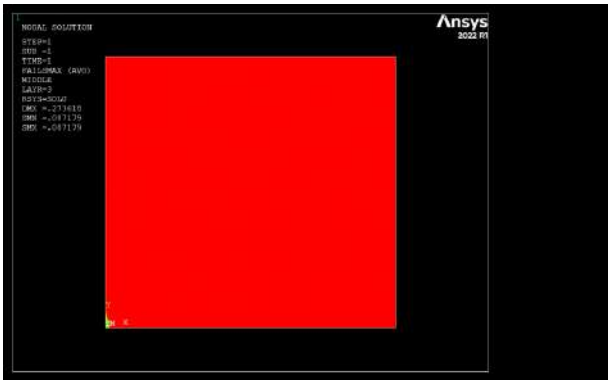

180N/mm

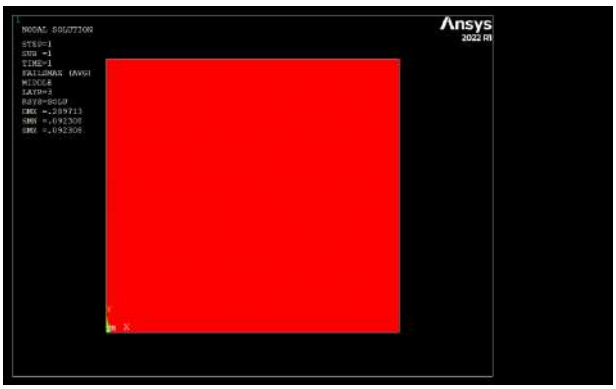

190N/mm

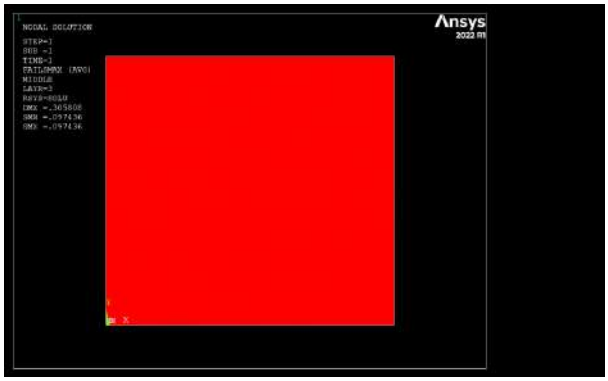

200N/mm

- **Tsai Hill IF- 150N/mm to 200N/mm**

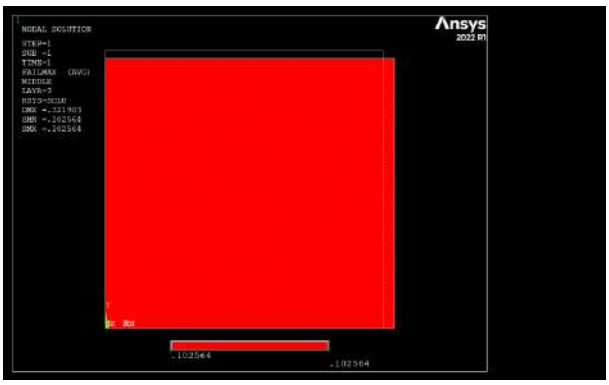

150N/mm

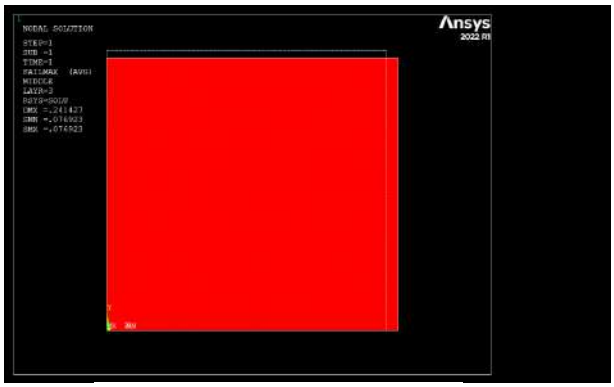

160N/mm

170N/mm

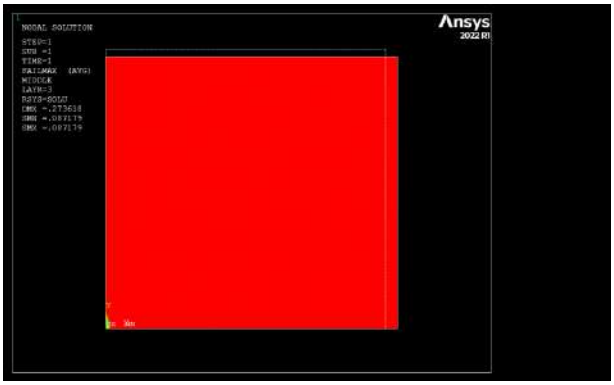

180N/mm

190N/mm

200N/mm

- **Tsai Wu IF- 150N/mm to 200N/mm**

150N/mm

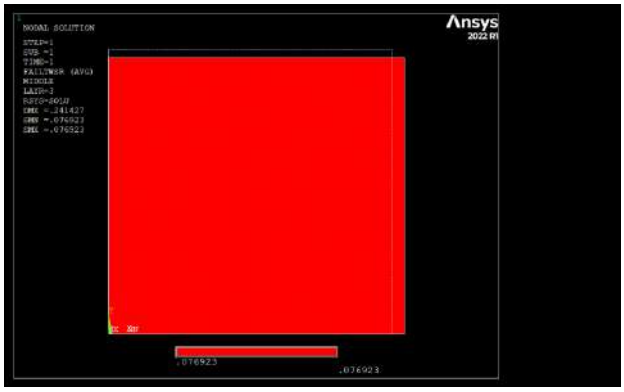

160N/mm

170N/mm

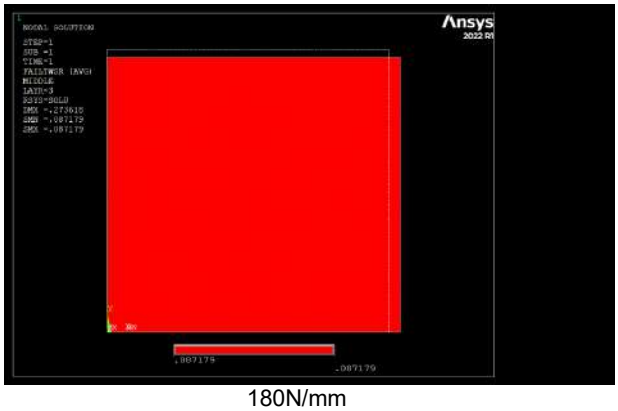

180N/mm

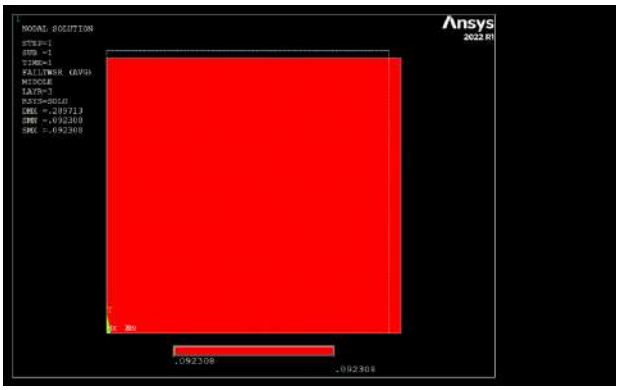

190N/mm

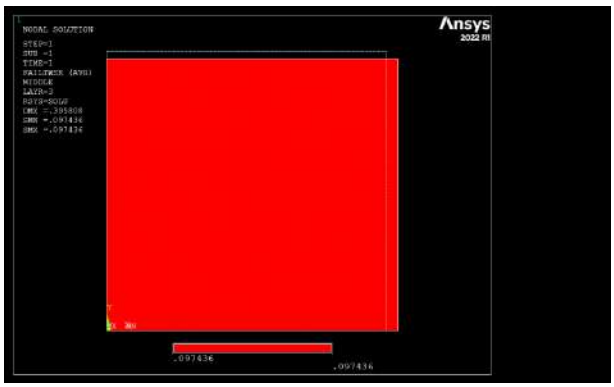

200N/mm

- **Maximum Displacement- 150N/mm to 200N/mm**

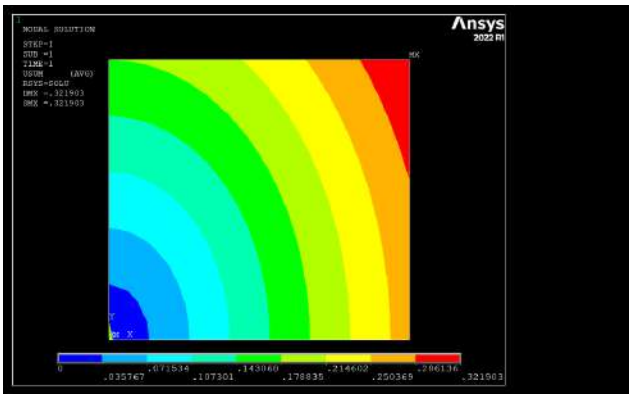

150N/mm

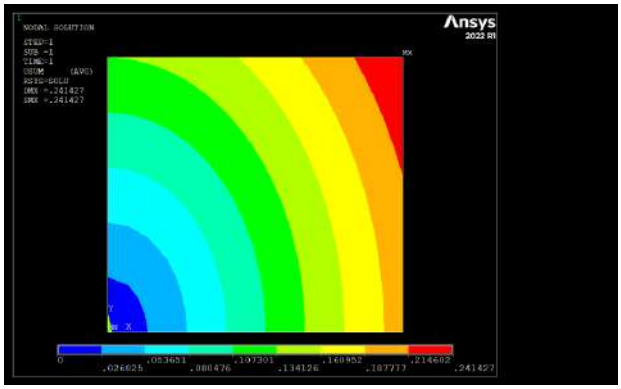

160N/mm

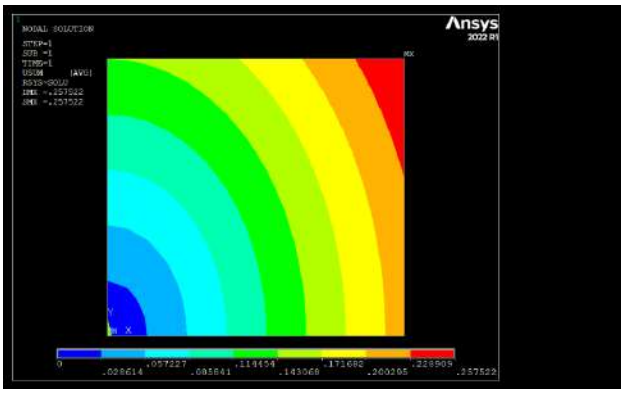

170N/mm

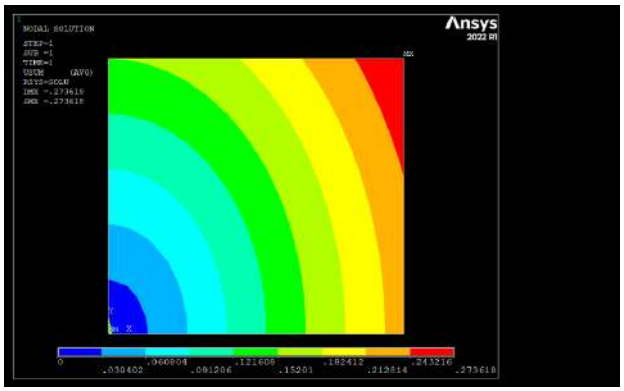

180N/mm

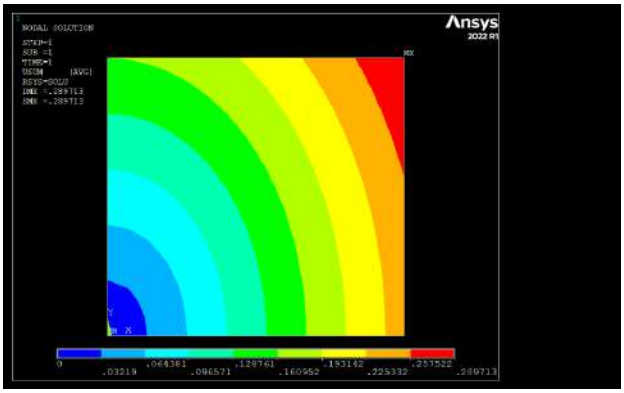

190N/mm

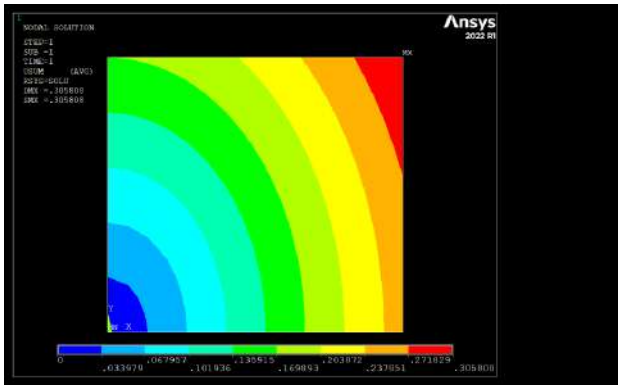

200N/mm

E1 Case Study

NXY Load Configuration

- **Hashin-Rottem IF- 150N/mm to 200N/mm**

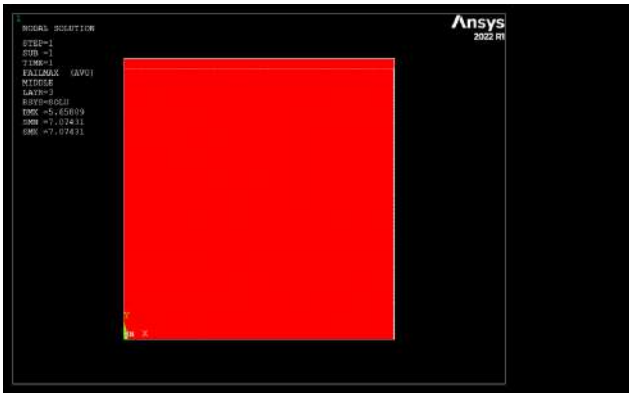

150N/mm

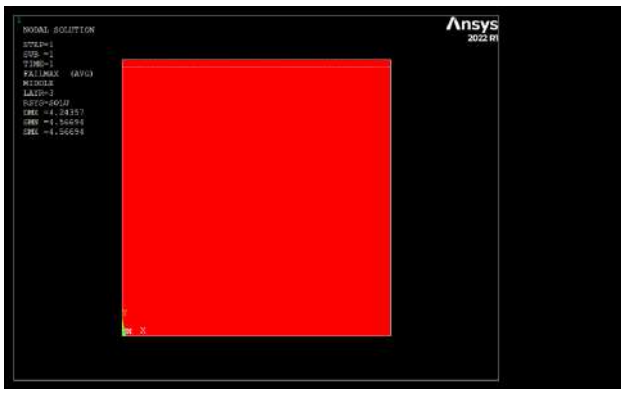

160N/mm

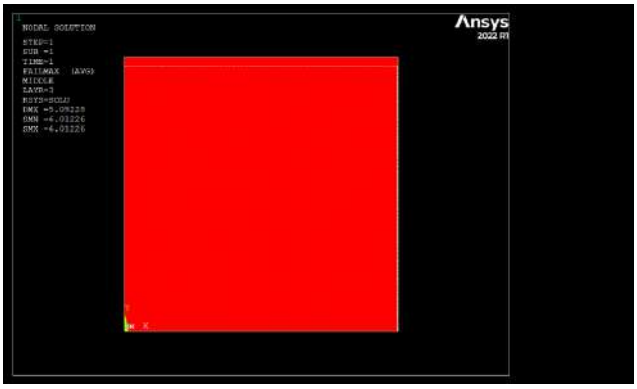

170N/mm

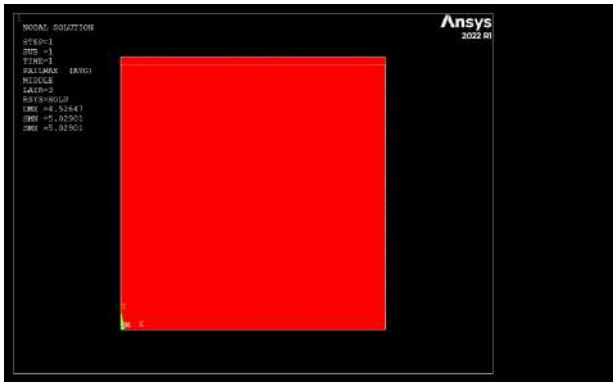

180N/mm

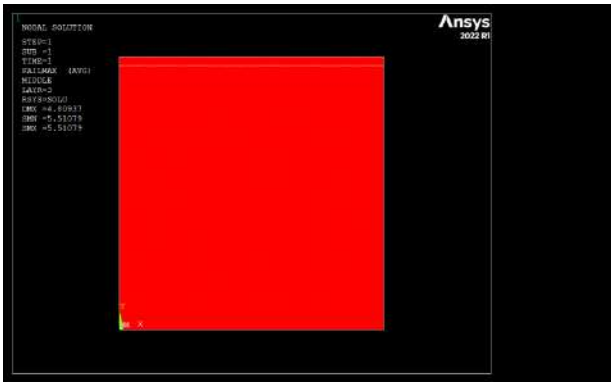

190N/mm

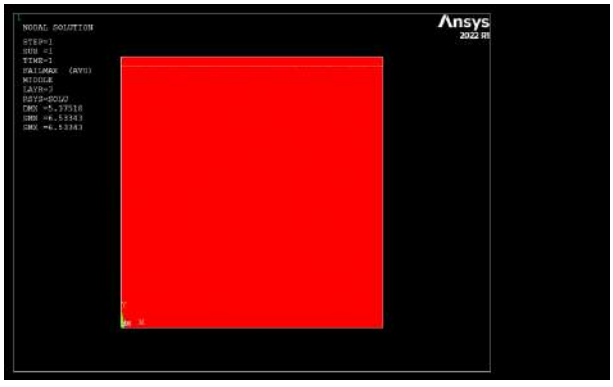

200N/mm

- **Max Stress IF- 150N/mm to 200N/mm**

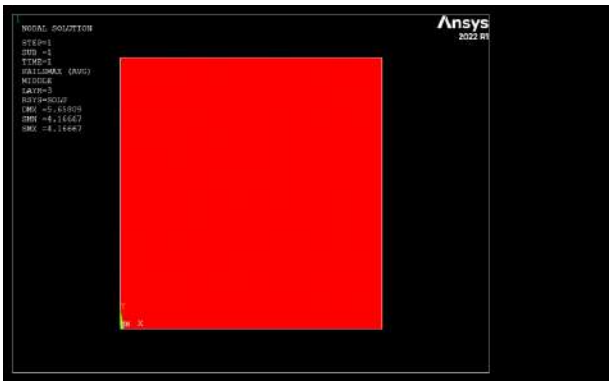

150N/mm

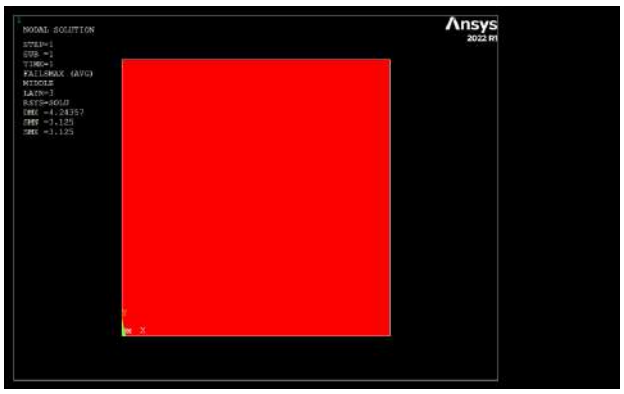

160N/mm

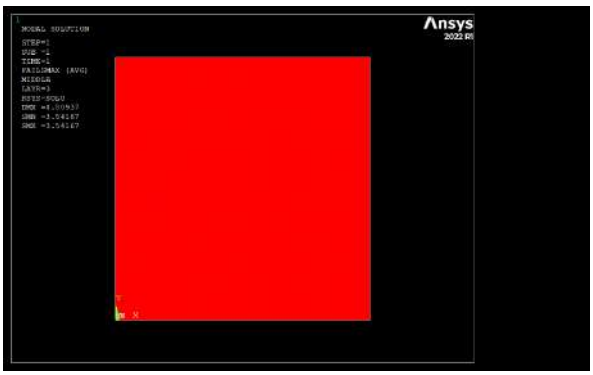

170N/mm

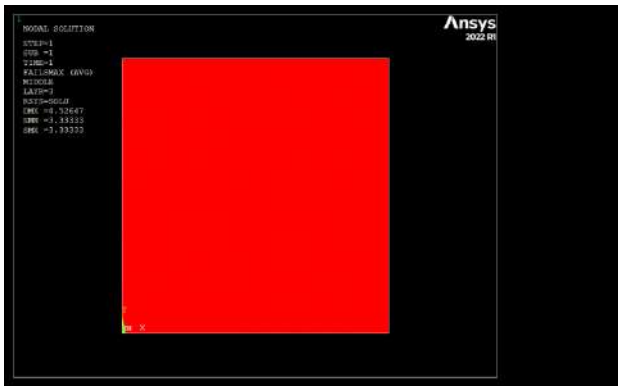

180N/mm

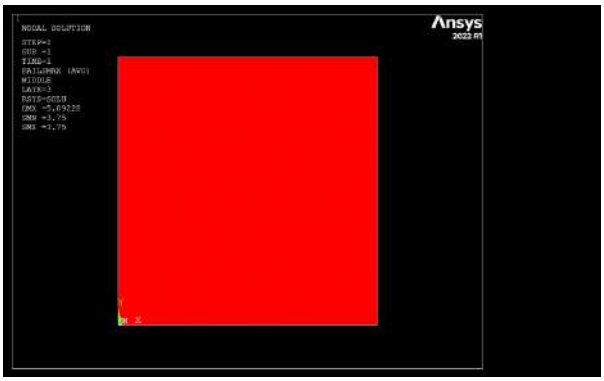

190N/mm

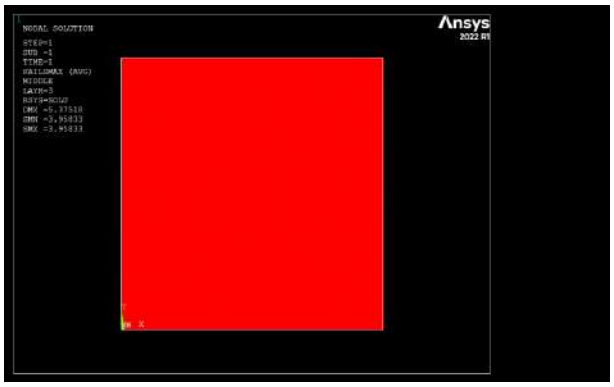

200N/mm

- **Tsai Hill IF- 150N/mm to 200N/mm**

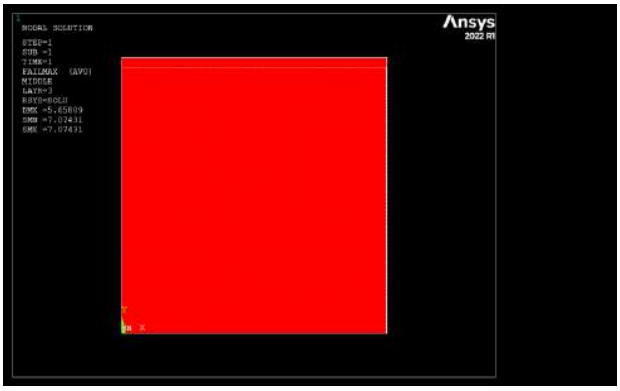

150N/mm

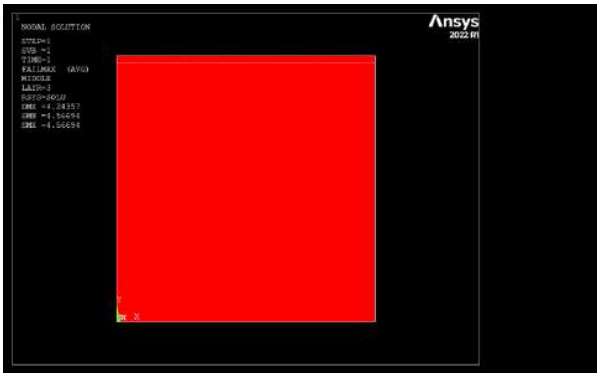

160N/mm

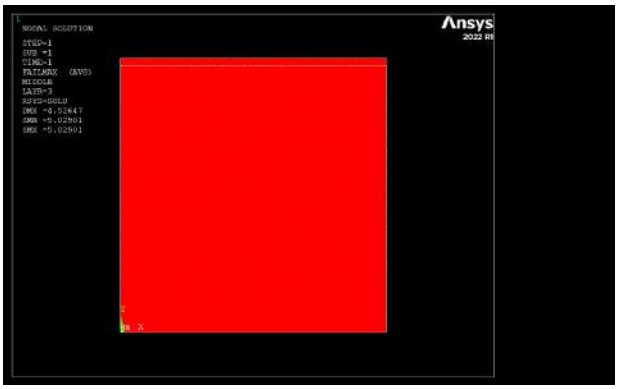

170N/mm

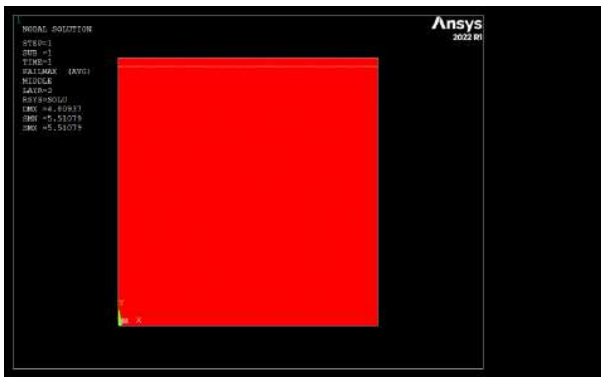

180N/mm

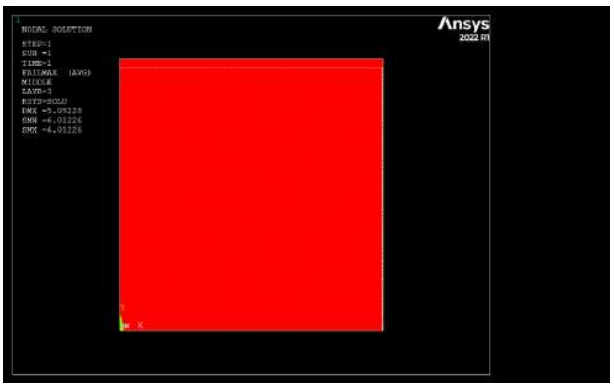

190N/mm

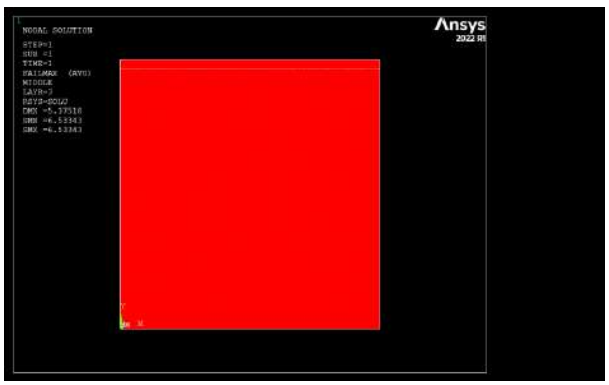

200N/mm

- **Tsai Wu IF- 150N/mm to 200N/mm**

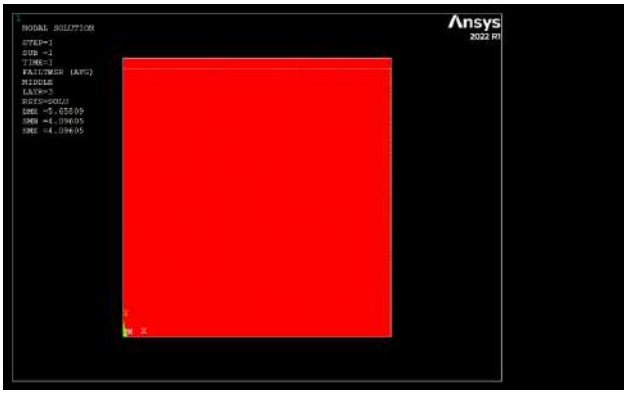

150N/mm

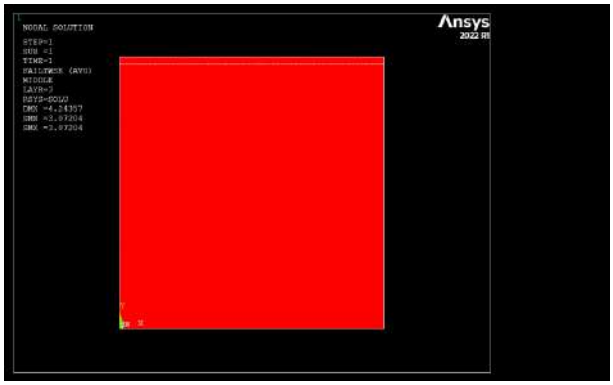

160N/mm

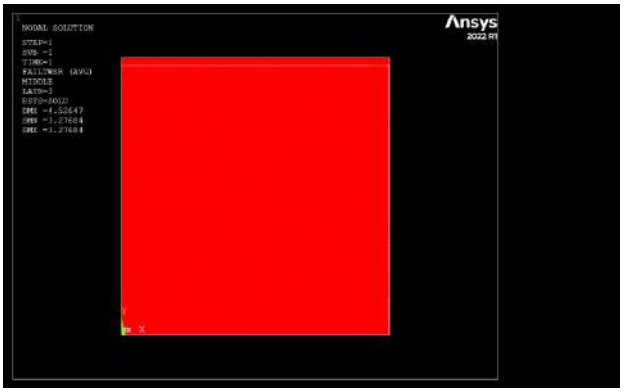

170N/mm

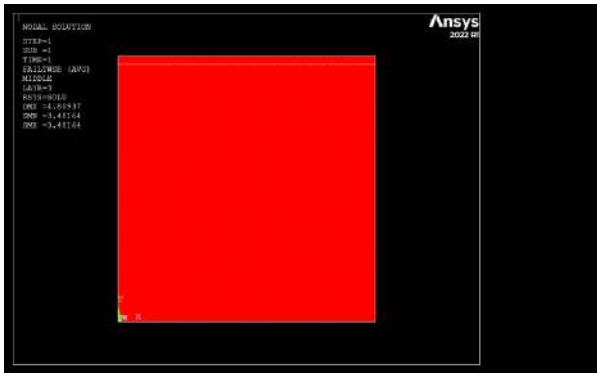

180N/mm

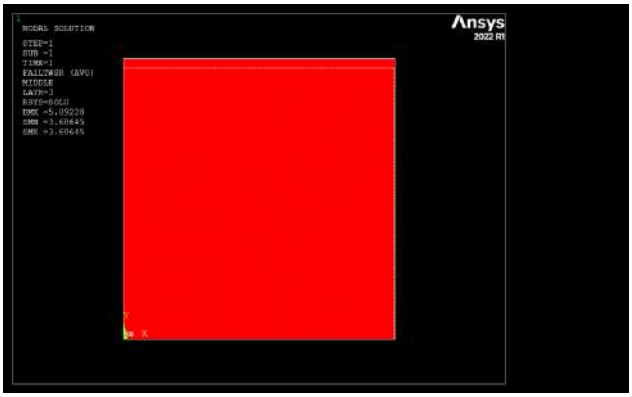

190N/mm

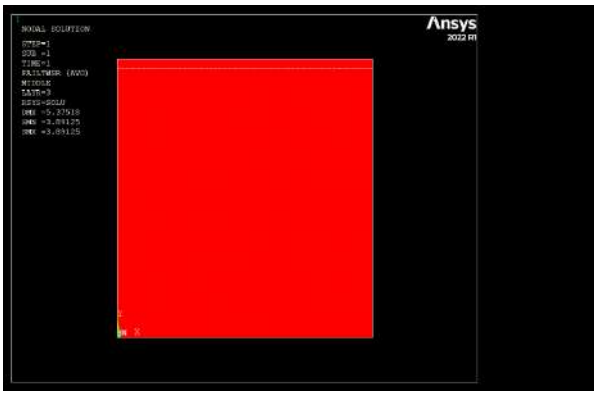

200N/mm

Maximum Displacement- 150N/mm to 200N/mm

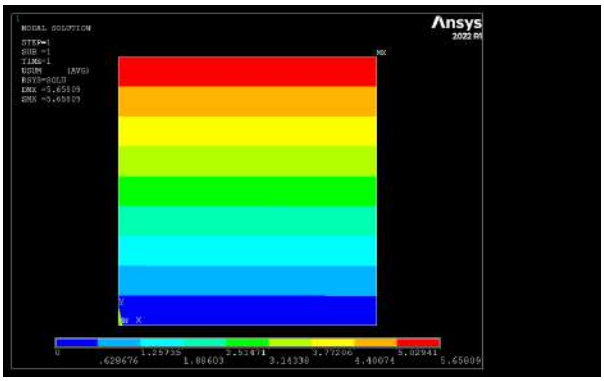

150N/mm

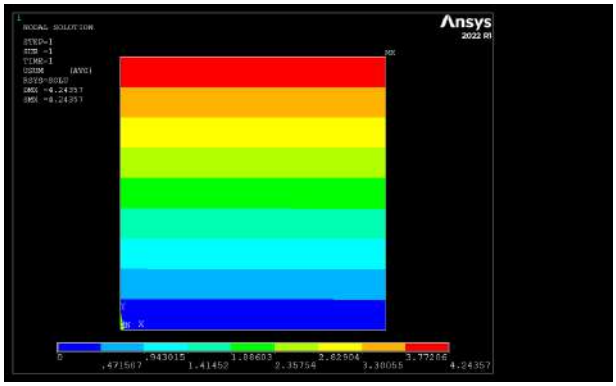

160N/mm

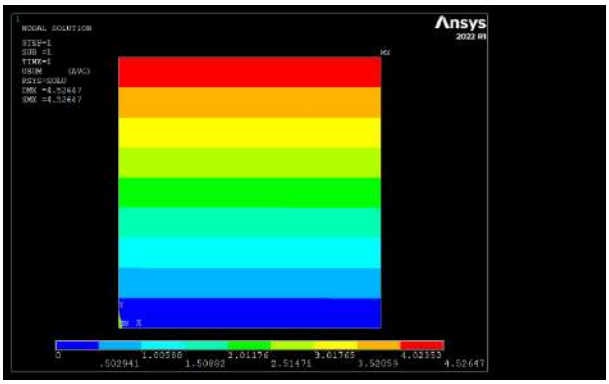

170N/mm

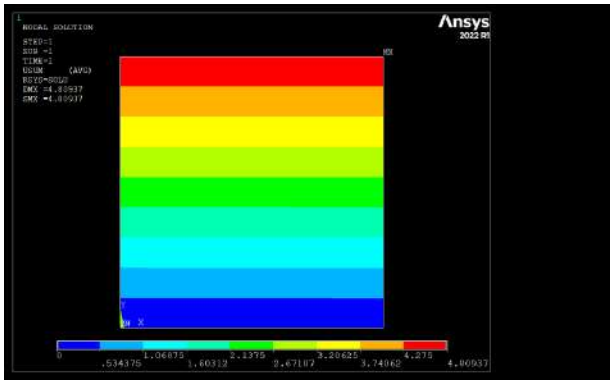

180N/mm

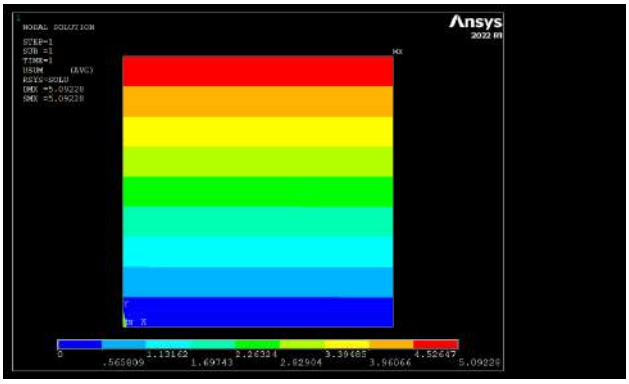

190N/mm

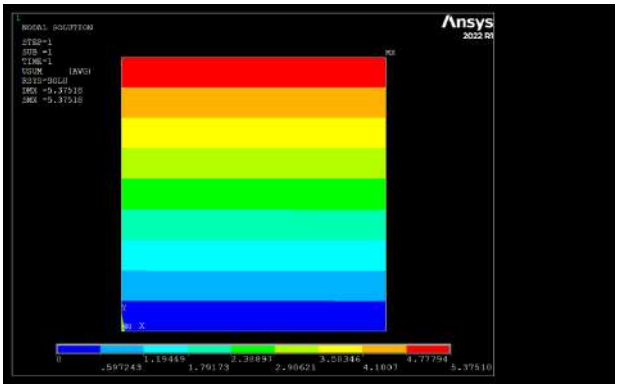

200N/mm

E1 Case Study

NY Load Configuration

- **Hashin-Rottem IF- 150N/mm to 200N/mm**

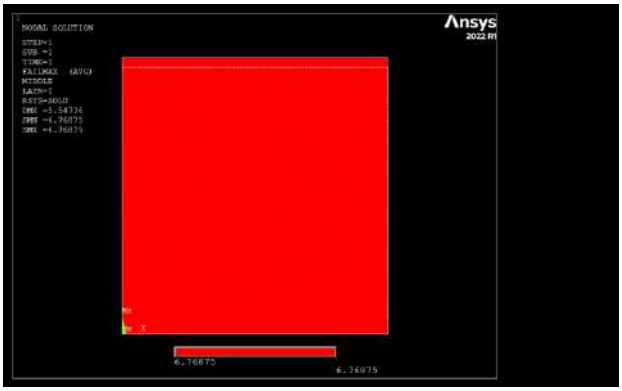

150N/mm

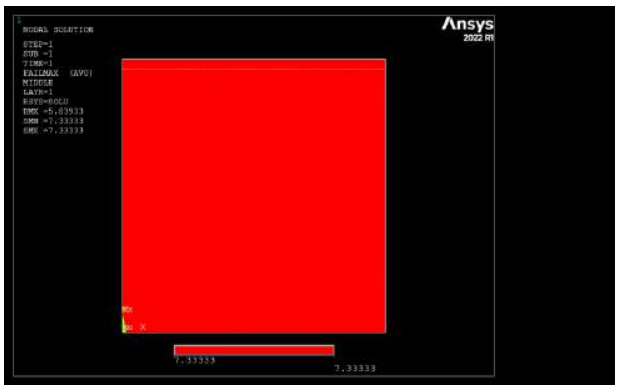

160N/mm

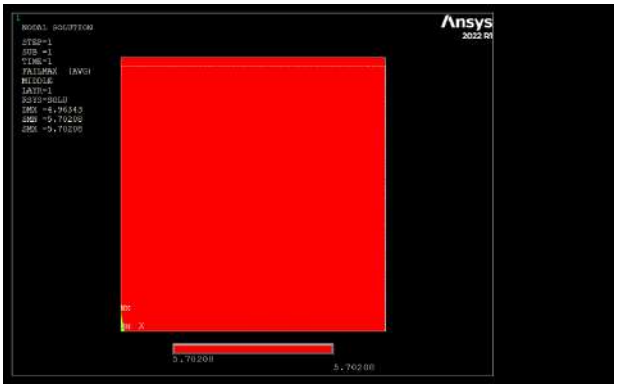

170N/mm

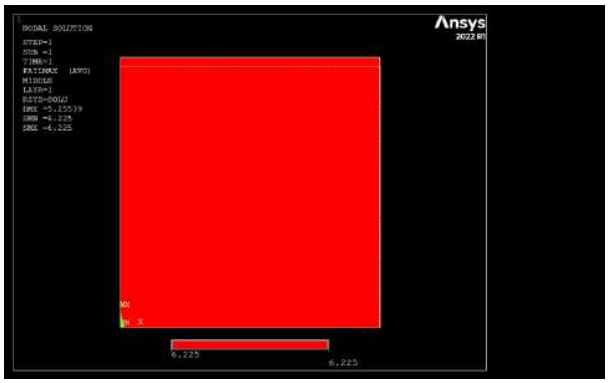

180N/mm

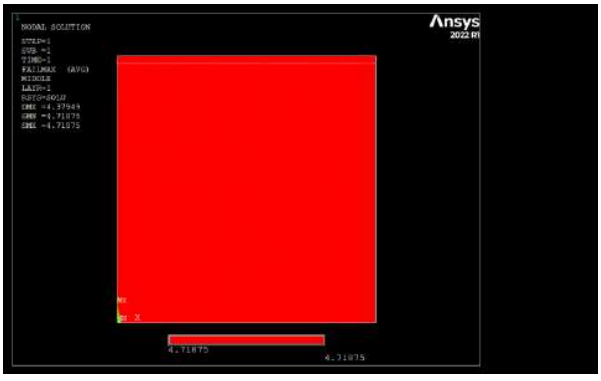

190N/mm

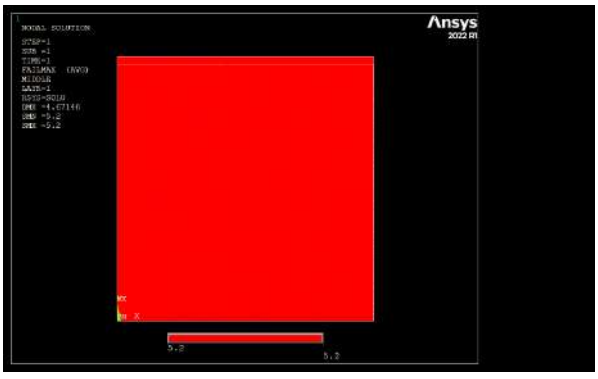

200N/mm

- **Max Stress IF- 150N/mm to 200N/mm**

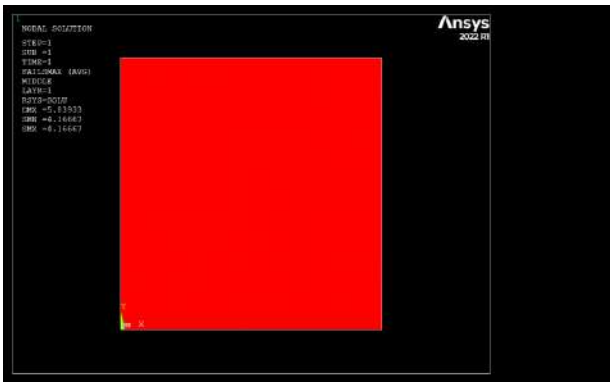

150N/mm

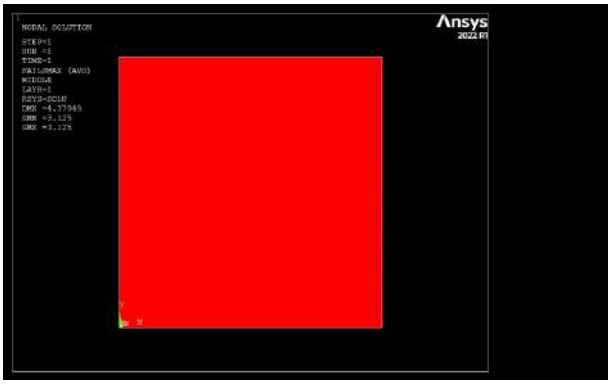

160N/mm

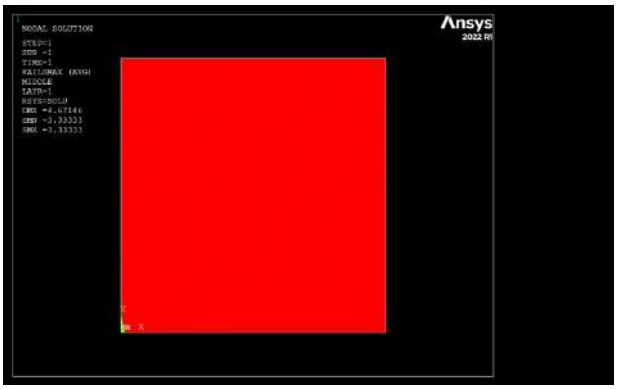

170N/mm

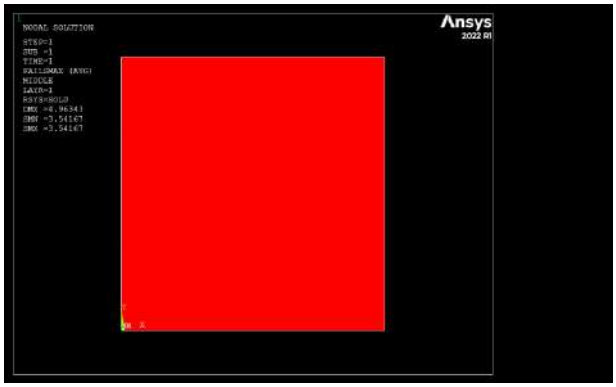

180N/mm

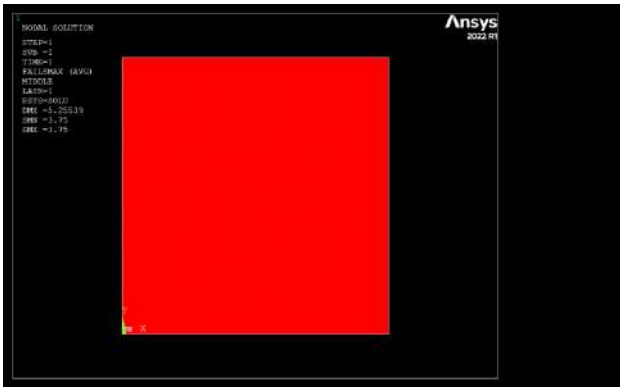

190N/mm

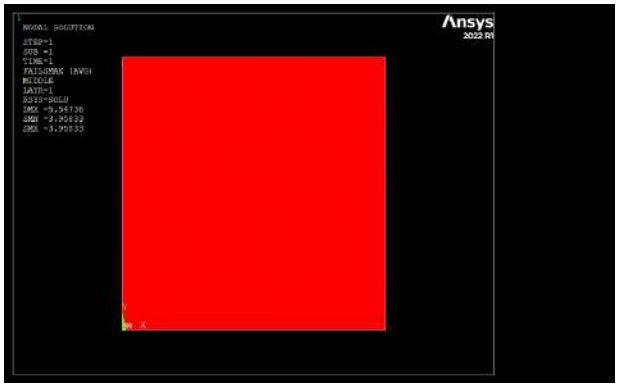

200N/mm

- **Tsai Hill IF- 150N/mm to 200N/mm**

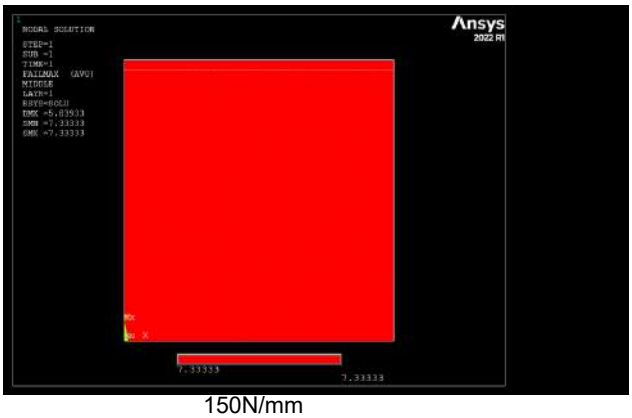

150N/mm

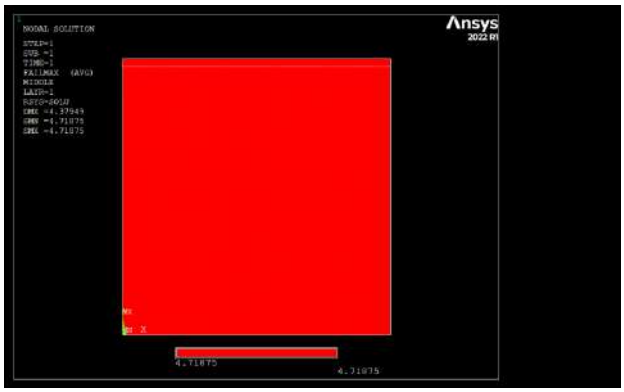

160N/mm

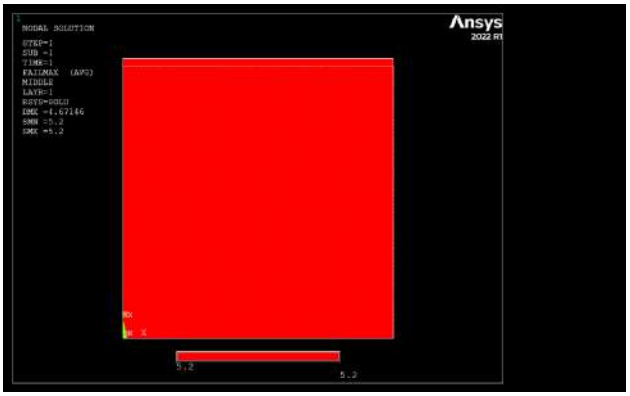

170N/mm

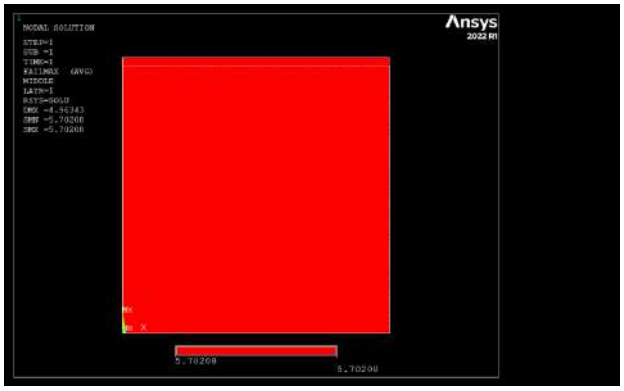

180N/mm

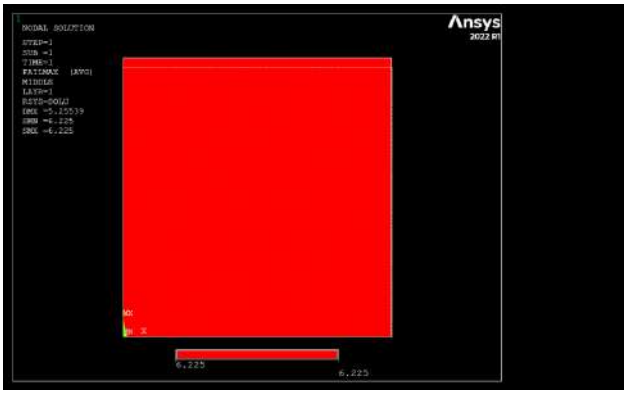

190N/mm

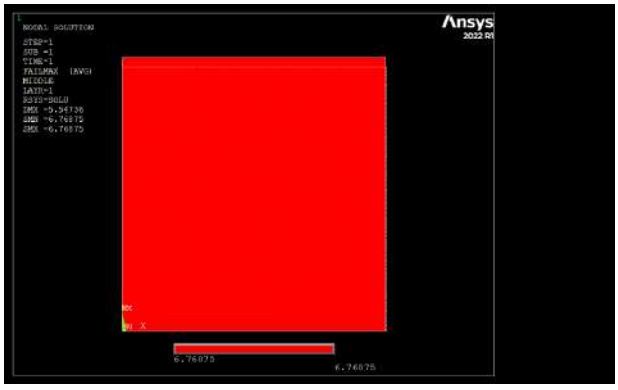

200N/mm

Tsai Wu IF- 150N/mm to 200N/mm

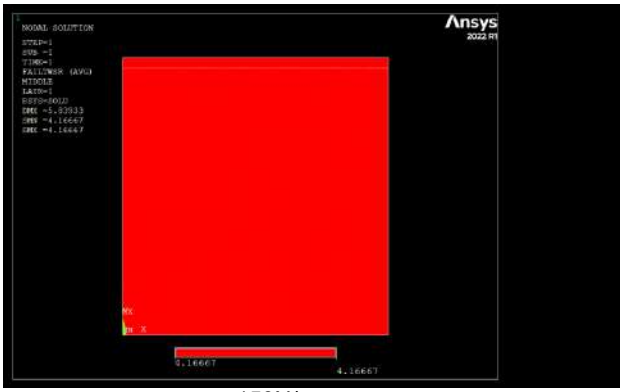

150N/mm

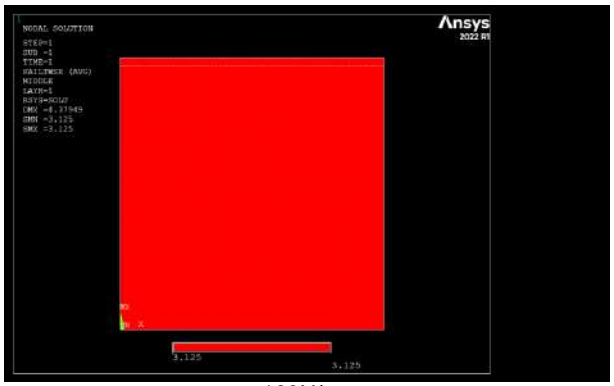

160N/mm

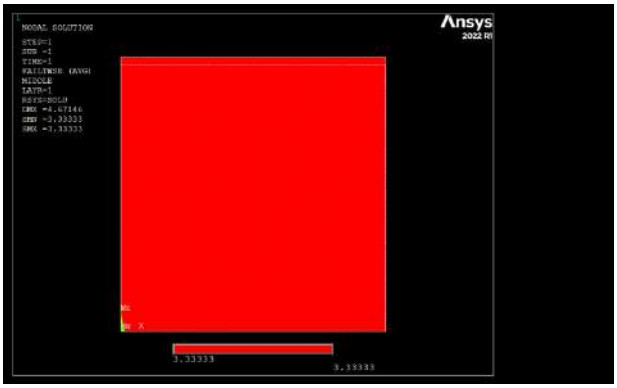

170N/mm

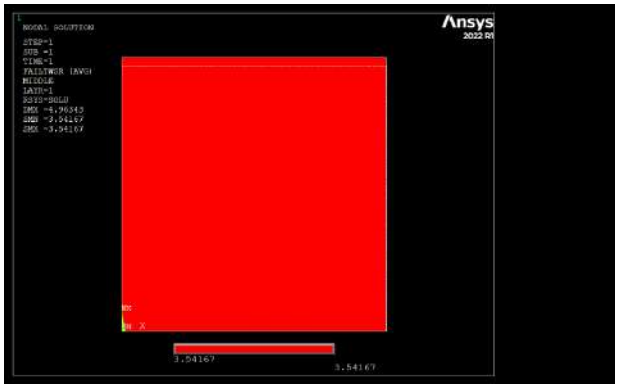

180N/mm

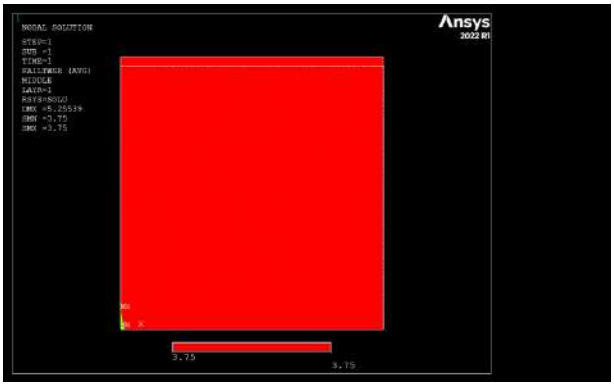

190N/mm

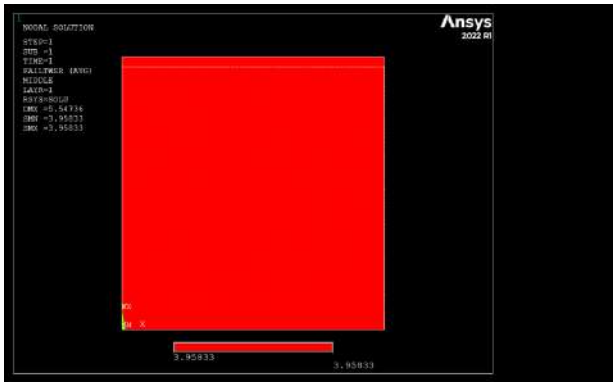

200N/mm

Maximum Displacement- 150N/mm to 200N/mm

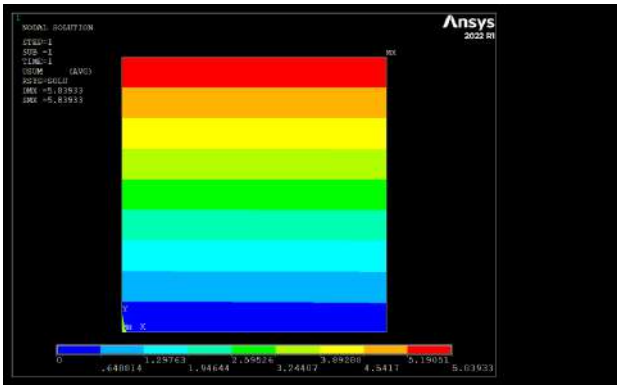

150N/mm

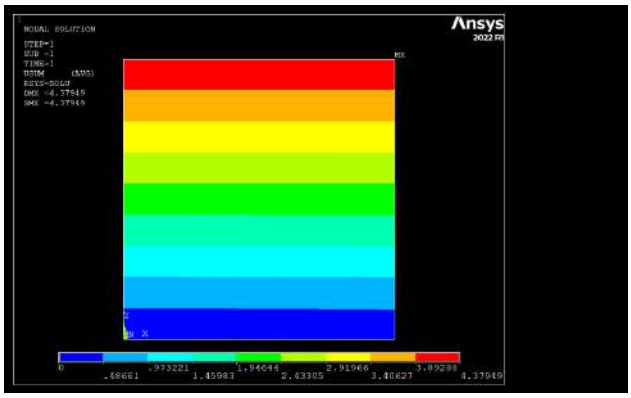

160N/mm

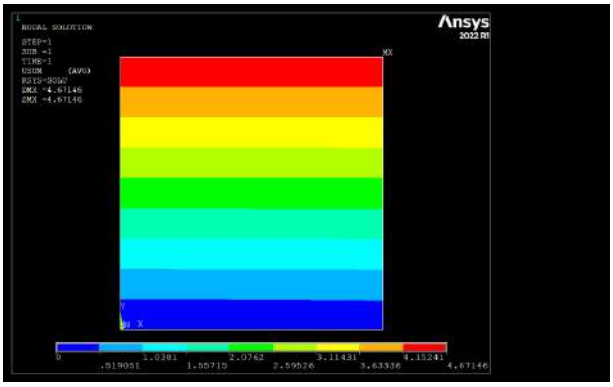

170N/mm

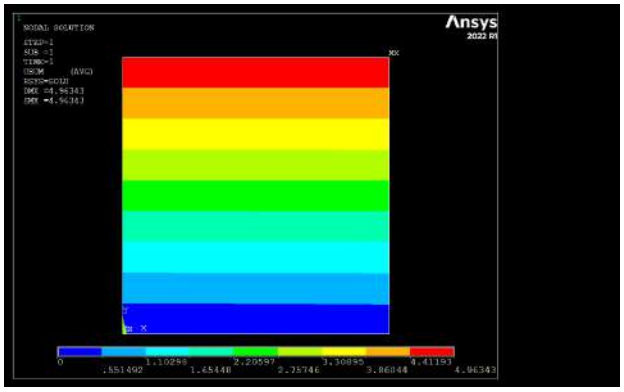

180N/mm

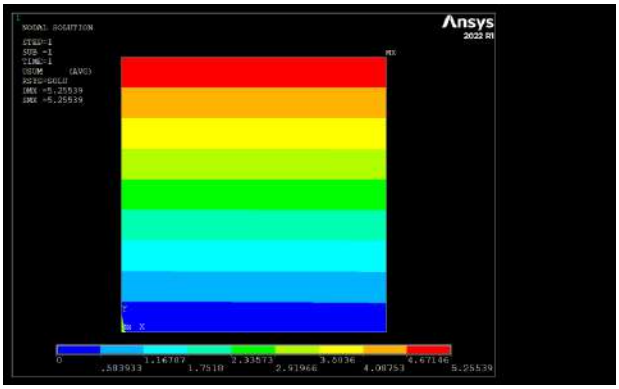

190N/mm

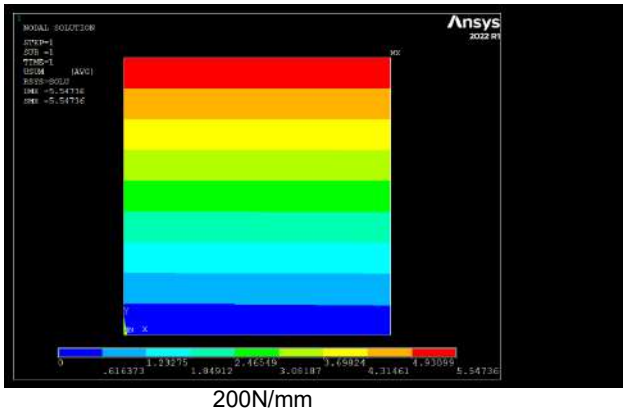

200N/mm

E2 Case Study

NX Load Configuration

- **Hashin-Rottem IF- 50N/mm to 100N/mm**

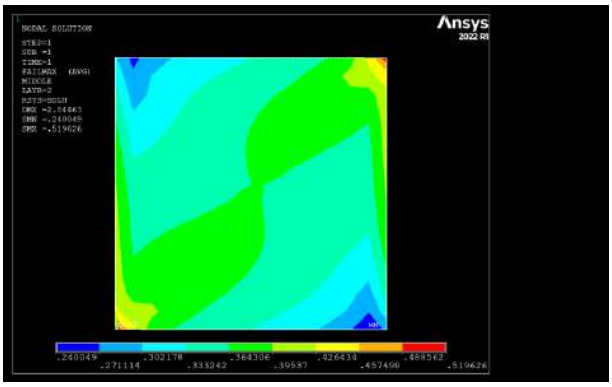

50N/mm

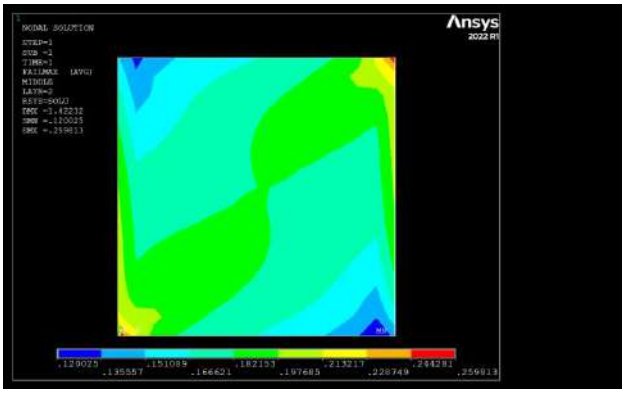

60N/mm

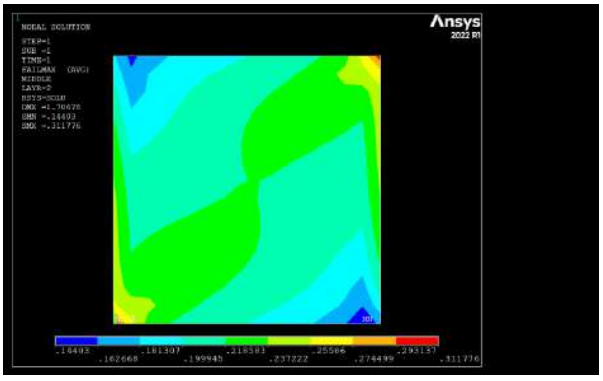

70N/mm

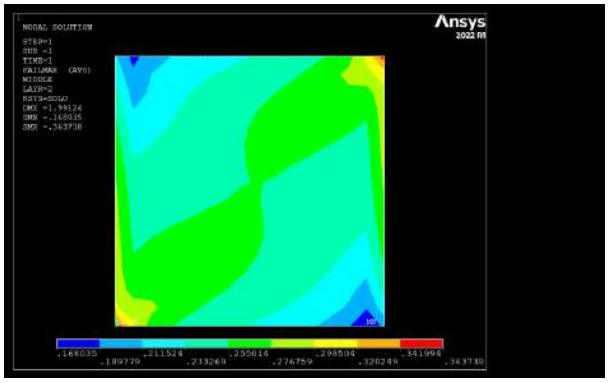

80N/mm

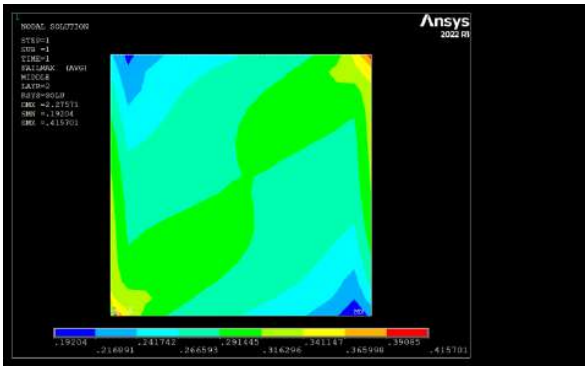

90N/mm

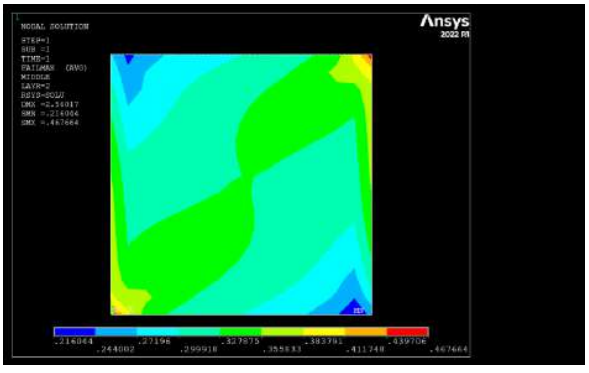

100N/mm

- **Max Stress IF- 50N/mm to 100N/mm**

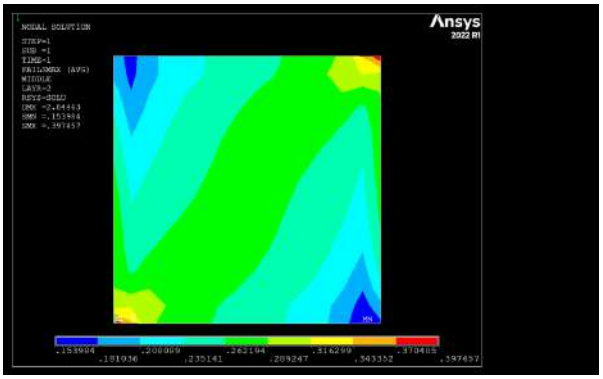

50N/mm

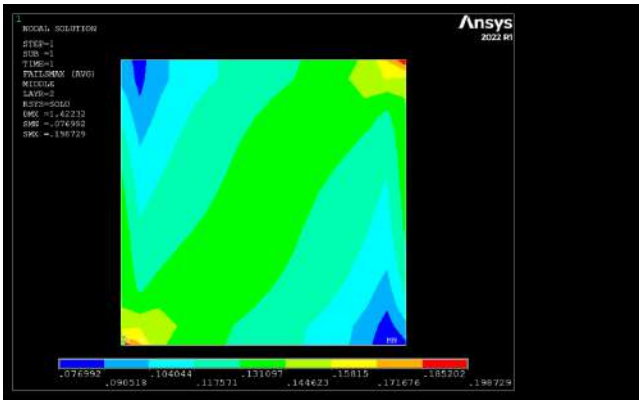

60N/mm

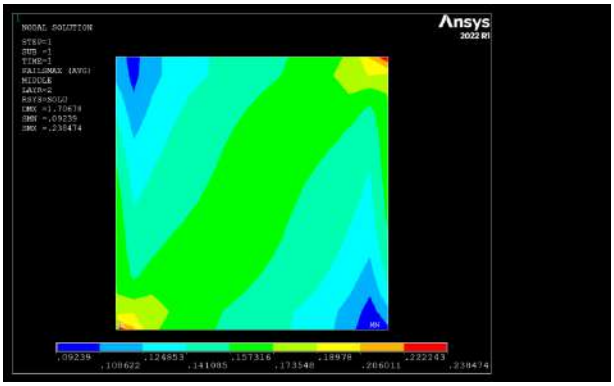

70N/mm

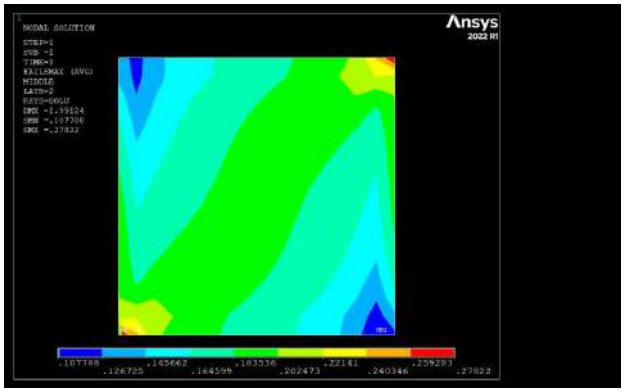

80N/mm

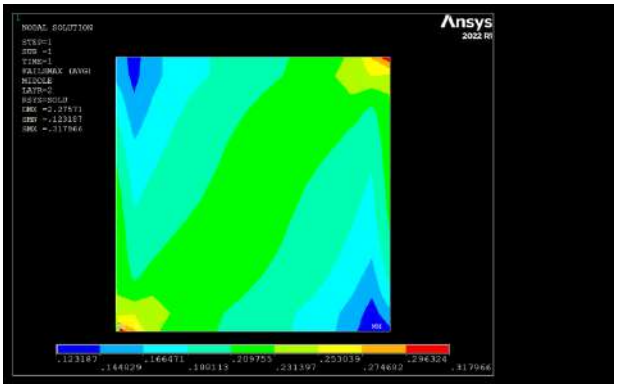

90N/mm

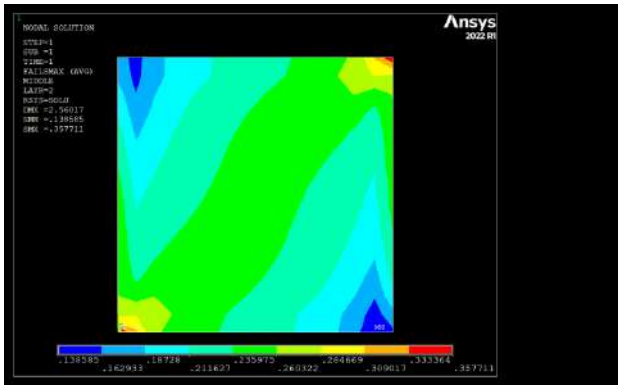

100N/mm

Tsai Hill IF- 50N/mm to 100N/mm

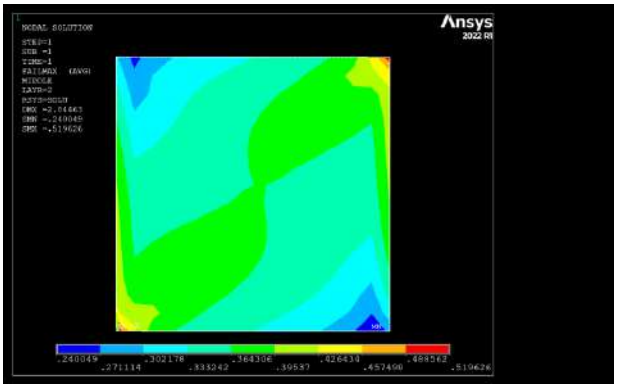

50N/mm

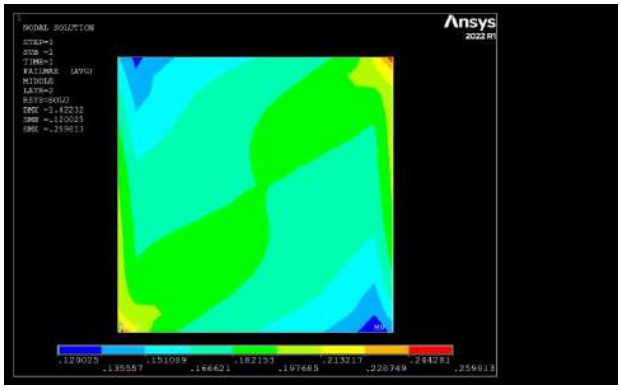

60N/mm

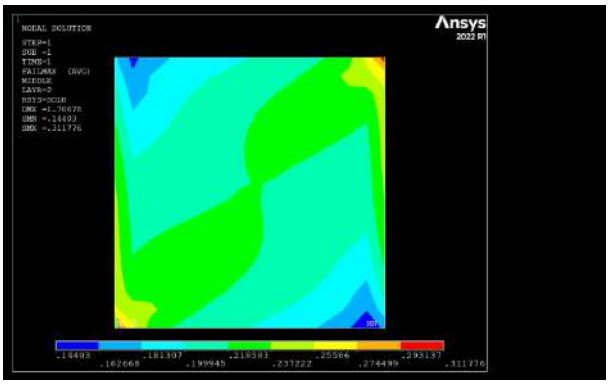

70N/mm

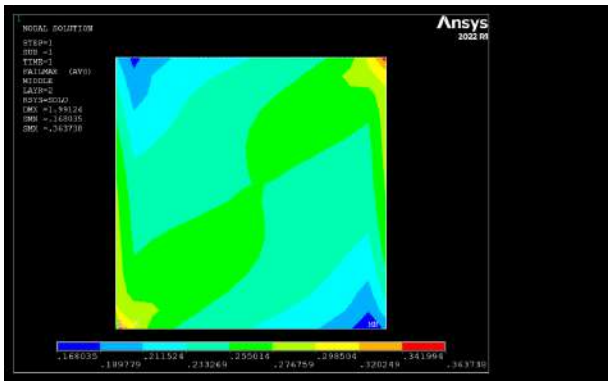

80N/mm

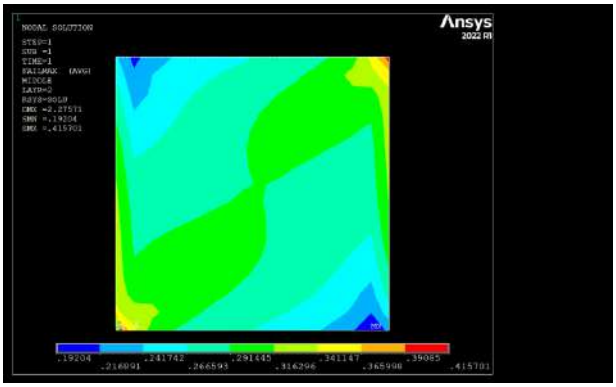

90N/mm

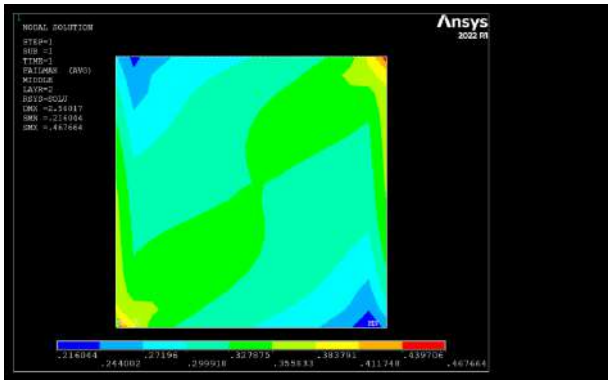

100N/mm

- **Tsai Wu IF- 50N/mm to 100N/mm**

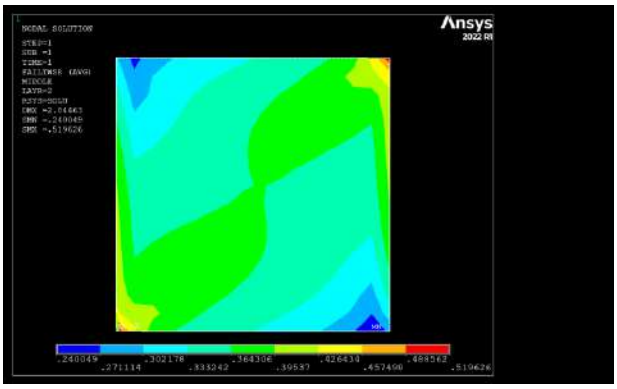

50N/mm

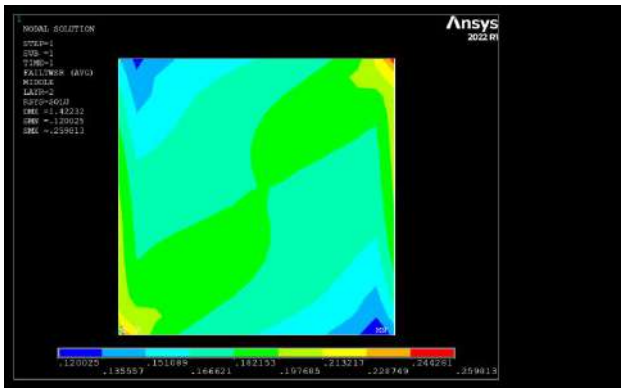

60N/mm

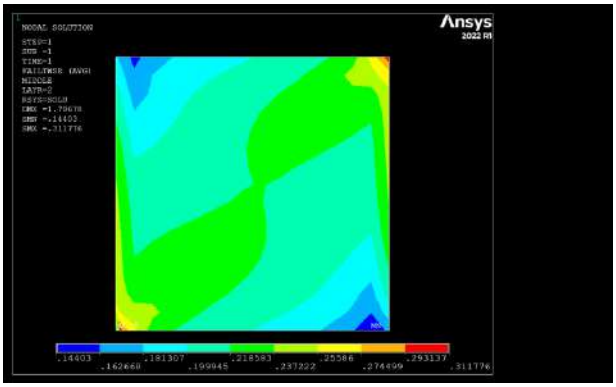

70N/mm

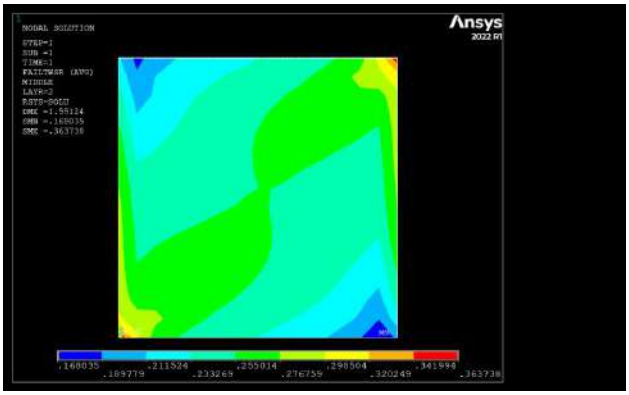

80N/mm

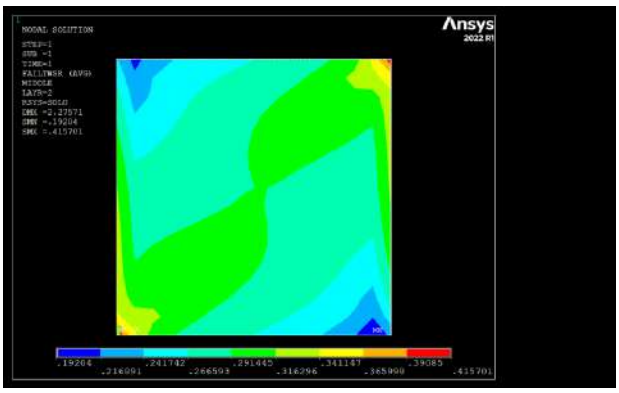

90N/mm

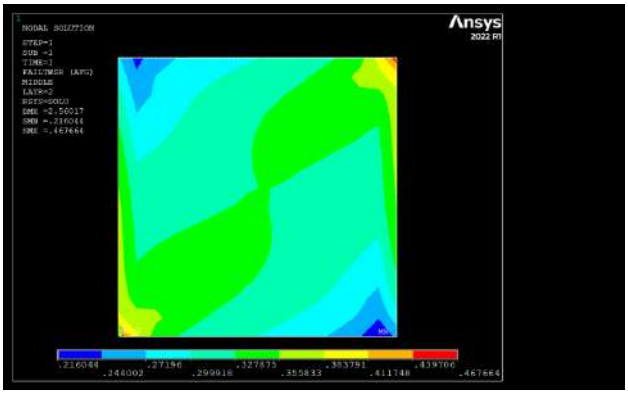

100N/mm

- **Maximum Displacement- 50N/mm to 100N/mm**

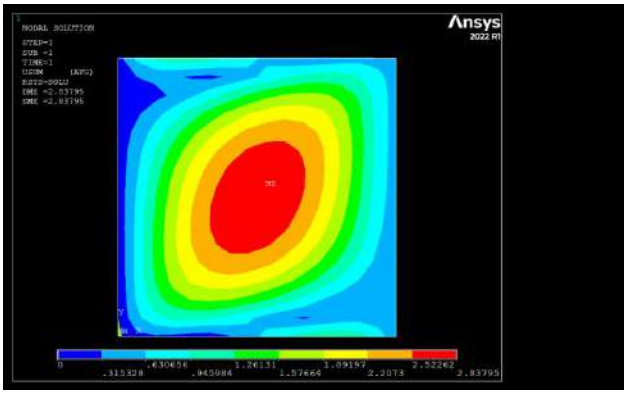

50N/mm

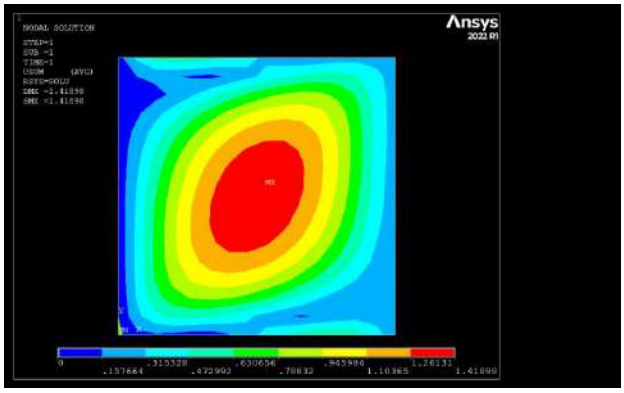

60N/mm

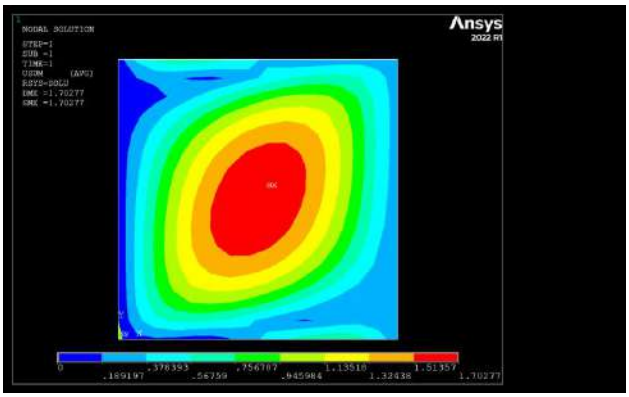

70N/mm

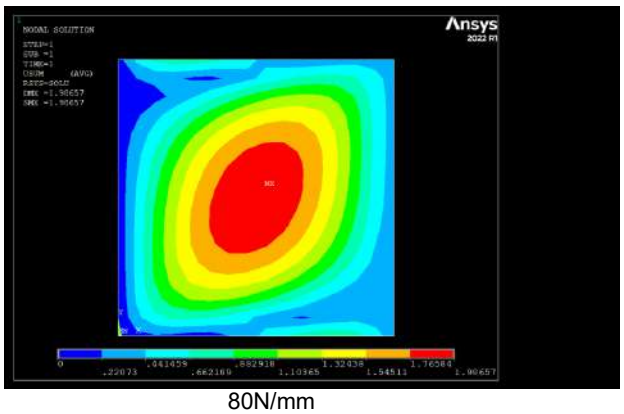

80N/mm

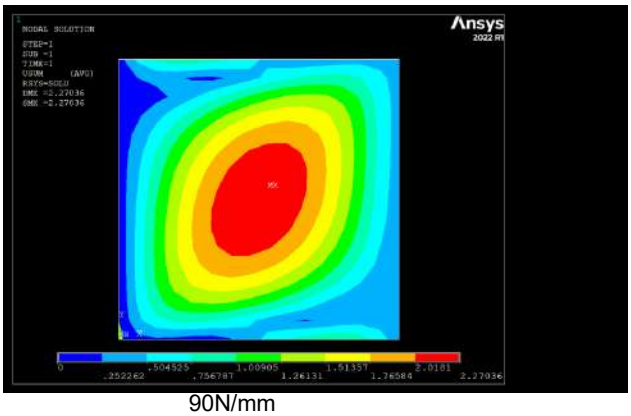

90N/mm

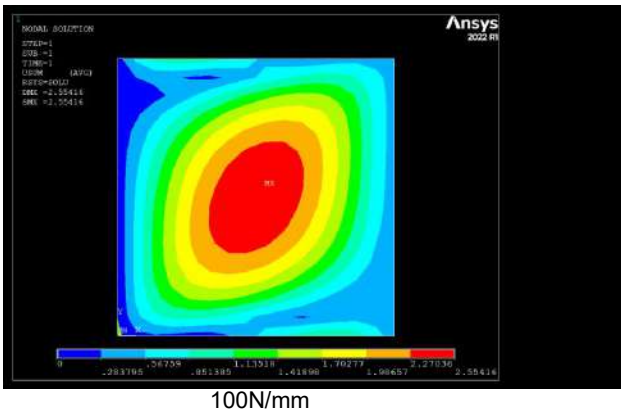

100N/mm

E1 Case Study

NXY Load Configuration

- **Hashin-Rottem IF- 150N/mm to 200N/mm**

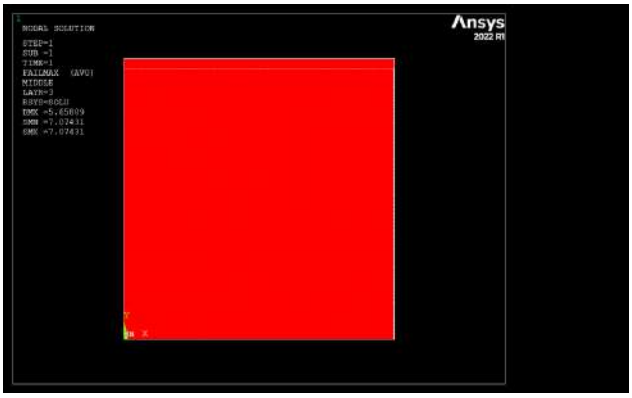

150N/mm

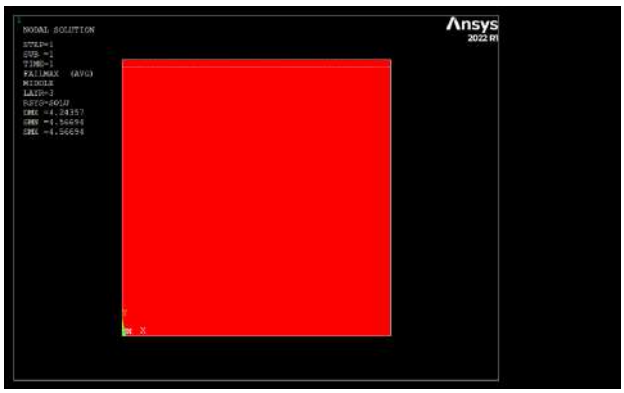

160N/mm

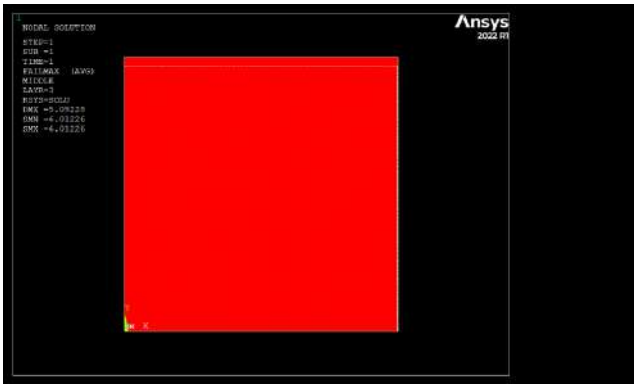

170N/mm

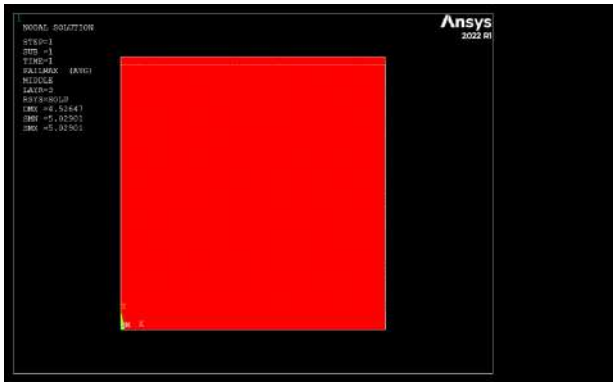

180N/mm

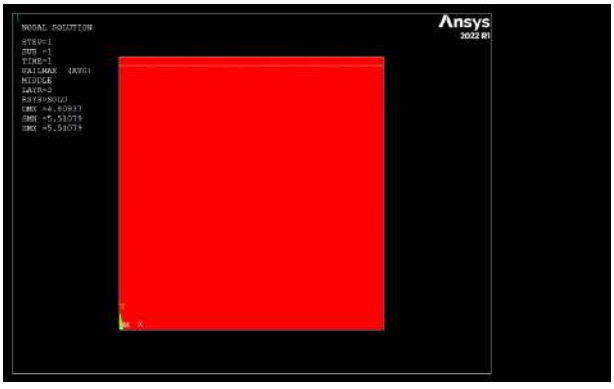

190N/mm

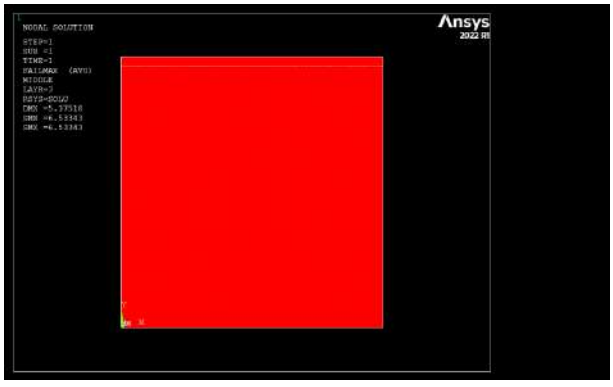

200N/mm

- **Max Stress IF- 150N/mm to 200N/mm**

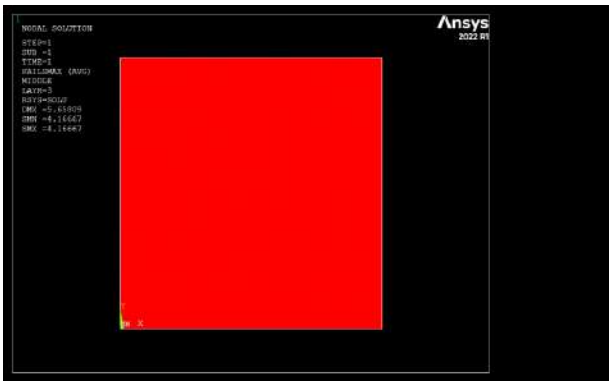

150N/mm

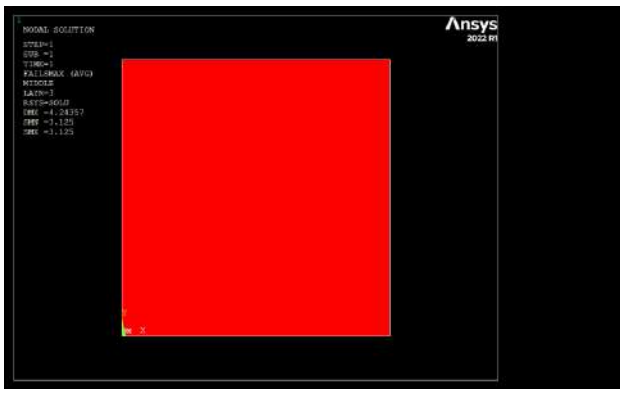

160N/mm

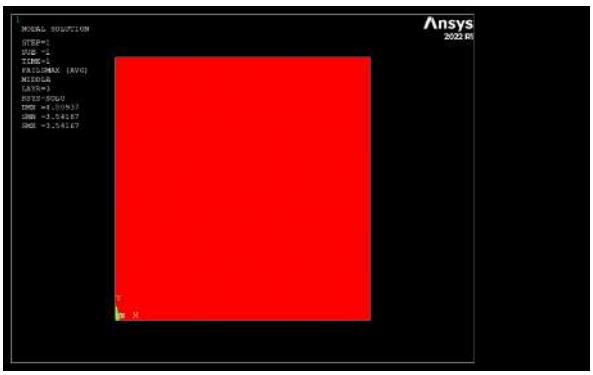

170N/mm

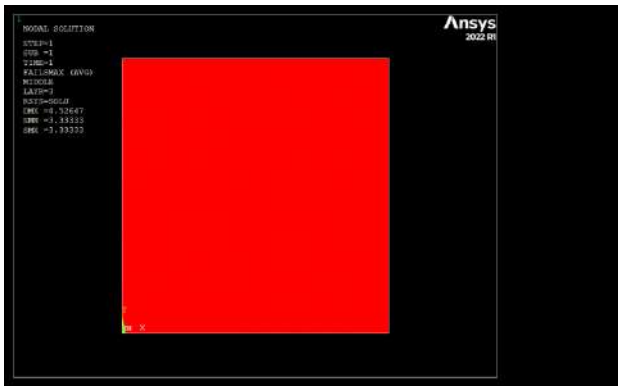

180N/mm

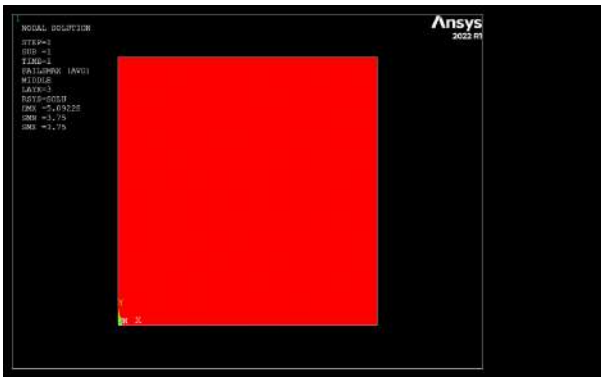

190N/mm

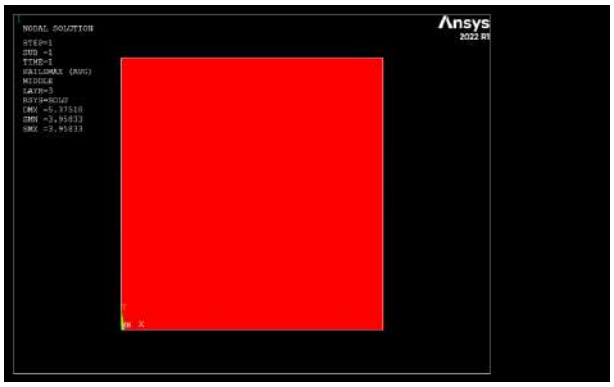

200N/mm

- **Tsai Hill IF- 150N/mm to 200N/mm**

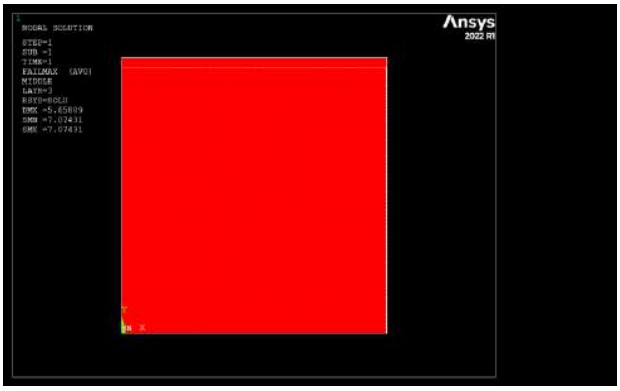

150N/mm

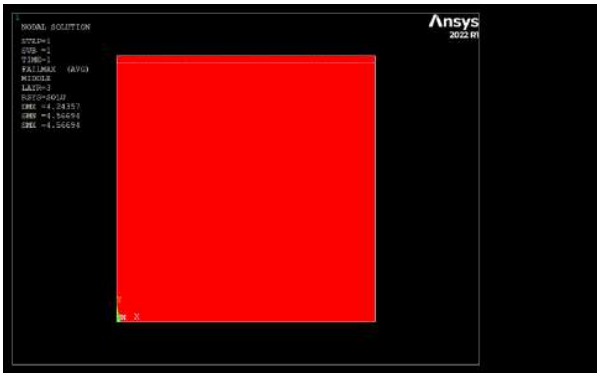

160N/mm

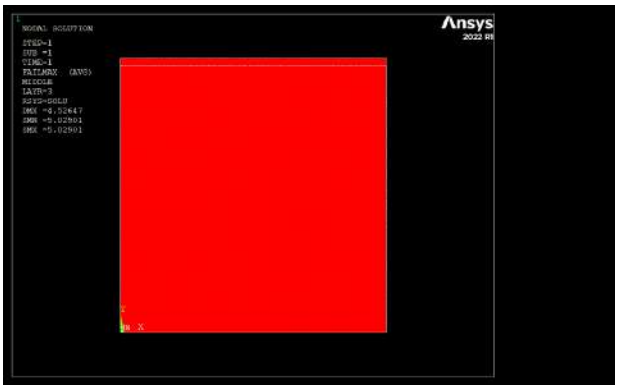

170N/mm

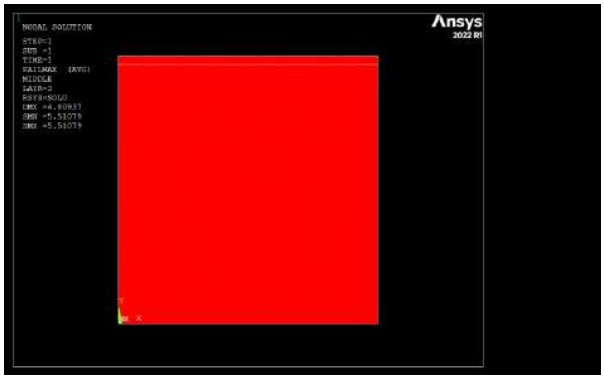

180N/mm

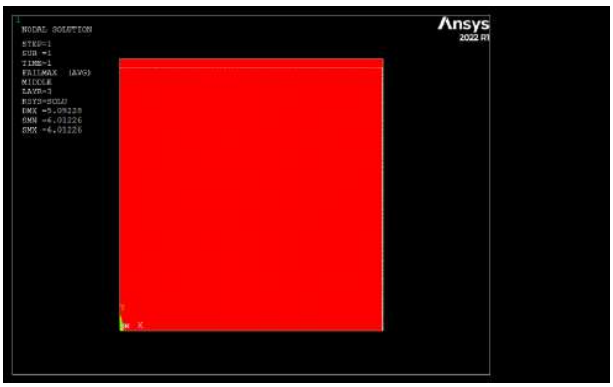

190N/mm

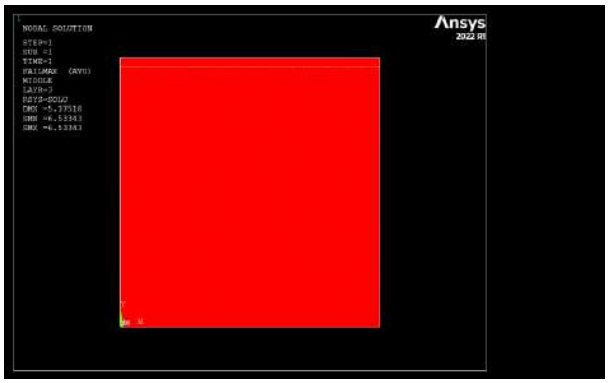

200N/mm

- **Tsai Wu IF- 150N/mm to 200N/mm**

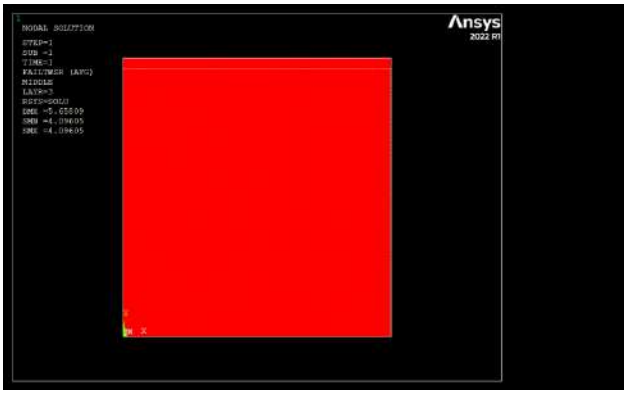

150N/mm

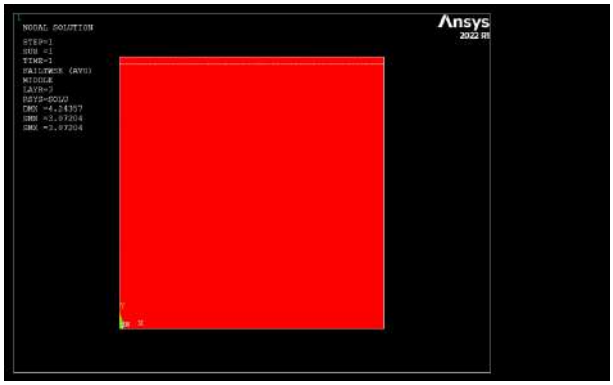

160N/mm

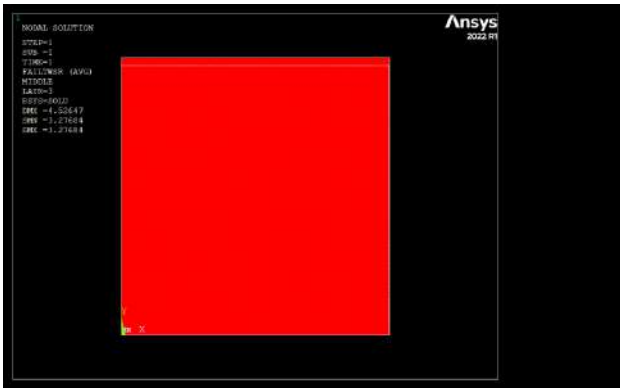

170N/mm

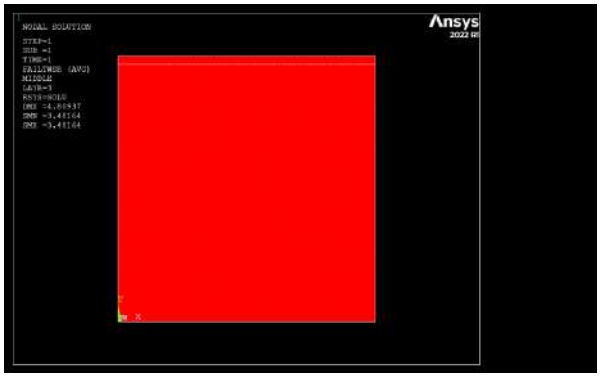

180N/mm

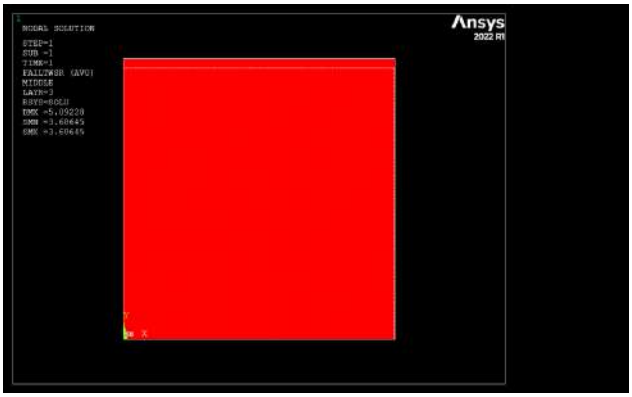

190N/mm

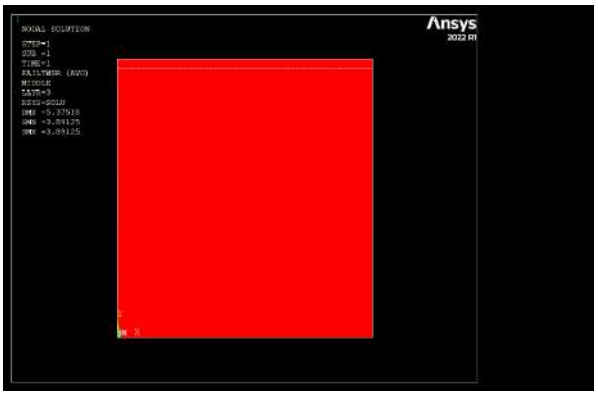

200N/mm

Maximum Displacement- 150N/mm to 200N/mm

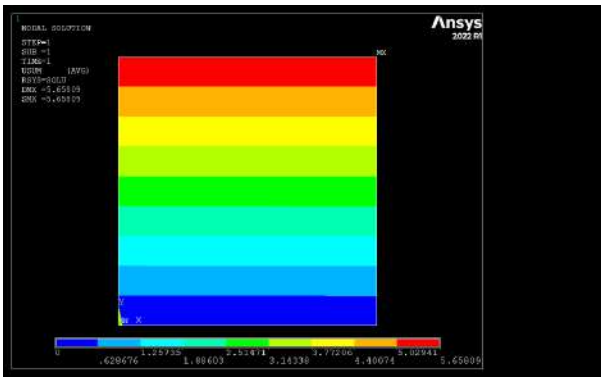

150N/mm

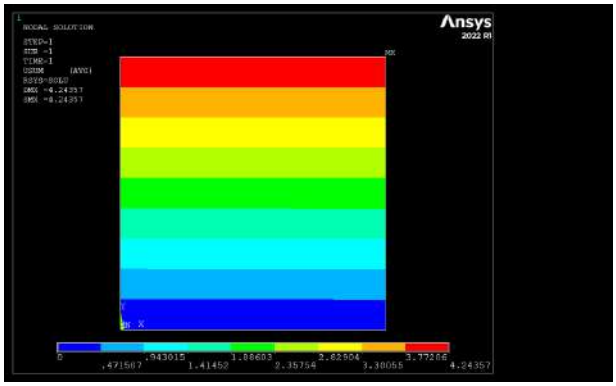

160N/mm

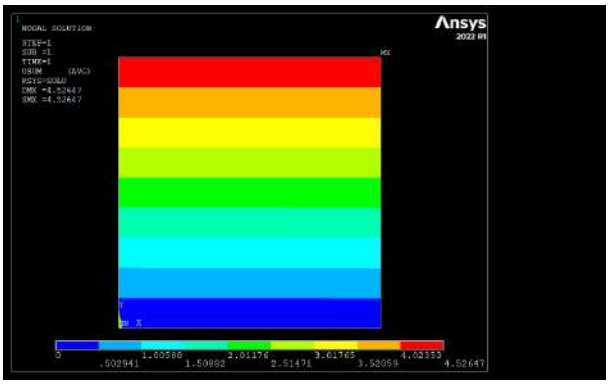

170N/mm

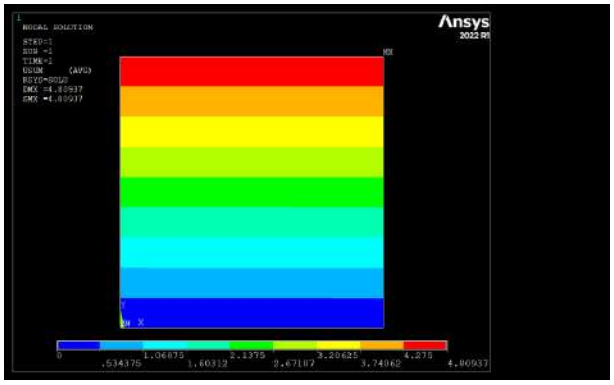

180N/mm

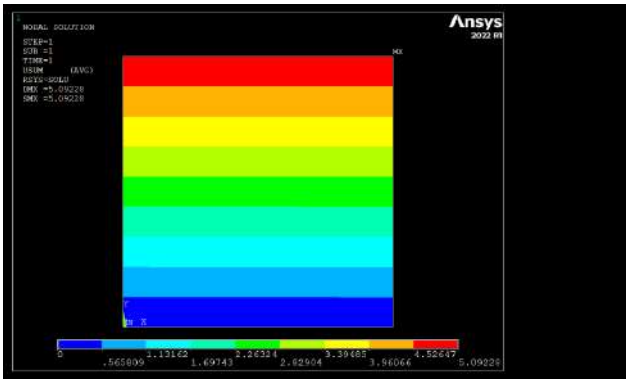

190N/mm

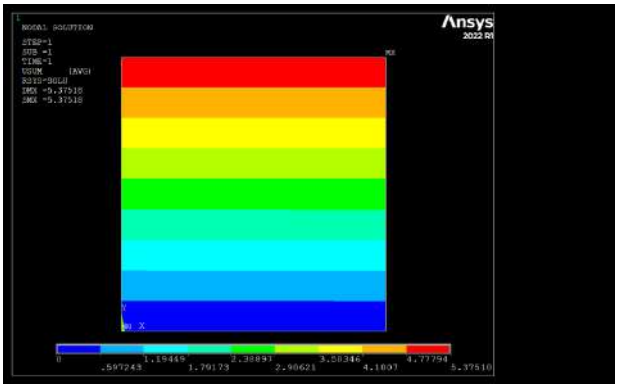

200N/mm

E1 Case Study

NY Load Configuration

- **Hashin-Rottem IF- 150N/mm to 200N/mm**

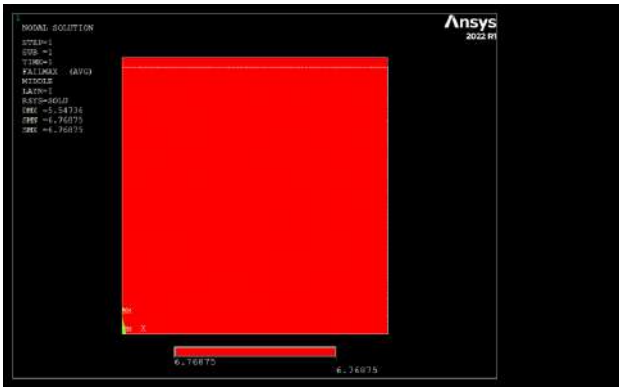

150N/mm

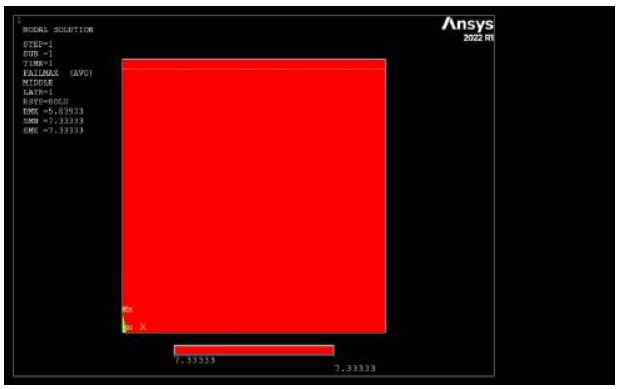

160N/mm

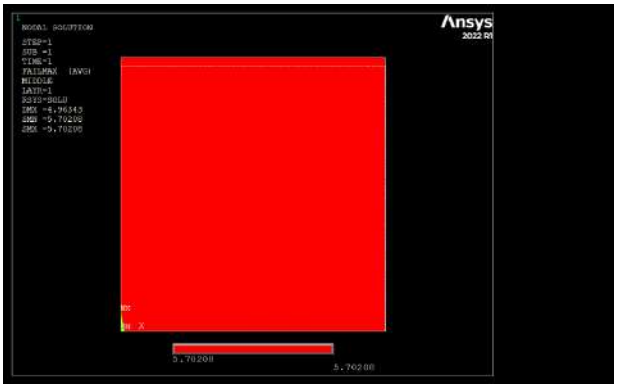

170N/mm

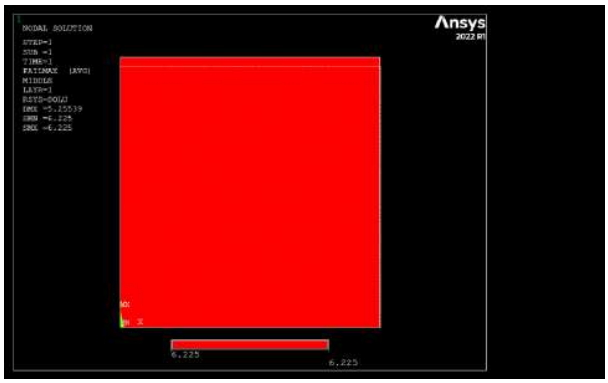

180N/mm

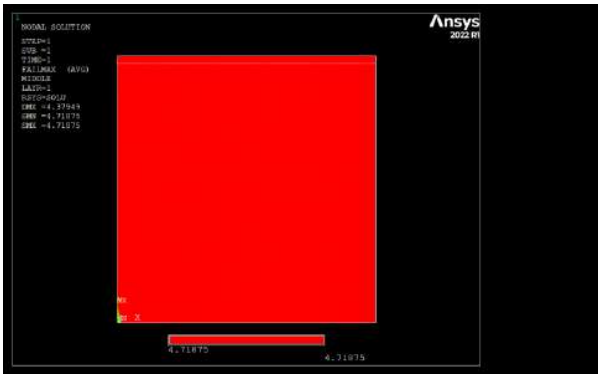

190N/mm

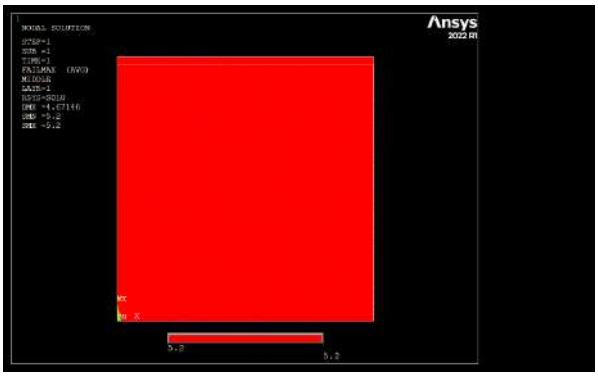

200N/mm

- **Max Stress IF- 150N/mm to 200N/mm**

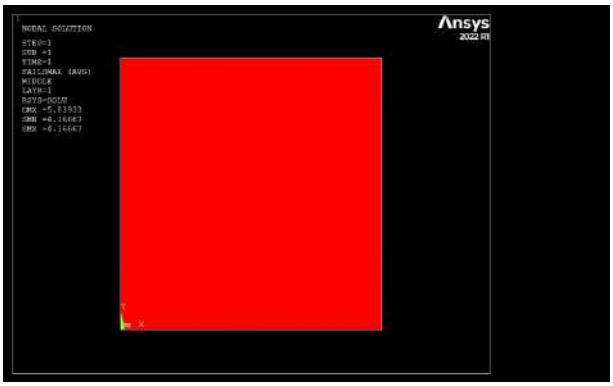

150N/mm

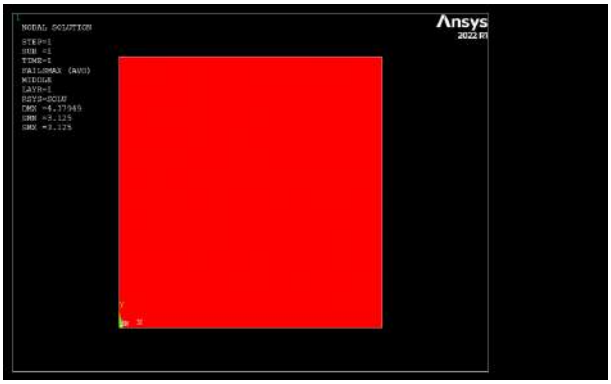

160N/mm

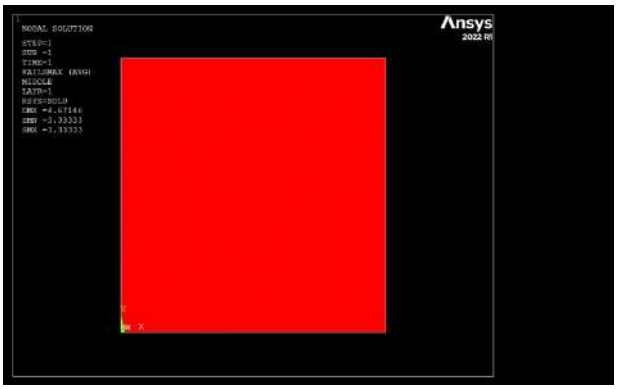

170N/mm

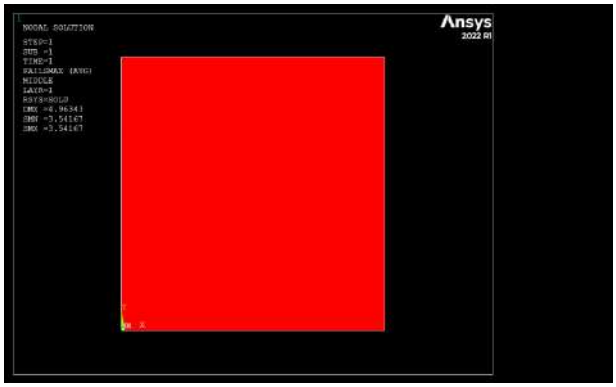

180N/mm

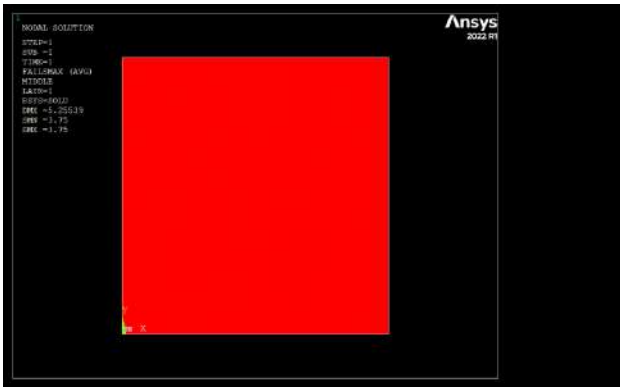

190N/mm

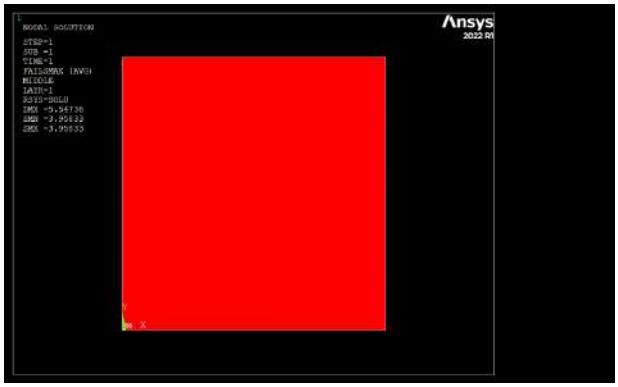

200N/mm

- **Tsai Hill IF- 150N/mm to 200N/mm**

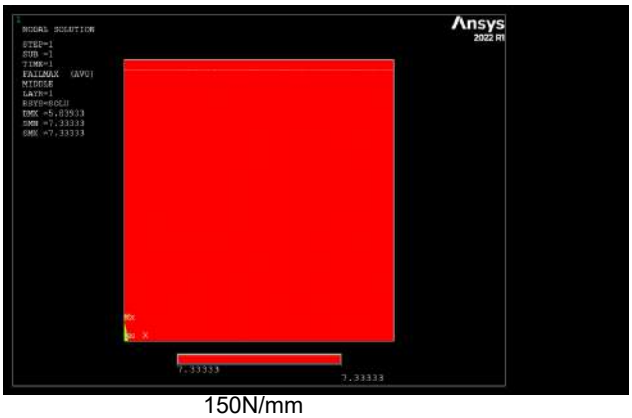

150N/mm

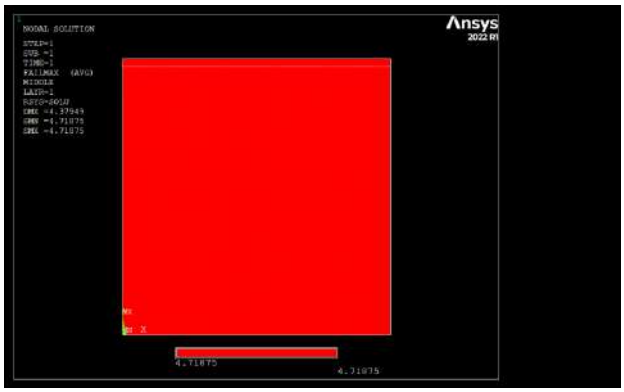

160N/mm

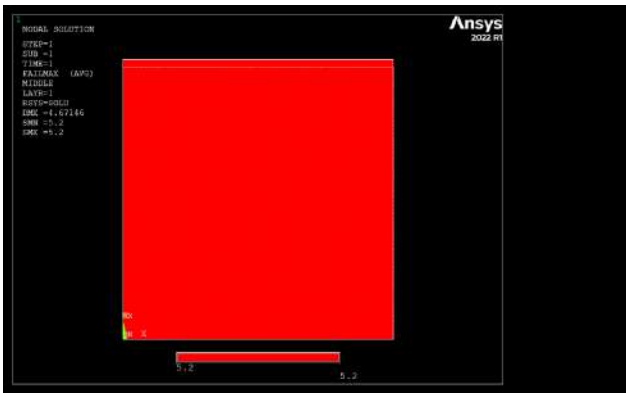

170N/mm

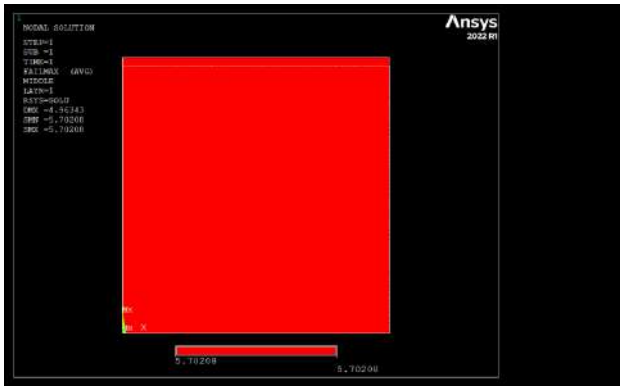

180N/mm

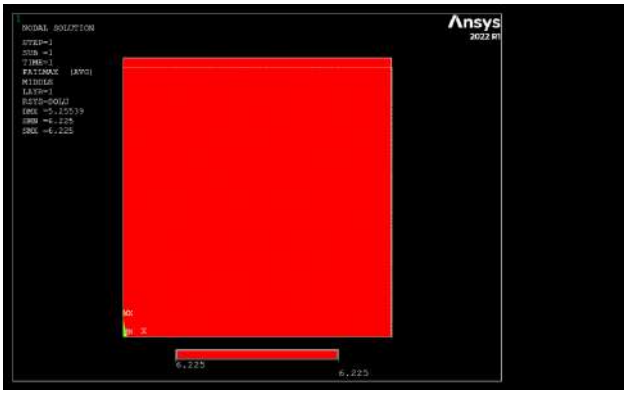

190N/mm

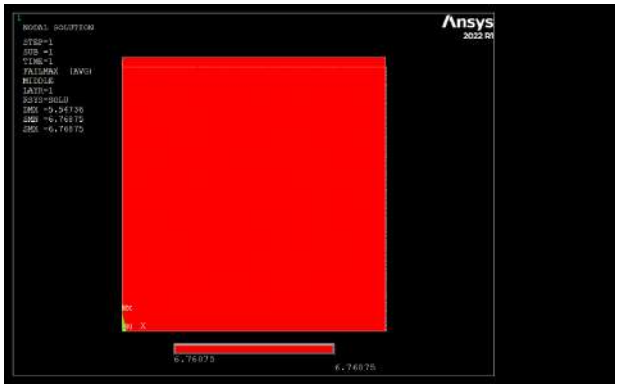

200N/mm

Tsai Wu IF- 150N/mm to 200N/mm

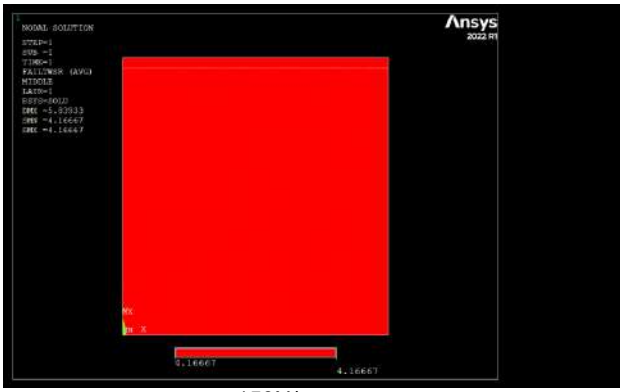

150N/mm

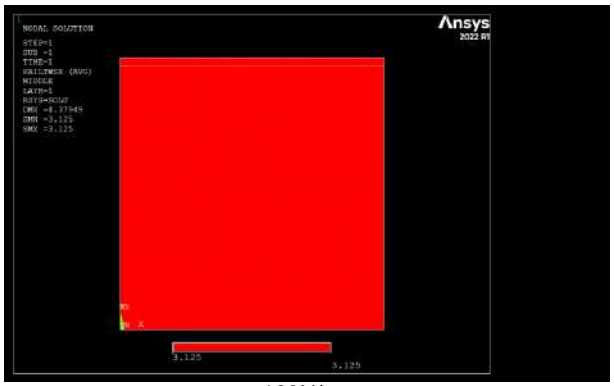

160N/mm

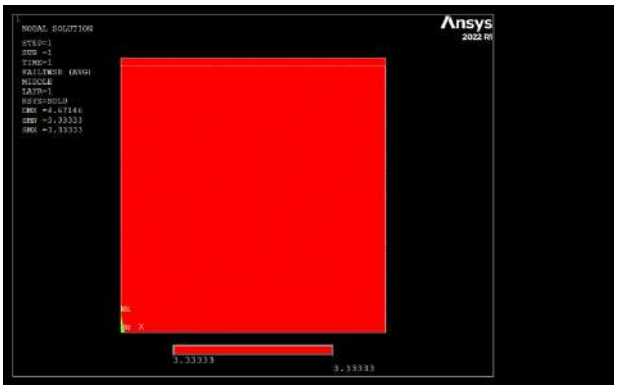

170N/mm

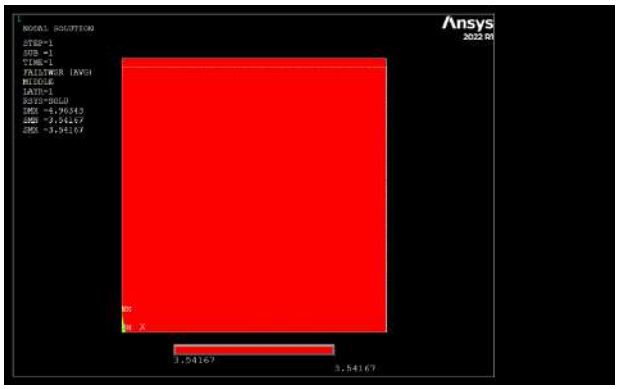

180N/mm

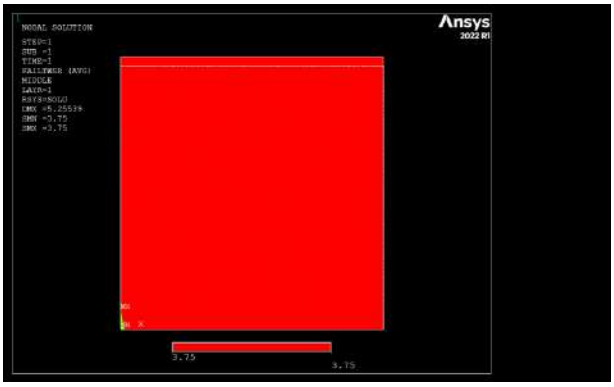

190N/mm

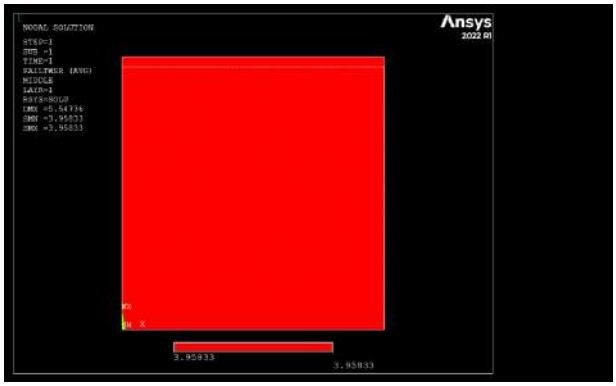

200N/mm

Maximum Displacement- 150N/mm to 200N/mm

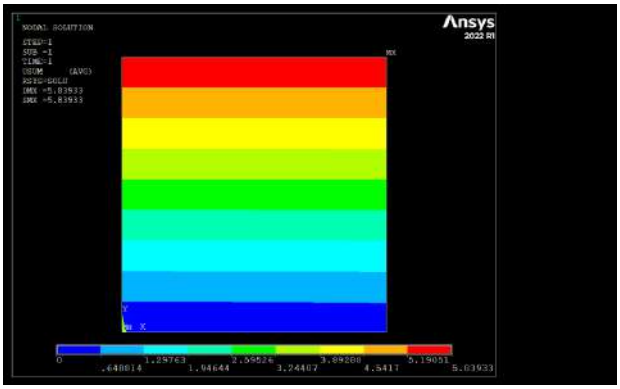

150N/mm

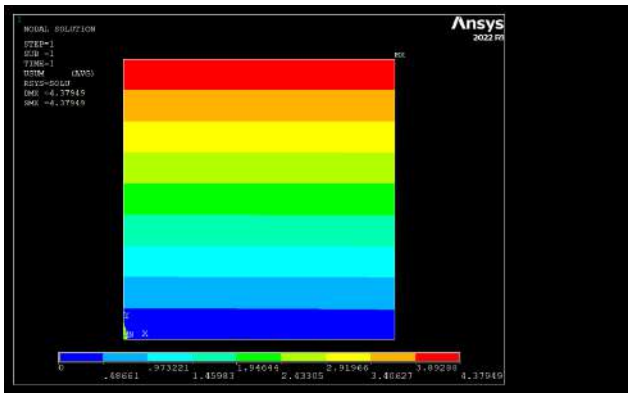

160N/mm

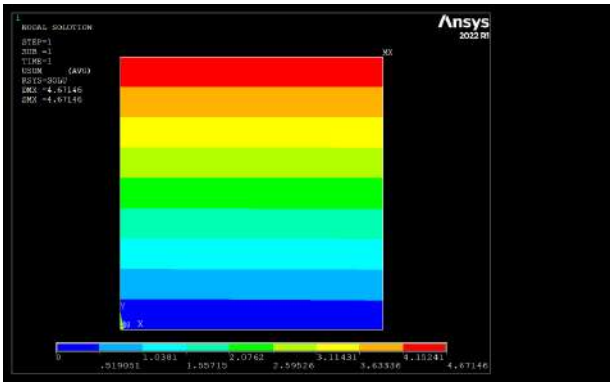

170N/mm

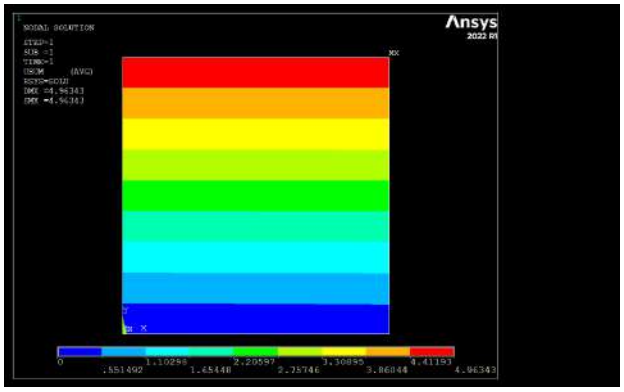

180N/mm

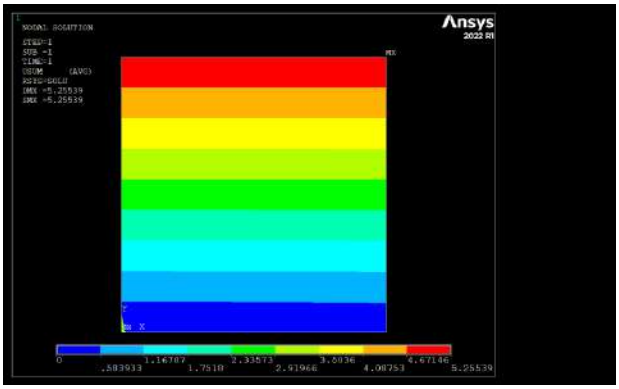

190N/mm

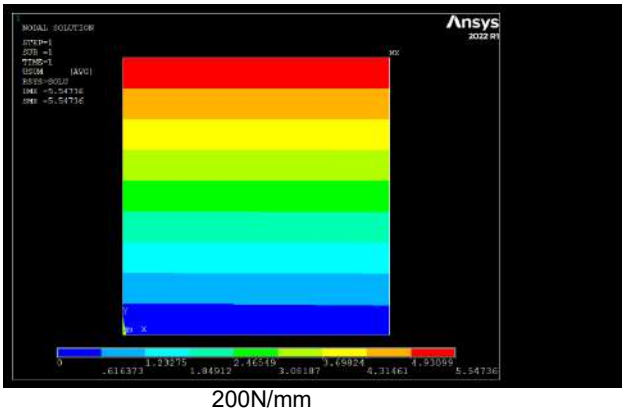

200N/mm